Stiffness and Strength Optimisation of the Anisotropy distribution for Laminated Structures

Anita Catapano

THÈSE DE DOCTORAT DE L'UNIVERSITÉ PIERRE ET MARIE CURIE

Spécialité: MÉCANIQUE

présentée par :
Anita CATAPANO

pour obtenir le titre de
DOCTEUR DE L'UNIVERSITÉ PIERRE ET MARIE CURIE

Stiffness and Strength Optimisation of the Anisotropy Distribution for Laminated Structures

4 Juin 2013
Composition du jury :

G. De Saxce	Pr.	LML, Université de Lille 1	Rapporteur
M. Potier-Ferry	Pr.	LEM3, Université de Lorraine	Rapporteur
J.F. Caron	DR	Institut NAVIER, ENPC	Examinateur
C. Fourcade	Dr.	Renault SAS	Examinateur
D. Kondo	Pr.	IJLRDA, Université Pierre et Marie Curie	Examinateur
P. Ladevèze	Pr.	LMT, ENS de Cachan	Examinateur
B. Desmorat	MdC	IJLRDA, Université Pierre et Marie Curie	Co-Directeur de Thèse
P. Vannucci	Pr.	LMV, Université de Versailles-St-Quentin	Directeur de Thèse

Institut Jean Le Rond d'Alembert
Université U.P.M.C. Paris VI / C.N.R.S. – UMR 7190

"Tutte le verità sono facili da capire
una volta che sono state rivelate. Il difficile è scoprirle..."
Galileo Galilei

"All truths are easy to understand
once they are discovered. The point is to discover them..."

Acknowledgements

I would like to thank Paolo Vannucci and Boris Desmorat for their supervision and their advices. It has been very interesting to perform this research and to sustain the numerous discussions on science with them; this allowed me to further expand my horizons and learn new concepts.

A sincere thanks goes also to my scientific supervisor at the Centre de Recherche Public Henri Tudor, Gaetano Giunta.

I am grateful to the National Research Fund (FNR) in Luxembourg, for supporting this work through Aides à la Formation Recherche Grant (PHD-09-184).

A very special thanks goes to my husband for his love and support in this experience and in the daily life. I wish to thank also my family: my parents, my sisters and my sweet nephews for believing and encouraging me in difficult moments.

Contents

Introduction

The objective of this thesis is to develop a new strategy for the analysis and the global optimal design of anisotropic structures. In particular, we propose a novel strategy able to include the optimisation of stiffness and strength into the same design process of a laminated structure. This is a relevant problem in structural design: both stiffness and strength are fundamental requirements for a structure. The purpose is to show that the simultaneous optimisation of two different characteristics of the structure can be effectively realised in order to obtain, hopefully, new interesting solutions for practical applications. In particular we consider structures with a given geometry but having variable stiffness and strength, because the anisotropy field is variable. We deal, by consequence, with a rather recent structural optimisation problem, that could be, by a slight abuse of language, qualified as the topological optimisation of anisotropy.

The thesis is mainly divided into three parts. In first part of the thesis, we briefly recall some basic points concerning the description of anisotropy. In particular, in Chapter 1 we introduce the tensorial representation of anisotropy and the *polar formalism*, used in this thesis for both the theoretical and numerical developments. Among its several advantages, we make use of the polar method for three main reasons: the possibility of describing the material symmetries in a very direct way, the advantage of letting appear the material orientation as an explicit term and the easiness in changing the reference frame. Finally, in this Chapter we recall also the mathematical bases of the Classical Laminated Plate Theory (CLPT) and its polar representation to describe the stiffness tensors of laminated structures.

Chapter 2 is dedicated to the description of the strength of orthotropic materials through failure criteria. We present some failure criteria used very often in the design of laminated structures: the polynomial failure criteria of Tsai-Hill, Hoffman, Tsai-Wu and the strain-based polynomial criterion of Zhang-Evans. The peculiarity of these criteria concerns their formulation, based upon a unique condition that algebraically can be interpreted to as a quadratic form. Moreover, we introduce, in this Chapter the "unified matrix formulation" of these criteria that will be the starting point for their invariant formulation described in Chapter 4.

In Chapter 3 we give a short overview on optimisation of laminates for what concerns the maximisation of stiffness and/or strength. Far from being exhaustive, its aim is to place in a bibliographic context our research.

The second part focuses on strength description and optimisation for orthotropic materials. In particular, we develop an appropriate formulation of strength criteria for orthotropic sheets and, subsequently, we search for an optimal material orientation to maximise their strength. In Chapter 4 we use the polar formalism to give, for all the above criteria, a unified formulation based upon the use of tensor invariants. Using these

results, in Chapter 5, we perform an analytical study to find the orientation of the the material that minimises the failure index. The objective function is the failure index of one amongst the polynomial failure criteria considered in Chapter 2.

In the third part of the thesis, we pass to the analysis of the optimal design of laminated structures. As said beforehand, the goal is to propose a strategy to include the optimisation of stiffness and strength in the same design process of a laminated structure.

The optimisation procedure that we have adopted is a two-step approach that can be interpreted as a model reduction for a passage from the meso-scale, the layers, to a macro-scale, the laminate. It can be resumed as follows:

- *First step (structural optimisation)*: the laminated structure is modelled as a single-layer homogeneous structure; the anisotropy field is optimised, leading to the optimal local mechanical properties of the structure, resumed in four fields of anisotropic polar parameters for stiffness and strength and in a field of orthotropy directions; hence, at the end of this step, the optimal mechanical response of the structure and the distribution of its anisotropic properties, for both stiffness and strength, are completely known;

- *Second step (lay up design)*: a suitable stacking sequence, giving the optimal response obtained at the end of the previous step, is looked for at each point of the structure; the outcome of this step is hence constituted by n orientation fields, n being the number of layers.

Such a two-step strategy is not new; in some way it can be reconducted to the first studies of Miki in 1982.

To be more specific, in Chapter 6 we formulate the general optimisation problem for stiffness and strength and precise the way that we use to describe the strength of the homogenised, single layer, fictitious plate of the first step. In order to better introduce such a procedure, we first recall the essential points of the analogous two-step approach, concerning only stiffness, already used by Jibawy *et al.*. Then, with the aim of extending the analytical approach introduced in Chapter 5 to the strength optimisation of laminated plates, we define an *homogenised failure criterion* giving a measure of the strength for the laminate. In this way we can define the functional, the laminate failure index, to be minimised in order to maximise the strength.

Concerning the stiffness functional, almost all of the works on stiffness optimisation take as objective function the compliance, which is a global functional, so its use introduce to a variational problem having a classical structure: the minimisation of a positive global functional. On the contrary, strength optimisation problems are not so easy to be deal with. Strength is always a local property, so any formulation of a strength maximisation problem gives rise to a variational problem with a local functional, hence to an intrinsically more complicate mathematical problem. In our approach, aiming to take into account at the same time for stiffness and strength, we need hence to formulate a mathematical problem where a local and a global functional are optimised at the same time.

In our approach a relevant assumption is that the design variables describing stiffness and strength, the anisotropic polar moduli, are independent. Nevertheless, the two anisotropy fields of stiffness and strength are not completely unrelated. They share common parameter, the material orientation.

For the first step of the strategy, we propose an optimisation process based upon a water-fall solution method: first we consider one of the two objectives as the leading

objective and we minimise it with respect not only to its polar moduli, but also to the orthotropy orientation; then, the other functional is minimised only with respect to the polar moduli while the orientation is given and fixed equal to that obtained minimising the leading objective. Therefore, in Chapter 6 we state two different optimisation problems, one taking the stiffness as the leading objective while in the second one it is the strength.

In Chapter 7 we present three different algorithms used to solve the first step of the hierarchical strategy. The first one is a simple modification of the optimisation algorithm introduced by Allaire and Kohn in 1993. Namely, we added a further phase to the original version of the algorithm in which we introduce the strength optimisation phase. We considered the stiffness as the main property to be maximised in terms of all the stiffness material parameters. On the contrary, the strength functional, i.e. the laminate failure index, is considered as the secondary property to be maximised.

The second algorithm can be considered, as the "converse" version of the previous one: the failure index is the leading objective while the complementary energy is the secondary one. Finally, we propose also a modified versions of this algorithm, more effective and robust than the previous one. Also, for this last algorithm we have been able to give a convergence proof, that is monotonic for complementary energy and alternate for strength. In all of these algorithms two functional are minimised, one being a global functional, the complementary energy, and the other a local one, the failure index. We give also an analytical solution for the minimisation of the strength functional, with respect to the material parameters. Finally, we present some numerical tests in order to prove the effectiveness and the robustness of the proposed algorithms and to evaluate the computational costs of this first step of the hierarchical strategy.

The last Chapter 8 concerns the second step, the lay-up design; the general numerical technique for obtaining a laminate having the optimal properties issued from the first step is described and discussed, a step for the layer wise check of strength is also introduced, and a numerical example given. As we show, following a general approach formulated by Vannucci and based upon the polar formalism, we show that it is really possible to design, without restricting a priori assumptions, laminates with any kind of elastic properties. The redundancy of solutions for the lay-up design problem appears to be, in our approach, a fundamental point that renders possible the existence of laminates satisfying the optimal requirements. We formulated the problem as an optimisation problem of minimum distance between the material parameters of the laminate solution and those issued from the structural optimisation step. In particular, this objective function is composed by nine semi-definite positive partial objectives, each one linked to one material parameter of the homogenised structure. Due to the non-convexity of the objective function, we solved this optimisation problem by the aid of the genetic code BIANCA, developed by Montemurro, Vincenti and Vannucci and used here in an automated procedure for the sequential solution of the lay-up problem for each one of the finite elements discretising the structure.

Finally, with this research we develop a new approach to the design of laminates, where stiffness and strength take part to a unique simultaneous optimisation procedure. The method presented here does not make use of simplifications usually adopted by laminates designers. So, at least in principle, true global minima can be obtained.

Conscious that we have not followed existing approaches in the domain, we hope that our research can be a starting point for future works that, integrating also technical requirements expressly let apart in this thesis, will lead it from an almost purely

mathematical achievement to a more appropriate technical solution.

Funding

This thesis is funded by the Fonds National de la Recherche (FNR) of Luxembourg through Aides à la Formation Recherche Grant (PHD-09-184). The work has been developed at the Institut Jean Le Rond d'Alembert of the Université Paris VI, at the Centre de Recherche Public Henri Tudor in Luxembourg and at Université de Versailles St. Quentin-en-Yvelines.

Part I

Introducing concepts and tools

1

Anisotropy and laminates classical theory

1.1 Introduction

Anisotropic materials, such as fiber reinforced composite materials, are extensively used in many industrial fields thanks to their mechanical performances. However, the design of structures constituted by such type of materials is very complex.

The main characteristic of an anisotropic material is the dependency of physical properties from the direction. A clue point in anisotropy, is to dispose of an appropriate mathematical model related to the physical behaviour of these materials: the tensorial representation. The combination of these two aspects, directionality of the material behaviour and tensorial representation, leads to the necessity of introducing an efficient formulation linked to the nature of the problem: the invariant formulation of tensors.

The most known "invariant" formulation is that introduced by Tsai and Pagano in 1968 [72], in particular they introduced 7 parameters whereof only 5 are invariants. Another invariant formulation, based upon a complex variable transformation and hence valid only for plane problems, is the *polar method* proposed by Verchery in 1979 [86].

In this Chapter we recall the mathematical representation of anisotropy, Secs. 1.2 and 1.3, and the classical laminated plate theory, Sec. 1.6, used in this thesis. Furthermore, in Sec. 1.4 to 1.5 we introduce the polar method and in Sec. 1.6 we use it to describe the behaviour of anisotropic structures in the framework of the Classical Laminated Plate Theory (CLPT).

1.2 3D anisotropic elasticity

1.2.1 The Hooke's law

Let us consider a three-dimensional medium constituted by a linear elastic anisotropic material and subjected to a stress state described by the Cauchy's stress tensor $\boldsymbol{\sigma}$. Denoting by $\mathbf{E}$ the elastic stiffness tensor, the generalised three-dimensional Hooke's law [33] is:

$$\boldsymbol{\sigma} = \mathbf{E}\boldsymbol{\varepsilon} \ , \tag{1.1}$$

where $\boldsymbol{\varepsilon}$ is the second order tensor of infinitesimal strains. $\mathbf{E}$ collects all the informations on the elastic behaviour of the material.

For an anisotropic material, the fourth order stiffness tensor $\mathbf{E}$ has the following tensorial symmetries:

$$\begin{array}{ll} \text{major symmetries :} & E_{ijkl} = E_{klij} \ , \\ \text{minor symmetries :} & E_{ijkl} = E_{jikl} = E_{jilk} = E_{ijlk} \ , \end{array} \quad \text{with } i,j,k,l = 1,2,3 \ . \tag{1.2}$$

The overall number of eqs. (1.2) is 60, hence, in the most general case of a completely anisotropic (triclinic) material the elasticity tensor has 21 independent components.
The compliance tensor $\mathbf{Z}$ is defined as the inverse of $\mathbf{E}$ and it has the same tensorial symmetries of $\mathbf{E}$. The inverse Hooke's law reads

$$\boldsymbol{\varepsilon} = \mathbf{Z}\boldsymbol{\sigma} \ . \tag{1.3}$$

Considering eq. (1.2), the Hooke's law (1.1) can be expressed in a compact matrix form using the Voigt's notation [90]:

$$\sigma_i = C_{ij}\varepsilon_i \ ; \quad i,j = 1,..,6 \quad \text{and } C_{ij} = C_{ji} \ , \tag{1.4}$$

with:

$$\{\sigma\} = \left\{ \begin{array}{c} \sigma_1 \\ \sigma_2 \\ \sigma_3 \\ \sigma_4 \\ \sigma_5 \\ \sigma_6 \end{array} \right\} ; \ \{\varepsilon\} = \left\{ \begin{array}{c} \varepsilon_1 \\ \varepsilon_2 \\ \varepsilon_3 \\ \varepsilon_4 = 2\varepsilon_{23} \\ \varepsilon_5 = 2\varepsilon_{13} \\ \varepsilon_6 = 2\varepsilon_{12} \end{array} \right\} \ ; \tag{1.5}$$

and $[C] \in \mathbb{R}^{6\times 6}$ being the stiffness matrix. The inverse of $[C]$ is the compliance matrix $[S]$. The relations of $[C]$ and $[S]$ with the tensors $\mathbf{E}$ and $\mathbf{Z}$ can be condensed in the following abridged matrix formulae:

$$[C] = \left[\begin{array}{ccc} E_{iijj} & | & E_{iikl} \\ -- & + & -- \\ E_{iikl} & | & E_{ijkl} \end{array} \right] , \ [S] = \left[\begin{array}{ccc} Z_{iijj} & | & 2Z_{iikl} \\ -- & + & -- \\ 2Z_{iikl} & | & 4Z_{ijkl} \end{array} \right] \ . \tag{1.6}$$

1.2.2 Elastic symmetries

As seen beforehand, a completely anisotropic material is characterised by 21 independent elastic components. However, anisotropic materials present often some material symmetries, providing an identical mechanical behaviour with respect to a set of directions: the *equivalent directions*. Depending on the number and type of material symmetries, the number of independent elastic moduli is reduced.

The possible symmetries of a material are:

1. Orthogonal symmetry with respect to a plane.
   The stiffness matrix is characterised by the following relations:

   $$C_{41} = C_{42} = C_{43} = C_{46} = C_{51} = C_{52} = C_{53} = C_{56} = 0 \ . \tag{1.7}$$

   The number of independent elastic moduli is reduced to 13. Such kind of material is called *monoclinic*.

2. Symmetry with respect to three orthogonal planes.
   The relations
   $$C_{61} = C_{62} = C_{63} = C_{45} = 0 \ , \tag{1.8}$$
   are verified along with eq. (1.7). The number of independent elastic moduli is reduced to 9. Such a kind of material is called *orthotropic*.

3. Symmetry of order n with respect to an axis.
   An axis, say the axis x_3, is an axis of symmetry of order n if the equivalent directions superimpose each other rotating by an angle $2\pi/n$ around x_3. In elasticity, only symmetries of order 2, 3, 4 and ∞ can exist:

   - 2^{nd} order, it can be easily proved that this symmetry is characterised by the same relations (1.7) of a monoclinic material. The number of independent elastic moduli is 13;
   - 3^{rd} order, the following relations among the components of $[C]$ exist:
     $$\begin{gathered} C_{16} = C_{26} = C_{34} = C_{35} = C_{45} = 0 \\ C_{22} = C_{11} \ , \quad C_{55} = C_{44} \ , \quad C_{23} = C_{13} \ , \quad C_{24} = -C_{14} \ , \\ C_{15} = -C_{25} \ , \quad C_{46} = C_{25} \ , \quad C_{56} = C_{14} \ , \quad C_{66} = \frac{C_{11} - C_{12}}{2} \ . \end{gathered} \tag{1.9}$$
     The number of independent elastic moduli is reduced to 7;
   - 4^{th} order, we can get
     $$\begin{gathered} C_{14} = C_{24} = C_{34} = C_{15} = C_{25} = C_{35} = C_{45} = C_{36} = C_{46} = C_{56} = 0 \\ C_{22} = C_{11} \ , \quad C_{23} = C_{13} \ , \quad C_{26} = -C_{16} \ , \quad C_{55} = -C_{44} \ . \end{gathered} \tag{1.10}$$
     Also in this case the number of independent elastic moduli is 7;
   - 6^{th} order, in this case it is
     $$\begin{gathered} C_{14} = C_{24} = C_{34} = C_{15} = C_{25} = C_{35} = C_{45} = C_{16} = C_{26} = C_{36} = C_{46} = C_{56} = 0 \\ C_{22} = C_{11} \ , \quad C_{23} = C_{13} \ , \quad C_{55} = C_{44} \ , \quad C_{66} = \frac{C_{11} - C_{12}}{2} \ . \end{gathered} \tag{1.11}$$
     The relations that characterise the independent elastic moduli of a material with a symmetry of 6^{th} order with respect to an axis are identical to those of a material that presents a rotational axis of symmetry (∞ order). Such materials are called *transversely isotropic*. The number of independent elastic moduli is 5 in both these cases;

4. Complete symmetry or isotropy.
   In this case the components of tensors $\mathbf{E}$ and $\mathbf{Z}$, and also of matrix $[C]$ and $[S]$ are invariant and do not change when varying the reference system. The number of independent elastic components is reduced to 2 (C_{11} and C_{12}).

1.3 The assumption of plane stress state

The hypothesis of plane stress state is justified when dealing with mechanical problems associated to thin plane structures. The relations that characterise a plane stress field

are, in the plane (x_1, x_2):

$$\left\{ \begin{array}{c} \sigma_3 \\ \sigma_4 \\ \sigma_5 \end{array} \right\} = \left\{ \begin{array}{c} 0 \\ 0 \\ 0 \end{array} \right\} \ . \tag{1.12}$$

As a consequence of eq. (1.12) the stress and strain vectors become:

$$\{\sigma\} = \left\{ \begin{array}{c} \sigma_1 \\ \sigma_2 \\ \sigma_6 \end{array} \right\} ; \ \{\varepsilon\} = \left\{ \begin{array}{c} \varepsilon_1 \\ \varepsilon_2 \\ \varepsilon_6 \end{array} \right\} . \tag{1.13}$$

The out-of-plane components of strains become, for an orthotropic material with x_1, x_2 and x_3 axes of orthotropy,

$$\left\{ \begin{array}{l} \varepsilon_3 = -\dfrac{C_{13}\varepsilon_1 + C_{23}\varepsilon_2}{C_{33}} \ , \\ \varepsilon_4 = 0 \ , \\ \varepsilon_5 = 0 \ . \end{array} \right. \tag{1.14}$$

In the transition from the three-dimensional stress state to the bi-dimensional one, the components of matrix $[S]$ do not vary while those of the in-plane stiffness matrix are obtained inverting the in-plane compliance matrix $[S]$ and are not not equal the components of the corresponding 3D case. For this reason the stiffness matrix is now called *reduced stiffness matrix* and it is introduced by $[Q]$; in particular we have

$$[Q] = [S]^{-1} \ \ \Rightarrow \ \ Q_{ij} = C_{ij} - \frac{C_{i3}C_{j3}}{C_{33}}, \ Q_{66} = C_{66} \ ; \tag{1.15}$$

and $i, j = 1, 2$.

1.3.1 Tensorial representation

The in-plane Hooke's law can be written

$$\{\sigma\} = [Q]\,\{\varepsilon\} \ . \tag{1.16}$$

The relation between the Voigt and the tensorial notations is:

$$\begin{array}{lll} Q_{11} = Q_{1111} \ , & Q_{12} = Q_{1122} \ , & Q_{16} = Q_{1112} \ , \\ Q_{22} = Q_{2222} \ , & Q_{26} = Q_{2212} \ , & Q_{66} = Q_{1212} \ , \end{array} \tag{1.17}$$

while for the compliance tensor one gets, see (1.6),

$$\begin{array}{lll} S_{11} = S_{1111} \ , & S_{12} = S_{1122} \ , & S_{16} = 2S_{1112} \ , \\ S_{22} = S_{2222} \ , & S_{26} = 2S_{2212} \ , & S_{66} = 4S_{1212} \ . \end{array} \tag{1.18}$$

1.3.2 Rotation of the reference frame

Let us consider two reference frames $\{0; x_1, x_2, x_3\}$ and $\{0; x, y, z = x_3\}$ rotated by an angle ϑ around x_3, Fig. 1.1. The tensor rotating (x_1, x_2) into (x, y) is:

$$\mathbf{U} = \left[\begin{array}{ccc} \cos\vartheta & -\sin\vartheta & 0 \\ \sin\vartheta & \cos\vartheta & 0 \\ 0 & 0 & 1 \end{array} \right] \ . \tag{1.19}$$

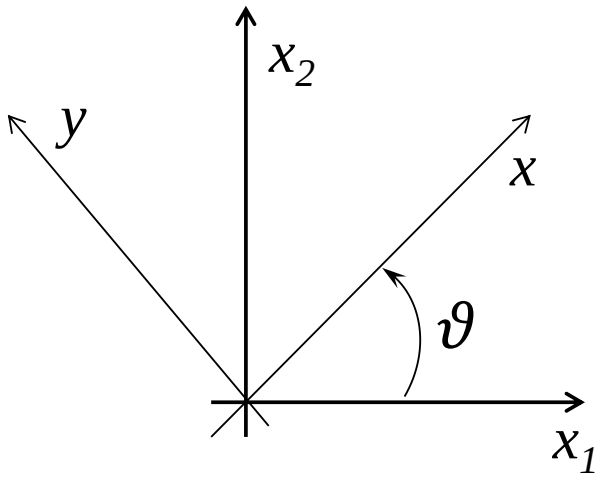

Figure 1.1: Principal and rotated reference systems.

If the components of the second order tensor $\boldsymbol{\sigma}$ are known in (x_1, x_2), its components in (x, y) are:

$$\boldsymbol{\sigma}' = \mathbf{U}^T \boldsymbol{\sigma}\ \mathbf{U}\ ; \tag{1.20}$$

in the matrix formulation we get

$$\{\sigma\}' = [T]\,\{\sigma\}\ , \tag{1.21}$$

where:

$$[T] = \begin{bmatrix} \cos^2\vartheta & \sin^2\vartheta & 2\sin\vartheta\cos\vartheta \\ \sin^2\vartheta & \cos^2\vartheta & -2\sin\vartheta\cos\vartheta \\ -\sin\vartheta\cos\vartheta & \sin\vartheta\cos\vartheta & \cos^2\vartheta - \sin^2\vartheta \end{bmatrix}\ . \tag{1.22}$$

is the rotation matrix.

For the strain tensor $\boldsymbol{\varepsilon}$, the transformation law of eq. (1.21) must be modified to take into account for the Voigt's notation:

$$\{\varepsilon\}' = [R]\,[T]^{-1}\,[R]^{-1}\,\{\varepsilon\}\ , \tag{1.23}$$

where:

$$[R] = \begin{bmatrix} 1 & 0 & 0 \\ 0 & 1 & 0 \\ 0 & 0 & 2 \end{bmatrix}\ , \tag{1.24}$$

is the Reuter matrix [33]. Because

$$[R]\,[T]^{-1}\,[R]^{-1} = \left([T]^T\right)^{-1}\ , \tag{1.25}$$

eq. (1.23) reads

$$\{\varepsilon\}' = \left([T]^T\right)^{-1}\{\varepsilon\}\ . \tag{1.26}$$

In matrix notation, the Hooke's law can be written in the frame (x, y) as follows:

$$\begin{array}{l} \{\sigma\} = [T]\,\{\sigma\}' \\ \{\varepsilon\} = [T]^T\,\{\varepsilon\}' \end{array} \implies [T]\,\{\sigma\}' = [Q]\,[T]^T\,\{\varepsilon\}'\ , \tag{1.27}$$

so:

$$\{\sigma\}' = [T]^{-1}\,[Q]\,[T]^{T}\,\{\varepsilon\}' \ . \tag{1.28}$$

The rotation law for the stiffness and compliance matrix is hence, respectively:

$$[Q]' = [T]^{-1}\,[Q]\,[T]^{T} \ ; \tag{1.29}$$

$$[S]' = \left([T]^{T}\right)^{-1}\,[S]\,[T] \ . \tag{1.30}$$

Eqs. (1.29) and (1.30) show that, when using the Cartesian representation for mechanical problems in plane anisotropy, the rotation laws increase the difficulties and make the solution more complicate to compute. This represents a major difficulty when dealing with the design problems of laminates. The orientation angles of the layers, normally the design variables, appears in the governing equations as arguments of fourth power of circular functions. It is, hence, interesting to see if an alternatively and more effective representation of tensors of anisotropy is available.

1.4 The polar method

A plane tensor representation, more effective for design problems, is the polar method introduced by Verchery [86] in 1979. His original work was focused on the representation of a fourth-order tensor of the elasticity type. There are several advantages in using the polar method; first of all, it is based on the use of invariants having a physical meaning (they have a direct link with the elastic symmetries) and secondly, the rotation of the frame is done in an easier way than with the Cartesian representation, [77].

The polar method is based upon a complex variable transformation that renders particularly simple to find the tensors invariants. We will not enter in its algebraic details that can be found in [77, 84] and more extensively in [76]. In the following, we will recall only the most important results, used in this thesis, of the polar method.

1.4.1 Representation of a second order tensor

Let us consider the second order tensor of Cauchy's stresses $\boldsymbol{\sigma}$ in the plane (x_1, x_2). The Cartesian components can be replaced by the polar ones (T, R, Φ):

$$\begin{cases} T = & \dfrac{\sigma_{11} + \sigma_{22}}{2} \ , \\ Re^{2i\Phi} = & \dfrac{\sigma_{11} - \sigma_{22}}{2} + i\sigma_{12} \ , \end{cases} \tag{1.31}$$

while the inverse law is

$$\begin{cases} \sigma_{11} = & T + & R\cos 2\Phi \ , \\ \sigma_{22} = & T - & R\cos 2\Phi \ , \\ \sigma_{12} = & & R\sin 2\Phi \ . \end{cases} \tag{1.32}$$

The polar parameters T and R are invariants, whereas the polar angle Φ gives the orientation, with respect to the reference system where the components σ_{ij}, of the first principal component of $\boldsymbol{\sigma}$ and is hence, frame dependent. T is linked to the spherical part of $\boldsymbol{\sigma}$, whereas $Re^{2i\Phi}$ to the deviatoric one, as it is apparent from eq. (1.31). The relations (1.31) and (1.32) expressed for the stress tensor $\boldsymbol{\sigma}$ are, of course, valid for any other second order

symmetric tensor.
In particular, the polar parameters associated to the second order strain tensor $\boldsymbol{\varepsilon}$ will be denoted by: t, r and ϕ.

1.4.2 Representation of a fourth order tensor of the elasticity type

Let us consider the fourth order stiffness tensor $\mathbf{Q}$ in the plane (x_1, x_2). The Cartesian components can be expressed by the polar ones $(T_0, T_1, R_0, R_1, \Phi_0, \Phi_1)$:

$$\left\{\begin{array}{llllll} 8T_0 & = Q_{1111} & -2Q_{1122} & +4Q_{1212} & & +Q_{2222}\ , \\ 8T_1 & = Q_{1111} & +2Q_{1122} & & & +Q_{2222}\ , \\ 8R_0e^{4i\Phi_0} & = Q_{1111} +4iQ_{1112} & -2Q_{1122} & -4Q_{1212} & -4iQ_{1222} & +Q_{2222}\ , \\ 8R_1e^{2i\Phi_1} & = Q_{1111} +2iQ_{1112} & & & +2iQ_{1222} & -Q_{2222}\ , \end{array}\right. \tag{1.33}$$

and inversely the Cartesian components can be given in terms of polar components:

$$\left\{\begin{array}{llllll} Q_{1111} = & T_0+ & 2T_1+ & R_0\cos 4\Phi_0+ & 4R_1\cos 2\Phi_1\ , \\ Q_{1112} = & & & R_0\sin 4\Phi_0+ & 2R_1\sin 2\Phi_1\ , \\ Q_{1122} = & -T_0+ & 2T_1- & R_0\cos 4\Phi_0 & \ , \\ Q_{1212} = & T_0- & & R_0\cos 4\Phi_0 & \ , \\ Q_{2212} = & & - & R_0\sin 4\Phi_0+ & 2R_1\sin 2\Phi_1\ , \\ Q_{2222} = & T_0+ & 2T_1+ & R_0\cos 4\Phi_0- & 4R_1\cos 2\Phi_1\ . \end{array}\right. \tag{1.34}$$

The polar moduli T_0, T_1, R_0, R_1 and the difference of the polar angles $\Phi_0 - \Phi_1$, are invariants. Finally, fixing one of the polar angles, corresponds to fixing a reference frame. Usually, and in the following of this thesis we will do the same. For instance, $\Phi_1 = 0$ corresponds, for an unidirectionally reinforced layer, to align the axis x_1 along the fibres.

The above representation can be, of course, applied to any other in-plane fourth order elasticity-like tensor, for instance the in-plane compliance tensor $\mathbf{S}$, whose polar parameter will be denoted by $t_0, t_1, r_0, r_1, \phi_0, \phi_1$.

1.4.3 Rotation of the reference system

The polar components of the second order tensor $\boldsymbol{\sigma}$, when passing from the frame $\{0; x_1, x_2, x_3\}$ to $\{0; x, y, z = x_3\}$ rotated of an angle ϑ, see Fig. 1.1, change as follows:

$$T, R, \Phi \quad \text{in} \quad \{0; x_1, x_2, x_3\} \longrightarrow T, R, \Phi - \vartheta \quad \text{in} \quad \{0; x, y, z\}\ . \tag{1.35}$$

As a consequence, the Cartesian components of $\boldsymbol{\sigma}$, in the frame $\{0; x, y, z\}$, are:

$$\left\{\begin{array}{llll} \sigma_{xx} = & T+ & R\cos 2(\Phi - \vartheta)\ , \\ \sigma_{yy} = & T- & R\cos 2(\Phi - \vartheta)\ , \\ \sigma_{xy} = & & R\sin 2(\Phi - \vartheta)\ . \end{array}\right. \tag{1.36}$$

In the same way, the polar components of tensor $\mathbf{Q}$ change, passing from the frame $\{0; x_1, x_2, x_3\}$ to $\{0; x, y, z\}$, as follows:

$$T_0, T_1, R_0, R_1, \Phi_0, \Phi_1 \quad \text{in} \quad \{0; x_1, x_2, x_3\} \longrightarrow T_0, T_1, R_0, R_1, \Phi_0 - \vartheta, \Phi_1 - \vartheta \quad \text{in} \quad \{0; x, y, z\}\ . \tag{1.37}$$

The Cartesian components of $\mathbf{Q}$, in the frame $\{0; x, y, z\}$ are:

$$\begin{cases} Q_{xxxx} = & T_0 + & 2T_1 + & R_0 \cos 4(\Phi_0 - \vartheta) + & 4R_1 \cos 2(\Phi_1 - \vartheta) \ , \\ Q_{xxxy} = & & & R_0 \sin 4(\Phi_0 - \vartheta) + & 2R_1 \sin 2(\Phi_1 - \vartheta) \ , \\ Q_{xxyy} = & -T_0 + & 2T_1 - & R_0 \cos 4(\Phi_0 - \vartheta) & \ , \\ Q_{xyxy} = & T_0 - & & R_0 \cos 4(\Phi_0 - \vartheta) & \ , \\ Q_{yyxy} = & & - & R_0 \sin 4(\Phi_0 - \vartheta) + & 2R_1 \sin 2(\Phi_1 - \vartheta) \ , \\ Q_{yyyy} = & T_0 + & 2T_1 + & R_0 \cos 4(\Phi_0 - \vartheta) - & 4R_1 \cos 2(\Phi_1 - \vartheta) \ . \end{cases} \tag{1.38}$$

The simplicity of the transformation laws of eqs. (1.38) with respect to eqs. (1.29) is evident.

1.5 Physical interpretation of polar invariants

Eqs. (1.38) show another very important peculiarity of the polar method: the moduli T_0 and T_1 represent the isotropic part of $\mathbf{Q}$, while R_0, R_1 and $\Phi_0 - \Phi_1$ represent its anisotropic part. So, the polar method allows for separating a tensor in its isotropic and anisotropic parts, which reveals to be very useful, under a mathematical point of view, when dealing with optimal design problems of laminates made by identical layers, see Sec. 1.6. Hereafter, we introduce two others physical meanings of the polar parameters: their energetic interpretation and their link with the elastic symmetries.

1.5.1 Energetic interpretation

The expression of the elastic energy density in terms of polar parameters is

$$W = \frac{1}{2}\boldsymbol{\sigma}\boldsymbol{\varepsilon} = Tt + Rr\cos 2(\Phi - \phi) \ . \tag{1.39}$$

The polar expression of the elastic energy density presents two separate quantities. The first one is composed by the spherical part of stresses and strains (Tt), while the second one by the deviatoric components of $\boldsymbol{\sigma}$ and $\boldsymbol{\varepsilon}$ ($Rr\cos 2(\Phi - \phi)$).
If we introduce the Hooke's law (1.16) in eq. (1.39), we get, using the relations (1.34), the elastic energy density in terms of $\mathbf{Q}$ and $\boldsymbol{\varepsilon}$, the so called strain energy:

$$W_s = 2T_0 r^2 + 4T_1 t^2 + 2R_0 r^2 \cos 4(\Phi_0 - \phi) + 8R_1 tr \cos 2(\Phi_1 - \phi) \ . \tag{1.40}$$

If we introduce the inverse of the Hooke's law (1.3) in eq. (1.39), we get, using the (1.34) written for the compliance tensor, the elastic energy density in terms of $\mathbf{S}$ and $\boldsymbol{\sigma}$, the so called complementary energy:

$$W_c = 2t_0 R^2 + 4t_1 T^2 + 2r_0 R^2 \cos 4(\phi_0 - \Phi) + 8r_1 TR \cos 2(\phi_1 - \Phi) \ . \tag{1.41}$$

The elastic energy density is an intrinsically positive quantity, for physical reasons: the mechanical work done to deform a body cannot be negative. By this fact, the strain energy gives the bounds on the moduli of an anisotropic material (see [55]); in terms of polar parameters, these bounds are reduced to only two:

$$\begin{aligned} &T_0 - R_0 > 0 \ , \\ &T_1(T_0^2 - R_0^2) - 2R_1^2[T_0 - R_0 \cos 4(\Phi_0 - \Phi_1)] > 0 \ . \end{aligned} \tag{1.42}$$

1.5.2 Elastic symmetries

The *orthotropy* symmetry in plane elasticity, for a material characterised by $R_0 \neq 0$ and $R_1 \neq 0$, is expressed in terms of polar components by the following invariant condition:

$$\Phi_0 - \Phi_1 = K\frac{\pi}{4}, \quad K = 0, 1 \ . \tag{1.43}$$

This condition, that intrinsically characterise the "ordinary orthotropy", shows that there are two types of orthotropy, for a given set of polar parameters T_0, T_1, R_0, R_1 depending on the value of K [77]: 0 and any other even value or 1 and any other odd value. K is an invariant too for an orthotropic material. It has been showed in several examples, see [75, 80, 88], that K plays a strange role in different optimisation problems. Actually, it is like a sort of switch, that transforms an optimal solution in an anti-optimal one, i.e. worst, when it switches from 0 to 1 and inversely. This fact, unknown before (Pedersen in [55], using the Tsai and Pagano invariants [72], realised a change in the shear stiffness that actually is linked to the value of K) is actually rather important because it affects very strongly the optimal solution.

The components of the fourth order orthotropic tensor $\mathbf{Q}$, expressed in a generic frame $\{0; x, y, z\}$, become:

$$\begin{cases} Q_{xxxx} = & T_0 + & 2T_1 + & (-1)^K R_0 \cos 4\Phi_1 + & 4R_1 \cos 2\Phi_1 \ , \\ Q_{xxxy} = & & & (-1)^K R_0 \sin 4\Phi_1 + & 2R_1 \sin 2\Phi_1 \ , \\ Q_{xxyy} = & -T_0 + & 2T_1 - & (-1)^K R_0 \cos 4\Phi_1 & \ , \\ Q_{xyxy} = & T_0 - & & (-1)^K R_0 \cos 4\Phi_1 & \ , \\ Q_{yyxy} = & & - & (-1)^K R_0 \sin 4\Phi_1 + & 2R_1 \sin 2\Phi_1 \ , \\ Q_{yyyy} = & T_0 + & 2T_1 + & (-1)^K R_0 \cos 4\Phi_1 - & 4R_1 \cos 2\Phi_1 \ . \end{cases} \tag{1.44}$$

The polar angle Φ_1 represents the direction of orthotropy and is frame dependent.

There are two other possible conditions, determining two special orthotropies:

1. R_0 orthotropy
$$R_0 = 0, \quad R_1 \neq 0 \ . \tag{1.45}$$
In this case only three polar invariants are sufficient to describe the material behaviour, see [76];

2. Square Orthotropy (the planar corresponding of the cubic symmetry)
$$R_1 = 0, \quad R_0 \neq 0 \ . \tag{1.46}$$
Also in this case only three polar invariants are sufficient to describe the material behaviour.

Finally, it is easy to see that isotropy corresponds to the condition:

$$R_0 = R_1 = 0 \ . \tag{1.47}$$

It is apparent, hence, that isotropy is the contemporary presence of the two special orthotropies.

Summarising, each elastic symmetry corresponds to the cancellation or to a precise value of the invariants: each invariant has a physical meaning directly linked to the symmetries and to the properties of the material. In particular, the orientation Φ_1 of the material symmetry and the type of orthotropy K are explicit terms of the tensors components, unlike the classical Cartesian representation.

1.6 The classical laminated plate theory

Unlike the case of homogeneous plates, where the design concerns mainly the thickness, the design of a laminate is much more complex: it depends upon several variables and multiple aspects, concerning its mechanical behaviour, must be taken into account. A laminate is a sort of complex structure, in the sense that its elastic behaviour can be different in extension and in bending and, in addition, these two behaviours can be coupled. When anisotropic layers are used, the design process must account for the elastic symmetries of the final plate. These considerations, developed in the following, let we quickly see that the optimal design of laminates is a difficult problem, with several aspects that need to be simultaneously considered.

The Classical Laminated Plate Theory (CLPT) is a mechanical model that, despite the well known diatribes on its mechanical consistence, has the property of precisely defining the tensors that describe the elastic response of the plate along with their elastic symmetries. That is why, it is a fundamental tool not only in analysis, but also in optimisation of laminated structures.

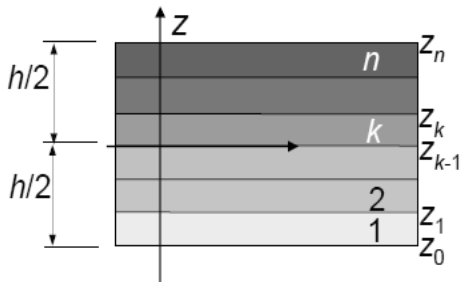

Figure 1.2: Sketch of the laminate layers and interfaces.

Let us consider a laminated plate made by a number n of plies laying in the plane (x, y) of a global frame, Fig. 1.2. Furthermore, each k^{th} ply is characterised by the position z_k of its top surface, its fibres' orientation δ_k with respect to the x axis (Fig. 1.3), its thickness h_k and its elastic properties defined by its in-plane reduced stiffness tensor $\mathbf{Q}(\delta_k)$.
The main assumptions of the CLPT are:

- linear elastic behaviour of the material;
- small displacements and deformations;
- Kirkhoff's kinematic model;
- plate's thickness, h, very small with respect to the other dimensions of the plate;
- perfect bonding between the plies.

The Kirkhoff's kinematic model leads to a strain field described by:

$$\boldsymbol{\varepsilon} = \boldsymbol{\varepsilon}_0 + z\boldsymbol{\chi} \ , \tag{1.48}$$

with

$$\boldsymbol{\varepsilon}_0 = \left\{ \begin{array}{c} \varepsilon_{xx} \\ \varepsilon_{yy} \\ 2\varepsilon_{xy} \end{array} \right\} \ , \quad \boldsymbol{\chi} = \left\{ \begin{array}{c} \chi_{xx} \\ \chi_{yy} \\ 2\chi_{xy} \end{array} \right\} . \tag{1.49}$$

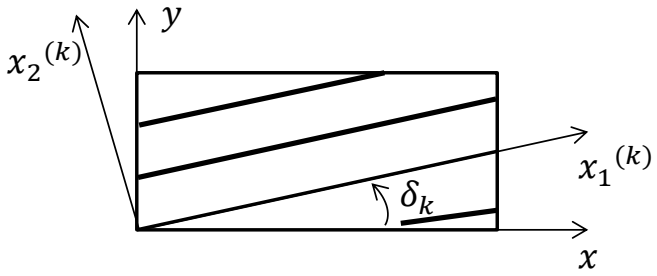

Figure 1.3: Global and local reference systems in the k^{th} ply of the laminated plate.

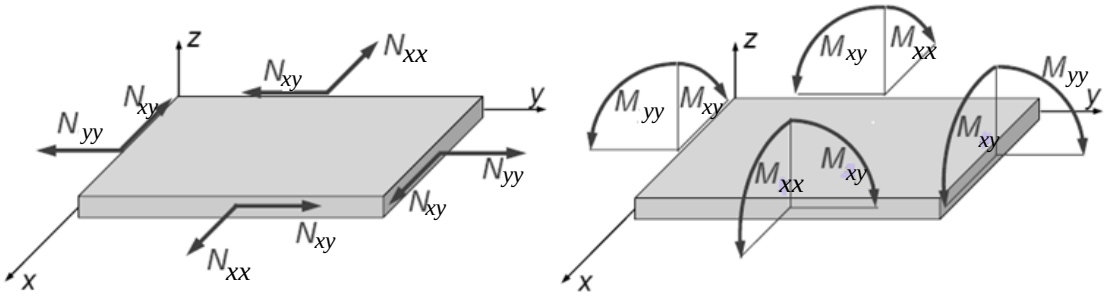

Figure 1.4: Internal forces of the plate.

$\boldsymbol{\varepsilon}_0$ and $\boldsymbol{\chi}$ are the in-plane strain and curvature tensors of the middle plane of the plate, respectively. Hence, in the CLPT the strain field is a *plane strain field*.

On the other side, the stress field $\boldsymbol{\sigma}$ linked to the strain field of eq. (1.48) is not plane. The out-of-plane component of $\boldsymbol{\sigma}$ are

$$\begin{aligned} \sigma_{yz} &= 0 \ , \\ \sigma_{xz} &= 0 \ , \\ \sigma_{zz} &\neq 0 \ . \end{aligned} \tag{1.50}$$

A further *assumption* in the CLPT, is hence:

$$\sigma_{zz} = 0 \ . \tag{1.51}$$

We can introduce the second order tensors $\mathbf{N}$ and $\mathbf{M}$ that represents respectively the in-plane forces and bending moments of the plate, see also Fig. 1.4:

$$\mathbf{N} = \int_{-h/2}^{h/2} \boldsymbol{\sigma} dz = \left\{ \begin{array}{c} N_{xx} \\ N_{yy} \\ N_{xy} \end{array} \right\} \ , \quad \mathbf{M} = \int_{-h/2}^{h/2} \boldsymbol{\sigma} z dz = \left\{ \begin{array}{c} M_{xx} \\ M_{yy} \\ M_{xy} \end{array} \right\} \ . \tag{1.52}$$

The CLPT provides the relations that link the internal forces of the plate with the strain field introduced beforehand:

$$\begin{aligned} \mathbf{N} &= \mathbf{A} \ \boldsymbol{\varepsilon}_0 + \mathbf{B} \ \boldsymbol{\chi} \ , \\ \mathbf{M} &= \mathbf{B} \ \boldsymbol{\varepsilon}_0 + \mathbf{D} \ \boldsymbol{\chi} \ . \end{aligned} \tag{1.53}$$

Eq. (1.53) shows that, in a laminate, the in-plane forces and bending moments depend on both the in-plane strains and the curvature of the middle plane of the plate. In other

words, *in a laminate there exist a coupling between in-plane forces and curvatures and between bending moments and in-plane strains*. Such effects are described by tensor **B**, the *membrane-bending coupling tensor*. On the other hand, tensors **A** and **D** characterise, respectively, the extension and bending stiffness of the homogenised laminated plate.

For a laminate composed by n plies, the expressions of **A**, **B** and **D** are:

$$\begin{aligned}
\mathbf{A} &= \sum_{k=-p}^{p} \mathbf{Q}_k\left(\delta_k\right)\left(z_k - z_{k-1}\right), \\
\mathbf{B} &= \frac{1}{2}\sum_{k=-p}^{p} \mathbf{Q}_k\left(\delta_k\right)\left(z_k^2 - z_{k-1}^2\right), \\
\mathbf{D} &= \frac{1}{3}\sum_{k=-p}^{p} \mathbf{Q}_k\left(\delta_k\right)\left(z_k^3 - z_{k-1}^3\right).
\end{aligned} \tag{1.54}$$

z_k and z_{k-1} represent the z coordinate of the bottom and top surface of the k^{th} ply; p is linked to the number of plies as follows, Fig. 1.2:

$$n = \begin{cases} 2p \text{ if even }, \\ 2p+1 \text{ if odd }. \end{cases} \tag{1.55}$$

Moreover, thanks to the symmetry of $\mathbf{Q}_k\left(\delta_k\right)$, also the tensors **A**, **B** and **D** are symmetric.

The composition laws (1.54) can be applied to any tensor representation, so to the polar formalism too. This, through some basic algebraic passages, lead us to introduce the polar parameters of **A**, **B** and **D** and their relation with the polar parameters of the plies that compose the laminate itself:

- polar parameters of **A**:

$$\begin{aligned}
T_0^A &= \sum_{k=-p}^{p} T_{0k}\left(z_k - z_{k-1}\right) \ , \\
T_1^A &= \sum_{k=-p}^{p} T_{1k}\left(z_k - z_{k-1}\right) \ , \\
R_0^A e^{4i\Phi_0^A} &= \sum_{k=-p}^{p} R_{0k} e^{4i(\Phi_{0k}+\delta_k)}\left(z_k - z_{k-1}\right) \ , \\
R_1^A e^{2i\Phi_1^A} &= \sum_{k=-p}^{p} R_{1k} e^{4i(\Phi_{1k}+\delta_k)}\left(z_k - z_{k-1}\right) \ ;
\end{aligned} \tag{1.56}$$

- polar parameters of **B**:

$$\begin{aligned}
T_0^B &= \frac{1}{2}\sum_{k=-p}^{p} T_{0k}\left(z_k^2 - z_{k-1}^2\right) \ , \\
T_1^B &= \frac{1}{2}\sum_{k=-p}^{p} T_{1k}\left(z_k^2 - z_{k-1}^2\right) \ , \\
R_0^B e^{4i\Phi_0^B} &= \frac{1}{2}\sum_{k=-p}^{p} R_{0k} e^{4i(\Phi_{0k}+\delta_k)}\left(z_k^2 - z_{k-1}^2\right) \ , \\
R_1^B e^{2i\Phi_1^B} &= \frac{1}{2}\sum_{k=-p}^{p} R_{1k} e^{4i(\Phi_{1k}+\delta_k)}\left(z_k^2 - z_{k-1}^2\right) \ ;
\end{aligned} \tag{1.57}$$

- polar parameters of $\mathbf{D}$:

$$\begin{aligned}
T_0^D &= \frac{1}{3}\sum_{k=-p}^{p} T_{0_k}\left(z_k^3 - z_{k-1}^3\right) \ , \\
T_1^D &= \frac{1}{3}\sum_{k=-p}^{p} T_{1_k}\left(z_k^3 - z_{k-1}^3\right) \ , \\
R_0^D e^{4i\Phi_0^D} &= \frac{1}{3}\sum_{k=-p}^{p} R_{0_k} e^{4i(\Phi_{0_k}+\delta_k)}\left(z_k^3 - z_{k-1}^3\right) \ , \\
R_1^D e^{2i\Phi_1^D} &= \frac{1}{3}\sum_{k=-p}^{p} R_{1_k} e^{4i(\Phi_{1_k}+\delta_k)}\left(z_k^3 - z_{k-1}^3\right) \ ;
\end{aligned} \tag{1.58}$$

In the above equations, T_{0_k}, T_{1_k}, R_{0_k}, R_{1_k}, Φ_{0_k} and Φ_{1_k} are the polar parameters of the k^{th} ply. Of course, the physical interpretations of the polar parameters of each one of the above tensors are completely analogue to those described in Sec. 1.5 for a generic anisotropic plate.
The tensors $\mathbf{A}$, $\mathbf{D}$ and $\mathbf{B}$ have the following dimensions:

$$[\mathbf{A}] = [\mathrm{F/L}] \ , [\mathbf{B}] = [\mathrm{F}] \ , [\mathbf{D}] = [\mathrm{F\ L}] \ . \tag{1.59}$$

Hence, such tensors cannot be directly compared. To circumvent this problem, the stiffness and coupling tensors of the CLPT are normalised, in order to have the same dimensions, in the following way:

$$\mathbf{A}^* = \frac{\mathbf{A}}{h} \ , \mathbf{B}^* = \frac{2\mathbf{B}}{h^2} \ , \mathbf{D}^* = \frac{12\mathbf{D}}{h^3} \ . \tag{1.60}$$

So, all the tensors share the same units, $[\mathrm{F/L^2}]$, and they express the elastic characteristics of a fictitious material constituting an *Equivalent Single Layer* (ESL) of the same thickness of the laminate.

We introduce, also, the so-called homogeneity tensor $\mathbf{C}$, expressing the difference between the membranal and bending behaviour of the plate:

$$\mathbf{C} = \mathbf{A}^* - \mathbf{D}^* \ . \tag{1.61}$$

Eqs. (1.56) to (1.58) are expressed in the most general case of a laminate composed by plies of different materials and thickness. Let us now consider a relevant case: that of a laminate composed by orthotropic layers that are all identical (i.e. same thickness and material). Then, choosing, as usually done, the material strong axis of k^{th} layer as the first axis , $x_1^{(k)}$, of the material frame of the layers, which correspond to putting $\Phi_1^{(k)} = 0$ (Fig. 1.3), eqs. (1.56) to (1.58) written directly for the normalised tensors and the components of $\mathbf{C}$, can be written as follows:

- polar parameters of $\mathbf{A}^*$:

$$\begin{aligned}
\overline{T}_0 &= T_0 \ , \\
\overline{T}_1 &= T_1 \ , \\
\overline{R}_0 e^{4i\overline{\Phi}_0} &= \frac{1}{n}(-1)^K R_0 \sum_{k=-p}^{p} e^{4i\delta_k} \ , \\
\overline{R}_1 e^{2i\overline{\Phi}_1} &= \frac{1}{n} R_1 \sum_{k=-p}^{p} e^{2i\delta_k} \ ;
\end{aligned} \tag{1.62}$$

- polar parameters of $\mathbf{B}^*$:

$$\begin{aligned}
&\widehat{T}_0 = 0 \ , \\
&\widehat{T}_1 = 0 \ , \\
&\widehat{R}_0 e^{4i\widehat{\Phi}_0} = \left(\frac{1}{n}\right)^2 (-1)^K R_0 \sum_{k=-p}^{p} b_k e^{4i\delta_k} \ , \\
&\widehat{R}_1 e^{2i\widehat{\Phi}_1} = \left(\frac{1}{n}\right)^2 R_1 \sum_{k=-p}^{p} b_k e^{2i\delta_k} \ ;
\end{aligned} \tag{1.63}$$

- polar parameters of $\mathbf{D}^*$:

$$\begin{aligned}
&\widetilde{T}_0 = T_0 \ , \\
&\widetilde{T}_1 = T_1 \ , \\
&\widetilde{R}_0 e^{4i\widetilde{\Phi}_0} = \left(\frac{1}{n}\right)^3 (-1)^K R_0 \sum_{k=-p}^{p} d_k e^{4i\delta_k} \ , \\
&\widetilde{R}_1 e^{2i\widetilde{\Phi}_1} = \left(\frac{1}{n}\right)^3 R_1 \sum_{k=-p}^{p} d_k e^{2i\delta_k} \ ;
\end{aligned} \tag{1.64}$$

- polar parameters of $\mathbf{C}$:

$$\begin{aligned}
&\breve{T}_0 = 0 \ , \\
&\breve{T}_1 = 0 \ , \\
&\breve{R}_0 e^{4i\overline{\Phi}_0} = \frac{1}{n^3}(-1)^K R_0 \sum_{k=-p}^{p} c_k e^{4i\delta_k} \ , \\
&\breve{R}_1 e^{2i\overline{\Phi}_1} = \frac{1}{n^3} R_1 \sum_{k=-p}^{p} c_k e^{2i\delta_k} \ .
\end{aligned} \tag{1.65}$$

In the previous equations, T_0, T_1, R_0, R_1, Φ_0 and Φ_1 are the polar parameters of the basic ply, while b_k, c_k and d_k are integer coefficients directly linked to the position k of each ply and to the total number n of the plies. In particular, we have

$$\begin{aligned}
n \ even: \quad & b_k = 2k - \frac{|k|}{k}, b_0 = 0 && ; \quad d_k = 12k^2 - 12|k| + 4, d_0 = 0 \quad ; \\
& c_k = 4p^2 - 12k^2 + 3|k| - 4, c_0 = 0 \\
n \ odd: \quad & b_k = 2k && ; \quad d_k = 12k^2 + 1 \quad ; \\
& c_k = 4p^2 + 4p - 12k^2
\end{aligned} \tag{1.66}$$

Thanks to eq. (1.66) is possible to verify that it is:

$$\sum_{k=-p}^{p} b_k = 0 \ , \ \sum_{k=-p}^{p} c_k = 0 \ , \ \sum_{k=-p}^{p} d_k = n^3 \ . \tag{1.67}$$

Eqs. (1.62) to (1.65) show something which is relevant in the optimisation problems of laminates. In fact, the separation between the isotropic and anisotropic parts is not only still existing, also for the laminate tensors, but more important, one can see that each one of the polar parameters of a laminate tensor depends only upon the corresponding polar parameter of the basic layer. In particular:

- the isotropic part of the tensors $\mathbf{B}^*$ and $\mathbf{C}$ are null: these two tensors are purely anisotropic (they have a null mean);
- the isotropic part of the tensors $\mathbf{A}^*$ and $\mathbf{D}^*$ are equal and the same of the basic layer; so, in a stack of identical layers only the anisotropic part can be tailored, but not the isotropic one; in other words, the isotropic polar parameters of a laminate composed of identical layers do not enter into the optimisation procedure, if the basic layer is chosen a priori, only the anisotropic part of $\mathbf{A}^*$ and $\mathbf{D}^*$ can be optimised.

There is, also, another aspect that needs to be emphasised: the concept of *quasi-homogeneity*. A laminate for which

$$\begin{aligned} \mathbf{B} &= 0 \ , \\ \mathbf{C} &= 0 \ . \end{aligned} \tag{1.68}$$

is said to be *quasi-homogeneous*, see [76].
For laminates composed by identical layers, $\mathbf{B}$ is null if, see (1.63):

$$\begin{aligned} \sum_{k=-p}^{p} b_k e^{4i\delta_k} &= 0 \ , \\ \sum_{k=-p}^{p} b_k e^{2i\delta_k} &= 0 \ , \end{aligned} \tag{1.69}$$

whilst $\mathbf{C}$ is null if, see (1.65):

$$\begin{aligned} \sum_{k=-p}^{p} c_k e^{4i\delta_k} &= 0 \ , \\ \sum_{k=-p}^{p} c_k e^{2i\delta_k} &= 0 \ . \end{aligned} \tag{1.70}$$

From a mechanical point of view, conditions (1.68) mean that the membrane and bending behaviour of a laminate are completely uncoupled and the membrane and bending stiffness tensors are identical. In other words, a quasi-homogeneous laminate behaves just like a plate composed by a unique equivalent layer, i.e. just like an homogeneous, but not necessary isotropic, plate.

1.6.1 Bounds on the laminate polar parameters

Tensors $\mathbf{A}^*$ and $\mathbf{D}^*$, as any other elasticity tensor, must be positive definite, hence, their polar parameters must satisfy conditions (1.42). Taking into account eq. (1.62), these conditions are for $\mathbf{A}^*$

$$\begin{aligned} &T_0 - \overline{R}_0 > 0 \ , \\ &T_1(T_0^2 - \overline{R}_0^2) - 2\overline{R}_1^2[T_0 - \overline{R}_0 \cos 4(\Phi_0 - \Phi_1)] > 0 \ . \end{aligned} \tag{1.71}$$

Similar conditions holds for $\mathbf{D}^*$ too. Nevertheless, it can be proved that these bounds can never be attained by the polar parameters of $\mathbf{A}^*$ and $\mathbf{D}^*$. In fact, when a laminate is composed by identical plies, eqs. (1.62) and (1.64) impose other bounds on the values of the polar parameters of $\mathbf{A}^*$ and $\mathbf{D}^*$. Such bound are named *geometric bounds* and it can be shown that they are always more restrictive than the elastic bounds (1.71), see [81].

In order to determine the polar parameters that correspond to a manufacturable laminate, the geometrical bounds cannot be violated. In the case of an orthotropic laminate composed by identical orthotropic plies, the geometric bounds for $\mathbf{A}^*$ are:

$$\begin{aligned} &2\left(\frac{\overline{R}_1}{R_1}\right)^2 - 1 \leq \frac{(-1)^{\overline{K}}\overline{R}_0}{(-1)^K R_0} \ , \\ &|(-1)^{\overline{K}}\overline{R}_0| \leq R_0 \ , \\ &\overline{R}_1 \geq 0 \ . \end{aligned} \tag{1.72}$$

Similar bounds holds for $\mathbf{D}^*$ too. In some sense, laminates constitute an elastic sub-class, smaller than that of elastic materials.

1.7 Concluding remarks

We have inroduced in this Chapter the polar formalism and its application to the CLPT. Some peculiarities of this method have also been introduced; they will reveal particularly useful in the followings Chapters, in the optimisation process. The polar method can be applied to different tensors, see [79, 84]. It will be used, in this thesis, to obtain an invariant form for some well known strength criteria of anisotropic layers.

2

Failure criteria in plane anisotropy

2.1 Introduction

Anisotropy influences strongly also the mechanical strength of a material, usually described by a *failure criterion*. The aim of a failure criterion is the evaluation of the *limit load* that the structure can tolerate before the failure arises. We can separate the failure criteria into two distinct classes: the phenomenological failure criteria [23, 28, 71, 73] and the physically-based failure criteria [58]. The phenomenological failure criteria are called in this way because, through the computation of a scalar indicator, the *failure index*, the occurrence of the failure is checked; in this case, an unique scalar condition has to be verified. Nevertheless, no indication is given about the mechanism of failure that has been activated. On the contrary, physically-based failure criteria check separately multiple failure mechanisms. In these criteria the different failure mechanisms are considered as independent and non-interacting phenomena and, so, the uniqueness of the failure index is lost.

Several failure criteria have been developed for composites materials, see [62]. The deepest assessment of failure criteria for composite laminates has been done in the World Wide Failure Exercise (WWFE) proposed by Hinton, Soden and Kaddour in 1998 [25–27]. It is important to note that all these failure criteria are "ply-level failure criteria", thus, when used to analyse the failure of laminated structures, such criteria are applied to each ply composing the structure determining the so-called *first-ply-failure*.

In the following sections we will present a detailed description of some phenomenological failure criteria. We will present the Tsai-Hill, Hoffman, Tsai-Wu and Zhang-Evans criteria. All of them are conceived for orthotropic plies. The Voigt's notation will be used in the material frame $\{0; x_1, x_2, x_3\}$, with the x_1 and x_2 axes lying in the plane of the layer.

2.2 Stress-based polynomial failure criteria

2.2.1 Tsai-Hill failure criterion

The Hill [23] yield criterion for orthotropic metals in the 3D space is:

$$\begin{gathered}(G+H)\sigma_1^2 + (F+H)\sigma_2^2 + (F+G)\sigma_3^2 - 2H\sigma_1\sigma_2 - \\ 2G\sigma_1\sigma_3 - 2F\sigma_2\sigma_3 + 2L\sigma_4^2 + 2M\sigma_5^2 + 2N\sigma_6^2 \leq 1 \ .\end{gathered} \tag{2.1}$$

The terms F, G, H, L, M and N are the strength parameters of Hill; they are linked to the limit values of the stresses, corresponding to yielding for ductile materials and to fracture for fragile materials. The fundamental assumption of the Hill criterion is that the strength properties of the material are identical in tension and compression, as it is usually the case of anisotropic metals. The following strength properties are introduced:

- X, strength along the direction x_1;
- Y, strength along the direction x_2;
- Z, strength along the direction x_3;
- S_{12}, S_{23}, S_{31}, shear strengths.

The relation between the Hill's parameters F, G, H, L, M, N of eq. (2.1) and the strength properties of the material are determined considering uniaxial loading cases.

For instance, if one considers the following stress state:

$$\begin{cases} \sigma_i = 0 \quad i = 1,2,3,4,5 \ , \\ \sigma_6 \neq 0 \ ; \end{cases} \tag{2.2}$$

the failure will arise when $2N\sigma_6^2 = 1$ with $\sigma_6 = S_{12}$ and we get:

$$N = \frac{1}{2S_{12}^2} \ . \tag{2.3}$$

If we do the same thing with every stress component, finally we obtain:

$$\begin{gathered} 2N = \frac{1}{S_{12}^2}, \ 2M = \frac{1}{S_{31}^2}, \ 2L = \frac{1}{S_{23}^2}, \\ 2H = \frac{1}{X^2} + \frac{1}{Y^2} - \frac{1}{Z^2}, \ 2G = \frac{1}{X^2} - \frac{1}{Y^2} + \frac{1}{Z^2}, \ 2F = -\frac{1}{X^2} + \frac{1}{Y^2} + \frac{1}{Z^2} \ . \end{gathered} \tag{2.4}$$

Hence eq. (2.1) can be written as follows:

$$\begin{aligned} F_{Hill} = \ & \left(\frac{\sigma_1}{X}\right)^2 + \left(\frac{\sigma_2}{Y}\right)^2 + \left(\frac{\sigma_3}{Z}\right)^2 - \left(\frac{1}{X^2} + \frac{1}{Y^2} - \frac{1}{Z^2}\right)\sigma_1\sigma_2 - \left(\frac{1}{X^2} + \frac{1}{Z^2} - \frac{1}{Y^2}\right)\sigma_1\sigma_3 - \\ & + \left(\frac{1}{Y^2} + \frac{1}{Z^2} - \frac{1}{X^2}\right)\sigma_2\sigma_3 + \left(\frac{\sigma_4}{S_{23}}\right)^2 + \left(\frac{\sigma_5}{S_{13}}\right)^2 + \left(\frac{\sigma_6}{S_{12}}\right)^2 \leq 1 \ . \end{aligned} \tag{2.5}$$

Tsai elaborated the criterion of Hill adapting it to the case of orthotropic composite sheets. In the case of plane stress state, condition (1.12) must be added to the formulation of the criterion.

For a sheet of a composite material which is always manufactured from a transversally isotropic material, we have:

$$Z = Y, \tag{2.6}$$

and we can denote $S_{12} = S$. Eq. (2.5) becomes, then:

$$F_{Hill} = \left(\frac{\sigma_1}{X}\right)^2 + \left(\frac{\sigma_2}{Y}\right)^2 - \frac{\sigma_1\sigma_2}{X^2} + \left(\frac{\sigma_6}{S}\right)^2 \leq 1 \ , \tag{2.7}$$

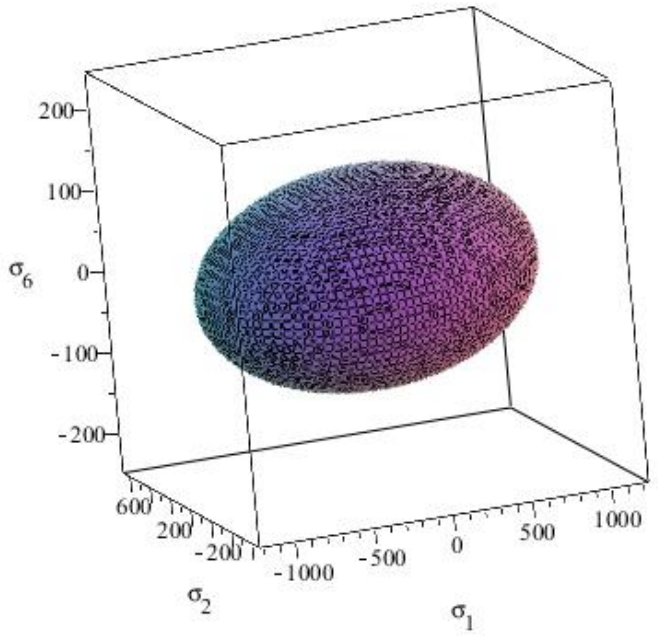

Figure 2.1: Limit surface of stresses obtained through the Tsai-Hill's criterion.

that represents the Tsai-Hill criterion for orthotropic sheets subject to plane stress state. In Fig. 2.1 is shown the corresponding graphical interpretation in the space $(\sigma_1, \sigma_2, \sigma_6)$ of the Tsai-Hill's failure criterion (2.7) for a generic E-Glass Epoxy orthotropic ply, whose strength properties are $X = 1080$ MPa, $Y = 39$ MPa and $S = 89$ MPa. This surface is an ellipsoid centered in the origin of the axes because of the assumption of identical strength behaviour in tension and compression.

It is possible, also, to write the criterion in matrix notation:

$$F_{Hill} = \{\sigma\}^T [F] \{\sigma\} \leq 1 \ , \tag{2.8}$$

with:

$$\{\sigma\} = \begin{Bmatrix} \sigma_1 \\ \sigma_2 \\ \sigma_6 \end{Bmatrix} , [F] = \begin{bmatrix} \frac{1}{X^2} & -\frac{1}{2X^2} & 0 \\ -\frac{1}{2X^2} & \frac{1}{Y^2} & 0 \\ 0 & 0 & \frac{1}{S^2} \end{bmatrix} \ . \tag{2.9}$$

2.2.2 Hoffman failure criterion

The formulation of the Hoffman criterion for orthotropic materials is [28]:

$$\begin{gathered} C_1(\sigma_2 - \sigma_3)^2 + C_2(\sigma_3 - \sigma_1)^2 + C_3(\sigma_1 - \sigma_2)^2 + \\ C_4\sigma_1 + C_5\sigma_2 + C_6\sigma_3 + C_7\sigma_4^2 + C_8\sigma_5 + C_9\sigma_6^2 \leq 1 \ . \end{gathered} \tag{2.10}$$

The failure criterion of Hoffman is a generalisation of the Hill's criterion, in which the difference of the strength properties in tension and compression is taken into account. The relation between the parameters C_1, C_2,...,C_9 and the strength properties of the

material can be obtained using a method similar to that used for the Tsai-Hill's criterion (i.e. uniaxial loading cases):

$$2C_1 = -\frac{1}{X_t X_c} + \frac{1}{Y_t Y_c} + \frac{1}{Z_t Z_c},\ \ 2C_2 = \frac{1}{X_t X_c} - \frac{1}{Y_t Y_c} + \frac{1}{Z_t Z_c},\ \ 2C_3 = \frac{1}{X_t X_c} + \frac{1}{Y_t Y_c} - \frac{1}{Z_t Z_c}$$
$$C_4 = \frac{1}{X_t} - \frac{1}{X_c},\ \ C_5 = \frac{1}{Y_t} - \frac{1}{Y_c},\ \ C_6 = \frac{1}{Z_t} - \frac{1}{Z_c},\ \ C_7 = \frac{1}{S_{23}^2},\ \ C_8 = \frac{1}{S_{31}^2},\ \ C_9 = \frac{1}{S_{12}^2}\ . \tag{2.11}$$

where the subscripts t and c stand for tension and compression.

In the case of plane stress state, condition (1.12) must be added to the formulation of the criterion and in addition, we have also, for a sheet manufactured from transversally isotropic material:

$$Z_t = Y_t,\ \ Z_c = Y_c, \tag{2.12}$$

and we can denote $S_{12} = S$.

It is possible to write the criterion in matrix notation:

$$F_{Hoff} = \{\sigma\}^T [F] \{\sigma\} + \{\sigma\}^T \{f\} \leq 1\ . \tag{2.13}$$

with:

$$[F] = \begin{bmatrix} \frac{1}{X_t X_c} & -\frac{1}{2X_t X_c} & 0 \\ -\frac{1}{2X_t X_c} & \frac{1}{Y_t Y_c} & 0 \\ 0 & 0 & \frac{1}{S^2} \end{bmatrix}, \{f\} = \begin{Bmatrix} \frac{X_c - X_t}{X_t X_c} \\ \frac{Y_c - Y_t}{Y_t Y_c} \\ 0 \end{Bmatrix}\ . \tag{2.14}$$

In Fig. 2.2 is shown the graphic interpretation in space $(\sigma_1, \sigma_2, \sigma_6)$ of the Hoffman's failure criterion (2.13) for the generic E-Glass Epoxy orthotropic ply whose strength properties are given in Tab. 2.1. This surface is still an ellipsoid but no more centered in the origin of the axis because of the assumption of different strength properties in tension and compression.

X_t	X_c	Y_t	Y_c	S
1080	620	39	128	89

Table 2.1: Strength properties of a generic E-Glass Epoxy lamina, [MPa].

2.2.3 Tsai-Wu failure criterion

The Tsai-Wu criterion [73], is:

$$F_{ij}\sigma_i\sigma_j + f_i\sigma_i \leq 1\ ; \tag{2.15}$$

where $i, j = 1, ..., 6$. The failure criterion of Tsai-Wu is conceived, differently from those of Tsai-Hill and Hoffman, for a completely anisotropic material. The difference of the strength for tension and compression is taken into account. In the original formulation of the criterion no one of the components of F_{ij} and f_i are neglected, but, the determination of these components has never been done. Nevertheless, if a material presents elastic

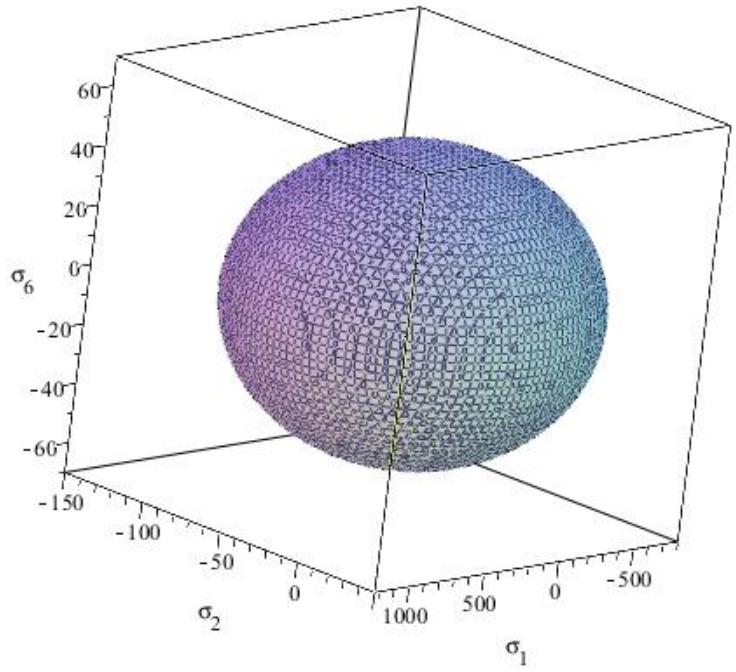

Figure 2.2: Limit surface of stresses obtained through the Hoffman's criterion.

symmetries, some terms of F_{ij} or f_i will be equal to zero.
In the case of an orthotropic layer and of plane stress state, the criterion becomes:

$$F_{11}\sigma_1^2 + F_{22}\sigma_2^2 + F_{66}\sigma_6^2 + 2F_{12}\sigma_1\sigma_2 + f_1\sigma_1 + f_2\sigma_2 \leq 1 \ , \tag{2.16}$$

where $i, j = 1, 2, 6$. The relations between the terms F_{ii} and f_i and the strength properties of the material X_t, X_c, Y_t, Y_c and S, are obtained through a procedure similar to the one adopted for the two previous criteria:

$$\begin{gathered} F_{11} = \frac{1}{X_t X_c}, \quad F_{22} = \frac{1}{Y_t Y_c}, \quad F_{66} = \frac{1}{S^2}, \\ f_1 = \frac{X_c - X_t}{X_t X_c}, \quad f_2 = \frac{Y_c - Y_t}{Y_t Y_c} \ . \end{gathered} \tag{2.17}$$

However, in the Tsai-Wu's criterion the term F_{12} is determined through a bi-axial test; if, for example, it is $\sigma_1 = \sigma_2 = \sigma$ and $\sigma_6 = 0$, then we get:

$$F_{12} = \frac{1}{2\sigma^2}\left[1 - \left(\frac{1}{X_t} + \frac{1}{X_c} + \frac{1}{Y_t} + \frac{1}{Y_c}\right)\sigma + \left(\frac{1}{X_t X_c} + \frac{1}{Y_t Y_c}\right)\sigma^2\right] \ ; \tag{2.18}$$

where the dependence on the value of the applied loading cannot be removed. Often, for composite materials F_{12} is written as:

$$F_{12} = \frac{F_{12}^*}{\sqrt{X_t X_c Y_t Y_c}} \ , \tag{2.19}$$

where the term F_{12}^* can take a value belonging to the range $[-1, 1]$, see [39]. The extreme values of this range are calculated through the condition:

$$F_{ii}F_{jj} - F_{ij} \geq 0 \ , \tag{2.20}$$

imposed on the components F_{ij} in [73] in order to ensure the failure envelope to be a closed surface. The criterion in matrix notation reads like:

$$F_{TW} = \{\sigma\}^T [F] \{\sigma\} + \{\sigma\}^T \{f\} \leq 1 \ , \tag{2.21}$$

where, for orthotropic layers it is:

$$[F] = \begin{bmatrix} \dfrac{1}{X_t X_c} & \dfrac{F_{12}^*}{\sqrt{X_t X_c Y_t Y_c}} & 0 \\ \dfrac{F_{12}^*}{\sqrt{X_t X_c Y_t Y_c}} & \dfrac{1}{Y_t Y_c} & 0 \\ 0 & 0 & \dfrac{1}{S^2} \end{bmatrix} \ ; \ \{f\} = \begin{Bmatrix} \dfrac{X_c - X_t}{X_t X_c} \\ \dfrac{Y_c - Y_t}{Y_t Y_c} \\ 0 \end{Bmatrix} \ . \tag{2.22}$$

Eq. (2.20) represents also a necessary, but not sufficient, condition for the positive definiteness of the matrix $[F]$.

2.3 Stress-based polynomial failure criteria expressed in terms of strains

The phenomenological criteria of Tsai-Hill, Hoffman and Tsai-Wu have been derived primarily in terms of stresses. There exists also an equivalent form of these criteria expressed in the strain space. It is worth noting, however, that such equivalent forms do not represent strain-based criteria for orthotropic materials. A fundamental assumption to write such criteria in the strain space is that of linear elastic behaviour of the material. Thanks to this assumption, the Hooke's law is used to express the stress-based criteria in terms of strains. The failure criteria of Tsai-Hill, Hoffman and Tsai-Wu, expressed in terms of strains, are introduced below.

2.3.1 Tsai-Hill failure criterion

The stress-based polynomial failure criterion of Tsai-Hill, under the assumption of plane stress state, is expressed in matrix notation by eq. (2.8). Injecting the Hooke's law (1.16) in (2.8), this last gives:

$$F_{Hill} = \{\varepsilon\}^T \left([Q]^T [F] [Q] \right) \{\varepsilon\} \leq 1 \ . \tag{2.23}$$

The double matrix product $[Q]^T [F] [Q]$ will be called in the rest of the thesis $[G]$ and denotes the matrix of strength properties of the stress-based failure criteria expressed in terms of strains as $[F]$ denotes the matrix of strength properties of the stress-based failure criteria expressed in terms of stresses. Hence we can write eq. (2.23) as:

$$F_{Hill} = \{\varepsilon\}^T [G] \{\varepsilon\} \leq 1 \ . \tag{2.24}$$

The components of the matrix $[G]$ are:

$$\begin{cases} G_{11} = & \dfrac{Q_{11}^2}{X^2} - \dfrac{Q_{11}Q_{12}}{X^2} + \dfrac{Q_{12}^2}{Y^2} \ , \\ G_{12} = & \dfrac{Q_{11}Q_{12}}{X^2} - \dfrac{Q_{11}Q_{22}}{2X^2} - \dfrac{Q_{12}^2}{2X^2} + \dfrac{Q_{12}Q_{22}}{Y^2} \ , \\ G_{16} = & 0 \ , \\ G_{22} = & \dfrac{Q_{12}^2}{X^2} - \dfrac{Q_{12}Q_{22}}{X^2} + \dfrac{Q_{22}^2}{Y^2} \ , \\ G_{26} = & 0 \ , \\ G_{66} = & \dfrac{Q_{66}^2}{S^2} \ ; \end{cases} \tag{2.25}$$

the components Q_{ij} in terms of the elastic properties, in the material frame, are:

$$[Q] = \begin{bmatrix} \dfrac{E_1}{1-\nu_{12}^2\dfrac{E_2}{E_1}} & \dfrac{\nu_{12}E_2}{1-\nu_{12}^2\dfrac{E_2}{E_1}} & 0 \\ \dfrac{\nu_{12}E_2}{1-\nu_{12}^2\dfrac{E_2}{E_1}} & \dfrac{E_2}{1-\nu_{12}^2\dfrac{E_2}{E_1}} & 0 \\ 0 & 0 & G_{12}^S \end{bmatrix} \ . \tag{2.26}$$

where E_i are the in-plane Young's moduli, G_{12}^S is the shear modulus and ν_{12} is the in-plane Poisson's ratio.

2.3.2 Hoffman failure criterion

Injecting in the stress-based polynomial failure criterion of Hoffman, written under the assumption of plane stress state, eq. (2.13), the Hooke's law (1.16), it gives:

$$F_{Hoff} = \{\varepsilon\}^T \left([Q]^T [F] [Q]\right) \{\varepsilon\} + \{\varepsilon\}^T [Q]^T \{f\} \leq 1 \ . \tag{2.27}$$

The matrix product $[Q]^T [F] [Q]$ is still called $[G]$, while the vector $[Q]^T \{f\}$ will be called $\{g\}$. So the previous equation can be written as:

$$F_{Hoff} = \{\varepsilon\}^T [G] \{\varepsilon\} + \{\varepsilon\}^T \{g\} \leq 1 \ . \tag{2.28}$$

In this case, the components of $[G]$ are:

$$\begin{cases} G_{11} = & \dfrac{Q_{11}^2}{X_t X_c} - \dfrac{Q_{11}Q_{12}}{X_t X_c} + \dfrac{Q_{12}^2}{Y_t Y_c} \ , \\ G_{12} = & \dfrac{Q_{11}Q_{12}}{X_t X_c} - \dfrac{Q_{11}Q_{22}}{2X_t X_c} - \dfrac{Q_{12}^2}{2X_t X_c} + \dfrac{Q_{12}Q_{22}}{Y_t Y_c} \ , \\ G_{16} = & 0 \ , \\ G_{22} = & \dfrac{Q_{12}^2}{X_t X_c} - \dfrac{Q_{12}Q_{22}}{X_t X_c} + \dfrac{Q_{22}^2}{Y_t Y_c} \ , \\ G_{26} = & 0 \ , \\ G_{66} = & \dfrac{Q_{66}^2}{S^2} \ ; \end{cases} \tag{2.29}$$

and the components of the vector $\{g\}$ are:

$$\{g\} = \begin{bmatrix} Q_{11}\dfrac{(X_c - X_t)}{X_t X_c} + Q_{12}\dfrac{(Y_c - Y_t)}{Y_t Y_c} \\ Q_{12}\dfrac{(X_c - X_t)}{X_t X_c} + Q_{22}\dfrac{(Y_c - Y_t)}{Y_t Y_c} \\ \\ 0 \end{bmatrix} . \tag{2.30}$$

The terms of Q_{ij} are defined in eq. (2.26).

2.3.3 Tsai-Wu failure criterion

Once again, substituting eq. (1.16) in eq. (2.21), the failure criterion of Tsai-Wu for a plane stress state gives:

$$F_{TW} = \{\varepsilon\}^T \left([Q]^T [F] [Q]\right) \{\varepsilon\} + \{\varepsilon\}^T [Q]^T \{f\} \leq 1 . \tag{2.31}$$

The above equation can still be written as eq. (2.28), but the components of the matrix $[G]$ are now:

$$\begin{cases} G_{11} = \dfrac{Q_{11}^2}{X_t X_c} + 2Q_{11}Q_{12}\dfrac{F_{12}^*}{\sqrt{X_t X_c Y_t Y_c}} + \dfrac{Q_{12}^2}{Y_t Y_c} , \\ G_{12} = \dfrac{Q_{11}Q_{12}}{X_t X_c} + Q_{11}Q_{22}\dfrac{F_{12}^*}{\sqrt{X_t X_c Y_t Y_c}} - Q_{12}^2\dfrac{F_{12}^*}{\sqrt{X_t X_c Y_t Y_c}} + \dfrac{Q_{12}Q_{22}}{Y_t Y_c} , \\ G_{16} = 0 , \\ G_{22} = \dfrac{Q_{12}^2}{X_t X_c} - 2Q_{12}Q_{22}\dfrac{F_{12}^*}{\sqrt{X_t X_c Y_t Y_c}} + \dfrac{Q_{22}^2}{Y_t Y_c} , \\ G_{26} = 0 , \\ G_{66} = \dfrac{Q_{66}^2}{S^2} . \end{cases} \tag{2.32}$$

The vector $\{g\}$ is equal to that of the Hoffman failure criterion, eq. (2.30), and the terms of Q_{ij} are still defined in eq. (2.26).

2.4 Strain-based polynomial failure criterion of Zhang-Evans

Almost all of the failure criteria, existing in literature, are formulated in the stress space. Nevertheless, in some cases the yield strain value can be more appropriate to describe the failure of a continuum: for example in the case of an elastic perfectly plastic material wherein the quantity that determines uniquely the failure is the yield strain.

A strain-based phenomenological failure criterion for orthotropic materials has been developed by Zhang and Evans in 1988 [92]. It is based on the same quadratic approximation used by Tsai and Wu. The 2D strain-based failure criterion of Zhang and Evans is:

$$F_{ZE} = \{\varepsilon\}^T [P] \{\varepsilon\} + \{\varepsilon\}^T \{p\} \leq 1 . \tag{2.33}$$

Let us introduce the following terms:

- X_ε, longitudinal yield strain along the fibres orientation;
- Y_ε, transverse yield strain perpendicular to the fibres orientation;
- S_ε, pure shear yield strain .

The components P_{ii} and p_i are determined through uniaxial ultimate tensile, compressive and shear strain tests:

$$\begin{aligned} P_{11} &= \frac{1}{X_{\varepsilon_t} X_{\varepsilon_c}} \ , \qquad P_{22} = \frac{1}{Y_{\varepsilon_t} Y_{\varepsilon_c}} \ , \qquad P_{66} = \frac{1}{S_\varepsilon^2} \ , \\ p_1 &= \frac{X_{\varepsilon_c} - X_{\varepsilon_t}}{X_{\varepsilon_t} X_{\varepsilon_c}} \ , \quad p_2 = \frac{Y_{\varepsilon_c} - Y_{\varepsilon_t}}{Y_{\varepsilon_t} Y_{\varepsilon_c}} \ , \qquad p_6 = 0 \ . \end{aligned} \tag{2.34}$$

where the subscripts t and c stand for tension and compression. On the contrary, the determination of the interaction term P_{12} is achieved through a uniaxial stress test that generates a biaxial strain state:

$$P_{12} = \frac{1}{2S_{11}S_{12}} \left[\frac{1 - (S_{11}p_1 + S_{21}p_2)X_t}{X_t^2} - (S_{11}^2 P_{11} + S_{22}^2 P_{22}) \right] \ . \tag{2.35}$$

where S_{ij} are the components of the compliance tensor:

$$[S] = \begin{bmatrix} \dfrac{1}{E_1} & -\dfrac{\nu_{12}}{E_1} & 0 \\ -\dfrac{\nu_{12}}{E_1} & \dfrac{1}{E_2} & 0 \\ 0 & 0 & \dfrac{1}{G_{12}^S} \end{bmatrix} \ . \tag{2.36}$$

Considering eq. (2.36), eq. (2.35) becomes:

$$P_{12} = -\frac{E_1^2}{2\nu_{12}} \left\{ \frac{1}{X_t^2} - \frac{1}{X_t E_1} \left[\frac{X_{\varepsilon_c} - X_{\varepsilon_t}}{X_{\varepsilon_t} X_{\varepsilon_c}} - \frac{\nu_{12}(Y_{\varepsilon_c} - Y_{\varepsilon_t})}{Y_{\varepsilon_t} Y_{\varepsilon_c}} \right] - \frac{1}{E_1^2} \left(\frac{1}{X_{\varepsilon_t} X_{\varepsilon_c}} + \frac{\nu_{12}^2}{Y_{\varepsilon_t} Y_{\varepsilon_c}} \right) \right\} \ . \tag{2.37}$$

Differently from the term F_{12} of the Tsai-Wu's criterion, the term P_{12} of the Zhang-Evans criterion is loading independent. The test to determine the coupling term in a strain-based criterion is completely different and easier than the test necessary for a stress-based criterion. This aspect is very important and interesting from a practical point of view because the value of the admissible strains can be easily and precisely determined. In addition, eq. (2.37) shows a very important result: no experimental evaluations are needed to determine the value of the interacting term of the criterion, it can be determined analytically because it depends only upon the uniaxial yield strains, the uniaxial strengths, the Young's modulus and the Poisson's ratio of the material.

A deeper comparison between stress and strain-based failure criteria can be found in [93].

2.5 Unified matrix formulation

As mentioned previously, it is possible to write all the stress-based criteria in matrix notation. A peculiarity of the terms that compose the matrix $[F]$, for each criterion,

concerns the position of the strength properties: they all appear at the denominator. So, we can assert that $[F]$ in stress-based criteria describes, in some sense, the inverse of the strength of the material: the *weakness*. Hence, we can consider the matrix $[F]$ as the analogous, for what concerns strength, of the compliance matrix $[S]$; then, we will call $[F]$ the *weakness matrix*. The matrix $[F]$, and for consistency, the vector $\{f\}$ will be expressed in a frame rotated by an angle $\pi/2$ around x_3. In this way, we will have the matrix $[F]$ described in the new reference system $\{0; x, y, z = x_3\}$ with the x-axis coincident with the direction of maximum weakness. We can express the three criteria by the general condition

$$F_{...} = \{\sigma\}^T [F] \{\sigma\} + \{\sigma\}^T \{f\} \leq 1 \; ; \tag{2.38}$$

with:

$$[F] = \begin{bmatrix} F_{xx} & F_{xy} & 0 \\ F_{xy} & F_{yy} & 0 \\ 0 & 0 & F_{ss} \end{bmatrix}, \{f\} = \begin{Bmatrix} f_x \\ f_y \\ 0 \end{Bmatrix} \; . \tag{2.39}$$

The values of matrix and vectorial components for each criterion are reported in Tabs. 2.2 and 2.3.

	Tsai-Hill	Hoffman	Tsai-Wu
F_{xx}	$\frac{1}{Y^2}$	$\frac{1}{Y_t Y_c}$	$\frac{1}{Y_t Y_c}$
F_{xy}	$-\frac{1}{2X^2}$	$-\frac{1}{2X_t X_c}$	$\frac{F_{12}^*}{\sqrt{X_t X_c Y_t Y_c}}$
F_{yy}	$\frac{1}{X^2}$	$\frac{1}{X_t X_c}$	$\frac{1}{X_t X_c}$
F_{ss}	$\frac{1}{S^2}$	$\frac{1}{S^2}$	$\frac{1}{S^2}$

Table 2.2: Components of $[F]$ for the three criteria.

	Tsai-Hill	Hoffman	Tsai-Wu
f_x	0	$\frac{Y_c - Y_t}{Y_t Y_c}$	$\frac{Y_c - Y_t}{Y_t Y_c}$
f_y	0	$\frac{X_c - X_t}{X_t X_c}$	$\frac{X_c - X_t}{X_t X_c}$
f_s	0	0	0

Table 2.3: Components of $\{f\}$ for the three criteria.

On the other hand, concerning the stress-based failure criteria expressed in terms of strains, we can consider the matrix $[G]$ as the analogous, for what concerns strength, of the stiffness matrix $[Q]$; then, we will call $[G]$ the *strength matrix*. We will express $[G]$, and for consistency, the vector $\{g\}$ in the material frame $\{0; x_1, x_2, x_3\}$ with the x_1 axis coincident with the direction of maximum strength. The general matrix formulation, for the three criteria, is:

$$F_{...} = \{\varepsilon\}^T [G] \{\varepsilon\} + \{\varepsilon\}^T \{g\} \leq 1 \; . \tag{2.40}$$

The components of $[G]$ and $\{g\}$ are reported in Tables 2.4 and 2.5; they all are dimensionless quantities. This is correct, because such terms represents, in some sense, the yield strain properties, so they are dimensionless like strains.

	Tsai-Hill	Hoffman
G_{11}	$\frac{Q_{11}^2 - Q_{11}Q_{12}}{X^2} + \frac{Q_{12}^2}{Y^2}$	$\frac{Q_{11}^2 - Q_{11}Q_{12}}{X_tX_c} + \frac{Q_{12}^2}{Y_tY_c}$
G_{12}	$\frac{Q_{11}Q_{12}}{X^2} - \frac{Q_{11}Q_{22} + Q_{12}^2}{2X^2} + \frac{Q_{12}Q_{22}}{Y^2}$	$\frac{Q_{11}Q_{12}}{X_tX_c} - \frac{Q_{11}Q_{22} + Q_{12}^2}{2X_tX_c} + \frac{Q_{12}Q_{22}}{Y_tY_c}$
G_{22}	$\frac{Q_{12}^2}{X^2} - \frac{Q_{12}Q_{22}}{X^2} + \frac{Q_{22}^2}{Y^2}$	$\frac{Q_{12}^2}{X_tX_c} - \frac{Q_{12}Q_{22}}{X_tX_c} + \frac{Q_{22}^2}{Y_tY_c}$
G_{66}	$\frac{Q_{66}^2}{S^2}$	$\frac{Q_{66}^2}{S^2}$

	Tsai-Wu
G_{11}	$\frac{Q_{11}^2}{X_tX_c} + 2Q_{11}Q_{12}\frac{F_{12}^*}{\sqrt{X_tX_cY_tY_c}} + \frac{Q_{12}^2}{Y_tY_c}$
G_{12}	$\frac{Q_{11}Q_{12}}{X_tX_c} + \frac{(Q_{11}Q_{22} - Q_{12}^2)F_{12}^*}{\sqrt{X_tX_cY_tY_c}} + \frac{Q_{12}Q_{22}}{Y_tY_c}$
G_{22}	$\frac{Q_{12}^2}{X_tX_c} - 2Q_{12}Q_{22}\frac{F_{12}^*}{\sqrt{X_tX_cY_tY_c}} + \frac{Q_{22}^2}{Y_tY_c}$
G_{66}	$\frac{Q_{66}^2}{S^2}$

Table 2.4: Components of $[G]$ for the three criteria.

	Tsai-Hill	Hoffman	Tsai-Wu
g_1	0	$Q_{11}\frac{(X_c - X_t)}{X_tX_c} + Q_{12}\frac{(Y_c - Y_t)}{Y_tY_c}$	$Q_{11}\frac{(X_c - X_t)}{X_tX_c} + Q_{12}\frac{(Y_c - Y_t)}{Y_tY_c}$
g_2	0	$Q_{12}\frac{(X_c - X_t)}{X_tX_c} + Q_{22}\frac{(Y_c - Y_t)}{Y_tY_c}$	$Q_{12}\frac{(X_c - X_t)}{X_tX_c} + Q_{22}\frac{(Y_c - Y_t)}{Y_tY_c}$
g_6	0	0	0

Table 2.5: Components of $\{g\}$ for the three criteria.

	Zhang-Evans
P_{11}	$\frac{1}{X_{\varepsilon_t}X_{\varepsilon_c}}$
P_{12}	$-\frac{E_1^2}{2\nu_{12}}\left\{\frac{1}{X_t^2} - \frac{1}{X_tE_1}\left[\frac{X_{\varepsilon_c} - X_{\varepsilon_t}}{X_{\varepsilon_t}X_{\varepsilon_c}} - \frac{\nu_{12}(Y_{\varepsilon_c} - Y_{\varepsilon_t})}{Y_{\varepsilon_t}Y_{\varepsilon_c}}\right] - \frac{1}{E_1^2}\left(\frac{1}{X_{\varepsilon_t}X_{\varepsilon_c}} + \frac{\nu_{12}^2}{Y_{\varepsilon_t}Y_{\varepsilon_c}}\right)\right\}$
P_{22}	$\frac{1}{Y_{\varepsilon_t}Y_{\varepsilon_c}}$
P_{66}	$\frac{1}{S_\varepsilon^2}$

Table 2.6: Components of $[P]$ for the criterion of Zhang-Evans.

	Zhang-Evans
p_1	$\frac{X_{\varepsilon_c} - X_{\varepsilon_t}}{X_{\varepsilon_t} X_{\varepsilon_c}}$
p_2	$\frac{Y_{\varepsilon_c} - Y_{\varepsilon_t}}{Y_{\varepsilon_t} Y_{\varepsilon_c}}$
p_6	0

Table 2.7: Components of $\{p\}$ for the criterion of Zhang-Evans.

We can do similar considerations also for the strain-based failure criterion of Zhang-Evans

$$F_{ZE} = \{\varepsilon\}^T [P] \{\varepsilon\} + \{\varepsilon\}^T \{p\} \leq 1 \ . \tag{2.41}$$

$[P]$, for analogy, will be called the *strength matrix*. We will express $[P]$, and for consistency, the vector $\{p\}$ in the material frame $\{0; x_1, x_2, x_3\}$ with the x_1 axis coincident with the direction of maximum strength. The values of the matrix and vectorial components of the strain-based criterion are reported in Tables 2.6 and 2.7.

Finally, we have expressed all the phenomenological failure criteria in a general matrix notation. All the criteria are characterised by the sum of a quadratic and a linear term. To this purpose, we prefer, for the sake of conciseness, to write all the described criteria in a *unified matrix formulation*:

$$F_{...} = \{v\}^T [H] \{v\} + \{v\}^T \{h\} \leq 1 \ , \tag{2.42}$$

where $\{v\}$, depending on the considered criterion, corresponds to $\{\sigma\}$ or $\{\varepsilon\}$, $[H]$ corresponds to $[F]$, $[G]$ or $[P]$ and $\{h\}$ corresponds to $\{f\}$, $\{g\}$ or $\{p\}$.

2.6 Concluding remarks

We have dedicated this Chapter to the description of the strength of orthotropic layers. Unlike the stiffness description, the strength behaviour of an anisotropic material is not represented by a unique law, like the Hooke's law, but by several criteria. We have considered some phenomenological criteria, in particular, we have described the criteria used very often in the design of laminated structures: the polynomial failure criteria of Tsai-Hill, Hoffman, Tsai-Wu and the strain-based criterion of Zhang-Evans. Their application to the design of laminated structures corresponds to a ply-by-ply verification of the strength. The peculiarity of these criteria concerns their formulation, based upon a unique condition whose quadratic term is not linked to the elastic stiffness matrix, like for strain energy, but to a matrix describing the strength properties of the material. The unified matrix formulation of these criteria, given in this Chapter, will be the starting point to an invariant formulation of such criteria presented in Chapter 4.

3

A state of the art on the optimisation of anisotropic laminated structures

3.1 Introduction

The design of an anisotropic laminated structure depends, very often, upon a large number of design variables: the material properties, the orientation angle and the thickness of each ply, along with the number of constitutive layers. The mechanical properties of such a structure can vary considerably with these design variables; therefore, unlike the case of metallic structures, the design of the laminated ones must include the design of the material (the so called "meso-scale") as a crucial phase of the whole design procedure.

The works on optimisation of laminated structures go back to the 70s. Those works studied the maximisation of classical mechanical properties such as stiffness, eigenfrequencies, limit loads and so on. For a general overview on structural optimisation applied to anisotropic structures the reader is addressed to [1, 3, 5, 21].

In this Chapter we give a short overview on optimisation of laminates for what concerns the maximisation of stiffness and/or strength. This presentation is split into three main parts. The first one concerns the optimal material orientation, the second one the optimisation of the material parameters of the structure and the third one the lay-up optimal design. We briefly describe only the studies that inspired the research work of the present thesis, aware that there are also other important works on the same subject.

3.2 Optimal material orientation for orthotropic sheets

3.2.1 Maximising stiffness

The problem of maximising the global stiffness of an elastic structure can be formulated through the minimisation of a global quantity defined on the structure: the *compliance*. The compliance of a body, in elasticity, corresponds to the global work done by the external forces for the field of the displacements that are solution of the elastic problem. Being the compliance a global and not a local quantity, it is a global functional for the stiffness optimisation problem. The firsts works on the minimisation of strain energy, for anisotropic plies, attempted to reach only one goal, i.e. the determination of the optimal material orientation, [9, 10, 54, 56], for fixed stiffness moduli of the material.

In [54], Pedersen showed a closed form analytical solution, in the bi-dimensional case, to determine the extreme values of the elastic strain energy density functional. The optimisation variable was the orientation of the orhotropic material. The objective function was expressed in terms of the principal strains, of the in-plane components of the stiffness matrix and of the angular difference ψ between the material orientation and the direction of the first principal strain. The value of ψ was determined in order to maximise or minimise the strain energy density. Results showed that the solution depends essentially upon the sign of a special parameter γ that reflects the relative shear stiffness of the material (classified as *low* or *high*). In particular, materials with *low* relative shear stiffness present a global minimum of energy density when the orientation of the maximum material stiffness coincides with the orientation of the minimum absolute value of principal strain components. This work was extended to the study of the extrema of the complementary energy in [10].

In 1991 Sacchi Landriani and Rovati [64] studied the problem of determining the optimal orientation of the stiffness properties for an orthotropic 2D continuum subject to a plane state of stress. The goal was still the maximisation of the stiffness of the structure. Also in this case, the problem was formulated through a variational approach and solved analytically. This work has been extended to the 3D case in [60]. Finally, in [61] the extreme values of the strain energy density functional are found in order to determine locally the orientations of the material symmetry axes for maximising stiffness. The strain field was fixed and the three-dimensional solid was an orthotropic material. The angular difference between the principal directions of strains and the axes of the material symmetry were described through the Euler's angles. The main result, found in all of the three previous works [60, 61, 64] is that a necessary condition for the stationarity of the strain energy density is the coaxiality of strain and stress tensors. Such condition leads to an important result for particular cases of material symmetries: the optimal solution corresponds to the simultaneous coincidence of the principal directions of strains, stresses and of the axes of symmetry.

In [41] Majak and Pohlak determined the optimal material orientation for three-dimensional linear and non-linear anisotropic materials. They used the Hooke and the Pedersen-Taylor [57] laws to describe the linear and non-linear constitutive relations, respectively. Two problems were considered: the minimisation of strain energy density and the minimisation of the Tsai-Hill and Tsai-Wu failure indexes. However, the strategy is described only for the first problem. They used the Euler's angles to determine the orientation of the material with respect to the direction of principal strains. Finally, the analytical solution was compared to the one obtained with the help of a hybrid genetic algorithm.

The outcome of all these works is that *the optimal material orientation, and particularly the direction of the symmetry axes, is always linked to the principal strain or stress directions.*

Innovative recent works on this theme are presented in [88] by Vincenti and Desmorat and in [80] by Vannucci. In these works the plane orthotropic elastic behaviour of the plane structure is described through six polar parameters (five polar invariants and a polar angle representing the orthotropy orientation). The problem of minimising the strain energy is discussed for a given state of stress and considering the polar terms as optimisation parameters. The formulation and the resolution method of this problem are the same described in [10], wherein the optimal orientation depends upon the sign of the parameter γ that reflects the relative shear stiffness of the material (*low* or *high*).

In [88] and in [80] thanks to the polar notation, the authors show that, actually, the optimal orientation to maximise the stiffness depends effectively upon a parameter, but this parameter represents the shape of orthotropy of the material. In this case, the solution of the optimal orthotropy orientation becomes very general and can be evaluated also in cases wherein the shear behaviour of the plate is not involved and, so, the shear parameter γ introduced by Pedersen does not take part into the problem resolution.

3.2.2 Maximising strength

In the literature, we can find a huge amount of works devoted to the problem of the maximisation of stiffness for composite materials and structures. A more complicated problem is the maximisation of strength: one possible reason is that the description of strength for anisotropic materials is more complicated and doubtful than the description of stiffness. The structural stiffness, from a variational point of view, can be described through a global functional, the compliance. On the other side, the strength is described through a local functional represented by phenomenological criteria. Several studies on strength optimisation of anisotropic materials have been conducted using the well-known phenomenological failure criteria of Tsai-Hill and Tsai-Wu.

One of the first works on the optimal material orientation maximising the strength was realised by Sandhu in 1969 [65]. He developed a parametric study on the Tsai-Hill's criterion applied to unidirectional composites. The criterion was parametrised in order to determine the maximum strength for a given set of stresses and admissible strengths. Results showed that the optimal material orientation depends upon the shear strength value. If the shear strength S is lower than the transverse strength Y, the orientation of the material that maximises the term (σ_1/X) corresponds to the principal stress orientation. If the shear strength is greater than the transverse strength no conclusion can be drown. For this last case, in 1970, Brandmaier [6] developed an analytical solution. The result was a relation between (σ_1/X) and the transverse and shear strengths. Such a solution for the optimal orientation is not generalised and has no links with the stress state of the material.

In some sense, Sandhu and Brandmaier anticipated the approach to find the optimal material orientation used by Pedersen *et al.* for maximising stiffness. The idea of parametrising and explicitly writing the orientation of the symmetry axis into the failure criterion is, today, usually exploited in approaches to the strength optimisation of composite structures. Majak and Hannus [40] formulated the Tsai-Hill [23] and Tsai-Wu [73] stress-based failure criteria in terms of strains for 3D and 2D orthotropic materials. The problem of the optimal material orientation was studied. The failure index was assumed as the objective function to be minimised and an analytical method, in the case of 2D orthotropic materials, was proposed to evaluate its minimum. The criteria were parametrised and the angular difference between the material orientation and the direction of the first principal strain component was explicitly introduced in the expression of the criteria. An analysis of global and local extrema was conducted in order to determine the relationship between the material orientation and the strain field. The results showed that the optimal material orientation depends upon two parameters, p and q, that depend upon the strength, the stiffness of the material and the strain state. As demonstrated by Sandhu and Brandmaier, the optimal orientation can be either coaxial with the principal direction of strains or it can depend upon the two parameters p and q. The work of Majak and Hannus is clearly an evolution of the those of Sandhu and Brandmaier. They pre-

sented an analytical expression of the optimal material orientation, in the bi-dimensional space, for any orthotropic material. Anyway, the terms p and q do not have, apparently, an explicit mechanical meaning; hence, when the optimal orientation depends upon p and/or q nothing can be said about its physical meaning.

In Chapters 4 and 5 we will deal with the same problem of finding the optimal material orientation to maximise strength in the 2D case. We give a new and more general approach to this problem and we find a physical meaning linked to all the optimal orientations.

3.3 Optimisation of anisotropic laminated structures

In Sec. 3.2 we have discussed some approaches to the problem of the optimal material orientation for an orthotropic ply. The solution, often analytical, of this problem allows for determining a link between the material orientation and the stress or strain state. In global optimisation of laminated structures, other mechanical properties of the structure must be taken into account: the material properties, the orientation and the thickness of every ply composing the structure as well as the number of plies. Of course, the increase in the number of design variables makes the solution of the optimisation problem more complex. We describe in this section some works that deal with this theme and make use of the CLPT to determine the optimal stiffness or strength of laminates.

3.3.1 Maximising stiffness

A great number of works on the optimal stiffness design of laminates achieves such a goal using the minimisation of the compliance [16, 43, 54, 67, 88]. When dealing with this problem, the most common assumption is the elastic uncoupling between extension and bending behaviour of the laminate, along with the use of a fixed number of plies. Once the material of the plies is fixed, almost all of the works on the optimal design of laminates make the assumption of identical plies with the material chosen *a priori*; then, the main optimisation variables are only the ply orientations and their thickness. Instead of working directly with these design variables, Miki [42, 43] was the first that used the so-called *lamination parameters* introduced by Tsai and Pagano in 1982 [72] to describe the classical stiffness tensors (membrane, bending and coupling) of the CLPT. In this way the optimal stiffness properties, in terms of lamination parameters, were easily obtained and the realisation of the stacking sequence corresponding to the optimal values of the laminate lamination parameters was postponed to a sub-sequent phase. The advantage of this strategy resides in the fact of having a simpler, linear and convex objective function, the compliance expressed in terms of lamination parameters, in the first phase of the design process. However, the method introduced by Miki presents a lack in the second phase of the strategy: it finds the solution in only one sub-set of stacking sequences, the angle-ply sequences. This two-step approach, introduced by Miki, was also used by other researchers, see [16, 17].

Hammer *et al.* in 1997 [22] used the lamination parameters as design variables for maximising the stiffness of orthotropic laminated plates subjected to single or multiple loads. In a first phase, the optimisation problem is initially simplified in order to reduce the design variables (e.g. adopting the CLPT and using the lamination parameters), then, in the second phase the lay-up is designed in order to match the values of the design variables (i.e. lamination parameters, thickness of the laminate, and so on) found during the first phase. Moreover, in the expression of the strain energy the lamination parameters

are locally defined, so they can change point wise. The local variation of the lamination parameters introduced the concept of *variable stiffness laminate* that represents the new class of the most performant composite structures. This strategy will be the core of our approach for the optimal design of laminated structures described in the third part of the present thesis (Chapters 6, 7 and 8).

An evolution and extension of this last work was presented by Jibawy *et al.* in 2011 [31]. The problem of minimising the complementary energy of a laminated structure for a given state of stress was addressed. They adopted a *hierarchical strategy* essentially base on two steps: a first step (structural optimisation) where the laminated structure is modelled as a single-layer homogeneous structure and the anisotropy distribution is optimised determining the optimal distribution of material parameters; then in the second step (lay up design) a suitable stacking sequence, giving the optimal response obtained at the end of the previous step, is looked for at each point of the structure. In this research the stiffness tensors of the laminate are represented using the polar method. An analytical solution is found for both the steps of the hierarchical strategy and the simplifications introduced by the polar method lead the authors to address the problem for pure membrane and pure bending loading cases.

3.3.2 Maximising strength

Maximising the strength of laminated structures is still more complex than maximising stiffness. Among the difficulties already existing for a single ply, in the case of a laminated structure, we do not dispose of a global quantity describing the strength for the homogenised structure. At the laminate level, the stiffness is still described by a global functional, the compliance, whilst the strength is described through a local functional, the failure criteria that needs to be analysed for each ply along the thickness of the structure; thus, the application of failure criteria, needs the knowledge of the laminate lay-up. However, during the first phase of the laminate design, the lay-up is not known. So, almost all of the works on optimal strength design of composite structures make use of a local approach: they determine n objective functions, one for each ply, describing the strength of the plies, [20, 36, 37, 52, 70]. The main optimisation variable, usually, is represented by the plies orientation.

For example, Park *et al.* [52] developed a strategy to maximise the strength of composite structures where the fibre orientations of the plies are the optimisation variables, while the geometry and the number of plies are fixed. The objective, in this work, was to minimise the maximum value of the failure index with respect to the fibres orientation. The stress field is determined through a Finite Element (FE) analysis using the penalty plate bending element of Reddy [59]. The stress field is, then, used to calculate the Tsai-Hill failure index, taken as the fitness function evaluated at each node for every ply.

A research on the optimum design of a composite box-beam structure subject to strength constraints was conducted by Kathiravan and Ganguli [35]. The analytical method of Ferrero et al [15] to solve the elastic problem of the composite box beam was used in order to reduce the computational efforts of the FE analysis. The number of layers of each wall were fixed, while the plies orientations were considered as the design variables in order to maximise the minimum reserve factor (the inverse of the failure index) obtained using the Tsai-Wu-Hann failure criterion. Both interactive descent method and a PSO (Particle Swarm Optimisation) method were used and a comparison between

results obtained using the two techniques was also presented.

Topal and Uzman [70] developed a numerical procedure to determine the optimum fibres orientations that maximise the load capacity of a structure. Simply supported and uncoupled laminated plates under biaxial tension and bending moment were considered. The optimisation problem was solved via a two-step method. At the first step a gradient based method is used to minimise the maximum value of the Tsai-Wu failure index and the optimisation variables are represented by the vector of plies orientations. In the second step, the load-bearing capacity is maximised in order to determine the maximum load before the first-ply-failure arises.

The way to proceed in all of these works is summarised below:

- one or more parallel stacking sequences are chosen (generally randomly);
- a FE analysis is used to determine the state of stress of each ply;
- all the plies for which the Tsai-Wu failure index is maximum withstand a variation of the fibres orientation.

The two last phases are repeated until the maximum value of the failure index is lower than a chosen value. Of course, such an approach does not provide any certitude to reach a global optimal solution. It is rather a procedure that is stopped once the obtained value of the failure index is considered as acceptable. Furthermore, the computation effort needed to study all the possible combinations of stacking sequences and the stress field associated (through FE analyses), is very high.

Some analytical approaches to the problem of strength maximisation in laminated structures have also been proposed. For example, Groenwold and Haftka [20] developed an analytical approach where Tsai-Wu and Tsai-Hill failure criteria were considered in order to minimise the local value of the failure index. In particular, the failure index is evaluated for each ply in terms of the "failure loading factor" and of the orientation of fibres with respect to the laminate frame. An angle-ply symmetric laminate is considered; hence, the variables, regardless the number of plies, are reduced to only one orientation.

Finally, an important step forward was made in 2008 by Ijsselmuiden et al [30]. They tried to approach the optimal strength design of a laminate made of unidirectional plies defining a *conservative failure envelope* valid for the whole laminate. They used the Tsai-Wu failure criterion expressed in terms of strains to obtain a conservative failure envelope extracting the internal area to all the failure envelopes for any possible orientation of plies. In this way they obtained a strength criterion, the failure envelope, valid for the whole laminate, with given strength properties. Such a failure index was the objective function to be minimised and the in-plane laminate strains were rewritten in terms of the in-plane stiffness tensor and the in-plane stress tensor of the homogenised plate. The optimisation variables were the lamination parameters of the in-plane stiffness tensor. In 2011 Khani et al [38] re-proposed the same work, but this time the same conservative envelope was formulated using the invariants of strains and a variable stiffness plate was optimised with respect to strength. The innovative aspect of this works concerns the approach to the definition of a unique failure criterion, the conservative failure envelope, valid for the whole laminate considered as an equivalent homogenised plate. On the other hand, we can say that the major lack of this work is the fact that the strength properties of the homogenised plate are given and do not take part into the optimisation process. In fact, the objective function, the conservative failure index, is minimised only with respect to the stiffness parameters of the material.

We will address the problem of the evaluation of an homogenised, through the thickness, failure criterion and its minimisation to maximise the strength of laminated structures in Chapters 6 and 7 of this thesis.

3.4 The lay-up design of laminates as an optimisation problem

As explained in Sec. 3.3, very often the stiffness optimisation of laminates is conducted, during a first phase, on an equivalent homogenised plate and the material parameters of such plate are considered as the optimisation variables. This phase, called *structural optimisation*, does not give a complete definition of the multi-layered plate. In fact the design process must include, also, the definition of a stacking sequence giving the distribution of material parameters issued from the structural optimisation phase.

Moreover, concerning the lay-up design phase, an important aspect needs to be emphasised: the relationship between the material properties of the homogenised plate and the stacking sequence is not bijective; this means that there are more solutions in terms of stacking sequence that can satisfy the same distribution of material parameters issued from the first step of the laminate design.

Due to the high non-convex relationships that subsist between the ply orientations and the laminate homogenised material parameters (lamination parameters, polar parameters and so on) several researchers use to simplify the design process, especially reducing the range of admissible orientation angles, classically chosen within the discrete set $0°$, $\pm 45°$, $90°$. Moreover, it is also very common to choose symmetric stacking sequences in order to satisfy the elastic uncoupling, or to use balanced or cross-ply laminates obtain orthotropy, [7, 69, 91].

All these simplifying hypothesis sensibly reduce the search space in the process of the optimal lay-up design of laminates. In fact, due to the non-bijectivity of the problem, it is also possible to obtain a laminate that attains the optimal material parameters of the equivalent homogenised plate with a free stacking sequence obtained without any simplifying assumption, see [34, 45, 89].

In [69] the stacking sequence of the optimised structure is designed to match the set of lamination parameters obtained with the structural optimisation phase. A Genetic Algorithm (GA) is used to obtain such stacking sequence. The laminate is required to be balanced and to have a number of contiguous plies less than or equal to 4 in order to meet aeronautical rules. In fact ply angles are limited to $0°$, $\pm 45°$ and $90°$, thus, the problem is formulated like a constrained combinatorial optimisation problem. The problem considered here belongs to the class of the minimum distance problems: the objective function is built as a sum of differences between the actual values of the lamination parameters and the expected ones. The constraints are considered adding penalty terms to the objective functions, see [48–50].

The stacking sequence linked to lamination parameters giving the minimisation of the strain energy, minimisation of certain displacements and maximisation of the first buckling factor is determined by Autio in [4]. Also in this case a genetic-based search strategy is employed. The objective function still consists of differences between the evaluated and target lamination parameters. This time the values of the adimissible plies orientations are: $0°$, $90°$, $\pm 45°$, $\pm 80°$, $\pm 70°$, $\pm 60°$, $\pm 30°$, $\pm 20°$, $\pm 10°$. This aspect is very important because it means the abandon of the standard sequences that limit so much the optimal

solutions. Moreover, such limitations on the orientations, often brings to the use of a higher number of plies in order to meet the expected material parameters.

A methodology is proposed in [74] to convert a known distribution of lamination parameters for a variable stiffness composite laminate into a realistic design in terms of fiber angles. The problem is formulated as a *global/local problem*. The local part consists in finding a realistic stacking sequence respecting the lamination parameter values. The global part concerns a manufacturing constraint on curvature of fibres from one point to the other. A GA is used to explore the design space of plies orientations. It consists in a set of angles belonging to the range $[0°; 90°]$ discretised with a step of $15°$.

The development of modern manufacture technologies leads the research to state the problem of the optimal lay-up design in a more general way. For instance, the design space of the plies orientation is discretised into more and more small steps: in [45] and [34] the search for an optimal stacking sequence through the genetic search method is conducted. The problem is still formulated as a minimum distance problem. In both these works, the material parameters are represented by the polar parameters of the equivalent homogenised plate introduced in Sec. 1.6. In [45] the laminate is considered composed by unidirectional plies, but the range of orientations $[0°; 90°]$ is discretised with a step of $1°$. By abandoning the assumption of using standard orientations, the authors found some realistic non-conventional stacks which show a lower weight than the standard ones. Moreover, in [34] the laminate is also considered as a variable stiffness laminate respecting the point-wise variation of the relative polar parameters.

The evolution presented in these three last works concerns the higher number of solutions found and, in [34, 74], it concerns also a variable fiber orientation in the same ply to match the spatial variation of laminated parameters. Such approach results in a more effective use of the directional properties, for both strength and stiffness, of fiber reinforced laminates. However, as it is shown in these works, the determination of the stacking sequence of a variable stiffness laminate that respects the optimal distribution of material parameters issued from the first step of the laminate design process, represents a very hard task.

We will introduce the problem of the optimal lay-up design in Chapter 8 of the present thesis.

3.5 Concluding remarks

In this Chapter we have presented a brief overview on the optimisation of anisotropic laminated structures. The chronological evolution of research in the field of stiffness and strength optimisation has been discussed. Particularly, we have presented the modern approach to variable stiffness and strength structures applied to laminated composites. On the base of the cited works, the following Chapters of this thesis will give a new and more general approach to:

- the problem of finding the optimal material orientation to maximise strength (Chapters 4 and 5);
- the hierarchical optimisation strategy to maximise the stiffness of a laminate, including the strength as a supplementary objective (Chapters 6, 7 and 8).

Part II

Optimal strength for orthotropic sheets

4

Invariant formulation of phenomenological failure criteria

4.1 Introduction

In this Chapter we present a new analytical approach to the formulation of strength criteria for linear elastic plane structures composed of orthotropic materials. The starting point is the choice to work with some polynomial failure criteria: we have considered the Tsai-Hill, Hoffman, Tsai-Wu and Zhang-Evans criteria, previously presented in Chapter 2 in their classical formulations. The aim of this Chapter is their formulation using the polar invariants.

The invariant formulation of polynomial failure criteria has been considered in other researches. For example, Hilton and Ariaratnam [24] reformulated the Shanley and Ryder [66] failure criterion through the invariants of the generalised stress tensors. This invariant failure criterion was used to solve deterministic and stochastic problems with large deformations and applied also to anisotropic materials. Another example is the strain invariant formulation of failure criteria for polymers in composite materials described by Gosse in [19].

In this thesis the invariant formulation, obtained through the polar formalism, has been chosen for investigating the physical link existing between the invariant terms and the strength properties of the material. Moreover, the unified matrix formulation of the phenomenological failure criteria described in Sec. 2.5 gives us the opportunity of having a *unified invariant formulation* of such criteria.

Finally the polar formalism has been chosen to easily express the link between the material orientation and the mechanical properties of the continuum. This will be, as shown in Chapter 5, particularly important during the study on the optimal material orientation for maximising strength.

4.2 Tensorial formulation of failure criteria

In Chapter 2 we have expressed the phenomenological failure criteria of Tsai-Hill, Hoffman, Tsai-Wu and Zhang-Evans in a unified matrix notation. All of them are characterised by the sum of a quadratic term and a linear term. We recall the 2D *unified matrix formulation* of failure indexes:

$$F_{...} = \{v\}^T [H] \{v\} + \{v\}^T \{h\} \leq 1 \ , \tag{4.1}$$

where $\{\upsilon\}$, depending on the considered criterion, corresponds to either $\{\sigma\}$ or $\{\varepsilon\}$, while $[H]$ and $\{h\}$ are, respectively, the matrix and vector of limit stresses or strains.

In order to use the polar formalism, we will consider, in the rest of the thesis, the tensorial representation of the matrix $[H]$ and of the vector $\{h\}$ within the framework of the unified matrix formulation of failure criteria for an orthotropic material with respect to the generic frame $\{0; x, y, z\}$. The link between the Voigt's notation and the Cartesian tensor components is

$$\begin{array}{lll} H_{xx} = H_{xxxx}, & H_{xs} = c_1 H_{xxxy}, & H_{xy} = H_{xxyy}, \\ H_{ss} = c_2 H_{xyxy}, & H_{ys} = c_1 H_{xyyy}, & H_{yy} = H_{yyyy}, \end{array} \tag{4.2}$$

and

$$h_x = h_{xx}, \quad h_y = h_{yy}, \quad h_s = c_1 h_{xy}, \tag{4.3}$$

with $c_1 = 2$ and $c_2 = 4$ for the weakness tensors ($\mathbf{F}$,$\mathbf{f}$), while $c_1 = c_2 = 1$ for the strength tensors ($\mathbf{G}$,$\mathbf{g}$ and $\mathbf{P}$,$\mathbf{p}$). The *unified tensorial formulation* of the considered failure criteria reads:

$$F_{\dots} = \boldsymbol{\upsilon}^T \mathbf{H} \boldsymbol{\upsilon} + \boldsymbol{\upsilon}^T \mathbf{h} \ . \tag{4.4}$$

4.3 Polar formulation of failure criteria

As tacitly assumed in classical criteria, like Tsai-Hill, Hoffman and Tsai-Wu, we also consider that the components of $[H]$ and $\{h\}$ correspond, through eqs. (4.2) and (4.3), respectively to the components of a fourth order tensor $\mathbf{H}$ and of a second order tensor $\mathbf{h}$. The tensor $\mathbf{H}$ is assumed to present all the tensorial symmetries of a classical elasticity tensor, while the second order tensor $\mathbf{h}$ is assumed to be symmetric: this characterisation is also implicit in the formulation of the considered criteria.

This assumptions correspond to admit that besides the elastic behaviour, also strength is represented by a fourth order tensor of the elasticity type and by a second rank symmetric tensor. Moreover, the material symmetries of elasticity and strength are supposed to be the same. Hence, if a material is orthotropic for its elastic behaviour, it is considered to be orthotropic also for its strength, and the orthotropy axes are the same for stiffness and strength, as well as for compliance and weakness.

Taking into account these points, we also assume the existence of such tensors, though their mechanical relevancy should, perhaps, be further investigated. Since we are using the tensorial formulation, it is possible to express these criteria through the polar formalism in order to explicitly write the invariant terms and find their physical meaning.

Let us consider, now, an orthotropic material for which x and y are symmetry axes. The Cartesian components of the fourth order orthotropic tensor $\mathbf{H}$ can be expressed using its polar parameters, $\Gamma_0, \Gamma_1, (-1)^L \Lambda_0, \Lambda_1, \Omega_1$ (see eqs. (1.34) for the case of the elasticity stiffness tensor):

$$\left\{ \begin{array}{lrcrcl} H_{xxxx} = & \Gamma_0 & +2\Gamma_1 & + & (-1)^L \Lambda_0 \cos 4\Omega_1 & +4\Lambda_1 \cos 2\Omega_1, \\ H_{xxxy} = & & & & (-1)^L \Lambda_0 \sin 4\Omega_1 & +2\Lambda_1 \sin 2\Omega_1, \\ H_{xxyy} = & -\Gamma_0 & +2\Gamma_1 & - & (-1)^L \Lambda_0 \cos 4\Omega_1 & , \\ H_{xyxy} = & \Gamma_0 & & - & (-1)^L \Lambda_0 \cos 4\Omega_1 & , \\ H_{xyyy} = & & & - & (-1)^L \Lambda_0 \sin 4\Omega_1 & +2\Lambda_1 \sin 2\Omega_1, \\ H_{yyyy} = & \Gamma_0 & +2\Gamma_1 & + & (-1)^L \Lambda_0 \cos 4\Omega_1 & -4\Lambda_1 \cos 2\Omega_1. \end{array} \right. \tag{4.5}$$

The polar components of $\mathbf{H}$ in terms of Cartesian components are obtained inverting eq. (4.5):

$$\begin{cases} 8\Gamma_0 & = H_{xxxx} & & -2H_{xxyy} & +4H_{xyxy} & & +H_{yyyy}, \\ 8\Gamma_1 & = H_{xxxx} & & +2H_{xxyy} & & & +H_{yyyy}, \\ 8(-1)^L\Lambda_0 e^{4i\Omega_1} & = H_{xxxx} & +4iF_{xxxy} & -2H_{xxyy} & -4H_{xyxy} & -4iH_{yyxy} & +H_{yyyy}, \\ 8\Lambda_1 e^{2i\Omega_1} & = H_{xxxx} & +2iF_{xxxy} & & & +2iH_{yyxy} & -H_{yyyy}. \end{cases} \tag{4.6}$$

The polar parameters $\Gamma_0, \Gamma_1, \Lambda_0, \Lambda_1$ are invariants. In particular Γ_0, Γ_1 represent the isotropic part of the tensor $\mathbf{H}$, while Λ_0 and Λ_1 represent the amplitude of the anisotropic part, so Λ_0 and Λ_1 are modules and can't be negative, see [86]. L is the orthotropy shape parameter and there are two types of orthotropy according to the possible values of L, see [76] and Sec. 1.5.2: 0 (and any other even value) or 1 (and any other odd value). The polar angle Ω_1 represents the direction of the main orthotropy axis and fixing its value corresponds to fix the frame, as still explained in Sec. 1.4.

Let us consider also the second order tensor $\mathbf{h}$, represented in the plane (x, y) by the vector $\{h\}$. The Cartesian components (h_{xx}, h_{yy}, h_{xy}) can be expressed using the polar ones, Γ, Λ, Ω:

$$\begin{cases} h_{xx} = & \Gamma + & \Lambda\cos 2\Omega, \\ h_{yy} = & \Gamma - & \Lambda\cos 2\Omega, \\ h_{xy} = & & \Lambda\sin 2\Omega. \end{cases} \tag{4.7}$$

Inversely,

$$\begin{cases} \Gamma = & \dfrac{h_{xx} + h_{yy}}{2}, \\ \Lambda e^{2i\Omega} = & \dfrac{h_{xx} - h_{yy}}{2} + ih_{xy}. \end{cases} \tag{4.8}$$

The polar parameters Γ and Λ are invariants, while the polar angle Ω gives the orientation, with respect to the reference system, of the first principal component of $\mathbf{h}$ and is hence, frame dependent. In addition, similarly to what happens for the fourth order tensor, Γ represents the spherical part of $\mathbf{h}$ while $\Lambda e^{2i\Omega}$ the deviatoric one.

In addition, the following consideration must be taken into account: the orientations Ω_1 and Ω of the tensors $\mathbf{H}$ and $\mathbf{h}$ are supposed to be equal because they describe the same property, the strength, of the same orthotropic bi-dimensional sheet.

In the following paragraphs we will introduce also the polar parameters U (spherical component), V (deviatoric component) and Υ (polar angle) of the second order tensor $\boldsymbol{v}$ representing the stresses/strains.

We have assumed that the material symmetries of elasticity and strength are the same, thus, as a consequence the strength symmetries, in terms of polar invariants, are characterised by the same conditions expressed in Sec. 1.5.2 for the stiffness tensor (for a deeper insight in the matter, the reader is addressed to [77]):

$$\begin{aligned} \text{ordinary orthotropy:} \quad & \Omega_0 - \Omega_1 = L\frac{\pi}{4} \text{ with } L = 0, 1, \\ R_0 \text{ orthotropy:} \quad & \Lambda_0 = 0, \\ \text{square orthotropy:} \quad & \Lambda_1 = 0, \\ \text{isotropy:} \quad & \Lambda_0 = \Lambda_1 = 0 \quad \text{for} \quad \mathbf{H}, \\ & \Lambda = 0 \quad \text{for} \quad \mathbf{h}; \end{aligned} \tag{4.9}$$

The orientation Ω_1 of the material symmetry and the type of orthotropy L are explicit terms of the tensors components. In an optimisation process this property reveals to be of the highest importance, see Chapter 5.

4.3.1 Invariant formulation of phenomenological failure criteria

We can now express the failure criteria with the polar formalism and we begin with the case of ordinary orthotropy. All the failure criteria get the same expression which, for a material with ordinary orthotropy is:

$$\begin{aligned} F_{...} = \; & 4V^2\left[\Gamma_0 + (-1)^L \Lambda_0 \cos 4(\Omega_1 - \Upsilon)\right] + 8U^2\Gamma_1 + 16UV\Lambda_1 \cos 2(\Omega_1 - \Upsilon) + \\ & + 2U\Gamma + 2V\Lambda \cos 2(\Omega - \Upsilon) \leq 1, \end{aligned} \tag{4.10}$$

that is the polar translation of eq. (4.4). As expected, the linear term does not add any coupling effect between the isotropic and anisotropic parts of tensors $\boldsymbol{\upsilon}$ and $\mathbf{h}$: indeed, the spherical and deviatoric parts of tensor $\boldsymbol{\upsilon}$ work only on the isotropic and anisotropic parts of $\mathbf{h}$, respectively.

Let us now consider some special cases of the stress/strain tensor and of isotropic materials.

Case 1: $V = 0$**.**

V represents the deviatoric part of the stress/strain tensor. So, if V is equal to zero then the stress/strain field is spherical: $\upsilon_{xx} = \upsilon_{yy} = U$ and $\upsilon_{xy} = 0$. By a simple substitution, eq. (4.10) becomes

$$F_{...} = 8U^2\Gamma_1 + 2U\Gamma \leq 1 \; . \tag{4.11}$$

Thus, only the spherical part of the criterion is present in this case and couples the spherical part of tensor $\boldsymbol{\upsilon}$ with one of the isotropic moduli of $\mathbf{H}$ and with the isotropic part of $\mathbf{h}$.

Case 2: $U = 0$**.**

When U is null, the stress/strain field is completely deviatoric with $\upsilon_{xx} = -\upsilon_{yy} = V\cos 2\Upsilon$ and $\upsilon_{xy} = V \sin 2\Upsilon$. The criteria become, hence:

$$F_{...} = 4V^2\left[\Gamma_0 + (-1)^L \Lambda_0 \cos 4(\Omega_1 - \Upsilon)\right] + 2V\Lambda \cos 2(\Omega - \Upsilon) \leq 1 \; . \tag{4.12}$$

Case 3: uniaxial stress/strain state along the x **axis,** $\upsilon_{xx} \neq 0$**,** $\upsilon_{yy} = \upsilon_{xy} = 0$**.**

In terms of polar parameters, tensor $\boldsymbol{\upsilon}$ becomes

$$\begin{array}{rcll} U + V\cos 2\Upsilon = & \upsilon_{xx} & \Longrightarrow & U = \upsilon_{xx}/2 \; , \\ U - V\cos 2\Upsilon = & 0 & \Longrightarrow & U = (-1)^k V, \quad k = 0, 1 \; , \\ V \sin 2\Upsilon = & 0 & \Longrightarrow & \Upsilon = k\pi/2, \quad k = 0, 1 \; . \end{array} \tag{4.13}$$

Hence, we get for the failure criteria (4.10)

$$F_{...} = 4U^2\left[\Gamma_0 + 2\Gamma_1 + (-1)^L \Lambda_0 \cos 4\Omega_1 + 4\Lambda_1 \cos 2\Omega_1\right] + 2U\left[\Gamma + \Lambda \cos 2\Omega\right] \leq 1 \; . \tag{4.14}$$

Case 4: uniaxial stress/strain state along the y axis, $\upsilon_{yy} \neq 0$, $\upsilon_{xx} = \upsilon_{xy} = 0$.

Tensor $\boldsymbol{\upsilon}$ becomes

$$\begin{array}{rcll} U + V\cos 2\Upsilon = & 0 & \Longrightarrow & U = -(-1)^k V, \quad k = 0,1\ , \\ U - V\cos 2\Upsilon = & \upsilon_{yy} & \Longrightarrow & U = \upsilon_{yy}/2\ , \\ V\sin 2\Upsilon = & 0 & \Longrightarrow & \Upsilon = k\pi/2, \qquad k = 0,1\ , \end{array} \tag{4.15}$$

and the failure criteria (4.10) read:

$$F_{...} = 4U^2\left[\Gamma_0 + 2\Gamma_1 + (-1)^L \Lambda_0 \cos 4\Omega_1 - 4\Lambda_1 \cos 2\Omega_1\right] + 2U\left[\Gamma - \Lambda\cos 2\Omega\right] \leq 1\ . \tag{4.16}$$

Case 5: a pure shear stress/strain state, $\upsilon_{xy} \neq 0$, $\upsilon_{xx} = \upsilon_{yy} = 0$.

Tensor $\boldsymbol{\upsilon}$ is

$$\begin{array}{rcll} U + V\cos 2\Upsilon = & 0 & \Longrightarrow & U = 0,\ \Upsilon = \dfrac{\pi}{4} + k\dfrac{\pi}{2}, \quad k = 0,1\ , \\ U - V\cos 2\Upsilon = & 0 & \Longrightarrow & U = 0,\ \Upsilon = \dfrac{\pi}{4} + k\dfrac{\pi}{2}\ , \\ V\sin 2\Upsilon = & \upsilon_{xy} & \Longrightarrow & (-1)^k V = \upsilon_{xy}, \qquad k = 0,1\ , \end{array} \tag{4.17}$$

and the failure criteria now look like:

$$F_{...} = 4V^2\left[\Gamma_0 - (-1)^L \Lambda_0 \cos 4\Omega_1\right] \leq 1\ . \tag{4.18}$$

Case 6: Isotropic material

The *complete symmetry* is expressed by the condition $\Lambda_0 = \Lambda_1 = 0$ and $\Lambda = 0$. In this way, only the isotropic parts of all the tensors appear within the criteria (the anisotropic ones being identically null):

$$F_{...} = \ 4V^2\Gamma_0 + 8U^2\Gamma_1 + 2U\Gamma \leq 1. \tag{4.19}$$

4.4 Physical interpretations

4.4.1 Remarks on the stress-based criteria

In the case of stress-based criteria, the tensors **H** and **h** represent the tensors **F** and **f**, respectively. It is possible to inject into eqs. (4.6) and (4.8) the relations giving, for each one of the three stress-based criteria, the Cartesian components of **F** and **f** as function of the strength properties (X_t, X_c, etc.), see Tabs. 2.2 and 2.3. In this Section we assume that (see Sec. 2.5) the x axis of the reference system is aligned with the direction of maximum weakness (in the case of an unidirectional ply, the fibres are perpendicular to the x axis).

The polar components of the weakness tensor **F**, for an orthotropic material, in terms of strength properties are:

$$\begin{cases} 8\Gamma_0 = & \dfrac{1}{X_tX_c} + \dfrac{1}{Y_tY_c} + \dfrac{1}{S^2} - 2F_{xxyy}, \\ 8\Gamma_1 = & \dfrac{1}{X_tX_c} + \dfrac{1}{Y_tY_c} + 2F_{xxyy}, \\ 8(-1)^L\Lambda_0 = & \dfrac{1}{X_tX_c} + \dfrac{1}{Y_tY_c} - \dfrac{1}{S^2} - 2F_{xxyy}, \\ 8\Lambda_1 = & \dfrac{1}{Y_tY_c} - \dfrac{1}{X_tX_c}, \end{cases} \tag{4.20}$$

with the term F_{xxyy} for each stress-based criterion reported in Tab. 2.2 as F_{xy}. Moreover, concerning the Tsai-Hill criterion the normal and transverse strength properties in are considered equivalent in tension and compression. A peculiar expression concerns the isotropic polar invariant Γ_1, in the Tsai-Hill criterion:

$$8\Gamma_1 = \frac{1}{Y^2}; \tag{4.21}$$

the above equation, that can be easily found using Tab. 2.2 along with eqs. (4.6), shows that Γ_1 is a direct measure of the transverse strength property Y.

Concerning the anisotropic terms of $\mathbf{F}$, we assume that Λ_0 and Λ_1 are positive or null as said in Sec. 1.4. Thus, if we impose that the third and fourth equations of (4.20) expressing Λ_0 and Λ_1 must be positive or null, we have the following conditions:

$$\left.\begin{array}{l} \dfrac{1}{X_tX_c} + \dfrac{1}{Y_tY_c} - 2F_{xxyy} \geq \dfrac{1}{S^2} \quad \text{if} \quad L = 0, \\ \dfrac{1}{X_tX_c} + \dfrac{1}{Y_tY_c} - 2F_{xxyy} \leq \dfrac{1}{S^2} \quad \text{if} \quad L = 1, \end{array}\right\} \text{with } Y_tY_c \leq X_tX_c \ . \tag{4.22}$$

Therefore, the type of orthotropy (value of the parameter L) take part into the conditions to ensure the positivity of Λ_0.

The polar components of $\mathbf{f}$, for an orthotropic material, in terms of the strength properties, can be obtained in the same way and are:

$$\begin{cases} 2\Gamma = & \dfrac{Y_c - Y_t}{Y_tY_c} + \dfrac{X_c - X_t}{X_tX_c}, \\ 2\Lambda = & \dfrac{Y_c - Y_t}{Y_tY_c} - \dfrac{X_c - X_t}{X_tX_c}. \end{cases} \tag{4.23}$$

This formulation is equivalent for the Tsai-Wu and Hoffman criteria, while for the Tsai-Hill criterion, tensor $\mathbf{f}$ is not present.

The value of the polar strength invariants for two orthotropic layers, see Tab. 4.1, are reported in Tabs. 4.2 to 4.4. Concerning the polar parameters of the Tsai-Hill fourth order tensor, four cases are presented for an E-glass epoxy lamina. This is due to the presence of two different values of normal strength properties in tension and compression that are used in relation with the sign of stress components σ_{xx} and σ_{yy}. This approach gives four different sets of invariants, one for the tension, one for the compression case, and the two others being a mix of tension and compression cases. In the case of the Hoffman failure criterion, the polar invariants are unique, see Tab. 4.3.

Material	X_t	X_c	Y_t	Y_c	S
E-Glass Epoxy	1080	620	39	128	89
Carbon/Epoxy	1447	1447	51.7	206	93

Table 4.1: Mechanical strength properties of two orthotropic materials, [MPa].

		$\times 10^{-5}$	$\times 10^{-6}$	$\times 10^{-6}$	$\times 10^{-6}$		
X	Y	Γ_0[MPa^{-2}]	Γ_1[MPa^{-2}]	Λ_0[MPa^{-2}]	Λ_1[MPa^{-2}]	L	Ω_1
X_t	Y_t	9.807	82.29	66.51	82.08	0	0
X_c	Y_c	2.373	7.955	7.826	7.304	1	0
X_t	Y_c	2.352	7.737	8.044	7.522	1	0
X_c	Y_t	9.829	82.51	66.73	81.86	0	0

Table 4.2: Weakness polar components for the generic E-Glass Epoxy in the Tsai-Hill failure criterion.

	$\times 10^{-5}$	$\times 10^{-5}$	$\times 10^{-6}$	$\times 10^{-5}$			$\times 10^{-3}$	$\times 10^{-3}$	
Material	Γ_0[MPa^{-2}]	Γ_1[MPa^{-2}]	Λ_0[MPa^{-2}]	Λ_1[MPa^{-2}]	L	Ω_1	Γ[MPa^{-1}]	Λ[MPa^{-1}]	Ω
E-Glass Epoxy	4.12	2.50	9.63	2.49	0	0	8.57	9.26	0
Carbon Epoxy	2.63	1.17	2.60	1.17	1	0	7.24	7.24	0

Table 4.3: Weakness polar components for orthotropic materials in the Hoffman failure criterion.

	$\times 10^{-5}$	$\times 10^{-5}$	$\times 10^{-6}$	$\times 10^{-5}$			$\times 10^{-3}$	$\times 10^{-3}$	
Material	Γ_0[MPa^{-2}]	Γ_1[MPa^{-2}]	Λ_0[MPa^{-2}]	Λ_1[MPa^{-2}]	L	Ω_1	Γ[MPa^{-1}]	Λ[MPa^{-1}]	Ω
E-Glass Epoxy	[4.53:3.67]	[2.09:2.96]	[13.8:5.12]	2.49	0	0	8.57	9.26	0
Carbon/ Epoxy	[2.79:2.46]	[1.01:1.35]	[0.98:4.33]	1.17	1	0	7.24	7.24	0

Table 4.4: Weakness polar components for orthotropic materials in the Tsai-Wu failure criterion.

Concerning the Tsai-Wu criterion, some polar parameters are linear functions of the term $F_{12}^* \in [-1;1]$ of eq. (2.19):

$$\begin{cases} 8\Gamma_0 = \dfrac{1}{X_tX_c} + \dfrac{1}{Y_tY_c} + \dfrac{1}{S^2} - 2\dfrac{F_{12}^*}{\sqrt{X_tX_cY_tY_c}}, \\ 8\Gamma_1 = \dfrac{1}{X_tX_c} + \dfrac{1}{Y_tY_c} + 2\dfrac{F_{12}^*}{\sqrt{X_tX_cY_tY_c}}, \\ 8(-1)^L\Lambda_0 = \dfrac{1}{X_tX_c} + \dfrac{1}{Y_tY_c} - \dfrac{1}{S^2} - 2\dfrac{F_{12}^*}{\sqrt{X_tX_cY_tY_c}}. \end{cases} \tag{4.24}$$

The range of their numerical values, considering that $F_{12}^* \in [-1;1]$, is presented in Tab. 4.4.

A general expression of the term F_{12}^* cannot be given because its value actually depends upon the stress state. Nevertheless, thanks to the polar formalism, we can see that the term F_{12}^* does not depend on the stress field in two cases.

The first one is obtained imposing $\Lambda_0 = 0$ in the third equation of (4.24):

$$F_{12}^* = \frac{\sqrt{X_t X_c Y_t Y_c}}{2}\left(\frac{1}{X_t X_c} + \frac{1}{Y_t Y_c} - \frac{1}{S^2}\right). \tag{4.25}$$

Eq. (4.25) represents a material with R_0-orthotropy, [76], for which the characterisation of the orthotropic weakness tensor $\mathbf{F}$ is given by three, instead of four, polar invariants: Γ_0, Γ_1 and Λ_1. Thus, for $\Lambda_0 = 0$ the term F_{12}^* of Tsai-Wu tensor $\mathbf{F}$ has a fixed value that depends only upon the properties of normal and shear strength of the material.

The second case is isotropy ($\Lambda_0 = \Lambda_1 = 0$). If we impose $\Lambda_1 = 0$ in the fourth equation of (4.20) we obtain:

$$X_t X_c = Y_t Y_c \ . \tag{4.26}$$

Combining eq. (4.26) with eq. (4.25), we get:

$$F_{12}^* = 1 - \frac{X_t X_c}{2S^2}. \tag{4.27}$$

Of course, in this case the further reduction of independent components, *a fortiori* leads to an explicit formulation of F_{12}^*.

The other polar terms of the Tsai-Wu tensors, not dependent on F_{12}^*, are equivalents to those of the Hoffman criterion.

Tsai-Hill criterion

The Tsai-Hill criterion in the case of ordinary orthotropy is:

$$F_{Hill} = 4V^2\left[\Gamma_0 + (-1)^L \Lambda_0 \cos 4(\Omega_1 - \Upsilon)\right] + 8U^2\Gamma_1 + 16UV\Lambda_1 \cos 2(\Omega_1 - \Upsilon) \leq 1. \tag{4.28}$$

Eq. (4.28) is formally identical to the corresponding one for the complementary energy W_c given in [88].

Let us now discuss some special cases, previously considered, of the stress tensor.

Case 1: $V = 0$.

Eq. (4.11) shows that only the spherical part of the criterion is present in this case coupling the spherical part of tensor $\boldsymbol{\sigma}$ with an isotropic component of $\mathbf{F}$. If we rewrite eq. (4.11) in Cartesian notation using eqs. (4.6) and (1.31) we get, in the case of a pure spherical stress field,

$$\sigma_{xx} = \sigma_{yy} \geq Y. \tag{4.29}$$

In this case the only property of resistance responsible for the failure is Y. This is a consequence of the tacit assumption, in the Tsai-Hill criterion, that the strength along the fibres direction, X, is greater than that in the transverse direction, Y.

Case 2: $U = 0$**.**

When U is null, the stress field is completely deviatoric with $\sigma_{xx} = -\sigma_{yy} = V\cos 2\Upsilon$ and $\sigma_{xy} = V\sin 2\Upsilon$. If we choose a frame putting $\Omega_1 = 0$, the criterion in terms of Cartesian components reads like

$$\sigma_{xx}^2\left(\frac{2}{X^2}+\frac{1}{Y^2}\right)+\frac{\sigma_{xy}^2}{S^2}\leq 1. \tag{4.30}$$

This relation corresponds to eq. (4.12) written in Cartesian notation using eqs. (4.6) and (1.31).

Case 3: Isotropic material.

The complete material symmetry is expressed by the condition $\Lambda_0 = \Lambda_1 = 0$. In this way the anisotropic part of the Tsai-Hill criterion is removed, eq. (4.11). Thus, it remains only the isotropic part of the criterion:

$$F_{Hill} = 8U^2\Gamma_1 + 4V^2\Gamma_0 \leq 1. \tag{4.31}$$

And in terms of strength properties:

$$X^2 = Y^2 = 3S^2. \tag{4.32}$$

The criterion in Cartesian components reads like:

$$F_{Hill} = \frac{1}{X^2}\left(\sigma_{xx}^2+\sigma_{yy}^2-\sigma_{xx}\sigma_{yy}+3\sigma_{xy}^2\right)\leq 1; \tag{4.33}$$

that corresponds to the Von Mises criterion in a plane stress state.

Hoffman and Tsai-Wu criteria

The general polar formulation of the two failure criteria is given in eq. (4.10). It is identical to that of the Tsai-Hill with two added terms that take into account for the linear contribution to the failure. In Tab. 4.5 some special cases, extensively discussed beforehand for the Tsai-Hill criterion, are reported for the cases of the Hoffman and Tsai-Wu criteria. The adopted approach is the same use for the Tsai-Hill criterion. The isotropic material case needs more attention an will be explained, apart, below.

Case 3: Isotropic material.

Hoffman's criterion: in terms of strength properties, the condition $\Lambda_0 = \Lambda_1 = 0$ and $\Lambda = 0$ corresponds to:

$$\begin{aligned} X_tX_c &= Y_tY_c = 3S^2, \\ X_c - X_t &= Y_c - Y_t. \end{aligned} \tag{4.34}$$

Thus, the Hoffman criterion in Cartesian components can be written as follows:

$$F_{Hoff} = \frac{1}{X_tX_c}\left(\sigma_{xx}^2+\sigma_{yy}^2-\sigma_{xx}\sigma_{yy}+3\sigma_{xy}^2\right)+(\sigma_{xx}+\sigma_{yy})\left(\frac{X_c-X_t}{X_tX_c}\right)\leq 1. \tag{4.35}$$

Case 1: $V = 0$	
Cartesian form.	$F_{Hoff} = \dfrac{\sigma^2}{Y_t Y_c} + \sigma\left(\dfrac{X_c - X_t}{X_t X_c} + \dfrac{Y_c - Y_t}{Y_t Y_c}\right),$
	$F_{TW} = \sigma^2\left(\dfrac{1}{Y_t Y_c} + \dfrac{2F_{12}^*}{\sqrt{X_t X_c Y_t Y_c}} + \dfrac{1}{X_t X_c}\right) + \sigma\left(\dfrac{X_c - X_t}{X_t X_c} + \dfrac{Y_c - Y_t}{Y_t Y_c}\right).$
Case 2: $U = 0$	
Cartesian form.	$F_{Hoff} = \sigma_{xx}^2\left(\dfrac{2}{X_t X_c} + \dfrac{1}{Y_t Y_c}\right) + \dfrac{\sigma_{xy}^2}{S^2} + \sigma_{xx}\left(\dfrac{Y_c - Y_t}{Y_t Y_c} - \dfrac{X_c - X_t}{X_t X_c}\right),$
	$F_{TW} = \sigma_{xx}^2\left(\dfrac{1}{X_t X_c} - \dfrac{2F_{12}^*}{\sqrt{X_t X_c Y_t Y_c}} + \dfrac{1}{Y_t Y_c}\right) + \dfrac{\sigma_{xy}^2}{S^2} + \sigma_{xx}\left(\dfrac{Y_c - Y_t}{Y_t Y_c} - \dfrac{X_c - X_t}{X_t X_c}\right).$

Table 4.5: Peculiar expressions of Hoffman and Tsai-Wu failure criteria in terms of stresses.

Eq. (4.35) can be rewritten in terms of principal stress components σ_I and σ_{II}. The relationship among the polar parameters U and V and the principal stresses is:

$$\begin{aligned} U &= \frac{\sigma_I + \sigma_{II}}{2}, \\ V &= \frac{\sigma_I - \sigma_{II}}{2}. \end{aligned} \tag{4.36}$$

Considering eq. (4.36), eq. (4.19) and eqs. (4.20), we obtain:

$$F_{Hoff} = \frac{1}{X_t X_c}\left(\sigma_I^2 + \sigma_{II}^2 - \sigma_I \sigma_{II}\right) + \left(\frac{X_c - X_t}{X_t X_c}\right)(\sigma_I + \sigma_{II}) \leq 1 \tag{4.37}$$

that corresponds to the Polynomial Invariants Failure Criterion of Christensen for isotropic materials, with different strength in tension and compression, developed from 1997 [11] to 2007 [12]. The failure criterion is valid for both ductile and brittle materials, it has a quadratic form similar to the Von Mises criterion but more general and applicable to a wider range of materials. Eq. (4.37) expresses a rather important result: thanks to the polar formalism we have shown, with few logical steps, that as well as the Tsai-Hill criterion is an extension of the Huber-Henky-Von Mises criterion, the Hoffman criterion can be considered as an extension of the Christensen criterion.

Tsai-Wu's criterion: in terms of strength properties, conditions $\Lambda_0 = \Lambda_1 = 0$ and $\Lambda = 0$ become now

$$\begin{aligned} X_t X_c = Y_t Y_c = 2S^2(1 - F_{12}^*), \\ X_c - X_t = Y_c - Y_t. \end{aligned} \tag{4.38}$$

Thus, the Tsai-Wu criterion in Cartesian components is, in this case,

$$F_{TW} = \frac{1}{X_t X_c}\left(\sigma_{xx}^2 + \sigma_{yy}^2 + 2F_{12}^* \sigma_{xx}\sigma_{yy} + \sigma_{xy}^2(1 - F_{12}^*)\right) + (\sigma_{xx} + \sigma_{yy})\left(\frac{X_c - X_t}{X_t X_c}\right) \leq 1; \tag{4.39}$$

but, using condition (4.27), valid for isotropic materials, eq. (4.39) becomes

$$F_{TW} = \frac{1}{X_t X_c}\left(\sigma_{xx}^2 + \sigma_{yy}^2\right) + \frac{1}{S^2}\left(\sigma_{xy}^2 - \sigma_{xx}\sigma_{yy}\right) + \left(\frac{X_c - X_t}{X_t X_c}\right)(\sigma_{xx} + \sigma_{yy}) \leq 1, \tag{4.40}$$

that represents the first formulation, to our knowledge, of failure criterion for isotropic materials derived from the most general criterion of Tsai-Wu for anisotropic materials.

4.4.2 Remarks on the stress-based criteria expressed in terms of strains

In the case of stress-based criteria expressed in terms of strains the tensors **H** and **h** represents the tensors **G** and **g**, respectively, Sec. 2.3.
It is possible, also in this case, to inject into eqs. (4.6) and (4.8) the relations giving, for each one of the three strength criteria expressed in terms of strains, the Cartesian components of **G** and $\boldsymbol{g}$, as functions of the strength and stiffness properties, see Tabs. 2.4 and 2.5. It is evident that, being such criteria the expression of the previous ones in terms of strains, the results and remarks are the same.

Thus, we will report only some numerical examples (Tab. 4.7) in order to compare the orthotropy orientations of the fourth order tensors involved in such formulation (**F**, **Q** and the combination of these two tensors: **G**). In particular, we will consider only the polar parameters of the Tsai-Hill criterion.

The mechanical properties of three materials are reported in Tab. 4.6. The reference system $\{0; x, y, z\}$ has, here, the x axis aligned with the direction of maximum stiffness and strength, hence, for an unidirectional ply the x axis is placed along the fibres direction (so, such a tensor is defined in a frame rotated of $\pi/2$ with respect to that used for **F**).

We recall, see Sec. 2.5, that the Cartesian components of **G** are dimensionless. Of course, this is true for the polar components of **G** as well. The main result observed in Tab. 4.7 is that while the orthotropy directions of tensors **F** and **Q** are always shifted of $\pi/2$, the orthotropy orientation of tensor **G** can be aligned either with **F** or **Q**, depending on the considered material.

	Carbon/Epoxy T300/5208	IM6/Epoxy Carbon/Epoxy	Generic E-Glass/Epoxy
E_1[MPa]	181000	203000	39000
E_2[MPa]	10300	11200	8600
G_{12}^S[MPa]	7170	8400	3800
ν_{12}	0.28	0.32	0.28
X[MPa]	1500	1540	620
Y[MPa]	246	56	39
S[MPa]	68	98	89

Table 4.6: Mechanical properties of a selected set of orthotropic materials

4.4.3 Remarks on the strain-based criterion

In the case of strain-based criteria the tensors **H** and **h** represents the tensors **P** and **p**, respectively, see Sec. 2.4. If we substitute in eqs. (4.6) the relations giving the Cartesian components of **P** and **p**, functions of the yield strain properties ($X_{\varepsilon_t}, X_{\varepsilon_C}$, etc.) reported

	Weakness tensor **F**					
	Γ_0 [MPa]$^{-2}$	Γ_1 [MPa]$^{-2}$	Λ_0 [MPa]$^{-2}$	Λ_1 [MPa]$^{-2}$	Ω_1	L
	$\times 10^{-5}$	$\times 10^{-5}$	$\times 10^{-5}$	$\times 10^{-5}$		
Carbon/Epoxy T300/5208	11.03	2.06	10.59	2.01	90	Even
IM6/Epoxy Carbon/Epoxy	5.29	3.98	2.69	3.98	90	Even
Generic E-Glass/Epoxy	9.86	8.21	6.70	8.18	90	Even
	Stiffness tensor **Q**					
	T_0 [MPa]	T_1 [MPa]	R_0 [MPa]	R_1 [MPa]	Φ_1	K
	$\times 10^3$	$\times 10^3$	$\times 10^3$	$\times 10^3$		
Carbon/Epoxy T300/5208	26.88	24.74	19.71	21.43	0	Even
IM6/Epoxy Carbon/Epoxy	30.22	27.82	21.82	24.11	0	Even
Generic E-Glass/Epoxy	7.34	6.66	3.54	3.86	0	Even
	Strength tensor **G**					
	Γ_0	Γ_1	Λ_0	Λ_1	Ω_1	L
	$\times 10^3$	$\times 10^3$	$\times 10^3$	$\times 10^3$		
Carbon/Epoxy T300/5208	7.52	2.12	3.59	1.60	0	Even
IM6/Epoxy Carbon/Epoxy	8.21	10.92	0.86	2.37	90	Even
Generic E-Glass/Epoxy	4.70	10.73	2.87	5.31	90	Even

Table 4.7: Polar Components for the tensors **F**, **Q** and **G** calculated in the material frame with x axis oriented along the direction of maximum strength, Tsai-Hill's criterion.

in Tabs. 2.6 and 2.7, we obtain:

$$\begin{cases} 8\Gamma_0 = \dfrac{1}{X_{\varepsilon_t} X_{\varepsilon_c}} + \dfrac{1}{Y_{\varepsilon_t} Y_{\varepsilon_c}} + \dfrac{4}{S_\varepsilon^2} - 2P_{xxyy}, \\ 8\Gamma_1 = \dfrac{1}{X_{\varepsilon_t} X_{\varepsilon_c}} + \dfrac{1}{Y_{\varepsilon_t} Y_{\varepsilon_c}} + 2P_{xxyy}, \\ 8(-1)^L \Lambda_0 = \dfrac{1}{X_{\varepsilon_t} X_{\varepsilon_c}} + \dfrac{1}{Y_{\varepsilon_t} Y_{\varepsilon_c}} - \dfrac{4}{S_\varepsilon^2} - 2P_{xxyy}, \\ 8\Lambda_1 = \dfrac{1}{X_{\varepsilon_t} X_{\varepsilon_c}} - \dfrac{1}{Y_{\varepsilon_t} Y_{\varepsilon_c}}. \end{cases} \tag{4.41}$$

in the material frame with x axis aligned with the direction of maximum strength and stiffness. The term P_{xxyy} is given in eq. (2.37) as P_{12}.

The anisotropic terms of $\mathbf{P}$, Λ_0 and Λ_1 are positive. This corresponds to the following conditions, the counterparts of eqs. (4.22):

$$\left.\begin{array}{ll} \dfrac{1}{X_{\varepsilon_t}X_{\varepsilon_c}}+\dfrac{1}{Y_tY_{\varepsilon_c}}-2P_{xxyy}\geq\dfrac{4}{S_\varepsilon^2} & \text{if} \quad L=0,\\ \dfrac{1}{X_{\varepsilon_t}X_{\varepsilon_c}}+\dfrac{1}{Y_{\varepsilon_t}Y_{\varepsilon_c}}-2P_{xxyy}\leq\dfrac{4}{S_\varepsilon^2} & \text{if} \quad L=1, \end{array}\right\} \text{with } Y_{\varepsilon_t}Y_{\varepsilon_c}\geq X_{\varepsilon_t}X_{\varepsilon_c}\ . \tag{4.42}$$

Therefore, the two types of orthotropy ($L=0$ or 1) are directly linked to the first two inequalities.

Thanks to the polar formalism, similarly to the case of the Tsai-Wu criterion, we can see that the term P_{xxyy} can be simplified with respect to eq. (2.35) in two cases:

$$\begin{aligned} \Lambda_0=0: \quad P_{xxyy}&=\frac{1}{2}\left(\frac{1}{X_{\varepsilon_t}X_{\varepsilon_c}}+\frac{1}{Y_{\varepsilon_t}Y_{\varepsilon_c}}-\frac{4}{S_\varepsilon^2}\right),\\ \text{Isotropy, i.e. } \Lambda_0=\Lambda_1=0: \quad P_{xxyy}&=\frac{1}{X_{\varepsilon_t}X_{\varepsilon_c}}-\frac{2}{S_\varepsilon^2}. \end{aligned} \tag{4.43}$$

The first one, $\Lambda_0=0$, represents a material with the so-called R_0-orthotropy ($\Lambda_0=0$) for which the characterisation of the orthotropic strength tensor $\mathbf{P}$ is given by four, and not five, polar invariants: Γ_0, Γ_1 and Λ_1. As shown in eq. (4.43), the term P_{12} of the Zhang-Evans tensor $\mathbf{P}$ depends only upon the properties of normal and shear yield strains, and not on other material properties like in (2.35). The second case of eq. (4.43) concerns the isotropic case. Of course, in this case the further reduction of independent components, *a fortiori* leads to a simplest formulation of P_{12}.

Similarly, the polar components of $\boldsymbol{p}$, for an orthotropic material, in terms of limit strain properties can be obtained from eqs. (4.8), and are

$$\left\{\begin{array}{ll} 2\Gamma= & \dfrac{X_{\varepsilon_c}-X_{\varepsilon_t}}{X_{\varepsilon_t}X_{\varepsilon_c}}+\dfrac{Y_{\varepsilon_c}-Y_{\varepsilon_t}}{Y_{\varepsilon_t}Y_{\varepsilon_c}},\\ 2\Lambda= & \dfrac{X_{\varepsilon_c}-X_{\varepsilon_t}}{X_{\varepsilon_t}X_{\varepsilon_c}}-\dfrac{Y_{\varepsilon_c}-Y_{\varepsilon_t}}{Y_{\varepsilon_t}Y_{\varepsilon_c}}. \end{array}\right. \tag{4.44}$$

Below, some special cases already considered in Sec. 4.3 are discussed. The way the Cartesian formulation is obtained is completely equivalent to that used for the stress-based criteria in Sec. 4.4.1.

Case 1: $V=0$**.**

Eq. (4.11) shows that only the spherical part of the criterion is present in this case coupling the spherical part of tensor $\boldsymbol{\varepsilon}$ with an isotropic component of $\mathbf{P}$. A spherical strain field ($V=0$) leads to failure when:

$$F_{ZE}=\varepsilon^2\left(\frac{1}{X_{\varepsilon_t}X_{\varepsilon_c}}+2P_{12}+\frac{1}{Y_{\varepsilon_t}Y_{\varepsilon_c}}\right)+\varepsilon\left(\frac{X_{\varepsilon_c}-X_{\varepsilon_t}}{X_{\varepsilon_t}X_{\varepsilon_c}}+\frac{Y_{\varepsilon_c}-Y_{\varepsilon_t}}{Y_{\varepsilon_t}Y_{\varepsilon_c}}\right)\geq 1. \tag{4.45}$$

This expression is very similar to that of the Tsai-Wu criterion in Tab. 4.5 for the case of spherical stress state. This time the quantities involved are the strains and the yield strain properties of the material.

Case 2: $U = 0$**.**

When U is null, the strain field is completely deviatoric with $\varepsilon_{xx} = -\varepsilon_{yy} = V\cos 2\Upsilon$ and $\varepsilon_{xy} = V\sin 2\Upsilon$. If we choose a frame in which $\Omega_1 = 0$, the criterion in terms of Cartesian components is:

$$\begin{aligned} F_{ZE} = \; & \varepsilon_{xx}^2\left(\frac{1}{X_{\varepsilon_t}X_{\varepsilon_c}} - 2P_{12} + \frac{1}{Y_{\varepsilon_t}Y_{\varepsilon_c}}\right) + 4\varepsilon_{xy}^2\left(\frac{1}{S_\varepsilon^2} + P_{12}\right) + \\ & + \varepsilon_{xx}\left(\frac{X_{\varepsilon_c} - X_{\varepsilon_t}}{X_{\varepsilon_t}X_{\varepsilon_c}} - \frac{Y_{\varepsilon_c} - Y_{\varepsilon_t}}{Y_{\varepsilon_t}Y_{\varepsilon_c}}\right) \leq 1. \end{aligned} \tag{4.46}$$

Case 3: Isotropic material.

Again in terms of strength properties, conditions $\Lambda_0 = \Lambda_1 = 0$ and $\Lambda = 0$ become now

$$\begin{gathered} X_{\varepsilon_t}X_{\varepsilon_c} = Y_{\varepsilon_t}Y_{\varepsilon_c} = S_\varepsilon^2/(S_\varepsilon^2 P_{12} + 2), \\ X_{\varepsilon_c} - X_{\varepsilon_t} = Y_{\varepsilon_c} - Y_{\varepsilon_t}. \end{gathered} \tag{4.47}$$

In this way, eq. (4.19) becomes

$$\begin{aligned} F_{ZE} = \; & \left(\frac{1}{X_{\varepsilon_t}X_{\varepsilon_c}} + \frac{1}{S_\varepsilon^2}\right)\left(\varepsilon_{xx}^2 + \varepsilon_{yy}^2\right) + \frac{8\varepsilon_{xy}^2}{S_\varepsilon^2} - 2\varepsilon_{xx}\varepsilon_{yy}\left(\frac{1}{X_{\varepsilon_t}X_{\varepsilon_c}} + \frac{2}{S_\varepsilon^2}\right) + \\ & + \left(\frac{X_{\varepsilon_c} - X_{\varepsilon_t}}{X_{\varepsilon_t}X_{\varepsilon_c}}\right)(\varepsilon_{xx} + \varepsilon_{yy}) \leq 1, \end{aligned} \tag{4.48}$$

that represents the first formulation, to our knowledge, of failure criterion for isotropic materials, with different strength in tension and compression, derived from the most general criterion of Zhang-Evans for anisotropic materials.

4.5 Concluding remarks

In this Chapter, four different polynomial failure criteria have been formulated within the framework of the polar formalism. The physical meaning of each one of the polar strength parameters has been examined. In particular, the polar angle Ω_1 represents the main strength orthotropy orientation and the value of the polar invariant L denotes two different types of ordinary strength orthotropy.

In Sec. 4.4.1, a new result has been obtained; the component F_{xxyy} of the Tsai-Wu fourth order tensor can get an exact value for two kinds of material: R_0-orthotropic materials and isotropic materials. In these two cases, the term F_{xxyy} depends on the normal and shear strength properties but not on the applied stresses, so it becomes a peculiar property of the material. Similarly, the component P_{xxyy} of the Zhang-Evans fourth order tensor can take a simpler expression for R_0-orthotropic materials and isotropic materials. In these two cases the term P_{xxyy} depends only upon the limit strain properties of the material and not also on the elastic moduli.

Moreover, in the case of a spherical stress/strain field with $\upsilon_{xx} = \upsilon_{yy}$, the failure indexes are every time equal to

$$F_{\dots} = 8U^2\Gamma_1 + 2U\Gamma. \tag{4.49}$$

This means that the failure is independent from the type of material symmetry and regards only the isotropic part of the weakness/strength tensors. A practical example of

this phenomenon can be that of the inflated membranes. In all the other cases the failure is influenced by anisotropy and hence by orientation.

The polar expression of the four criteria has been determined also for isotropic materials with different strength in tension and compression. In particular, the Hoffman criterion gives, for an isotropic material, the condition of the recently formulated Christensen criterion, so it can be considered as an extension of this last one, whereas the Tsai-Wu and Zhang-Evans criteria give two new formulations for the prediction of failure in isotropic materials that, to the best of our knowledge, are not present in the literature.

5

Optimal material orientation through minimisation of failure indexes

5.1 Introduction

In Chapter 4 we have expressed the unified formulation of the failure criteria of Tsai-Hill, Hoffman, Tsai-Wu and Zhang-Evans through invariants. In this Chapter we will use such invariant formulation as a functional in order to maximise the strength of an orthotropic ply, taking as design variable the orthotropy direction, Ω_1. The objective function is the failure index of one among the polynomial failure criteria considered in Chapter 2. We will separate the failure indexes into two main groups:

- the quadratic failure indexes: we put in this group all the failure criteria characterised only by quadratic terms, namely the Tsai-Hill criterion expressed in terms of stresses or strains;
- the quadratic *plus* linear failure indexes: in this class, we group all the failure criteria characterised by quadratic and linear terms, like the Tsai-Wu criterion expressed in terms of stresses or strains.

The aim is to find the orientation of the orthotropy axes of the material minimising the objective function, written using the polar formalism, which presents the following advantages:

1. the use of material intrinsic, i.e. frame independent, quantities;
2. the possibility of stating, by these quantities, the material symmetries;
3. the fact that the material orientation, denoted by Ω_1, appears explicitly among the variables;

5.2 Minimising the quadratic failure indexes

In Sec. 4.4.1 we have yet expressed the failure index (in terms of stresses or strains) for an orthotropic material with a given principal orthotropic direction Ω_1. Now, the angle

Ω_1 becomes the design variable. The failure index for an orthotropic material when using a quadratic failure criterion is

$$F_{Quad} = 4V^2 \left[\Gamma_0 + (-1)^L \Lambda_0 \cos 4\left(\Omega_1 - \Upsilon\right)\right] + 8U^2\Gamma_1 + 16UV\Lambda_1 \cos 2\left(\Omega_1 - \Upsilon\right), \quad (5.1)$$

where the relation between the polar parameters U, V and the principal stress/strain components $\upsilon_I, \upsilon_{II}$ is given in eq. (4.36). The polar angle Υ represents the direction of the higher principal stress/strain component. Eq. (5.1) is the objective function to be minimised. Therefore the minimisation problem can be defined as follow:

$$\min_{\Omega_1} F_{Quad}\left(\Gamma_0, \Gamma_1, \Lambda_0, \Lambda_1, L, \Omega_1, U, V, \Upsilon\right). \quad (5.2)$$

Problem (5.2) is completely analogous to the minimisation problem of the strain energy density with "fixed strain state", see [88], with only one design variable: the angle Ω_1. The next step concerns the analytical search of the stationary points of F_{Quad}, i.e. of the directions of the maximum weakness/strength. Putting the first derivative to zero gives:

$$\frac{\partial F_{Quad}}{\partial \Omega_1} = -32V \sin 2\left(\Omega_1 - \Upsilon\right)\left[(-1)^L \Lambda_0 V \cos 2\left(\Omega_1 - \Upsilon\right) + \Lambda_1 U\right] = 0. \quad (5.3)$$

Eq. (5.3) is satisfied by anyone of the following conditions:

$$\begin{cases} V = 0: \text{ spherical stress/strain field,} \\ \Lambda_0 = \Lambda_1 = 0: \text{ isotropic material,} \\ \sin 2\left(\Omega_1 - \Upsilon\right) = 0 \;\Rightarrow\; \Omega_1 - \Upsilon = \left\{0, \dfrac{\pi}{2}\right\}, \\ \cos 2\left(\Omega_1 - \Upsilon\right) = -\dfrac{\Lambda_1 U}{(-1)^L \Lambda_0 V}, \text{ with } \dfrac{|\,U\,|}{V} \leq \dfrac{\Lambda_0}{\Lambda_1}. \end{cases} \quad (5.4)$$

The first two cases are trivial and exclude any possible optimisation of the strength by varying the orthotropy direction, but the last two give three different stationary points to be compared:

$$\begin{aligned} \Omega_1 &= \Upsilon, && \text{denoted as solution} \quad x_a, \\ \Omega_1 &= \Upsilon + \pi/2, && \text{denoted as solution} \quad x_b, \\ \Omega_1 &= \Upsilon \pm \frac{1}{2} \arccos\left[-(-1)^L \frac{\Lambda_1 U}{\Lambda_0 V}\right], && \text{denoted as solution} \quad x_c\,. \end{aligned} \quad (5.5)$$

The third solution, x_c, exist only for $\dfrac{|\,U\,|}{V} \leq \dfrac{\Lambda_0}{\Lambda_1}$. The orthotropy direction Ω_1 minimising F_{Quad} is directly linked to the direction Υ of the higher principal stress/strain υ_I.

We can, now, evaluate the sign of the second order derivative to check the local conditions of minimum or maximum of F_{Quad} at the stationary points given in eq. (5.5):

$$\frac{\partial^2 F_{Quad}}{\partial \Omega_1^2} = -64V\left[(-1)^L \Lambda_0 V \cos 4(\Omega_1 - \Upsilon) + \Lambda_1 U \cos 2(\Omega_1 - \Upsilon)\right]. \quad (5.6)$$

In addition, the following condition on the stress/strain tensor $\boldsymbol{\upsilon}$ will be taken into account:

$$\text{if } \upsilon_I \geq \upsilon_{II}, \text{ then } \begin{cases} U \leq 0 \;\Leftrightarrow\; |\upsilon_I| \leq |\upsilon_{II}|, \\ U \geq 0 \;\Leftrightarrow\; |\upsilon_I| \geq |\upsilon_{II}|, \end{cases} \quad (5.7)$$

with $U = (\upsilon_I + \upsilon_{II})/2$.

The type of ordinary orthotropy affects the solution of this problem. We consider separately the two cases of $L = 0$ and $L = 1$.

1) $L = 0$
Eq. (5.6) in the stationary local points of eq. (5.5) becomes

$$\begin{aligned}
\left.\frac{\partial^2 F_{Quad}}{\partial \Omega_1^2}\right|_{x_a} &= -64V\left[\Lambda_0 V + \Lambda_1 U\right] > 0 \qquad \text{if} \qquad \frac{U}{V} < -\frac{\Lambda_0}{\Lambda_1},\\
\left.\frac{\partial^2 F_{Quad}}{\partial \Omega_1^2}\right|_{x_b} &= -64V\left[\Lambda_0 V - \Lambda_1 U\right] > 0 \qquad \text{if} \qquad \frac{U}{V} > \frac{\Lambda_0}{\Lambda_1},\\
\left.\frac{\partial^2 F_{Quad}}{\partial \Omega_1^2}\right|_{x_c} &= -64V\left[\frac{\Lambda_1^2 U^2 - \Lambda_0^2 V^2}{\Lambda_0 V}\right] > 0 \quad \text{if} \quad -\frac{\Lambda_0}{\Lambda_1} < \frac{U}{V} < \frac{\Lambda_0}{\Lambda_1}.
\end{aligned} \tag{5.8}$$

Each term of eq. (5.8) is a positive quantity excepting for U. Moreover, the sign of the second derivative depends on the ratio of the stress components U/V with respect to Λ_0/Λ_1. All the conditions of eqs. (5.8) that concern U/V belong to different and independent ranges of values of U/V. Moreover, the third solution of (5.8) respect the bounds on the last condition of eq. (5.4), so, the stationary points of (5.5) are solutions for the maximum of strength.

2) $L = 1$
Eq. (5.6) in the stationary local points of eq. (5.5) becomes

$$\begin{aligned}
\left.\frac{\partial^2 F_{Quad}}{\partial \Omega_1^2}\right|_{x_a} &= -64V\left[-\Lambda_0 V + \Lambda_1 U\right] > 0 \qquad \text{if} \quad \frac{U}{V} < \frac{\Lambda_0}{\Lambda_1},\\
\left.\frac{\partial^2 F_{Quad}}{\partial \Omega_1^2}\right|_{x_b} &= 64V\left[\Lambda_0 V + \Lambda_1 U\right] > 0 \qquad \text{if} \quad \frac{U}{V} > -\frac{\Lambda_0}{\Lambda_1},\\
\left.\frac{\partial^2 F_{Quad}}{\partial \Omega_1^2}\right|_{x_c} &= -64V\left[\frac{-\Lambda_1^2 U^2 + \Lambda_0^2 V^2}{\Lambda_0 V}\right] > 0 \quad \text{if} \quad \frac{U}{V} > \frac{\Lambda_0}{\Lambda_1}, \frac{U}{V} < -\frac{\Lambda_0}{\Lambda_1}.
\end{aligned} \tag{5.9}$$

In this case, the last equation is never satisfied because the value of U/V violates the boundaries on solution x_c imposed in the last equation of (5.4). Hence, only the first two stationary points can be a minimum. We can compare, in this case, the value of F_{Quad} in this two points:

$$F_{Quad}|_{x_a} - F_{Quad}|_{x_b} = 32UV\Lambda_1. \tag{5.10}$$

The minimum of F_{Quad} depends strictly from the sign of U. For $U > 0$ the solution is given by x_b, while for $U < 0$ the solution is given by x_a.

In Fig. 5.1, we show a summary of the solutions found above; in this figure, μ is the direction angle of the principal stress having the least absolute value, i.e.

$$\mu = \mathrm{dir}\left(\min\left\{|\upsilon_I|, |\upsilon_{II}|\right\}\right), \tag{5.11}$$

and

$$\xi = \frac{1}{2}\arccos\left[-(-1)^L \frac{\Lambda_1 U}{\Lambda_0 V}\right]. \tag{5.12}$$

As Υ is the direction of the principal stress/strain υ_I, taking into account eq. (5.7), it is $\mu = \Upsilon$ for $U < 0$, while $\mu = \Upsilon + \pi/2$ for $U > 0$. The use of the angle μ is useful in

strength problems, because it represents the direction of the least stress/strain for the material. This figure shows that for $\dfrac{|U|}{V} > \dfrac{\Lambda_0}{\Lambda_1}$ the optimal solution Ω_1^{opt} is equal for the two types of orthotropy ($L = 0$ and $L = 1$), while for $\dfrac{|U|}{V} < \dfrac{\Lambda_0}{\Lambda_1}$ the solution Ω_1^{opt} for $L = 0$ becomes anti-optimal for $L = 1$. Therefore, the type of orthotropy plays a decisive role in the optimisation of strength. This kind of influence of the type of orthotropy upon an optimal solution has been already found in other problems concerning the elastic response of anisotropic structures, see [80].

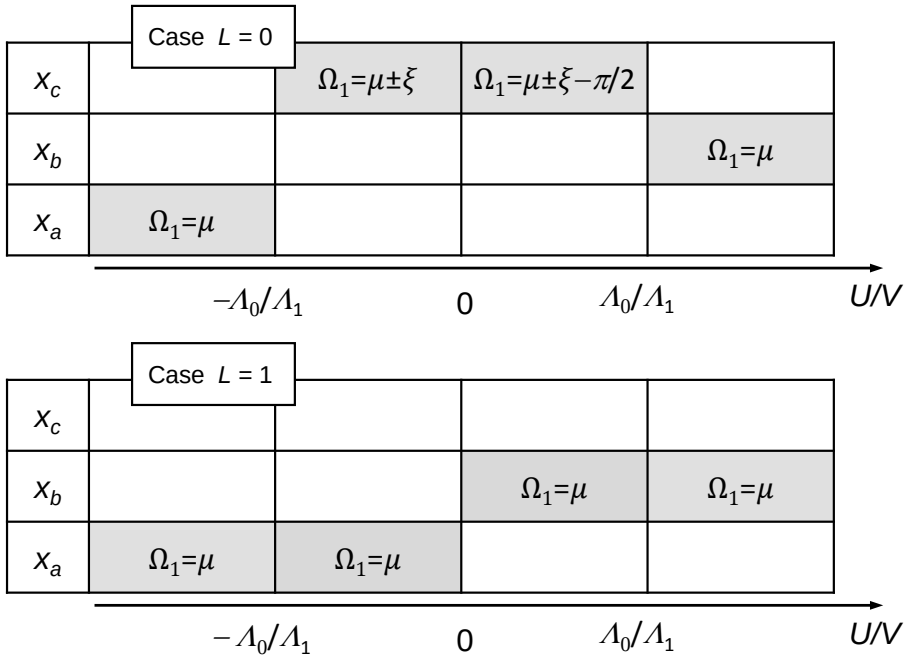

Figure 5.1: Optimal orthotropy orientation minimising the failure index of *quadratic* criteria.

A last remark: the above results clearly show, by an invariant relation, the link between the anisotropy strength properties of the material and the stress/strain field for obtaining the optimal orientation of the material. A similar result, will be obtained in the next section, where the *Quadratic plus Linear* (QL) criteria are considered.

5.3 Minimising the quadratic *plus* linear failure indexes

Proceeding in a similar way, the quadratic *plus* linear failure index F_{QL} for an orthotropic material is

$$\begin{aligned} F_{QL} = \; & 4V^2\left[\Gamma_0 + (-1)^L \Lambda_0 \cos 4\left(\Omega_1 - \Upsilon\right)\right] + 8U^2\Gamma_1 + 16UV\Lambda_1 \cos 2\left(\Omega_1 - \Upsilon\right) + \\ & + 2U\Gamma + 2V\Lambda \cos 2\left(\Omega_1 - \Upsilon\right). \end{aligned} \tag{5.13}$$

The minimisation problem is equivalent to (5.2). In addition, as mentioned in Sec. 4.3, the orthotropic orientations Ω_1 and Ω of the tensors $\mathbf{H}$ and $\mathbf{h}$ are assumed to be the same.

The minimum of the objective function F_{QL} with respect to the principal orthotropic direction Ω_1 can be calculated using the same procedure used in the previous Section. First, we impose the first derivative to be null:

$$\frac{\partial F_{QL}}{\partial \Omega_1} = -4V \sin 2\left(\Omega_1 - \Upsilon\right)\left[8(-1)^L \Lambda_0 V \cos 2\left(\Omega_1 - \Upsilon\right) + 8\Lambda_1 U + \Lambda\right] = 0; \tag{5.14}$$

this equation is satisfied when

$$\begin{cases} V = 0: \text{ spherical stress/strain field,} \\ \Lambda_0 = \Lambda_1 = \Lambda = 0: \text{ isotropic material,} \\ \sin 2\left(\Omega_1 - \Upsilon\right) = 0 \;\Rightarrow\; \Omega_1 - \Upsilon = \left\{0, \dfrac{\pi}{2}\right\}, \\ \cos 2\left(\Omega_1 - \Upsilon\right) = -\dfrac{(8\Lambda_1 U + \Lambda)}{8(-1)^L \Lambda_0 V}, \text{ with } -\dfrac{(8\Lambda_0 V + \Lambda)}{8\Lambda_1} \leq U \leq \dfrac{8\Lambda_0 V - \Lambda}{8\Lambda_1}. \end{cases} \tag{5.15}$$

We can notice that, due to the introduction of linear terms in the expression of these criteria, isotropy, for strength, is characterised by three parameters, not by two, like in elasticity and in the quadratic criteria (and, also, there are three invariant conditions of isotropic strength for these criteria). This time, differently from the simple quadratic case, the range of existence of U for the third stationary point depends on the anisotropic polar parameters of $\mathbf{H}$ and $\mathbf{h}$ and also on the deviatoric component of the stress/strain tensor υ that cannot be separated from the weakness/strength polar parameters.

A comparison must be done between the values of F_{QL} for

$$\begin{aligned} \Omega_1 = \Upsilon, &\quad \text{denoted as solution} \quad x_a, \\ \Omega_1 = \Upsilon + \pi/2, &\quad \text{denoted as solution} \quad x_b, \\ \Omega_1 = \Upsilon \pm \frac{1}{2}\arccos\left[-(-1)^L \frac{(8\Lambda_1 U + \Lambda)}{8\Lambda_0 V}\right], &\quad \text{denoted as solution} \quad x_c. \end{aligned} \tag{5.16}$$

We can analyse the second order derivatives to verify the conditions of minimum or maximum of F_{QL} with respect to the stationary points given by eq. (5.16):

$$\frac{\partial^2 F_{QL}}{\partial \Omega_1^2} = -8V\left[8(-1)^L \Lambda_0 V \cos 4(\Omega_1 - \Upsilon) + (8\Lambda_1 U + \Lambda)\cos 2(\Omega_1 - \Upsilon)\right]. \tag{5.17}$$

Again, two cases have to be considered separately.

1) $L = 0$

If we impose $L = 0$, eq. (5.17), evaluated in the stationary points of eq. (5.16), becomes

$$\begin{aligned} \left.\frac{\partial^2 F_{QL}}{\partial \Omega_1^2}\right|_{x_a} &= -8V\left[8\Lambda_0 V + 8\Lambda_1 U + \Lambda\right] > 0 \qquad \text{if} \quad U < -\frac{(8\Lambda_0 V + \Lambda)}{8\Lambda_1}, \\ \left.\frac{\partial^2 F_{QL}}{\partial \Omega_1^2}\right|_{x_b} &= -8V\left[8\Lambda_0 V - 8\Lambda_1 U - \Lambda\right] > 0 \qquad \text{if} \quad U > \frac{8\Lambda_0 V - \Lambda}{8\Lambda_1}, \\ \left.\frac{\partial^2 F_{QL}}{\partial \Omega_1^2}\right|_{x_c} &= 8V\left[8\Lambda_0 V - \frac{(8\Lambda_1 U - \Lambda)^2}{8\Lambda_0 V}\right] > 0 \quad \text{if} \quad -\frac{(8\Lambda_0 V + \Lambda)}{8\Lambda_1} < U < \frac{8\Lambda_0 V - \Lambda}{8\Lambda_1}. \end{aligned} \tag{5.18}$$

If we consider that each term in eq. (5.18) is a polar invariant, they all are positive quantities except for U, so, an evaluation of the sign of U is necessary to determine the sign of the second derivative. There is also a second condition that concerns the value of

U with respect to $(8\Lambda_0 V \pm \Lambda)/8\Lambda_1$. Finally, with an analysis on the sign and on the value of U we can determine the global minimum of the F_{QL} and the optimal orientation Ω_1 to maximise the strength behaviour of the continuum. All the conditions of eqs. (5.18) belong to different and independent ranges of values of U. Moreover, the third solution of (5.18) respects the bounds on the last condition of eq. (5.15), so, the stationary points of (5.16) are solutions for the maximum of strength.

2) $L = 1$
Eq. (5.17) in the stationary local points of eq. (5.16) becomes

$$\begin{aligned}
&\left.\frac{\partial^2 F_{QL}}{\partial \Omega_1^2}\right|_{x_a} = -8V\left[-8\Lambda_0 V + 8\Lambda_1 U + \Lambda\right] > 0 \quad \text{if} \quad U < \frac{8\Lambda_0 V - \Lambda}{8\Lambda_1},\\
&\left.\frac{\partial^2 F_{QL}}{\partial \Omega_1^2}\right|_{x_b} = 8V\left[8\Lambda_0 V + 8\Lambda_1 U + \Lambda\right] > 0 \qquad \text{if} \quad U > -\frac{8\Lambda_0 V + \Lambda}{8\Lambda_1},\\
&\left.\frac{\partial^2 F_{QL}}{\partial \Omega_1^2}\right|_{x_c} = 8V\left[\frac{(8\Lambda_1 U + \Lambda)^2}{8\Lambda_0 V} - 8\Lambda_0 V\right] > 0 \quad \text{if} \quad U < -\frac{(8\Lambda_0 V + \Lambda)}{8\Lambda_1}, U > \frac{8\Lambda_0 V - \Lambda}{8\Lambda_1}.
\end{aligned} \tag{5.19}$$

Eqs. (5.19) give us the ranges of values for which the second derivative is positive in the stationary points. The third condition violates the bound on the last condition of eqs. (5.15), while the first two can be satisfied independently. The difference between the values of F_{QL} in the first two stationary points is

$$F_{QL}|_{x_a} - F_{QL}|_{x_b} = 32UV\Lambda_1 + 4V\Lambda. \tag{5.20}$$

Hence, the solution depends on the value of U with respect to the ratio $-\Lambda/8\Lambda_1$.

Fig. 5.2 summarises the results obtained beforehand, for the cases of the *quadratic plus linear* failure indexes; the direction angle ψ is

$$\psi = \frac{1}{2}\arccos\left[-(-1)^L \frac{8\Lambda_1 U + \Lambda}{8\Lambda_0 V}\right] \tag{5.21}$$

For the sake of clarity, we have used two separate figures, when $L = 0$, depending upon the value of V with respect to $\Lambda/8\Lambda_0$. In this case, the range $-\dfrac{\Lambda}{8\Lambda_1} < U < 0$ of $L = 0$ gives a value of Ω_1^{opt} that is anti-optimal for the same range when $L = 1$, hence the difference between the two types of orthotropy ($L = 0$ and $L = 1$) must be taken into account because the solution is strictly dependent from this parameter.

5.4 Comparison between optimal material orientations

Figs. 5.1 and 5.2 resume the solutions maximising the strength of orthotropic materials with respect to the direction of maximum weakness/strength Ω_1. We have shown the possibility of having two different groups of solutions, depending upon the type of ordinary orthotropy L.

The polar formulation of the quadratic failure criteria, very close to that of the strain energy density, leads the strength optimisation to the same type of solutions obtained for the stiffness optimisation [88]. Namely, for $L = 0$ one optimal orientation of Ω_1 depends

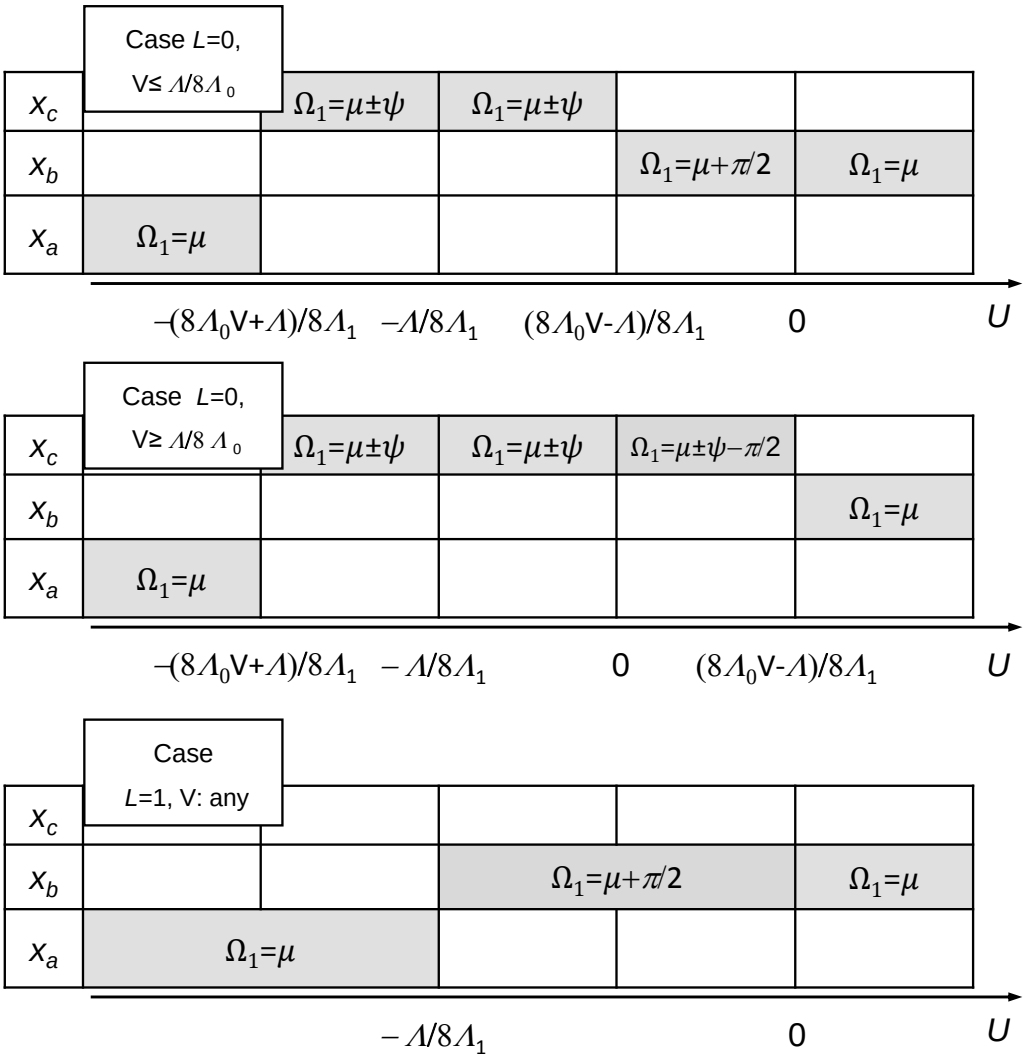

Figure 5.2: Optimal orthotropy orientation minimising the failure index of *quadratic plus linear* criteria.

only upon Υ, while the other one depends also upon the stress/strain tensor (U,V) and on the anisotropic part of the weakness/strength tensor $\mathbf{H}$, (Λ_0,Λ_1). In this sense, the solution is qualitatively similar to that of maximal compliance/stiffness but the actual values of the orthotropy direction minimising compliance and strength may be different, in general. On the other hand, for $L = 1$ the solutions give an orientation of Ω_1 aligned with the principal stress/strain component that has the minimum absolute value. Hence, in this case the optimal orientation of an orthotropic material to maximise the strength is always aligned with the one maximising the stiffness.

Some considerations are also important for the minimisation of the quadratic plus linear failure indexes. The solution to this problem may be different from that obtained using the quadratic criteria: this is due to the presence of the linear terms. For $L = 1$, a different range of values of U with respect to the ratio $\dfrac{\Lambda}{8\Lambda_1}$ is obtained to separate the optimal solutions. The first and last ones give an optimal orientation aligned with the principal stress/strain component having the minimum absolute value that corresponds

to the optimal orientation obtained using the quadratic criteria, while the second range of U gives a Ω_1^{opt} aligned with the principal stress/strain component having the maximum absolute value. In a similar way, new types of solutions appear for $L = 0$: they are function of the principal stress/strain component having the maximum absolute value. Hence the correspondence of the directions maximising strength and stiffness, observed in the case of the quadratic criteria, is present, in the case of the quadratic plus linear criteria, only in the first and last cases of $L = 0$ and $L = 1$ and in some intermediary cases of $L = 0$.

In conclusion, we can assert that the optimal orthotropy orientation to maximises the strength, depending on the type of orthotropy L and on the values U and V of the stress/strain tensor $\boldsymbol{\upsilon}$ with respect to the anisotropic part of the weakness/strength tensors $\mathbf{H}$ and $\mathbf{h}$, can be equal or different to the one that maximise the stiffness and can also be the same or different for the considered criteria. A last remark: as it is apparent from Figs. 5.1 and 5.2, in some cases the uniqueness of the optimal solution is lost; this occurrence depends always upon a particular combination of the values of the polar invariants of the stress/strain state and of the tensors describing the strength criterion.

5.5 Concluding remarks

Strength optimisation for an orthotropic ply has been considered in this Chapter. The polar formulation of the failure indexes has been taken as objective function, while the ordinary orthotropy direction has been considered as the optimisation variable. We have shown the possibility of having two different groups of solutions, depending upon the type of orthotropy. For the two groups, we derived analytically the different solution with respect to the polar components of the failure criteria. Results show that the type of orthotropy plays a decisive role in the optimisation of strength and that, depending on the values of the stresses/strains and of the polar parameters of the failure criteria, the optimal orientation of the material that maximises strength can be equal to or different from the one that maximises stiffness and can also be the same or not for the different criteria. This means that it is possible to obtain *in some cases* an orthotropic plate that is simultaneously optimised with respect to two important engineering requirements, stiffness and strength.

The way we deal with the problem of finding the optimal material orientation to maximise strength is very similar to the analytical approach presented in [40] by Majak and Hannus. They presented an analytical expression of the optimal material orientation, in the bi-dimensional space, for any orthotropic material considering the Tsai-Hill and Tsai-Wu criteria. The solution depended upon some terms that do not have, at least apparently, an explicit mechanical meaning. On the other hand, in our work, thanks also to the polar formalism, we give a new and more general approach to this problem. The results found in this Chapter, are essentially two. First of all we present a very general analytical solution whose formulation is valid for more different criteria that can be expressed, indifferently, in terms of stresses or strains. Secondly, the parameters L, Λ_0 and Λ_1 on which the solution depends have a clear physical meaning and, so, they directly give a mechanical appraisal of the optimal orientation.

Part III

Optimising stiffness and strength of laminated structures: a two-step strategy

6

Introducing an optimisation strategy for the simultaneous maximisation of stiffness and strength

6.1 Introduction

As previously discussed in Chapter 3, unlike the design procedures for metallic structures, the optimal design of a laminated structure needs a further phase to take into account for the material design. The design of anisotropic laminated structures depends upon a large number of design variables: the material properties, the orientation angle and the thickness of each ply, along with the number of constitutive layers. Thus, accounting for all these design variables make the design process of composite materials and structures a very complex task. For this reason, several authors use a sort of model reduction, splitting the optimum problem into two subsequent and coupled problems. Concerning the stiffness and strength optimisation of a structure, almost all the works, in the literature, focus on the maximisation of only one of these two properties. When the second one is considered, it is usually included into the optimisation process as a constraint.

In this Chapter we introduce a problem for the simultaneous maximisation of both stiffness and strength of a laminated structure. The aim is to include the strength optimisation into an existing strategy developed to maximise uniquely the stiffness of composite structures: the two-step hierarchical optimisation strategy for laminated plates using the polar formulation [31].

6.2 The optimisation problem of stiffness and strength and the hierarchical resolution strategy

6.2.1 Statement of the optimisation problem

The goal of the present study is to propose a novel strategy to include the optimisation of stiffness and strength in the same design process of a laminated structure. This is a relevant problem in structural design: both stiffness and strength are fundamental requirements for a structure. Nevertheless, rarely they are taken into account simultaneously as leading objectives in an optimum design. More often, stiffness is considered as the leading objective and strength is taken into account as a constraint to the design.

In other cases, a vectorial optimum problem, i.e. with the two objectives, is formulated. Unlike these cases, the problem that we consider is the following one:

To determine the best distribution of the anisotropy for a laminated structure that has to be simultaneously the stiffest and the strongest one.

Some details must, of course, be given to render the above problem well posed; hence, let us list the assumptions and basic points of our research, so as to precise the exact context of our study:

1. we consider a laminated structure, whose *geometry, boundary conditions and applied loads are knowns and fixed*;
2. the stacking sequence is composed by *identical plies*, i.e. by plies all composed of the same material and having the same thickness;
3. the material composing the basic plies is *chosen a priori once and for all*; hence, it does not take part into the optimisation process;
4. each ply is constituted by an *orthotropic material*, whose behaviour is sensibly *linearly elastic up to its ultimate load*;
5. the total thickness h of the laminate is fixed and is the same everywhere; as a consequence, by assumption 2, the number of layers is *fixed and known a priori* as well: it cannot be modified during the optimisation process;
6. the structure is subject to only *in-plane loads*;
7. the laminate has to be *orthotropic everywhere*;
8. the laminate has to be *extension-bending uncoupled everywhere*;
9. the design variables describing stiffness are *independent* from those describing strength;
10. the only common parameter of stiffness and strength is the *direction*: we assume that the laminate is orthotropic not only for the stiffness, but also for the strength, and that the *direction of the orthotropy axes is exactly the same (or turned of $\pi/2$) for both the cases*;
11. the strength properties of the laminate can be condensed in the *components of an elasticity-like fourth order plane tensor*;
12. the relevant mechanical parameters for the optimisation of the laminated structure stiffness and strength are the *polar invariants* of the tensors describing the different mechanical properties;
13. we take the CLPT as kinematic model for the laminate;
14. the limit state is modelled by the Tsai-Hill failure criterion.

Some commentaries about the above assumptions are needed; they are given in the following section.

6.2.2 Discussion of the assumptions

First of all, we do not act upon the geometry, nor upon the boundary conditions to enhance the mechanical performances of the structure, but upon the *distribution of anisotropy*. In some sense, with a slight abuse of language taken from classical topology structural optimisation, where the optimal geometry is looked for in the case of a known material composing the system, we could class such a type of problem as an *anisotropy topology optimisation problem*.

So, we act on the distribution of anisotropy to enhance the mechanical performances of the structure. Nevertheless, such anisotropy is not completely free: it is actually the anisotropic behaviour of a laminate composed by a fixed number of plies of a chosen material. As such, it cannot take all the possible values for its elastic and strength moduli. In fact, a laminate is a sort of *restricted class* of elastic materials, [81], and this point gives, as a consequence, some constraints to the optimum problem, see Sec. 1.6.1 and Chapter 7.

However, what is completely free is the orientation of the anisotropy. One has hence a certain interest in using a mathematical representation of anisotropy that allows, on one side, to let appear directly the orientation of the mechanical anisotropic behaviour, and on the other side to let disappear from the problem, and in particular from the set of unknowns, the elastic and strength moduli that cannot be modified by the optimisation process. In fact, the use of identical layers has an immediate consequence: the elastic or strength behaviour of the laminate cannot be completely designed by the optimisation process, but only a part of it, namely its anisotropic part, while its isotropic part remains unaffected and equal to that of the basic ply, [83], recall also what said in Sec. 1.6. The polar method, allowing all of these points, seems to be the best mathematical representation of anisotropy for such a kind of problems; that is why we have used it.

Concerning assumptions 2 and 3, they are rather usually done in such a kind of problems, while assumption 4 corresponds to the most part of composite materials normally employed in structural applications, such as pre-pregs layers in carbon-epoxy or glass-epoxy.

Assumption 5 is introduced for two reasons: first of all, we do not focus here on the optimisation of the structural weight, but of the anisotropy field; then, this assumption is necessary to render the structural optimisation problem well posed, both for strength and for stiffness. In fact, without this assumption, that actually constitutes the well known iso-perimetric constraint of a classical, e.g., stiffness maximisation problem, the problem itself would be meaningless; the stiffest and strongest structure would be simply the one having an infinite thickness.

Assumption 6 is only slightly limiting our study, but in this phase it is still necessary. Taking into account for both the extension and bending behaviour in the optimisation of a laminated structure is still an open problem: the size of the problem increases, in the sense that the design space has a greater dimension, but its topology is still unknown, because the relations between the design variables concerning extension and bending are still not known, in general. So, we have preferred to concentrate our study on a general procedure for the simultaneous maximisation of stiffness and strength and to apply it to the more important case, for applications, of in-plane loads, that is what mainly happens to slender, stiffened structures, as those normally constituted by laminates. We precise also that the translation of the present work to unstretched bended laminated structures is almost straightforward.

Assumptions 7 and 8 are classical assumptions in laminate design; anyway, we precise

since now that, unlike what normally done in the largest part of works in the matter, we do not make use of *short-cuts* usually employed by designers to obtain orthotropy and/or uncoupling (typically, for the case of in-plane orthotropy the use of balanced symmetric stacks). In fact, we state the problem as completely free: orthotropy and uncoupling take part to the optimisation problem, i.e. they compose the objective function, namely for the second step problem, see Chapter 8. In this way, the search for the optimal stack is completely free and general, it happens in the largest dimensional space allowed by the problem, i.e. in the space of orientations, whose dimension is $n-1$, n being the number of plies, not restricted by some a priori assumptions (for instance, the use of symmetric stacks divides by two the dimension of the search space). This is rather important in our approach: because of the subsequent assumption 9, it is worth to search for the optimal stack, matching the requirements on stiffness and strength, over the largest possible search domain. Actually, restricting this last, by the use of a priori assumptions, can simply lead to no solutions.

Assumption 9 is rather important; mathematically, this allows to completely split stiffness from strength, except for the direction of orthotropy, see assumption 10, and hence to precisely define the dimensionality of the optimum problem.

About assumption 10, it is based upon a physical reasonable rationale: for a simple ply, the geometrical disposition of the matter or of the phases, i.e. of the reinforcing fibers, naturally induces orthotropy for both the stiffness and strength properties, and with the same axes. So inspired, we enforce such a circumstance also for the whole laminate.

Assumption 11 is also a rationale suggested by what has been discussed in Chapters 2 and 4: because the phenomenological criteria considered in this thesis and valid for orthotropic plies are actually based upon such an assumption, we enforce it also for the same criteria when used for the strength of the laminate considered as a whole, a homogenised plate (see Sec. 6.4).

Concerning assumption 12, it is in fact a choice: the description of all the anisotropic tensors is done by their polar invariants, plus the anisotropy direction (which is also a polar parameter, but not of course an invariant). The reason for that has been already discussed above and the multiple advantages of this choice will be more evident in the following of this thesis, Chapters 7 and 8.

For what concerns assumption 13, it is motivated by two facts: we are mainly interested in the anisotropy and in the overall behaviour of slender structures, well caught by the CLPT, and, thanks to assumptions 6 and 8, only the in-plane behaviour is considered herein. Of course, we left apart here some phenomena, like delamination under in-plane loads, that can occur and cause the loss of the structure: they should be considered in a subsequent study. The choice of another kinematic model for the laminate is however still possible, it does not alter fundamentally the procedure described in this thesis (for instance, the definition of the anisotropy tensors $\mathbf{A}^*$, $\mathbf{B}^*$ and $\mathbf{D}^*$ does not change).

Finally, about the last assumption 14, we have chosen to develop the procedure only for the Tsai-Hill criterion for the sake of brevity, the goal being to assess the effectiveness of a new computational strategy for the strength optimisation of laminated structures, not to validate a given strength criterion. Anyway, the procedure sketched in the following of this manuscript can be modified, with a slight effort, to be adapted to another of the failure criteria considered in the previous chapters.

6.2.3 Interpreting the optimisation problem

As a consequence of the above assumptions, it is clear now that our goal is to determine the optimal value that the orthotropy directions plus the anisotropy polar parameters of stiffness and strength for the laminate should get, at each point in the structure domain, in order to optimise simultaneously its stiffness and strength. To be more precise about the objective, we try to give an answer to the following question: is it possible to consider stiffness and strength at the same time, not as *competitive* objects, but, in a sense that will be clearer in the next chapter, as *collaborative* objectives? In practice, in our approach one of the two objectives will be still considered as the leading objective, but the other one will also enter the design process, and not as a constraint nor as a competitor to the leading objective. Actually, two cases will be considered: one, with the stiffness and the other one with the strength as fundamental objective, see Chapter 7, where the core of the problem is described in detail.

Of course, such an approach gives necessarily rise to a new interpretation of the problem at hand; actually, different levels of analysis are to be introduced, and it is worth to give since now a quick appraisal of such aspects, that will be developed in the following of this thesis.

First of all, some mathematical considerations; the optimisation of stiffness is without any doubt the most studied problem in structural optimisation. The reason for that is not only a mechanical one (stiffness is of course a fundamental property for a structure), but also, and perhaps more important, a mathematical one. In fact, almost all of the works on stiffness optimisation take as objective function, i.e. as *measure* of the stiffness, the *compliance*, which is the overall mechanical work made by the applied forces through the actual displacements of the structure and as such, always positive. Compliance is linked, as well known, to the elastic energy stored by the structure itself. The reason for taking compliance as a relevant measure for the stiffness of a structure can be subjected to discussion (some counterexamples can be given), but actually it is almost exclusively due to the fact that compliance is a *good mathematical* quantity: it is a global functional, by its same nature, so its use introduce to a variational problem having a classical, well-known, structure: the minimisation of a positive global functional.

Unlike the case of stiffness, strength optimisation problems are not so easy to be formulated. First of all, and of an uttermost importance, strength is always a *local property*, so any formulation of a strength maximisation problem gives rise to a variational problem with a *local functional*, hence to an intrinsically more complicate mathematical problem. In our approach, aiming to take into account at the same time for stiffness and strength, we need hence to formulate a mathematical problem where a local and a global functional are optimised at the same time. Such a situation has a direct consequence, of course, on the algorithm to be cast for the solution search: Chapter 7 is essentially devoted to this topic.

Then, some mechanical considerations: what does it mean, from a mechanical point of view, to optimise the strength along with stiffness or vice-versa? Well, let us consider the case of a structure designed to maximise its stiffness. Then, a local optimisation of its strength means to look for the structure that, still conserving its best stiffness, maximises, point wise, its strength. Hence, it means to look for, among all the possible structures realising the same optimal stiffness, the strongest one. This is an engineering relevant problem: how to better strengthen a structure designed with respect to stiffness? Dually, when a stiffness optimisation is performed on an anisotropy field giving the strongest structure, one obtains the stiffest solution for a fixed optimum strength. For the engineer,

this means to improve at its best the stiffness of a structure designed to withstand some applied loads.

It is worth noting that the above interpretation, and more properly such a kind of dual problems, is possible and meaningful just for the case at hand. In fact, just because the design variables concerning stiffness are assumed to be, for the laminate, completely independent from those resuming strength, assumption 9, it is possible, for an optimal distribution of stiffness, to look *also* for a local optimal strength. And the possibility of looking for a solution to such a problem is rendered possible (though its existence cannot be demonstrated a priori) by the *great redundancy of stacks corresponding to a set of optimal design variables*. This consideration is valid also for the dual case of an optimal distribution of strength for which a local maximisation of the stiffness is performed.

6.2.4 The optimisation procedure

We arrive now to a key point of our approach, that will introduce us also to the subsequent general organisation of the strategy for the search of a solution to the problem formulated in this section: the redundancy of the stacks. Eqs. (1.54) show that, for a given basic layer, to a set of orientation angles δ_k, $k = 1, ..., n$, corresponds a *unique* set of tensors $\mathbf{A}^*$, $\mathbf{B}^*$ and $\mathbf{D}^*$. In other words, as obvious, the elastic behaviour is uniquely determined by a stacking sequence of identical plies. The converse, however, is not true: *the correspondence between the elastic behaviour of a laminate and the stacks is not bijective*. Different stacks of the same plies can give rise to the same final elastic behaviour or, more precisely, it is possible to obtain the same mechanical response with laminates that, though constituted by the same number of plies of the same material, are different.

This circumstance is well known; less known is the great redundancy of the stacks: the number of laminates giving rise to the same elastic behaviour is extremely large and very rapidly increasing with the layers number. In fact, the usual rules employed by designers to obtain laminates of a certain type (balanced, symmetric, angle-ply, cross-ply laminates) shrink so much and so quickly the existence domain of solutions for a laminate that the enormous wealth of solutions of the general case is completely hidden and greatly reduced, to such a point that it looses its real importance: the fact that it gives to the designer a great number of possibilities, provided that he is able to include in the design process those properties that are commonly asked for a laminate (uncoupling, orthotropy and so on).

As we will show in Chapter 8, following a general approach formulated by Vannucci [78], and based upon the polar formalism, it is really possible to design, without restricting a priori assumptions, laminates with any kind of elastic properties; so, we can exploit profitably the redundancy of the stacks to look for a laminate having some optimal properties. This redundancy appears hence to be, in our approach, a fundamental point that, far from being a strange and unusual fact, renders possible the existence of laminates satisfying the optimal requirements.

We remark again, however, that it is not possible, in the general case, to ensure a priori the existence of a laminate having some prescribed properties. Montemurro *et al.*, [45] have given a partial response to such a kind of problem: they looked for the minimal number of layers giving a laminate with certain fixed properties. The result, that was found numerically as the solution to a minimum problem, cannot be generalised, and of course is strongly problem-dependent.

The non bijectivity between the elastic properties and the stacks leads us to another

crucial point and inspires our strategy for the search of the solutions. In fact, the relevant mechanical fact of non bijectivity is that the stacking sequence is not needed to describe the elastic response of the laminate. Some other parameters, whose number does not depend upon the plies number, are sufficient for that: the components of tensors $\mathbf{A}^*$, $\mathbf{B}^*$ and $\mathbf{D}^*$.

Practically, we look at the laminate as a homogeneous anisotropic plate, i.e. as it was constituted by a single layer, whose anisotropy has to be designed point wise, and we give its mechanical properties by the aid of some relevant parameters: the polar parameters of $\mathbf{A}^*$ (thanks to assumptions 6 and 8, tensors $\mathbf{B}^*$ and $\mathbf{D}^*$ are discarded in this work). For what concerns strength, a similar procedure can be adopted too, but only once a homogenisation procedure for the strength properties has been introduced; this is the topic of Sec. 6.3.

In a subsequent phase, once the optimal polar parameters are known, we pass to determine a laminate among all the possible stacking sequences giving rise to the optimal set of polar parameters. Hence, we outline here what will be the optimisation procedure that we have adopted, in its general lines: a two-step approach, resumed as follows:

- *First step (structural optimisation)*: the laminated structure is modelled as a single-layer homogeneous structure; the anisotropy field is optimised, leading to the optimal local mechanical properties of the structure, resumed in four fields of anisotropic polar parameters for stiffness and strength and in a field of orthotropy directions; hence, at the end of this step, the optimal mechanical response of the structure and the distribution of its anisotropic properties, for both stiffness and strength, are completely known;

- *Second step (lay up design)*: a suitable stacking sequence, giving the optimal response obtained at the end of the previous step, is looked for at each point of the structure; the outcome of this step is hence constituted by n orientation fields.

Such a two-step strategy, that is not new but rather ancient, the oldest example seems in fact to go back to the method of Miki in 1982 [42] is a sort of *model reduction* from a *meso-scale*, the layers, to a *macro-scale*, the laminate.

During the first step, the structural optimisation is not performed in the *geometrical space* of the ply orientations, but in a *mechanical space*, constituted by the polar anisotropy invariants of stiffness and strength, plus the orthotropy direction shared by stiffness and strength. While the dimension of the geometrical space is $n-1$, the dimension of the mechanical space is fixed and always equal to 5: the two anisotropy polar parameters of stiffness and strength plus the orthotropy direction. In usual applications, $n \gg 5$, so the reduction of the model obtained in the mechanical space, at the macro-scale level, can be considerable and really simplify the computational effort, that could be, in a direct approach, too big.

A last remark: the use of a two-step approach has a mathematical consequence, already introduced in Sec. 6.2.2: the first step, in fact, cannot be considered a completely *free material approach*. In fact, the homogenised single layer, object of the optimisation during the first step, is only a *mechanical condensation* of a laminate composed by n layers, and as such it is not, by no means, a completely free structure to be designed. It is subjected to the restrictions on the mechanical properties dues to the assemblage of n identical plies, see [81] and Sec. 1.6.1, that renders a laminate a sort of *meta-material* belonging to a restricted elastic class. Some bounds, called *geometrical bounds*, eq. (1.72), are to be

imposed to the first step problem, in order to finally obtain mechanical parameters that can be, subsequently, really get by the superposition of n plies (see Chapter 7).

At this point, we can outline the content of the following part of this manuscript: in this Chapter 6, we formulate the general optimisation problem for stiffness and strength and give the way that we use to describe the strength of the homogenised, single layer, fictitious plate of the first step. In order to better introduce such a procedure, we first recall the essential points of the analogous two-step approach, concerning only stiffness, already used by Jibawy *et al.*, [31].

Chapter 7 is devoted to the first step, the structural optimisation: the algorithm, for both the cases of stiffness or strength leading objective, is presented and its convergence proved. For the case of strength as leading objective, two variants of the algorithm are given and discussed. Some numerical examples end the chapter.

Finally, Chapter 8 concerns the second step, the lay-up design; the general numerical technique for obtaining a laminate having the optimal properties issued from the first step is described and discussed, a step for the layer wise check of strength is also introduced, and a numerical example given.

6.3 Description of the hierarchical stiffness optimisation strategy

6.3.1 First step: structural stiffness optimisation

The first step focuses on the definition of the optimal distribution of the laminate stiffness polar parameters [31, 32, 34]. The solution of the structural optimisation problem is searched for an orthotropic uncoupled homogenised plate subject to a given pure membrane or bending loading condition.

The objective of maximising the global stiffness of the plate is realised through the minimisation of the *complementary energy* W_c that corresponds to the half of the compliance. For the sake of brevity we will consider only the pure membrane case. The distributed design variables are the orthotropy orientation and the anisotropic polar moduli of tensor $\mathbf{A}^*$:

$$\overline{\Phi}_1,\ \beta_m \quad \text{with} \quad m = 1, 2\ ; \tag{6.1}$$

they depend upon the coordinates (x, y) and in particular we put

$$\begin{aligned} \beta_1 &= (-1)^{\overline{K}}\overline{R}_0, \\ \beta_2 &= \overline{R}_1\ , \end{aligned} \tag{6.2}$$

while the isotropic polar moduli of $\mathbf{A}^*$ are identical to the ones of the basic ply, see eq. (1.62). As the basic ply has been chosen *a priori* the isotropic elastic moduli do not take part to the optimisation problem. The optimisation problem can be mathematically formalised as follows:

$$\min_{\left\{\overline{\Phi}_1,\ \beta_m\right\}} \min_{N_{ij}} \left[W_c = \int_{S_p} A^{-1}_{ijkl}(\overline{\Phi}_1,\ \beta_m) N_{ij} N_{kl} dS_p\right] \quad \text{with} \quad i, j, k, l = x, y;$$

$$\text{with} \begin{cases} 2\left(\dfrac{\overline{R}_1}{R_1}\right)^2 - 1 \leq \dfrac{(-1)^{\overline{K}}\overline{R}_0}{(-1)^K R_0}, \\ |(-1)^{\overline{K}}\overline{R}_0| \leq R_0, \\ \overline{R}_1 \geq 0. \end{cases} \tag{6.3}$$

In (6.3) N_{ij} is a statically admissible state of in-plane forces, S_p represents the plate surface, the terms $(-1)^K R_0$ and R_1 are the anisotropic polar parameters of the reduced stiffness tensor $\mathbf{Q}$ of the basic ply, see Sec. 1.4, and the constraints are the *geometric bounds* introduced in Sec. 1.6.1. The geometry is fixed. Problem (6.3) has been solved using the optimisation algorithm introduced by Allaire and Kohn [2]. It is characterised by the following phases:

- initialisation : the stiffness distribution on the structure is initialised. Therefore, a first Finite Element (FE) analysis is conducted in order to determine the initial stress field;
- local minimisation : search for a new anisotropic stiffness distribution $(\overline{\Phi}_1^{(n+1)}, \beta_m^{(n+1)})$ that solves the problem of eq. (6.3) for a fixed stress state: the optimal polar parameters are determined locally, for each finite element discretising the plate;
- global minimisation : definition of the in-place forces field $(N_{ij}^{(n+1)})$ linked to the new stiffness distribution $(\overline{\Phi}_1^{(n+1)},\ \beta_m^{(n+1)})$ by a FE analysis.

These last two phases are repeated until convergence. A classical demonstration proves the monotonic convergence of this procedure. We sketch it hereafter, in the framework of the polar formalism.

Convergence proof

We consider the anisotropic stiffness distribution $(\overline{\Phi}_1^{(n)},\ \beta_m^{(n)})$ and its corresponding in-plane forces field $\mathbf{N}^{(n)}$, at the iteration n. The local minimisation consists in finding the minimum of the energy density:

$$\min_{\{\overline{\Phi}_1,\ \beta_m\}} \left[A^{-1}_{ijkl}(\overline{\Phi}_1,\ \beta_m) N^{(n)}_{ij} N^{(n)}_{kl} \right] \ , \tag{6.4}$$

defined at each point (in the discretised model: at each element) of the structure assuming a fixed field $\mathbf{N}^{(n)}$. Using the polar formalism, it is possible to find analytically the solution to problem (6.4) with the constraints in eq. (6.3). Such a solution is presented in Tab. 6.1 and described at the end of this proof.

Thanks to this analytical solution, we obtain the new stiffness distribution $(\overline{\Phi}_1^{(n+1)},\ \beta_m^{(n+1)})$ that satisfies the following inequality:

$$A^{-1}_{ijkl}(\overline{\Phi}_1^{(n+1)},\ \beta_m^{(n+1)}) N^{(n)}_{ij} N^{(n)}_{kl} \leq A^{-1}_{ijkl}(\overline{\Phi}_1^{(n)},\ \beta_m^{(n)}) N^{(n)}_{ij} N^{(n)}_{kl} \ , \tag{6.5}$$

and, thus

$$\int_{S_p} A^{-1}_{ijkl}(\overline{\Phi}_1^{(n+1)},\ \beta_m^{(n+1)}) N^{(n)}_{ij} N^{(n)}_{kl} dS_p \leq \int_{S_p} A^{-1}_{ijkl}(\overline{\Phi}_1^{(n)},\ \beta_m^{(n)}) N^{(n)}_{ij} N^{(n)}_{kl} dS_p \ . \tag{6.6}$$

The global minimisation phase consists in determining the new field $\mathbf{N}^{(n+1)}$ solution to the elastic problem determined by the stiffness distribution $(\overline{\Phi}_1^{(n+1)},\ \beta_m^{(n+1)})$. Using the complementary energy theorem we get

$$\int_{S_p} A^{-1}_{ijkl}(\overline{\Phi}_1^{(n+1)},\ \beta_m^{(n+1)}) N^{(n+1)}_{ij} N^{(n+1)}_{kl} dS_p \leq \int_{S_p} A^{-1}_{ijkl}(\overline{\Phi}_1^{(n+1)},\ \beta_m^{(n+1)}) N^{(n)}_{ij} N^{(n)}_{kl} dS_p \ . \tag{6.7}$$

Combining eq. (6.6) with eq. (6.7) we obtain:

$$\int_{S_p} A^{-1}_{ijkl}(\overline{\Phi}_1^{(n+1)},\ \beta_m^{(n+1)}) N_{ij}^{(n+1)} N_{kl}^{(n+1)} dS_p \leq \int_{S_p} A^{-1}_{ijkl}(\overline{\Phi}_1^{(n)},\ \beta_m^{(n)}) N_{ij}^{(n)} N_{kl}^{(n)} dS_p\ , \tag{6.8}$$

i.e.

$$W_c^{(n+1)} \leq W_c^{(n)}. \tag{6.9}$$

Hence, W_c is a positive quantity that reduces at each iteration; this proves the monotonic convergence of the algorithm.

We ponder now on the analytical solutions to the local minimisation phase in the previous procedure, eq. (6.4) along with the constraints (6.3). The analytical resolution to such a problem was extensively studied in [31, 34]. Nevertheless in those works, the geometric constraint on the polar parameters was not taken into account, but they considered only the thermodynamic constraints on the polar moduli. Tab. 6.1 summarises the optimal value, using the geometric constraints, of the stiffness polar parameters of tensor $\mathbf{A}^*$, for a basic ply with $K = 0$. These results show that the solution depends upon the polar parameters of the in-plane stress tensor $\mathbf{N}$. In particular, T and R are the spherical and deviatoric parts of the tensor, respectively, while Φ represents the direction of the first principal component of $\mathbf{N}$. We want to highlight a particular aspect, extensively discussed in [34], concerning the solution of type 1 in Tab. 6.1: the stiffness distribution linked to such a solution generates a pure spherical strain field, while the stress field has both spherical and deviatoric components, see [34].

	$(-1)^{\overline{K}^{opt}}\overline{R}_0^{opt}$	$\overline{R}_1^{opt}$	$\overline{\Phi}_1^{opt}$
Solution type: 1 $0 \leq \frac{R}{\lvert T\rvert} \leq \frac{R_1}{T_1}$	$\left[R_0\left(2\left(\frac{RT_1}{\lvert T\rvert R_1}\right)^2 - 1\right); R_0\right]$	$T_1\frac{R}{\lvert T\rvert}$	direction(max($\lvert N_I\rvert$, $\lvert N_{II}\rvert$))
Solution type: 2 $\frac{R_1}{T_1} \leq \frac{R}{\lvert T\rvert} \leq \frac{T_0+R_0}{2R_1}$	R_0	R_1	direction(max($\lvert N_I\rvert$, $\lvert N_{II}\rvert$))
Solution type: 3 $\frac{R}{\lvert T\rvert} \geq \frac{T_0+R_0}{2R_1}$	R_0	$\frac{T_0+R_0}{2(R/\lvert T\rvert)}$	direction(max($\lvert N_I\rvert$, $\lvert N_{II}\rvert$))

Table 6.1: Optimal values of stiffness polar parameters to maximise the plate stiffness fora basic ply with $K = 0$.

6.3.2 Second step: lay-up design

The design process turns now on the definition of the stacking sequence satisfying the optimal distribution of polar parameters issued from the firs step. The problem of the lay-up design can be stated as follows:

find, for a given set $\left\{\overline{K}^{opt}, \overline{R}_0^{opt}, \overline{R}_1^{opt}, \overline{\Phi}_1^{opt}\right\}$,
a vector of plies orientations $(\delta_1, \delta_2, ..., \delta_n)$ such that:

$$\begin{cases} \overline{R}_0 = \overline{R}_0^{opt} \ , \\ \overline{R}_1 = \overline{R}_1^{opt} \ , \\ \overline{\Phi}_0 - \overline{\Phi}_1 = \overline{K}^{opt} \dfrac{\pi}{4} \ , \\ \overline{\Phi}_1 = \overline{\Phi}_1^{opt} \ , \\ \mathbf{B} = \mathbf{O} \ , \end{cases} \tag{6.10}$$

In eq. (6.10), the first three conditions concern the anisotropy moduli of the optimal laminate, the fourth one the orientation of anisotropy and the last one the bending-extension uncoupling.

The problem of defining a laminate stacking sequence having a given elastic behaviour is rather cumbersome and difficult due to the fact that the laminate properties depend upon a combination of powers of circular functions of the layers orientations. As a consequence, researchers usually limit the search of solutions to a restricted class of stacking sequences, as for example symmetric stacking sequences to ensure bending-extension uncoupling or balanced sequences to have in-plane orthotropy.

As discussed in Sec. 6.2.4, eqs. (1.62) and (1.64) show that the correspondence between the elastic behaviour of a laminate and the stacks is not bijective. This means that it is possible to obtain the same mechanical parameters with several stacking sequences, although they are characterised by the same number of identical plies. Moreover, the number of laminates having the same elastic behaviour is extremely large and rapidly increases with the layers number. Therefore, the classical solutions often employed by designers (balanced, symmetric, angle-ply, cross-ply stacks) reduce the width of the solution space.

The problem of designing laminates with given elastic properties as a global optimisation problem, without restricting a priori assumptions on the stacking sequence, was formulated in a completely general way with the works of Vannucci *et al.* [78,82,85]. The redundancy of the solutions is, in this approach, a fundamental point that renders possible the existence of laminates satisfying several optimal requirements. Thanks to the polar method, the problem is stated through the formulation of an unique objective function which takes into account for several sub-objectives, one for each desired elastic property, such as uncoupling, orthotropy and so on. In particular, the problem is formulated as a minimum distance problem in the space of the polar parameters, the design variables being the plies orientations. The general problem is, hence, reduced to a classical form and its solutions are the minima of a highly non-convex function in the design space of the layers orientations:

$$\min_{\delta_k} \ I(f_i(\delta_k)) = \sum_j f_j^2(\delta_k) \text{ with } \ k = 1, 2, .., n \ , \tag{6.11}$$

where the $f_j(\delta_k)$ are the partial terms, i.e. the sub-objectives, composing the distance function between the laminate elastic properties and their target values. For such a general approach, however, a numerical efficient procedure is needed. For more details on the definition of this objective function for different combinations of elastic symmetries the reader is addressed to [45,78,85].

In some cases, namely when some assumptions are made, analytical solutions can be obtained; for instance, Vannucci and Verchery have proved the existence of a particular class of uncoupled (**B**=**O**) or quasi-homogeneous (**B**=**C**=**O**) laminates, the *quasi-trivial solutions*, so called because the equations leading to them do not need a direct solution, but can be found by an enumerating method working on combinations of integer coefficients,

see [82, 83]. Also, in [31] a closed form solution is found to obtain stacking sequences satisfying the requirements in Tab. 6.1. In particular, they find, analytically, two kind of stacking sequences satisfying the solution of type 1:

- a quasi-homogeneous angle-ply, which corresponds to the lowest value of the interval of $(-1)^{\overline{K}^{opt}}\overline{R}_0^{opt}$, with

$$\delta_k = \pm\alpha \text{ and } \alpha^{opt} = \frac{1}{2}\arccos\frac{T_1 R}{R_1|T|} \ , \tag{6.12}$$

- a symmetric cross-ply, which corresponds to the highest value of the interval of $(-1)^{\overline{K}^{opt}}\overline{R}_0^{opt}$, with

$$\eta^{0\ opt} = \frac{1}{2}\left(1 + \frac{\overline{R}_1^{opt}}{R_1}\right) \ , \tag{6.13}$$

where $\eta^{0\ opt} = n^0/n^{90}$ is the ratio between the number of plies at 0° and the number of plies at 90°.

The stacking sequence satisfying the solution of type 2 corresponds to an unidirectional laminate. Finally, the stacking sequence satisfying the solution of type 3 can be reached by a asymmetric cross-ply with:

$$\eta^{0\ opt} = \frac{1}{2}\left(1 + \frac{|T|(T_0 + R_0)}{2RR_1}\right) \ . \tag{6.14}$$

6.4 Taking into account for strength

In this Section, we propose a method to generalise the procedure for stiffness optimisation presented in Sec. 6.3 with the aim of introducing strength in the optimisation process. Strength is usually described through *failure criteria*. It is important to note that almost all of the failure criteria for composite materials are "ply-level failure criteria", i.e. the criterion is applied to each ply composing the laminated structure.

In Chapter 5 and in [8] we have stated the problem of optimising the strength of elastic plane structures composed of orthotropic materials. We have formulated the phenomenological failure criteria, described in Chapter 2, through invariants using the polar method and we have maximised the strength of a generic orthotropic sheet in terms of its material orientation.

With the aim of extending the analytical approach introduced in Chapter 5 to the strength optimisation of laminated plates, we define a *homogenised failure criterion* giving a measure of the strength for the laminate.

In the literature some works deal with this problem: the evaluation of a *laminate-level failure criterion*, [13, 14, 51]. In 1983, De Buhan [13] presented a study on the strength homogenisation of a generic composite material. He considered a heterogeneous continuum composed by two constituents. The strength homogenisation was evaluated at both the mesoscopic and macroscopic level. At the macroscopic scale, the strength is given by a sum of the strengths of each constituent, weighted by the corresponding material volume fraction. In 1991, De Buhan and Taliercio [14] addressed the same problem reformulating the theory developed in the previous work: the constituents are identified as the matrix, the fibres and the interfaces. The strength domain is assumed to vary point-wise and it is approximated by an homogenised strength field given by the sum of the isotropic part of strength, that does not depends upon the volume fraction, and of the anisotropic part of strength, this one depending on the phase volume fractions.

6.4.1 Evaluation of the laminate strength using an homogenised criterion

In the first part of this Section, we formulate a homogenised failure criterion that gives a measure of the strength of the laminate. Then, in order to give a mechanical relevant meaning to the homogenised failure criterion, we define in an explicit way its link with the first-ply-failure approach. In the second part of this section, such a criterion is used in the problem of the simultaneous maximisation of both stiffness and strength of a laminated structure. In particular, in order to include the strength optimisation into the first step of the hierarchical optimisation strategy presented beforehand, the homogenised criterion will represent the strength functional to be minimised, when the laminate is considered as an equivalent homogenised plate. Finally, in the third part of this section we define the problem of the lay-up design when the homogenised failure criterion is used in the first part of the hierarchical strategy.

6.4.1.1 The homogenised laminate strength

Let us consider a laminated plate with n plies. Let be $\{0; x, y, z\}$ the laminate global frame. The generic k^{th} ply is characterised by the position of its bottom and top surfaces, z_{k-1} and z_k as shown in Fig. 1.2, its fibre orientations δ_k, its elastic properties $\mathbf{Q}_k(\delta_k)$ and its strength properties $\mathbf{G}_k(\delta_k)$. In the following description we will consider the Tsai-Hill's failure criterion as an example to show how we can obtain a homogenised failure criterion. The procedure is completely general and can be applied to any other polynomial failure criterion, as for instance, the Hoffman or the Tsai-Wu criterion, the only difference resides in the addition of the linear terms that, anyway, does not change the overall procedure.

The stress-based polynomial failure criterion of Tsai-Hill expressed in terms of strains for a generic orthotropic ply, eq. (2.23), is:

$$F_{Hill}^{Ply} = \boldsymbol{\varepsilon}^T \mathbf{G} \boldsymbol{\varepsilon} \leq 1 \ , \tag{6.15}$$

where $\mathbf{G}$ is the *strength tensor* introduced in Sec. 2.3.1. In the framework of the CLPT the strain field is:

$$\boldsymbol{\varepsilon} = \boldsymbol{\varepsilon_0} + \boldsymbol{\chi} \ z \ . \tag{6.16}$$

where the in-plane strain $\boldsymbol{\varepsilon_0}$ and the curvature $\boldsymbol{\chi}$ tensors do not depend upon the z coordinate.

Introducing eq. (6.16) into eq. (6.15) we obtain:

$$F_{Hill}^{Ply} = \boldsymbol{\varepsilon_0}^T \mathbf{G} \boldsymbol{\varepsilon_0} + \boldsymbol{\chi}^T \mathbf{G} \boldsymbol{\chi} \ z^2 + 2 \ \boldsymbol{\varepsilon_0}^T \mathbf{G} \boldsymbol{\chi} \ z \leq 1 \ . \tag{6.17}$$

We recall the polar parameters of $\mathbf{G}$ introduced in Sec. 4.4.2:

- Γ_0 and Γ_1 represent the isotropic polar moduli (the corresponding of T_0 and T_1 for stiffness);
- Λ_0 and Λ_1 represent the anisotropic polar moduli (the corresponding of R_0 and R_1 for stiffness);
- Ω_1 represents the polar angle and, so, the orthotropy orientation (the corresponding of Φ_1 for stiffness);
- L represents the orthotropy shape parameter (the corresponding of K for stiffness).

Being t, r and ϕ the polar parameters of the strain tensor $\boldsymbol{\varepsilon}$, we can write the F_{Hill}^{Ply} as follows, see Sec. 4.3:

$$F_{Hill} = 4r^2\Gamma_0 + 8t^2\Gamma_1 + 4(-1)^L\Lambda_0 r^2\cos 4\left(\Omega_1 - \phi\right) + 16tr\Lambda_1\cos 2\left(\Omega_1 - \phi\right) \ . \tag{6.18}$$

To evaluate the failure index of the laminate, we integrate eq. (6.17) through the thickness of the plate:

$$F_{Hill}^{Lam} = \frac{1}{h}\int_h F_{Hill}^{Ply}(z)dz \leq 1, \tag{6.19}$$

and divide by h in order to have still a dimensionless failure index. In this way we evaluate, in some sense, an averaged strength (through the thickness) starting from the strengths of all the plies composing the laminate. This approach is completely similar to the determination of the laminate stiffness in the CLPT. Since the in-plane strain tensor $\boldsymbol{\varepsilon}_0$ and the curvature tensor $\boldsymbol{\chi}$ do not depend upon the z coordinate, eq. (6.19) becomes:

$$F_{Hill}^{Lam} = \frac{1}{h}\left[\boldsymbol{\varepsilon}_0\left(\int_h \mathbf{G}dz\right)\ \boldsymbol{\varepsilon}_0 + \boldsymbol{\chi}\left(\int_h \mathbf{G}z^2dz\right)\ \boldsymbol{\chi} + 2\boldsymbol{\varepsilon}_0\left(\int_h \mathbf{G}zdz\right)\ \boldsymbol{\chi}\right] \leq 1 \ . \tag{6.20}$$

Developing layer-wise the previous integrals into a sum of contributions, we obtain:

$$\begin{aligned}
\mathbf{G}^A &= \sum_{k=1}^{n}\mathbf{G}_k\left(\delta_k\right)\left(z_k - z_{k-1}\right), \\
\mathbf{G}^B &= \frac{1}{2}\sum_{k=-p}^{p}\mathbf{G}_k\left(\delta_k\right)\left(z_k^2 - z_{k-1}^2\right), \\
\mathbf{G}^D &= \frac{1}{3}\sum_{k=-p}^{p}\mathbf{G}_k\left(\delta_k\right)\left(z_k^3 - z_{k-1}^3\right).
\end{aligned} \tag{6.21}$$

In this way we have determined the strength tensors of the equivalent homogenised plate. As $\mathbf{G}^A$, $\mathbf{G}^B$ and $\mathbf{G}^D$ derives from the sum of symmetric elasticity-like tensors $\mathbf{G}_k\left(\delta_k\right)$, also $\mathbf{G}^A$, $\mathbf{G}^B$ and $\mathbf{G}^D$ are symmetric tensors possessing all the tensorial symmetries of a classical elasticity tensor.
Injecting eq. (6.21) into eq. (6.20), it gives:

$$F_{Hill}^{Lam} = \frac{1}{h}\left(\boldsymbol{\varepsilon}_0\mathbf{G}^A\boldsymbol{\varepsilon}_0 + \boldsymbol{\chi}\mathbf{G}^D\boldsymbol{\chi} + 2\boldsymbol{\varepsilon}_0\mathbf{G}^B\boldsymbol{\chi}\right) \leq 1. \tag{6.22}$$

Eq. (6.22) represents the "Tsai-Hill laminate-level failure criterion" for a laminated plate modelled as an Equivalent Single Layer (ESL) having the same thickness h of the laminate. This will be the starting point to the strength optimisation for a laminated plate, the optimisation variables being the polar components of the tensors $\mathbf{G}^A, \mathbf{G}^B$ and $\mathbf{G}^D$.

It is evident that it exists an analogy between eqs. (6.21) and (1.54). Therefore we can assume that tensors $\mathbf{G}^A$, $\mathbf{G}^B$ and $\mathbf{G}^D$ are the *strength counterpart* of the laminate stiffness tensors $\mathbf{A}$, $\mathbf{B}$ and $\mathbf{D}$. We can normalise such tensors as already done in eq. (1.60) and introduce the polar parameters of $\mathbf{G}^{A*}$, $\mathbf{G}^{B*}$ and $\mathbf{G}^{D*}$ as long as their relations with the polar parameters of the plies composing the laminate itself. In particular, for an orthotropic laminated plate composed by identical orthotropic plies, we have:

- Polar parameters of $\mathbf{G}^{A*}$:

$$\begin{aligned}
&\overline{\Gamma}_0 = \Gamma_0 \ , \\
&\overline{\Gamma}_1 = \Gamma_1 \ , \\
&(-1)^{\overline{L}}\overline{\Lambda}_0 e^{4i\overline{\Omega}_1} = \frac{1}{n}(-1)^L\Lambda_0 e^{4i\Omega_1}\sum_{k=1}^{n}e^{4i\delta_k} \ , \\
&\overline{\Lambda}_1 e^{2i\overline{\Omega}_1} = \frac{1}{n}\Lambda_1 e^{2i\Omega_1}\sum_{k=1}^{n}e^{2i\delta_k} \ .
\end{aligned} \tag{6.23}$$

- Polar parameters of $\mathbf{G}^{B*}$:

$$\begin{aligned}
&\widehat{\Gamma}_0 = 0 \ , \\
&\widehat{\Gamma}_1 = 0 \ , \\
&(-1)^{\widehat{L}}\widehat{\Lambda}_0 e^{4i\widehat{\Omega}_1} = \frac{1}{n^2}(-1)^L \Lambda_0 e^{4i\Omega_1}\sum_{k=1}^{n} b_k e^{4i\delta_k} \ , \\
&\widehat{\Lambda}_1 e^{2i\widehat{\Omega}_1} = \frac{1}{n^2}\Lambda_1 e^{2i\Omega_1}\sum_{k=1}^{n} b_k e^{2i\delta_k} \ .
\end{aligned} \tag{6.24}$$

- Polar parameters of $\mathbf{G}^{D*}$:

$$\begin{aligned}
&\widetilde{\Gamma}_0 = \Gamma_0 \ , \\
&\widetilde{\Gamma}_1 = \Gamma_1 \ , \\
&(-1)^{\widetilde{L}}\widetilde{\Lambda}_0 e^{4i\widetilde{\Omega}_1} = \frac{1}{n^3}(-1)^L \Lambda_0 e^{4i\Omega_1}\sum_{k=1}^{n} d_k e^{4i\delta_k} \ , \\
&\widetilde{\Lambda}_1 e^{2i\widetilde{\Omega}_1} = \frac{1}{n^3}\Lambda_1 e^{2i\Omega_1}\sum_{k=1}^{n} d_k e^{2i\delta_k} \ .
\end{aligned} \tag{6.25}$$

Γ_0, Γ_1, Λ_0, Λ_1, L and Ω_1 are the polar parameters of tensor $\mathbf{G}$ of the basic ply, while coefficients b_k and d_k are exactly the same introduced for tensors $\mathbf{B}^*$ and $\mathbf{D}^*$, respectively, eqs. (1.63) and (1.64). Eqs. (6.23) and (6.25) impose the same kind of *geometric bounds* on the polar parameters of $\mathbf{G}^{A*}$ and $\mathbf{G}^{D*}$, already introduced for $\mathbf{A}^*$ and $\mathbf{D}^*$, eq. (1.72):

$$\begin{cases}
2\left(\dfrac{\overline{\Lambda}_1}{\Lambda_1}\right)^2 - 1 \leq \dfrac{(-1)^{\overline{L}}\overline{\Lambda}_0}{(-1)^L\Lambda_0} \ , \\
|(-1)^{\overline{L}}\overline{\Lambda}_0| \leq \Lambda_0 \ , \\
\overline{\Lambda}_1 \geq 0 \ .
\end{cases} \tag{6.26}$$

In order to determine the polar parameters that correspond to a manufacturable laminate, the geometrical bounds cannot be violated.

There is, also, another aspect deserving attention: for a laminate made of identical plies the following relation subsists:

$$\mathbf{B} = 0 \ \Leftrightarrow \ \mathbf{G}^B = 0 \ , \tag{6.27}$$

because $\mathbf{B}$ and $\mathbf{G}^B$ are nulls if and only if:

$$\begin{aligned}
&\sum_{k=-p}^{p} b_k e^{4i\delta_k} = 0 \ , \\
&\sum_{k=-p}^{p} b_k e^{2i\delta_k} = 0 \ ,
\end{aligned} \tag{6.28}$$

at the same time. From a mechanical point of view, eq. (6.27) means that the elastic uncoupling of a laminate implies the strength uncoupling and vice-versa.

Eq. (6.17) represents the most general case in which membrane and flexural loadings are acting simultaneously on the plate. For an uncoupled plate subject to a pure membrane loading ($\boldsymbol{\chi} = 0 \Rightarrow \boldsymbol{\varepsilon} = \boldsymbol{\varepsilon_0}$), eq. (6.22) reads:

$$F_{Hill}^{Lam} = \boldsymbol{\varepsilon}^T \mathbf{G}^{A*} \boldsymbol{\varepsilon} \ , \tag{6.29}$$

or, in terms of polar parameters,

$$F_{Hill}^{Lam} = 4r^2\Gamma_0 + 8t^2\Gamma_1 + 4(-1)^{\overline{L}}\overline{\Lambda}_0 r^2 \cos 4\left(\overline{\Omega}_1 - \phi\right) + 16tr\overline{\Lambda}_1 \cos 2\left(\overline{\Omega}_1 - \phi\right) \ . \quad (6.30)$$

In eq. (6.30), the first two terms are the isotropic part of the criterion; when the material of the constitutive layer is chosen, these terms are fixed. The last two terms involve the anisotropic moduli of the material and the orthotropy orientation of the homogenised plate, thus, these parameters are the terms that can be designed in order to maximise the strength of the structure.

6.4.1.2 Comparison between the strength of the ply and of the homogenised laminate

We have defined an homogenised failure criterion in order to include strength in the optimal design process of a laminated structure: our goal is to maximise the strength of the structure. However, we have already recalled that unlike stiffness when measured by compliance, strength is measured by a local quantity, the failure index.

The through the thickness strength homogenisation method that we have proposed in the previous Section can be considered, in some sense, a little bit arbitrary: we homogenise a quantity, strength, that is typically local. In order to validate this homogenised model, we discuss the comparison between the strength of the ply and that of the homogenised laminate in order to take into account, during the design process, also for the first-ply-failure.

The adopted Kirkhoff's kinematic model implies an unique strain field $\boldsymbol{\varepsilon}$ that varies linearly and continuously through the thickness. When an uncoupled plate is subject to a pure membrane loading ($\boldsymbol{\chi} = 0$), the strain field of the whole laminate is identical to that of each constitutive layer.

Let us consider a homogenised plate whose stiffness and strength characteristics are known; hence, its F_{Hill}^{Lam} is known at any point, for a given strain state. Being the strain field of the homogenised plate identical to that of each constitutive layer thanks to assumptions 6 and 8 of Sec. 6.2.1, we can compare the value of the F_{Hill}^{Lam} with that of the single ply defining the ratio η. We have:

$$\eta = \frac{F_{Hill}^{Ply}}{F_{Hill}^{Lam}} = \frac{4r^2\Gamma_0 + 8t^2\Gamma_1 + 4(-1)^L\Lambda_0 r^2 \cos 4\left(\Omega_1 - \phi\right) + 16tr\Lambda_1 \cos 2\left(\Omega_1 - \phi\right)}{F_{Hill}^{Lam}} \ . \quad (6.31)$$

In eq. (6.31), F_{Hill}^{Lam}, the strain field (t, r, ϕ) and the polar parameters of tensor $\mathbf{G}$ of the basic ply (Γ_0, Γ_1,$(-1)^L\Lambda_0$,Λ_1) are given quantities. We let only free the orthotropy direction Ω_1 of the ply, evaluated with respect to the global frame of the laminate.

Depending on the ply orientation, we can consider three separate cases:

1. $\eta < 1 \Longrightarrow F_{Hill}^{Ply} < F_{Hill}^{Lam}$: this case represents a safe situation because the failure index of the laminate is greater than that of the single ply. This means that, in this case, the homogenised failure criterion is conservative;

2. $\eta = 1 \Longrightarrow F_{Hill}^{Ply} = F_{Hill}^{Lam}$: this case represents the limit condition, because the failure index of the laminate is equal to that of the single ply. The failure of both laminate and ply occurs at the same time, hence, the homogenised failure criterion is still conservative;

3. $\eta > 1 \Longrightarrow F_{Hill}^{Ply} > F_{Hill}^{Lam}$: this case represents an unsafe situation because the failure index of the laminate is lower than that of the single ply. The failure of a ply can occur for a laminate failure index lower than 1. In this case, the homogenised failure criterion is not conservative and we have to find a way to determine *a priori* the conditions that lead to such a situation.

Therefore, concerning this last case, we need to evaluate the orthotropy orientation Ω_1 of the ply which maximises F_{Hill}^{Ply} and, by consequence η. Such value will represent the worst situation that can be achieved. The failure index of the single ply is given in eq. (6.18) and the maximisation problem can be formulated as follows:

$$\max_{\Omega_1} F_{Hill}^{Ply}\left(\Gamma_0, \Gamma_1, \Lambda_0, \Lambda_1, L, \Omega_1, t, r, \phi\right). \tag{6.32}$$

This problem admits an analytical resolution that is similar to the minimisation problem solved in Chapter 5. Firstly, we write the derivative:

$$\frac{\partial F_{Hill}^{Ply}}{\partial \Omega_1} = -32r\sin 2\left(\Omega_1 - \phi\right)\left[(-1)^L \Lambda_0 r\cos 2\left(\Omega_1 - \phi\right) + \Lambda_1 t\right] = 0. \tag{6.33}$$

The solution of eq. (6.33) gives us the stationary points of F_{Hill}^{Ply}:

$$\begin{cases} r = 0: \text{ spherical strain field,} \\ \Lambda_0 = \Lambda_1 = 0: \text{ isotropic material,} \\ \sin 2\left(\Omega_1 - \phi\right) = 0 \;\Rightarrow\; \Omega_1 - \phi = \left\{0, \dfrac{\pi}{2}\right\}, \\ \cos 2\left(\Omega_1 - \phi\right) = -\dfrac{\Lambda_1 t}{(-1)^L \Lambda_0 r}, \text{ with } \dfrac{\mid t \mid}{r} \leq \dfrac{\Lambda_0}{\Lambda_1}. \end{cases} \tag{6.34}$$

The last two conditions have three different solutions to be compared:

$$\begin{aligned} \Omega_1 &= \phi, && \text{denoted as solution} \quad x_a, \\ \Omega_1 &= \phi + \pi/2, && \text{denoted as solution} \quad x_b, \\ \Omega_1 &= \phi \pm \frac{1}{2}\arccos\left[-(-1)^L \frac{\Lambda_1 t}{\Lambda_0 r}\right], && \text{denoted as solution} \quad x_c\,. \end{aligned} \tag{6.35}$$

Eq. (6.35) shows that the orthotropy direction Ω_1 maximising F_{Hill}^{Ply} is directly linked to the direction ϕ of the higher principal strain ε_I.

The second derivative reads:

$$\frac{\partial^2 F_{Hill}^{Ply}}{\partial \Omega_1^2} = -64r\left[(-1)^L \Lambda_0 r\cos 4(\Omega_1 - \phi) + \Lambda_1 t\cos 2(\Omega_1 - \phi)\right]. \tag{6.36}$$

The following property of the polar parameter t of the stress tensor $\boldsymbol{\varepsilon}$ has to be taken into account:

$$\text{if } \varepsilon_I \geq \varepsilon_{II}, \text{ then } \begin{cases} t \leq 0 & \Leftrightarrow & |\varepsilon_I| \leq |\varepsilon_{II}|, \\ t \geq 0 & \Leftrightarrow & |\varepsilon_I| \geq |\varepsilon_{II}|, \end{cases} \tag{6.37}$$

with $t = (\varepsilon_I + \varepsilon_{II})/2$.

We can separate the resolution into two main cases that depend upon the value of L.

1) $L = 0$

$$\begin{aligned}
\left.\frac{\partial^2 F_{Hill}^{Ply}}{\partial \Omega_1^2}\right|_{x_a} &= -64r\left[\Lambda_0 r + \Lambda_1 t\right] < 0 \qquad \text{if} \qquad \frac{t}{r} > -\frac{\Lambda_0}{\Lambda_1},\\
\left.\frac{\partial^2 F_{Hill}^{Ply}}{\partial \Omega_1^2}\right|_{x_b} &= -64r\left[\Lambda_0 r - \Lambda_1 t\right] < 0 \qquad \text{if} \qquad \frac{t}{r} < \frac{\Lambda_0}{\Lambda_1},\\
\left.\frac{\partial^2 F_{Hill}^{Ply}}{\partial \Omega_1^2}\right|_{x_c} &= -64r\left[\frac{\Lambda_1^2 t^2 - \Lambda_0^2 r^2}{\Lambda_0 r}\right] < 0 \quad \text{if} \quad \frac{t}{r} < -\frac{\Lambda_0}{\Lambda_1}; \frac{t}{r} > \frac{\Lambda_0}{\Lambda_1}.
\end{aligned} \tag{6.38}$$

The last equation is never satisfied because the values of t/r are outside the interval of existence of the solution x_c imposed by the last equation of (6.34). Hence, the solution concerns only the first two stationary points, and

$$F_{Hill}^{Ply}\big|_{x_a} - F_{Hill}^{Ply}\big|_{x_b} = 32tr\Lambda_1. \tag{6.39}$$

The minimum of F_{Hill}^{Ply} depends, hence, on the sign of t. For $t > 0$ the solution is given by x_a, while for $t < 0$ the solution is given by x_b.

2) $L = 1$

$$\begin{aligned}
\left.\frac{\partial^2 F_{Hill}^{Ply}}{\partial \Omega_1^2}\right|_{x_a} &= -64r\left[-\Lambda_0 r + \Lambda_1 t\right] < 0 \qquad \text{if} \quad \frac{t}{r} > \frac{\Lambda_0}{\Lambda_1},\\
\left.\frac{\partial^2 F_{Hill}^{Ply}}{\partial \Omega_1^2}\right|_{x_b} &= 64r\left[\Lambda_0 r + \Lambda_1 t\right] < 0 \qquad \text{if} \quad \frac{t}{r} < -\frac{\Lambda_0}{\Lambda_1},\\
\left.\frac{\partial^2 F_{Hill}^{Ply}}{\partial \Omega_1^2}\right|_{x_c} &= -64r\left[\frac{-\Lambda_1^2 t^2 + \Lambda_0^2 r^2}{\Lambda_0 r}\right] < 0 \quad \text{if} \quad -\frac{\Lambda_0}{\Lambda_1} < \frac{t}{r} < \frac{\Lambda_0}{\Lambda_1}.
\end{aligned} \tag{6.40}$$

All the conditions of eqs. (6.40) that concern t/r belongs to different and independent range of values of t/r. Moreover, the third solution of (6.40) respect the bounds on the last condition of eq. (6.34), so, the stationary points of (6.35) are solutions for the maximum of F_{Hill}^{Ply}.

In Fig. 6.1 we give a summary of the solutions, where

$$\kappa = \mathrm{dir}\left(\max\left\{|\varepsilon_I|, |\varepsilon_{II}|\right\}\right), \tag{6.41}$$

and

$$\rho = \frac{1}{2}\arccos\left[-(-1)^L \frac{\Lambda_1 t}{\Lambda_0 r}\right]. \tag{6.42}$$

These orientations give us the maximum value of F_{Hill}^{Ply}, and thus the maximum value of η, that can be achieved for a given strain state.

In conclusion, thanks to the polar method and to the Kirkhoff's kinematic model, we are able to

1. evaluate *a priori* the maximum value of F_{Hill}^{Ply} at the end of the first step of the hierarchical strategy, when the lay-up is not known;

2. validate the proposed strength homogenisation criterion because it allows us to check the first-ply-failure when we are still designing the homogenised plate, see Sec. 7.6;

Moreover, the value of $\max(\eta)$ will be taken into account also in the phase of the lay-up design, as it will be detailed in Chapter 8, in order to be able to find admissible lay-up with respect to the first-ply-failure in cases for which $F_{Hill}^{Ply} > 1$ and $F_{Hill}^{Lam} < 1$.

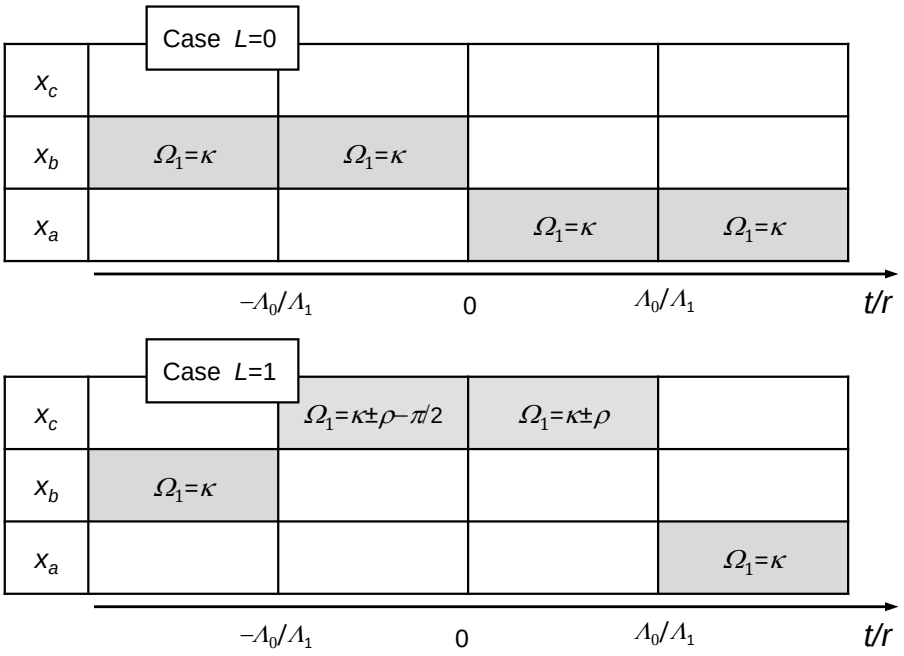

Figure 6.1: Orthotropy orientation maximising the failure index of the Tsai-Hill criterion.

6.4.2 First step: structural optimisation

After defining the homogenised failure criterion for the laminate, we have to consider, now, how to use such a criterion in the first step of the hierarchical strategy for the maximisation of strength. As a consequence of the assumptions made for the problem (see Sec. 6.3) and of what has been previously shown in this Chapter, the stiffness and the strength of the homogenised plate can be described, respectively, by the following quadratic functions:

$$\text{Complementary Energy: } W_c = \int_{S_p} \mathbf{N}^T \mathbf{A}^{-1}(\overline{\Phi}_1, (-1)^{\overline{K}}\overline{R}_0, \overline{R}_1)\mathbf{N} dS_p \ , \tag{6.43}$$

$$\text{Failure index: } F_{Hill}^{Lam} = \left[\boldsymbol{\varepsilon}^T \mathbf{G}^{A*}(\overline{\Omega}_1, (-1)^{\overline{L}}\overline{\Lambda}_0, \overline{\Lambda}_1)\boldsymbol{\varepsilon}\right] \ . \tag{6.44}$$

Eqs. (6.43) and (6.44) deserve some important remarks:

- the design variables of the structural optimisation step are the 8 polar parameters necessary to characterise the in-plane stiffness and strength behaviour, i.e. $(\overline{\Phi}_1, \overline{K}, \overline{R}_0, \overline{R}_1)$ and $(\overline{\Omega}_1, \overline{L}, \overline{\Lambda}_0, \overline{\Lambda}_1)$ for $\mathbf{A}^*$ and $\mathbf{G}^{A*}$, respectively;
- we recall, as already said in Sec. 6.2.3, that there are two functional to be minimised: the complementary energy, a global functional, and the laminate failure index, that is, on the contrary, a local functional. From a variational point of view the difficulty of this problem is increased because we have to minimise simultaneously, not one, but two objectives linked to two different variational problems, the former concerning a global functional and the later a local one.

The previous aspects are to be taken into account when developing an algorithm able to deal with the optimisation problem at hand.

We come, now, to a key point of our approach; the mathematical consequence of assumption 10, Sec. 6.2.1, along with the polar formalism gives the following condition:

$$\overline{\Phi}_1 = \begin{cases} \overline{\Omega}_1 \ , \\ \overline{\Omega}_1 \pm \pi/2 \ . \end{cases} \tag{6.45}$$

In addition we put, for having a more compact notation,

$$\begin{aligned} \overline{R}_{0K} &= (-1)^{\overline{K}} \overline{R}_0 \ , \\ \overline{\Lambda}_{0L} &= (-1)^{\overline{L}} \overline{\Lambda}_0 \ , \end{aligned} \tag{6.46}$$

that are still tensor invariants because obtained as a combination of invariants.

In this way the number of independent design variables for the problem of the first step is reduced to 5: $\overline{R}_{0K}$, $\overline{R}_1$, $\overline{\Lambda}_{0L}$, $\overline{\Lambda}_1$ and the orthotropy orientation. We recall that assumption 9 implies, for the structural optimisation step which involves an homogenised plate, that the stiffness anisotropic polar parameters, $\overline{R}_{0K}$ and $\overline{R}_1$, are independent from the corresponding parameters for strength, $\overline{\Lambda}_{0L}$ and $\overline{\Lambda}_1$.

All the assumptions and considerations lead us to state the following generalised optimisation problem:

$$\begin{aligned} &\text{Sub-problem 1:} \quad \min_{\{\vartheta,\ a_i\}} F_I(\vartheta,\ a_i) \ , \\ &\text{Sub-problem 2:} \quad \min_{\{b_i\}} F_{II}(\vartheta,\ b_i) \ ; \end{aligned} \tag{6.47}$$

where F_I and F_{II} are, indifferently, one the stiffness and the other the strength functional, and a_i and b_i are the respective anisotropic polar moduli, $i = 1, 2$. Eqs. (6.47) represent an optimisation problem having two functional to be minimised. The alignment of the symmetry axis for stiffness and strength leads to a unique quantity in both the functional, the orthotropy orientation ϑ.

The solution method for these two minimisations is a "waterfall method": at the first stage, we minimise the first functional with respect to its polar moduli and the orthotropy orientation, then, during a second stage, we minimise the second functional with respect to its polar moduli and we impose the orthotropy orientation to be the one found in the solution of the first minimisation. It is hence clear that, thanks to the independence of the anisotropic polar moduli of stiffness and strength, the two sub-problems of the first step of our approach are completely unrelated unless for the orthotropy orientation that constitutes the mathematical and mechanical link between the optimisation of stiffness and strength.

Finally, due to the interchangeability of the stiffness and strength functional in the two sub-problems of (6.47), we can state the two following dual but different optimisation problems:

- Optimisation problem I.

$$\begin{aligned} &\text{Sub-problem 1:} \quad \min_{\left\{\overline{\Phi}_1,\ \overline{R}_{0K},\ \overline{R}_1\right\}} W_c(\overline{\Phi}_1,\ \overline{R}_{0K},\ \overline{R}_1) \ , \\ &\text{Sub-problem 2:} \quad \min_{\left\{\overline{\Lambda}_{0L},\ \overline{\Lambda}_1\right\}} F_{Hill}^{Lam}(\overline{\Phi}_1, \overline{\Lambda}_{0L},\ \overline{\Lambda}_1) \ ; \end{aligned} \tag{6.48}$$

- Optimisation problem II.

$$\begin{aligned} &\text{Sub-problem 1:} \quad \min_{\left\{\overline{\Omega}_1,\ \overline{\Lambda}_{0L},\ \overline{\Lambda}_1\right\}} F^{Lam}_{Hill}(\overline{\Omega}_1, \overline{\Lambda}_{0L},\ \overline{\Lambda}_1)\ , \\ &\text{Sub-problem 2:} \quad \min_{\left\{\overline{R}_{0K},\ \overline{R}_1\right\}} W_c(\overline{\Omega}_1,\ \overline{R}_{0K},\ \overline{R}_1)\ ; \end{aligned} \tag{6.49}$$

The structural problem that we consider is, now, well stated in its two variants; in the first one, eq. (6.48), the leading objective is stiffness, while in the second one, eq. (6.49), it is strength. What is to be remarked for both of them, is that these are by no means multi-objective problems, but really something different.

6.4.3 Second step: lay-up design

Just like in the case of the stiffness optimisation, Sec. 6.3.2, the second step is needed to obtain a stacking sequence realising, at the same time, the optimal parameters of strength and stiffness found at the end of the previous step. We state the lay-up problem in a way similar to that introduced in Sec. 6.3.2. The optimisation problem of the lay-up design phase is:

$$\begin{gathered} \text{find, for a given set} \\ \left\{\overline{K}^{opt}, \overline{R}_0^{opt}, \overline{R}_1^{opt}, \overline{L}^{opt}, \overline{\Lambda}_0^{opt}, \overline{\Lambda}_1^{opt}, \overline{\Phi}_1^{opt}\right\} \\ \text{a vector of plies orientations } (\delta_1, \delta_2, ..., \delta_n) \text{ such that:} \end{gathered}$$

$$\begin{cases} \overline{R}_0 = \overline{R}_0^{opt}\ , \\ \overline{R}_1 = \overline{R}_1^{opt}\ , \\ \overline{\Lambda}_0 = \overline{\Lambda}_0^{opt}\ , \\ \overline{\Lambda}_1 = \overline{\Lambda}_1^{opt}\ , \\ \overline{\Phi}_0 - \overline{\Phi}_1 = \overline{K}^{opt}\pi/4\ , \\ \overline{\Omega}_0 - \overline{\Omega}_1 = \overline{L}^{opt}\pi/4\ , \\ \overline{\Phi}_1 - \overline{\Omega}_1 = 0; \pi/2\ , \\ \overline{\Phi}_1 = \overline{\Phi}_1^{opt}\ , \\ \mathbf{B} = \mathbf{O}\ . \end{cases} \tag{6.50}$$

A supplementary check on a possible first-ply-failure of the layers composing the optimal laminate can be taken into account within this second phase of the design procedure. To this purpose, the evaluation of $\max(\eta)$, eq. (6.31), will be very helpful, as will be discussed in Chapter 8 where the development of the numerical strategy to solve the optimisation problem of the lay-up design will be described.

It is evident that problem (6.50) is more complex than problem (6.10) concerning uniquely the stiffness optimal design. In this case, the requirements to be satisfied by the lay-up solution are increased because we added also the strength parameters issued from the first step of the strategy. Despite the complexity of (6.50), the non-bijectivity of the problem and, so, the existence of more stacking sequences solution allows us for having an important redundancy on the choice of the final solution. We know from previous studies on the lay-up design, [45,82], that the number of staking sequences, solution of the lay-up design problem, increase significantly along with the number of plies [82].
Again, the non-bijectivity can help us when the check on the first-ply-failure forces us to remove some stacking sequences from the solution space of the problem (6.50).

6.5 Concluding remarks

In this Chapter we have formulated the problem of simultaneous stiffness and strength optimisation for a laminated structure. This approach, declined into two different versions, has been inspired by an existing hierarchical strategy for the only stiffness maximisation.

We focused firstly on the *formulation of a strength functional valid for the equivalent homogenised plate*, in order to include the strength in the first step of the hierarchical strategy. Particularly we integrated through the thickness the expression of Tsai-Hill's failure criterion, in terms of strains, averaging the strength of the plies and obtaining an *homogenised failure criterion* formulated through invariants using the polar formalism.

Then, according to the general assumptions introduced for the problem at hand, we have proved that the first step can be alternatively stated as two dual problems, characterised by a different leading objective. Each one of these problems is almost independent from the other in terms of anisotropic polar moduli, but they are linked in terms of orthotropy orientation. This last aspect allows us to not fall in the frame of a multi-objective problem: stiffness and strength are separately and sequentially maximised, preserving only the orthotropy direction.

If we compare this work with the most recent works on the same theme, for instance [30, 38], we can assert that its most important innovation concerns the definition of a new laminate level failure criterion that leads us to introduce the laminate strength parameters into the optimisation variables. In [30, 38] the laminate-level failure criterion was represented by a conservative envelope characterised by fixed strength properties in order to avoid the first-ply-failure of the laminate plies. The strength properties in the laminate failure criterion introduced in this Chapter, on the other hand, can vary in order to minimise the laminate failure index.

Thanks to the polar notation and to the use of the failure criteria expressed in terms of strains for both the laminate and the ply, we proved that we are able to compare, in the first phase of the laminate design when the staking sequence is still unknown, the failure index of the laminate and that of the ply in order to check the first-ply-failure.

In Chapters 7 and 8 the development and resolution of the two steps of the hierarchical strategy will be discussed.

7

First step: structural optimisation of laminates including strength

7.1 Introduction

This Chapter describes the theoretical and numerical development of the first step of the hierarchical optimisation strategy sketched in the previous Chapter. The outcome of this first step will be the optimal distribution of anisotropy, through the definition of the optimal value of the material parameters maximising stiffness and strength for a given structure. In Sec. 7.2 and 7.3, we describe two optimisation algorithms for the resolution of the optimisation problems stated in Sec. 6.4.2, while Sec. 7.4 is devoted to the resolution procedures used for the local minimisation phases of the algorithms. Moreover, in Sec. 7.4.1, a new analytical solution to the problem of optimising the strength of plane structures made of linear elastic orthotropic materials, is proposed.

Finally, several numerical test cases are presented, proving the effectiveness and the robustness of the proposed approaches.

7.2 The stiffness optimisation algorithm with *a posteriori* local maximisation of strength

We have already introduced the first step, i.e. what we call the structural optimisation phase, in the previous Chapter (Sec. 6.4.2). In this section, we consider the first optimisation problem announced therein, the one where stiffness is considered as the leading objective. In other words, we focus here on problem (6.48).

This first structural optimisation algorithm consists in the sequential use of of the optimisation algorithm introduced by Allaire and Kohn [2], already described in Sec. 6.3.1, and of a second phase wherein we introduce the strength optimisation. This approach consists, then, in *a posteriori* maximisation of strength to an already stiffness optimised structure.

The optimisation parameters are:

$$\overline{\Phi}_1,\ \beta_m,\ \alpha_m \quad \text{with} \quad m = 1, 2\ . \tag{7.1}$$

They are local quantities, i.e. they are functions depending upon the coordinates (x, y) in the plate global frame. $\overline{\Phi}_1$ is the stiffness orthotropy orientation, β_m is defined in eq. (6.2),

α_m is defined as

$$\begin{aligned} \alpha_1 &= \overline{\Lambda}_{0L}, \\ \alpha_2 &= \overline{\Lambda}_1 \ . \end{aligned} \tag{7.2}$$

The optimisation problem, eqs. (6.48), is formulated as follows:

$$\begin{aligned} &\text{Sub-problem 1:} \quad \min_{\left\{\overline{\Phi}_1,\ \beta_m\right\}} \ \min_{N_{ij}} W_c(\overline{\Phi}_1,\ \beta_m,\ N_{ij}) \ , \\ &\text{Sub-problem 2:} \quad \min_{\alpha_m} F_{Hill}^{Lam}(\overline{\Phi}_1, \alpha_m) \ ; \end{aligned} \tag{7.3}$$

subject to the *geometric bounds* of eqs. (6.3) and (6.26).
The geometry, the loading conditions and the material properties of the basic ply are given quantities.

The algorithm to solve such a problem, sketched by a flow-chart diagram in Fig. 7.1, can be divided into the following phases:

1. initialisation : the stiffness and strength distributions on the structure are initialised, for instance they can be randomly sorted. Then, a first FE analysis is conducted in order to determine the initial stress and strain fields;

2. local minimisation of the local complementary energy W_c^l: local definition of a new anisotropic stiffness distribution ($\overline{\Phi}_1^{(n+1)}$, $\beta_m^{(n+1)}$) minimising the local complementary energy for a fixed field ($\mathbf{N}^{(n)}$);

3. global minimisation of W_c: definition of the new internal actions ($\mathbf{N}^{(n+1)}$) and strain ($\boldsymbol{\varepsilon}^{(n+1)}$) fields linked to the new stiffness distribution ($\overline{\Phi}_1^{(n+1)}$, $\beta_m^{(n+1)}$) through a FE analysis;

4. local minimisation of F_{Hill}^{Lam} *after the convergence*: local definition of the anisotropic strength distribution (α_m) that minimises the failure index F_{Hill}^{Lam} linked to the optimal strain field $\boldsymbol{\varepsilon}^{opt}$:
$$\min_{\alpha_m} \left[G_{ijkl}^{A*}(\overline{\Phi}_1^{opt}, \alpha_m) \varepsilon_{ij}^{opt} \varepsilon_{kl}^{opt} \right] \ . \tag{7.4}$$

The second and third phases, repeated in loop until convergence, correspond exactly to the algorithm presented in Sec. 6.3.1 (which was proved to be convergent).

We see here what announced in Sec. 6.4.2: the assumption concerning the alignment of the orthotropy directions for stiffness $\mathbf{A}^*$ and strength $\mathbf{G}^{A*}$ tensors combined with the assumption that the design variables β_m are independent from α_m, gives the only link between the stiffness and the strength optimisation phases. In this algorithm, we impose the global complementary energy as the leading objective to be minimised with respect to all of the optimisation parameters ($\overline{\Phi}_1$ and β_m). On the contrary, the strength functional, the failure index, is considered here as the secondary objective to be minimised, once the optimum for stiffness has been reached. In the optimisation phase concerning F_{Hill}^{Lam}, the parameters involved in the optimisation process are only the polar moduli (α_m), while the strength orthotropy orientation $\overline{\Omega}_1$ is given by the optimal value found for $\overline{\Phi}_1$ (see eq. (6.45) and assumption 10 of Sec. 6.2.1).

This assumption, allowing for a minimisation of F_{Hill}^{Lam} only with respect to α_m, leads to an important consequence: the local minimisation of F_{Hill}^{Lam} can be placed outside

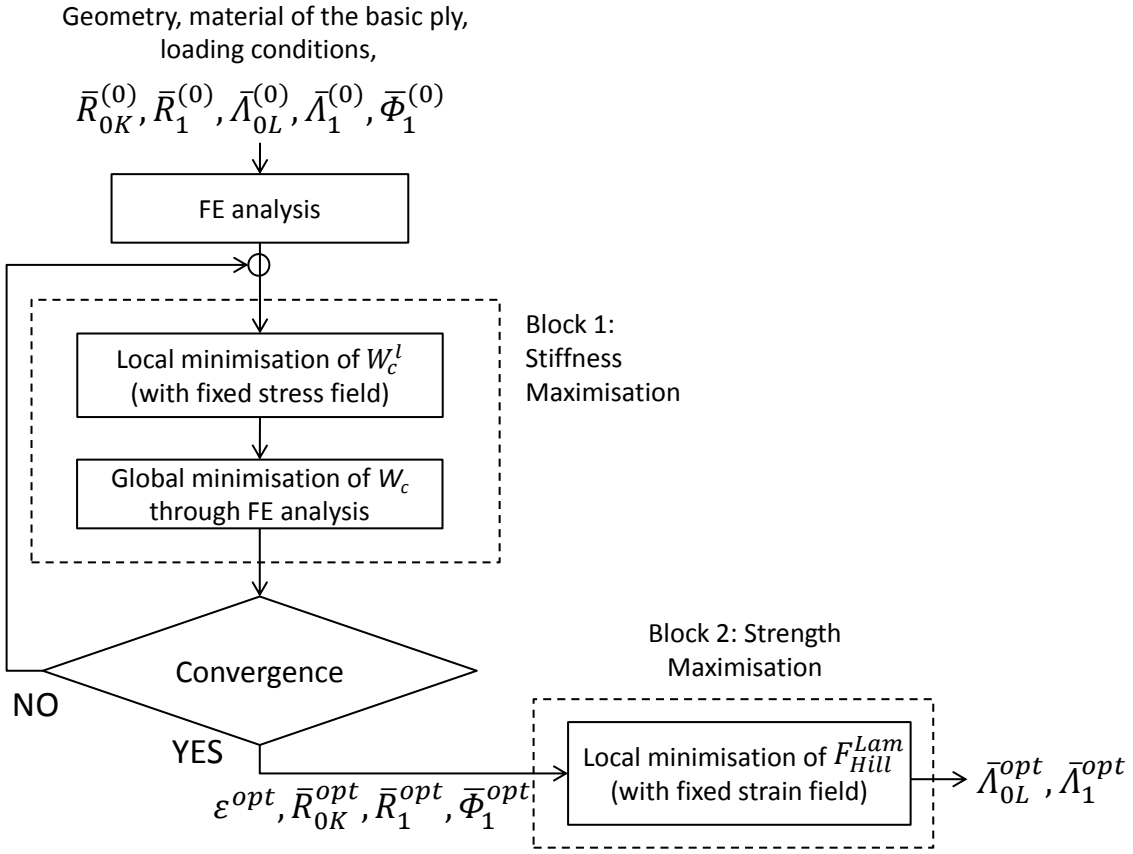

Figure 7.1: The iterative process to optimise the stiffness of laminated structures with *a posteriori* local maximisation of strength.

the iterative loop, after the convergence of the stiffness solution. This happens because the parameters α_m characterising the strength distribution do not take part to the FE analysis, nor to the evaluation of the complementary energy. Hence, the evaluation of α_m does not alter the iterative loops that lead to convergence for stiffness.

In Sec. 6.4.1 we have shown the advantages of using the failure criterion expressed in terms of strains. However, we can also express the problem (7.4) in terms of stresses and nothing will change in the mathematical formulation of the problem itself. The F_{Hill}^{Lam} written in terms of stresses is:

$$F_{Hill}^{Lam} = (\mathbf{N}^{opt})^T((\mathbf{A}^{opt})^{-1})^T\mathbf{G}^{A*}(\mathbf{A}^{opt})^{-1}(\mathbf{N})^{opt} \ , \tag{7.5}$$

with

$$\boldsymbol{\varepsilon}^{opt} = (\mathbf{A}^{opt})^{-1}\mathbf{N}^{opt} \ . \tag{7.6}$$

Thus, F_{Hill}^{Lam} of eq. (7.5) is equivalent to F_{Hill}^{Lam} of eq. (7.4). Therefore, when using the present algorithm, the expression of the F_{Hill}^{Lam} in terms of stresses or strains is equivalent.

7.3 The structural optimisation algorithm with *a priori* local maximisation of strength

This algorithm can be considered, in some sense, as the dual version of the previous one: here, strength is the primary property to be maximised while stiffness is the secondary

one. The optimisation parameters are:

$$\overline{\Omega}_1,\ \beta_m,\ \alpha_m\ , \tag{7.7}$$

$\overline{\Omega}_1$ is the strength orthotropy orientation, β_m is defined in eq. (6.2) and α_m is defined in eq. (7.2). The problem, (6.49), is composed as follows:

$$\begin{aligned} &\text{Sub-problem 1:} \quad \min_{\{\overline{\Omega}_1,\alpha_m\}} F_{Hill}^{Lam}(\overline{\Omega}_1,\alpha_m)\ , \\ &\text{Sub-problem 2:} \quad \min_{\beta_m}\min_{N_{ij}} W_c(\overline{\Omega}_1,\ \beta_m,\ \mathbf{N})\ ; \end{aligned} \tag{7.8}$$

subject to the *geometric bounds* of eqs. (6.3) and (6.26).

7.3.1 Optimisation algorithm: a first version

7.3.1.1 Description of the algorithm

The algorithm to solve such a problem, sketched in Fig. 7.2, can be divided into the following phases:

1. initialisation: the stiffness and strength distribution over the structure are initialised in some way, for instance they can be randomly sorted. Then, a first FE analysis is done to determine the starting stress and strain fields;

2. local minimisation of F_{Hill}^{Lam}: local determination of the new anisotropic strength distribution ($\overline{\Omega}_1^{(n+1)}$, $\alpha_m^{(n+1)}$) minimising the failure index F_{Hill}^{Lam} with a fixed strain field ($\boldsymbol{\varepsilon}^{(n)}$);

3. local minimisation of W_c^l: local definition of a new anisotropic stiffness distribution ($\beta_m^{(n+1)}$) that minimises the complementary energy with an imposed orthotropy orientation ($\overline{\Omega}_1^{(n+1)}$) and a fixed field ($\mathbf{N}^{(n)}$) of internal actions;

4. global minimisation of W_c: definition of the new internal actions ($\mathbf{N}^{(n+1)}$) and strain ($\boldsymbol{\varepsilon}^{(n+1)}$) fields linked to the new stiffness distribution ($\beta_m^{(n+1)}$, $\overline{\Omega}_1^{(n+1)}$) through a FE analysis.

The last three phases are repeated until convergence.

Just like in the previous case, the assumption concerning the alignment of the orthotropy directions for stiffness $\mathbf{A}^*$ and strength $\mathbf{G}^{A*}$ tensors combined with the assumption that the design variables β_m are independent from α_m, gives the only link between the strength and the stiffness optimisation phases. The strength functional, the laminate failure index, is minimised with respect to all of the optimisation parameters involved in it ($\overline{\Omega}_1$ and α_m). On the contrary, the stiffness functional, the complementary energy, is minimised only with respect to the polar moduli β_m, while the stiffness orthotropy orientation $\overline{\Phi}_1$ is given by the optimal value taken by $\overline{\Omega}_1$, eq. (6.45).

As the stiffness orthotropy orientation is given by the local minimisation of F_{Hill}^{Lam}, in this algorithm we cannot put outside the iterative loop, as an independent numerical phase, the strength optimisation phase, because the orthotropy orientation $\overline{\Omega}_1$ takes part to the evaluation of the complementary energy W_c, see eqs. (7.8). Therefore, the minimisation of F_{Hill}^{Lam} must be included into the iterative process and it is placed before the local

minimisation of W_c^l in order to determine the new optimal value of $\overline{\Omega}_1$, with strength as leading objective.

Differently from the previous optimisation algorithm, F_{Hill}^{Lam} cannot be expressed in both stress or strain terms. The laminate failure index in terms of internal forces at the iteration n is

$$F_{Hill}^{Lam} = (\mathbf{N}^{EF(n-1)})^T((\mathbf{A}^{(n)})^{-1})^T\mathbf{G}^{A*}(\mathbf{A}^{(n)})^{-1}(\mathbf{N})^{EF(n-1)} \ . \tag{7.9}$$

In eq. (7.9) the stresses are known as an output of the FE analysis at the iteration $(n-1)$ while the elasticity tensor is characterised by the anisotropy parameters $\beta_m^{(n)}$ that will be determined only after the local maximisation of stiffness. Thus, at the iteration n during the local minimisation of F_{Hill}^{Lam}, the stiffness tensor $\mathbf{A}^{(n)}$ in eq. (7.9) is not known. On the other hand, the F_{Hill}^{Lam} written in terms of strains

$$F_{Hill}^{Lam} = (\boldsymbol{\varepsilon}^{EF(n-1)})^T\mathbf{G}^{A*}(\boldsymbol{\varepsilon})^{EF(n-1)} \ , \tag{7.10}$$

is characterised by known quantities, in fact the strains are known as an output of the FE analysis at the previous iteration $n-1$. The only unknowns are the optimisation parameters α_m and $\overline{\Omega}_1$. Therefore, only the formulation in terms of strains can be used to solve the problem of local maximisation of strength in the framework of the present algorithm.

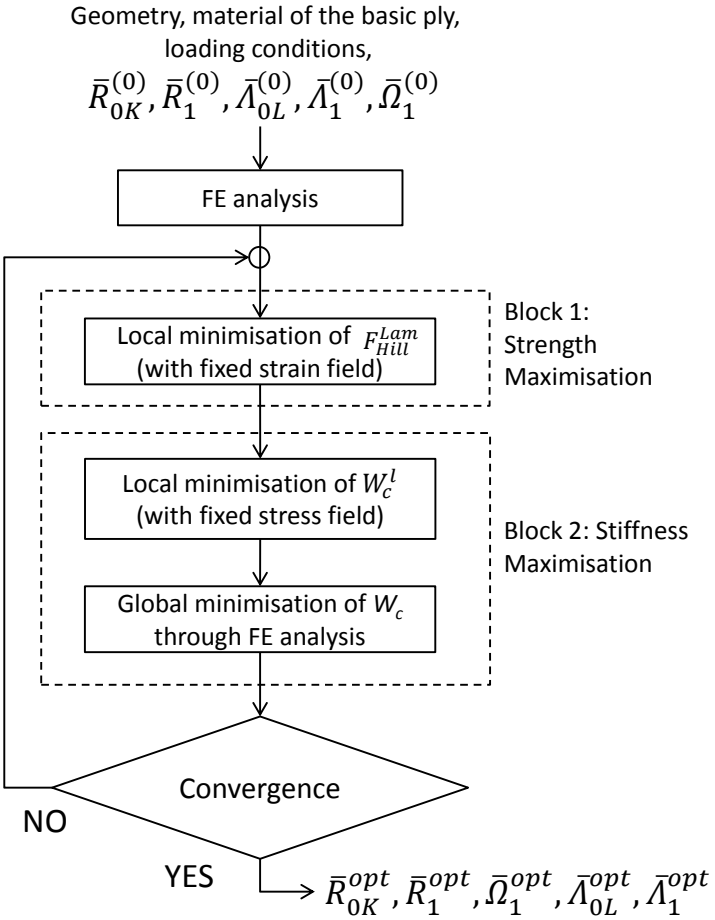

Figure 7.2: The iterative process of the first version of the algorithm with *a priori* maximisation of strength.

7.3.1.2 Discussion about convergence

Let us consider the anisotropic stiffness and strength parameters ($\beta_m^{(n)}$,$\alpha_m^{(n)}$,$\overline{\Omega}_1^{(n)}$) and the internal actions $\mathbf{N}^{(n)}$ and strain $\boldsymbol{\varepsilon}^{(n)}$ fields at the iteration n.

The local minimisation of F_{Hill}^{Lam} consists in finding the strength distribution $\alpha_m^{(n+1)}$ and $\overline{\Omega}_1^{(n+1)}$ such that

$$G_{ijkl}^{A*}(\overline{\Omega}_1^{(n+1)}, \alpha_m^{(n+1)})\varepsilon_{ij}^{(n)}\varepsilon_{kl}^{(n)} = \min_{\{\overline{\Omega}_1,\ \alpha_m\}} \left[G_{ijkl}^{A*}(\overline{\Omega}_1, \alpha_m)\varepsilon_{ij}^{(n)}\varepsilon_{kl}^{(n)}\right] , \tag{7.11}$$

defined at each point of the structure with a fixed strain field $\boldsymbol{\varepsilon}^{(n)}$.
The local minimisation of the complementary energy consists in finding the new stiffness distribution $\beta_m^{(n+1)}$ such that:

$$A_{ijkl}^{-1}(\beta_m^{(n+1)}, \overline{\Omega}_1^{(n+1)})N_{ij}^{(n)}N_{kl}^{(n)} = \min_{\beta_m} \left[A_{ijkl}^{-1}(\beta_m, \overline{\Omega}_1^{(n+1)})N_{ij}^{(n)}N_{kl}^{(n)}\right] , \tag{7.12}$$

at each point of the structure for a fixed field $\mathbf{N}^{(n)}$. This local minimisation, enforces the global inequality

$$\int_{S_p} A_{ijkl}^{-1}(\beta_m^{(n+1)}, \overline{\Omega}_1^{(n+1)})N_{ij}^{(n)}N_{kl}^{(n)}dS_p \leq \int_{S_p} A_{ijkl}^{-1}(\beta_m^{(n)}, \overline{\Omega}_1^{(n+1)})N_{ij}^{(n)}N_{kl}^{(n)}dS_p \ . \tag{7.13}$$

The global minimisation consists in determining the new fields $\mathbf{N}^{(n+1)}$ and $\boldsymbol{\varepsilon}^{(n+1)}$, solution to the elastic problem determined by the stiffness distribution ($\beta_m^{(n+1)}$, $\overline{\Omega}_1^{(n+1)}$). By the complementary energy theorem, we have

$$\int_{S_p} A_{ijkl}^{-1}(\beta_m^{(n+1)}, \overline{\Omega}_1^{(n+1)})N_{ij}^{(n+1)}N_{kl}^{(n+1)}dS_p \leq \int_{S_p} A_{ijkl}^{-1}(\beta_m^{(n+1)}, \overline{\Omega}_1^{(n+1)})N_{ij}^{(n)}N_{kl}^{(n)}dS_p \tag{7.14}$$

Combining eq. (7.13) with eq. (7.14) we obtain:

$$\int_{S_p} A_{ijkl}^{-1}(\beta_m^{(n+1)}, \overline{\Omega}_1^{(n+1)})N_{ij}^{(n+1)}N_{kl}^{(n+1)}dS_p \leq \int_{S_p} A_{ijkl}^{-1}(\beta_m^{(n)}, \overline{\Omega}_1^{(n+1)})N_{ij}^{(n)}N_{kl}^{(n)}dS_p \ , \tag{7.15}$$

so

$$W_c(\beta_m^{(n+1)}, \overline{\Omega}_1^{(n+1)}, \mathbf{N}^{(n+1)}) \leq W_c(\beta_m^{(n)}, \overline{\Omega}_1^{(n+1)}, \mathbf{N}^{(n)}) \ . \tag{7.16}$$

Eq. (7.16) shows that, concerning this second algorithm, only the reduction of the complementary energy from the local to the global minimisation phase is ensured. The reduction of W_c from the iteration n to the consecutive $(n+1)$ is no more ensured. We have:

$$W_c(\beta_m^{(n+1)}, \overline{\Omega}_1^{(n+1)}, \mathbf{N}^{(n+1)}) \lessgtr W_c(\beta_m^{(n)}, \overline{\Omega}_1^{(n)}, \mathbf{N}^{(n)}) \ . \tag{7.17}$$

This is due to the evaluation of the new field $\mathbf{N}^{(n+1)}$ that is linked to a stiffness distribution composed by two quantities, the modules β_m, that come from the local minimisation of the local complementary energy and by a third quantity, the orthotropy orientation $\overline{\Omega}_1$, that comes from the solution of another optimisation problem, the local minimisation of the laminate failure index. This means that, inside the convergent optimisation algorithm introduced by Allaire and Kohn [2], we introduce a quantity, the orthotropy orientation $\overline{\Omega}_1$, that takes part to the stiffness optimisation algorithm and that is calculated not to minimise the stiffness functional W_c but to minimise another quantity, the laminate

failure index. Such an alteration, introduced within the stiffness optimisation algorithm causes the loss of the convergence proof.

The monotonic decrease of the failure index, through the iterations, is also not ensured, i.e.:

$$F_{Hill}^{Lam}(\alpha_m^{(n+1)}, \overline{\Omega}_1^{(n+1)}, \boldsymbol{\varepsilon}^{(n+1)}) \lesseqgtr F_{Hill}^{Lam}(\alpha_m^{(n)}, \overline{\Omega}_1^{(n)}, \boldsymbol{\varepsilon}^{(n)}) \ . \tag{7.18}$$

This happens because the strength parameters, $\overline{\Omega}_1$ and α_m, are determined through the local minimisation of the laminate failure index but the strain field is the one obtained through the solution of an other optimisation problem: the global minimisation of the complementary energy.

The consequence is an oscillation of the values of W_c and F_{Hill}^{Lam} along the iterations. For this reason, we have modified this algorithm in order to recover the monotonic decrease of the complementary energy through the iterations, and thus, the convergence of the global procedure.

7.3.2 Optimisation algorithm: a second version

Concerning the first version of the optimisation algorithm with *a priori* maximisation of strength, we have highlighted an important aspect: the cause of the oscillation of the values of F_{Hill}^{Lam} and W_c is to be searched into the way the orthotropy orientation is determined. In order to avoid such an oscillation and ensure the convergence of the algorithm, we have developed a modified version of the previous algorithm.

7.3.2.1 Description of the algorithm

The main phases of this version of the algorithm, sketched in Fig. 7.3, are:

1. initialisation: the stiffness and strength distributions over the structure are initialised and a first FE analysis is conducted;

2. constrained local minimisation of F_{Hill}^{Lam}: local definition of the anisotropic strength distribution ($\alpha_m^{(n+1)}$, $\overline{\Omega}_1^{(n+1)}$) that minimise F_{Hill}^{Lam} with fixed strain field ($\boldsymbol{\varepsilon}^{(n)}$):

$$\min_{\{\overline{\Omega}_1,\ \alpha_m\}} \left[G_{ijkl}^{A*}(\overline{\Omega}_1, \alpha_m) \varepsilon_{ij}^{(n)} \varepsilon_{kl}^{(n)} \right] \ , \tag{7.19}$$

   with $\overline{\Omega}_1$ constrained by the condition

$$\min_{\beta_m} \left[A_{ijkl}^{-1}(\beta_m, \overline{\Omega}_1) N_{ij}^{(n)} N_{kl}^{(n)} \right] \leq A_{ijkl}^{-1}(\beta_m^{(n)}, \overline{\Omega}_1^{(n)}) N_{ij}^{(n)} N_{kl}^{(n)} \ ; \tag{7.20}$$

3. local minimisation of W_c^l: local definition of a new anisotropic stiffness distribution ($\beta_m^{(n+1)}$) that minimises the complementary energy with an imposed orthotropy orientation ($\overline{\Omega}_1^{(n+1)}$) and a fixed field ($\mathbf{N}^{(n)}$) of internal actions;

4. global minimisation of W_c: definition of the new internal actions $\mathbf{N}^{(n+1)}$ and strain $\boldsymbol{\varepsilon}^{(n+1)}$ fields linked to the new stiffness distribution ($\beta_m^{(n+1)}$, $\overline{\Omega}_1^{(n+1)}$) through a FE analysis;

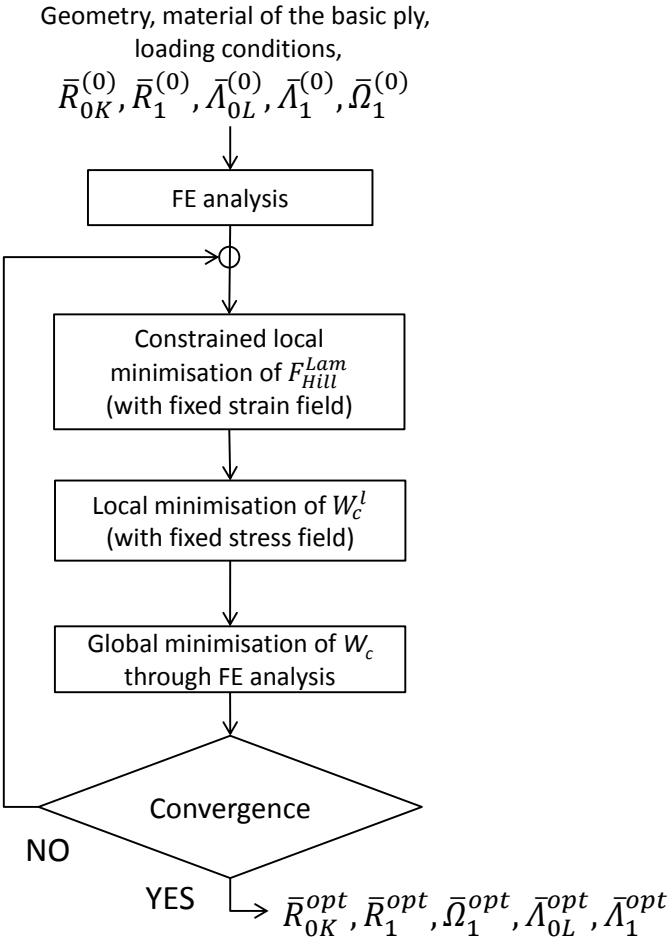

Figure 7.3: The iterative process of the second version of the algorithm with *a priori* maximisation of strength.

The three last phases are repeated until convergence of W_c.

Concerning this modified version of the algorithm *a priori*, we have simply inserted a constraint on the evaluation of the orthotropy orientation $\overline{\Omega}_1$: the optimal value of $\overline{\Omega}_1$, determined through the local minimisation of F_{Hill}^{Lam}, has to belong to a domain of orientations such that the reduction of the complementary energy, through the iterations, is ensured. Of course, in this algorithm, only the monotonic decrease of the complementary energy is ensured, while the value of F_{Hill}^{Lam} can oscillate along the iterations.

7.3.2.2 Convergence proof

Let us consider the anisotropic stiffness and strength distribution $(\beta_m^{(n)}, \alpha_m^{(n)}, \overline{\Omega}_1^{(n)})$ and the internal actions $\mathbf{N}^{(n)}$ and strain $\boldsymbol{\varepsilon}^{(n)}$ fields at the iteration n.

The local minimisation of F_{Hill}^{Lam} consists in finding the strength distribution $\alpha_m^{(n+1)}$ and $\overline{\Omega}_1^{(n+1)}$ such that

$$G_{ijkl}^{A*}(\overline{\Omega}_1^{(n+1)}, \alpha_m^{(n+1)})\varepsilon_{ij}^{(n)}\varepsilon_{kl}^{(n)} = \min_{\{\overline{\Omega}_1,\ \alpha_m\}} \left[G_{ijkl}^{A*}(\overline{\Omega}_1, \alpha_m)\varepsilon_{ij}^{(n)}\varepsilon_{kl}^{(n)} \right] , \tag{7.21}$$

at each point of the structure, with $\overline{\Omega}_1$ constrained by the condition

$$\min_{\beta_m}\left[A^{-1}_{ijkl}(\beta_m,\overline{\Omega}_1)N^{(n)}_{ij}N^{(n)}_{kl}\right] \leq A^{-1}_{ijkl}(\beta^{(n)}_m,\overline{\Omega}^{(n)}_1)N^{(n)}_{ij}N^{(n)}_{kl} \ , \tag{7.22}$$

This constraint, at least, is satisfied for $\overline{\Omega}_1 = \overline{\Omega}^{(n)}_1$, that leads to the same value of W^l_c calculated at the previous iteration. The range of orientations $\overline{\Omega}_1$ satisfying such a constraint will be formally written in the form

$$\overline{\Omega}_1 \in \left[\overline{\Omega}_{1_a},\overline{\Omega}_{1_b}\right] \tag{7.23}$$

though the domain of $\overline{\Omega}_1$ satisfying (7.22) could possibly be composed by several distinct intervals. The local minimisation of the complementary energy is performed in order to find the new stiffness distribution:

$$A^{-1}_{ijkl}(\beta^{(n+1)}_m,\overline{\Omega}^{(n+1)}_1)N^{(n)}_{ij}N^{(n)}_{kl} = \min_{\beta_m}\left[A^{-1}_{ijkl}(\beta_m,\overline{\Omega}^{(n+1)}_1)N^{(n)}_{ij}N^{(n)}_{kl}\right] \ , \tag{7.24}$$

considering that $\overline{\Omega}^{(n+1)}_1$ determined through the local minimisation of F^{Lam}_{Hill} satisfies the condition (7.22), we have:

$$\int_{S_p} A^{-1}_{ijkl}(\beta^{(n+1)}_m,\overline{\Omega}^{(n+1)}_1)N^{(n)}_{ij}N^{(n)}_{kl}dS_p \leq \int_{S_p} A^{-1}_{ijkl}(\beta^{(n)}_m,\overline{\Omega}^{(n)}_1)N^{(n)}_{ij}N^{(n)}_{kl}dS_p \ . \tag{7.25}$$

The global minimisation consists in determining the new stress ($\mathbf{N}^{(n+1)}$) and strain ($\boldsymbol{\varepsilon}^{(n+1)}$) fields, solution to the elastic problem linked to the stiffness distribution ($\beta^{(n+1)}_m,\overline{\Omega}^{(n+1)}_1$). Thanks to the complementary energy theorem, the following inequality

$$\int_{S_p} A^{-1}_{ijkl}(\beta^{(n+1)}_m,\overline{\Omega}^{(n+1)}_1)N^{(n+1)}_{ij}N^{(n+1)}_{kl}dS_p \leq \int_{S_p} A^{-1}_{ijkl}(\beta^{(n+1)}_m,\overline{\Omega}^{(n+1)}_1)N^{(n)}_{ij}N^{(n)}_{kl}dS_p \ , \tag{7.26}$$

is verified. In addition, combining eq. (7.25) with eq. (7.26) we obtain:

$$\int_{S_p} A^{-1}_{ijkl}(\beta^{(n+1)}_m,\overline{\Omega}^{(n+1)}_1)N^{(n+1)}_{ij}N^{(n+1)}_{kl}dS_p \leq \int_{S_p} A^{-1}_{ijkl}(\beta^{(n)}_m,\overline{\Omega}^{(n)}_1)N^{(n)}_{ij}N^{(n)}_{kl}dS_p \ , \tag{7.27}$$

so

$$W^{(n+1)}_c \leq W^{(n)}_c \ , \tag{7.28}$$

which proves the monotonic convergence of the algorithm for what concerns W_c. Since W_c reduces at each iteration and converges, F^{Lam}_{Hill} will converge to a value due to the convergence of the strain field.

Some remarks on this second version of the algorithm *a priori* are mandatory. First of all, in order to prove the convergence of the algorithm we inserted a constraint on the evaluation of the optimal orthotropy orientation; such a value has to ensure the reduction of the local complementary energy from an iteration to the consecutive. The orthotropy orientations satisfying such a constraint include the optimal orientation of the previous iteration and, generally, are more than only one. Then, we choose, among them, the orientation that gives the minimum value of F^{Lam}_{Hill}.

Therefore, in this new version of the algorithm we are still favouring the strength but with a limit on the solution space linked to the optimal orientation. At each iteration, the optimum value of F^{Lam}_{Hill} is still a minimum, but its search is limited to a given domain of

orientations. Such a value, hence, could not be the global minimum that we can obtain for a given strain field, like what happens in the first version of the algorithm where no limits are imposed on the search space of the optimal values of $\overline{\Omega}_1$ to minimise F_{Hill}^{Lam}. As a consequence, even if F_{Hill}^{Lam} converges to a value, its convergence could not be monotonic.

Concluding, we can assert that this second version of the algorithm is slightly different from the previous one, it ensures the monotonic convergence of W_c and the oscillating convergence of F_{Hill}^{Lam}.

7.4 Solution of local minimisations

In this Section we determine the solution, analytical or numerical, of the local minimisation phases belonging to the optimisation algorithms described in Secs. 7.2 and 7.3.

7.4.1 Analytical solution for minimum laminate failure index

7.4.1.1 First local minimisation problem: fixed orthtotropy orientation

The optimisation problem is:

$$\underset{\left\{\overline{\Lambda}_{0L},\overline{\Lambda}_1\right\}}{min} F_{Hill}^{Lam}\left(\overline{\Lambda}_{0L},\overline{\Lambda}_1,\overline{\Omega}_1^{opt}\right) \ , \tag{7.29}$$

with:

$$\begin{cases} 2\left(\dfrac{\overline{\Lambda}_1}{\Lambda_1}\right)^2 - 1 \leq \dfrac{\overline{\Lambda}_{0L}}{(-1)^L\Lambda_0} \ , \\ |\overline{\Lambda}_{0L}| \leq \Lambda_0 \ , \\ \overline{\Lambda}_1 \geq 0 \ . \end{cases} \tag{7.30}$$

and

$$\overline{\Omega}_1 = \begin{cases} \overline{\Phi}_1^{opt} \ or \\ \overline{\Phi}_1^{opt} + \pi/2 \ . \end{cases} \tag{7.31}$$

This local minimisation problem takes part to:

- the *a posteriori* local minimisation phase of F_{Hill}^{Lam} in the "algorithm *a posteriori*", eq. (7.4);
- the constrained local minimisation of F_{Hill}^{Lam} in the second version of the "algorithm *a priori*", as we will show in Sec. 7.5.2;

The constraints (7.30) are the *geometric bounds* already introduced and written here in a slight different way from eqs. (6.26) to take into account for variable $\overline{\Lambda}_{0L}$, eq. (6.46).

The extended expression of the objective function is, eq. (6.30):

$$F_{Hill}^{Lam} = 4r^2\Gamma_0 + 8t^2\Gamma_1 + 4\overline{\Lambda}_{0L}r^2\cos 4\left(\overline{\Omega}_1 - \phi\right) + 16tr\overline{\Lambda}_1\cos 2\left(\overline{\Omega}_1 - \phi\right) \ . \tag{7.32}$$

The two partial derivatives of F_{Hill}^{Lam} with respect to $\overline{\Lambda}_{0L}$ and $\overline{\Lambda}_1$ are:

$$\begin{aligned} \frac{\partial F_{Hill}^{Lam}}{\partial\overline{\Lambda}_{0L}} &= 4r^2\cos 4(\overline{\Omega}_1 - \phi) \ , \\ \frac{\partial F_{Hill}^{Lam}}{\partial\overline{\Lambda}_1} &= 16tr\cos 2(\overline{\Omega}_1 - \phi) \ . \end{aligned} \tag{7.33}$$

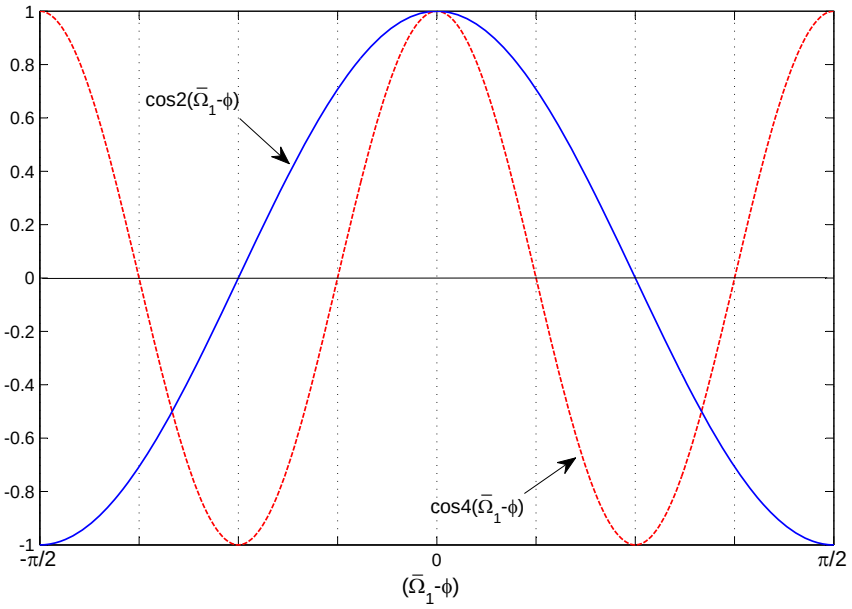

Figure 7.4: Diagram of the two functions $\cos 4\left(\overline{\Omega}_1 - \phi\right)$ and $\cos 2\left(\overline{\Omega}_1 - \phi\right)$.

Both the derivatives are constant for a fixed strain field. F_{Hill}^{Lam} is a linear function of $\overline{\Lambda}_{0L}$ and $\overline{\Lambda}_1$. Therefore, the minimum value of F_{Hill}^{Lam} necessarily lies on the boundary of the domain defined in the plane $(\overline{\Lambda}_{0L}, \overline{\Lambda}_1)$ by eqs. (7.30). Moreover, the sign of the partial derivatives (7.33) depends upon the signs of $\cos 4\left(\overline{\Omega}_1 - \phi\right)$ and $\cos 2\left(\overline{\Omega}_1 - \phi\right)$, Fig. 7.4), and upon the sign of t, the spherical part of strains. In addition, the area of admissible values of $\overline{\Lambda}_{0L}$ and $\overline{\Lambda}_1$ changes together with the value of the orthotropy shape parameter L of the basic ply, see eq. (7.30). This suggest that it is worth to separate the solutions into two main groups, depending on the value L of the basic ply.

Before introducing such solutions, we have to consider another important case: the spherical strain field, characterised by $r = 0$. If we impose $r = 0$ in eq. (7.32), the two optimisation parameters are not longer present in the equation of F_{Hill}^{Lam}. This means that, for a spherical strain field, any value of $\overline{\Lambda}_{0L}$ and $\overline{\Lambda}_1$ within the admissible design region can be optimal for the failure index functional. From a mechanical point of view this means that when the strain field is purely spherical, we can place the fibres, of the corresponding laminate, in any direction and we will have still an optimal solution in terms of homogenised strength.

All the following cases will be characterised by $r \neq 0$.

Let us, then, consider the first case of a basic ply with $L = 0$. As the solution depends upon the sign of t, $\cos 4\left(\overline{\Omega}_1 - \phi\right)$ and $\cos 2\left(\overline{\Omega}_1 - \phi\right)$, we start our analysis by considering the case

$$t > 0 \text{ and } \left(\overline{\Omega}_1 - \phi\right) \in \left]-\frac{\pi}{8}, \frac{\pi}{8}\right[,$$

for which all the above three quantities are positive.

In this case we have at the same time:

$$\frac{\partial F_{Hill}^{Lam}}{\partial \overline{\Lambda}_{0L}} > 0, \quad \frac{\partial F_{Hill}^{Lam}}{\partial \overline{\Lambda}_1} > 0 \ . \tag{7.34}$$

The two design variables $\overline{\Lambda}_{0L}$ and $\overline{\Lambda}_1$ being independent, the point corresponding to the minimum of F_{Hill}^{Lam} is point A in Fig. 7.5, where $\overline{\Lambda}_{0L}$ and $\overline{\Lambda}_1$ get their lowest admissible

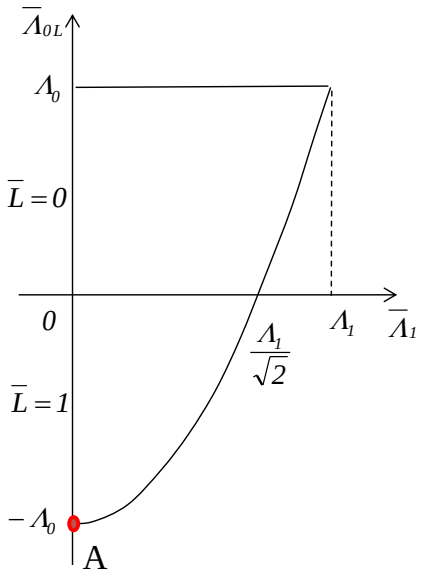

Figure 7.5: Admissible domain of $\overline{\Lambda}_{0L}$ and $\overline{\Lambda}_1$ for a basic ply with $L = 0$.

value:

$$\begin{aligned} \overline{\Lambda}_{0L}^{opt} &= -\Lambda_0, \\ \overline{\Lambda}_1^{opt} &= 0 \ . \end{aligned} \tag{7.35}$$

The objective function takes, thus, the following value:

$$F_{Hill}^{Lam} = 4r^2\Gamma_0 + 8t^2\Gamma_1 - 4\Lambda_0 r^2 \cos 4\left(\overline{\Omega}_1 - \phi\right) \ . \tag{7.36}$$

The remaining cases, characterised by other combinations of the signs of t, $\cos 4\left(\overline{\Omega}_1 - \phi\right)$ and $\cos 2\left(\overline{\Omega}_1 - \phi\right)$, can be treated in the same way. The complete discussion of all the cases is rather lengthy, and for a better appraisal of the general procedure, presented it in Appendix A.1.

A complete summary of the solutions of the local minimisation of F_{Hill}^{Lam} for $L = 0$ is presented in Tab. 7.1. The angular range of $\left(\overline{\Omega}_1 - \phi\right)$ is considered only between 0 and $\pi/2$ because of the symmetry of the solutions that are symmetric with respect to the axis $\left(\overline{\Omega}_1 - \phi\right) = 0$. Moreover, in Table 7.1 we numerate the solutions in order to map the "solution type" linked to the local minimisation of F_{Hill}^{Lam} over the surface of the structures considered in the numerical examples of Sec. 7.6. The numeration associates in a unique value of "solution type" all optimal solutions having the same optimal values of $\overline{\Lambda}_{0L}$ and $\overline{\Lambda}_1$. In particular, the solution type 0 has been associated to a specific solution, that obtained whit a purely spherical strain field.

Let us now turn the attention on the case $L = 1$ of the basic ply. Also in this case, in order to find the best value of the two design variables $\overline{\Lambda}_{0L}$ and $\overline{\Lambda}_1$, we have to distinguish different cases, depending upon the sign of t, $\cos 4\left(\overline{\Omega}_1 - \phi\right)$ and $\cos 2\left(\overline{\Omega}_1 - \phi\right)$. The way to get the optimal values of $\overline{\Lambda}_{0L}$ and $\overline{\Lambda}_1$ is completely similar to that sketched above for $L = 0$. For the sake of brevity, the results concerning the case $L = 1$, are not reported here but are simply summarised in Tab. 7.2. The numeration of solution associate in a unique value of "solution type" all optimal solutions having the same optimal values of $\overline{\Lambda}_{0L}$ and $\overline{\Lambda}_1$. Again, the solution type 0 is associated to the solution obtained whit a purely

$(\overline{\Omega}_1 - \phi)$	$[0, \frac{\pi}{8}[$	$\frac{\pi}{8}$	$]\frac{\pi}{8}, \frac{\pi}{4}[$	$\frac{\pi}{4}$	$]\frac{\pi}{4}, \frac{3\pi}{8}[$	$\frac{3\pi}{8}$	$]\frac{3\pi}{8}, \frac{\pi}{2}]$
$\mathbf{r = 0}$, $\forall$t, Solution Type = 0							
$\overline{\Lambda}_{0L}^{opt}$	*any*						
$\overline{\Lambda}_1^{opt}$	*any*						
$\mathbf{t > 0}$, $\mathbf{r \neq 0}$							
Solution Type :	**1**	**5**	**2**	**6**	**3**		**4**
$\overline{\Lambda}_{0L}^{opt}$	$-\Lambda_0$	$[-\Lambda_0, \Lambda_0]$	Λ_0				$\left(\frac{2(\overline{\Lambda}_1^{opt})^2}{\Lambda_1^2} - 1\right)\Lambda_0$; Λ_0 (*)
$\overline{\Lambda}_1^{opt}$	0			$[0, \Lambda_1]$	Λ_1		$\frac{t\lvert \cos 2\left(\overline{\Omega}_1 - \phi\right)\rvert \Lambda_1^2}{r\Lambda_0 \cos 4\left(\overline{\Omega}_1 - \phi\right)}$; Λ_1 (*)
$\mathbf{t = 0}$, $\mathbf{r \neq 0}$							
Solution Type :	**1**	**7**	**6**		**7**		**1**
$\overline{\Lambda}_{0L}^{opt}$	$-\Lambda_0$	*any*	Λ_0		*any*		$-\Lambda_0$
$\overline{\Lambda}_1^{opt}$	0	*any*	$[0, \Lambda_1]$		*any*		0
$\mathbf{t < 0}$, $\mathbf{r \neq 0}$							
Solution Type :	**4**	**3**	**6**	**2**	**5**		**1**
$\overline{\Lambda}_{0L}^{opt}$	$\left(\frac{2(\overline{\Lambda}_1^{opt})^2}{\Lambda_1^2} - 1\right)\Lambda_0$; Λ_0 (*)	Λ_0			$[-\Lambda_0, \Lambda_0]$		$-\Lambda_0$
$\overline{\Lambda}_1^{opt}$	$\frac{\lvert t\rvert \cos 2\left(\overline{\Omega}_1 - \phi\right) \Lambda_1^2}{r\Lambda_0 \cos 4\left(\overline{\Omega}_1 - \phi\right)}$; Λ_1 (*)	Λ_1	$[0, \Lambda_1]$		0		

(*) the first solution is valid for $\frac{|t|}{r} < \frac{\Lambda_0 \cos 4\left(\overline{\Omega}_1 - \phi\right)}{\Lambda_1 \lvert \cos 2\left(\overline{\Omega}_1 - \phi\right)\rvert}$

Table 7.1: Solutions for $L = 0$, local minimisation of F_{Hill}^{Lam} with an imposed value of $\overline{\Omega}_1$.

$(\overline{\Omega}_1 - \phi)$	$\left[0, \frac{\pi}{8}\right[$	$\frac{\pi}{8}$	$\left]\frac{\pi}{8}, \frac{\pi}{4}\right[$	$\frac{\pi}{4}$	$\left]\frac{\pi}{4}, \frac{3\pi}{8}\right[$	$\frac{3\pi}{8}$	$\left]\frac{3\pi}{8}, \frac{\pi}{2}\right]$
$\mathbf{r = 0}$, $\forall$t, Solution Type = 0							
$\overline{\Lambda}_{0L}^{opt}$	*any*						
$\overline{\Lambda}_{1}^{opt}$	*any*						
$\mathbf{t > 0},\ \mathbf{r \neq 0}$							
Solution Type :	**1**	**5**	**2**		**8**	**9**	
$\overline{\Lambda}_{0L}^{opt}$	$-\Lambda_0$	$[-\Lambda_0, \Lambda_0]$	Λ_0		$\left(1 - \frac{2(\overline{\Lambda}_1^{opt})^2}{\Lambda_1^2}\right)\Lambda_0$; $-\Lambda_0$ (*)	$-\Lambda_0$	
$\overline{\Lambda}_{1}^{opt}$	0				$\frac{t\cos 2\left(\overline{\Omega}_1 - \phi\right)\Lambda_1^2}{r\cos 4\left(\overline{\Omega}_1 - \phi\right)\Lambda_0}$; Λ_1 (*)	Λ_1	
$\mathbf{t = 0},\ \mathbf{r \neq 0}$							
Solution Type :	**10**	**7**	**2**			**7**	**10**
$\overline{\Lambda}_{0L}^{opt}$	$-\Lambda_0$	*any*	Λ_0			*any*	$-\Lambda_0$
$\overline{\Lambda}_{1}^{opt}$	$[0, \Lambda_1]$	*any*	0			*any*	$[0, \Lambda_1]$
$\mathbf{t < 0},\ \mathbf{r \neq 0}$							
Solution Type :	**9**		**4**	**2**		**5**	**1**
$\overline{\Lambda}_{0L}^{opt}$	$-\Lambda_0$		$\left(\frac{2(\overline{\Lambda}_1^{opt})^2}{\Lambda_1^2} - 1\right)\Lambda_0$; Λ_0 (*)	Λ_0		$[-\Lambda_0, \Lambda_0]$	$-\Lambda_0$
$\overline{\Lambda}_{1}^{opt}$	Λ_1		$\frac{t\cos 2\left(\overline{\Omega}_1 - \phi\right)\Lambda_1^2}{r\cos 4\left(\overline{\Omega}_1 - \phi\right)\Lambda_0}$; Λ_1 (*)	0			

(*) the first solution is valid for $\dfrac{t}{r} < \dfrac{\Lambda_0 \cos 4\left(\overline{\Omega}_1 - \phi\right)}{\Lambda_1 \cos 2\left(\overline{\Omega}_1 - \phi\right)}$

Table 7.2: Solutions for $L = 1$, local minimisation of F_{Hill}^{Lam} with an imposed value of $\overline{\Omega}_1$.

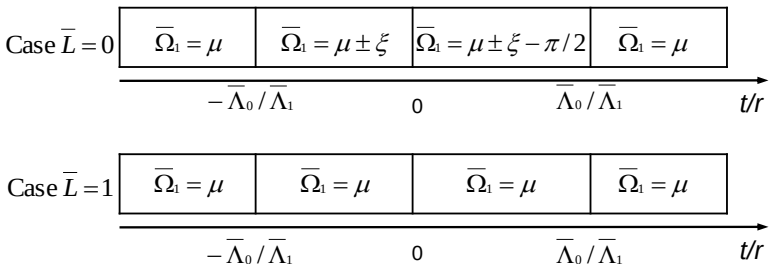

Figure 7.6: Optimal orthotropy orientation to minimise F_{Hill}^{Lam}.

spherical strain filed. The reader can find the complete discussion of all the possible cases corresponding to $L = 1$ in Appendix A.1.

7.4.1.2 Second local minimisation problem: including the orthotropy orientation as an optimisation variable

The optimisation problem can be formalised as:

$$\underset{\left\{\overline{\Lambda}_{0L},\overline{\Lambda}_1,\overline{\Omega}_1\right\}}{min} F_{Hill}^{Lam}\left(\overline{\Lambda}_{0L},\overline{\Lambda}_1,\overline{\Omega}_1\right) \ , \tag{7.37}$$

along with the constraints (7.30). The objective function is:

$$F_{Hill}^{Lam} = 4r^2\Gamma_0 + 8t^2\Gamma_1 + 4\overline{\Lambda}_{0L}r^2\cos 4\left(\overline{\Omega}_1-\phi\right) + 16tr\overline{\Lambda}_1\cos 2\left(\overline{\Omega}_1-\phi\right) \ . \tag{7.38}$$

This local minimisation problem takes part to the local minimisation phase of F_{Hill}^{Lam} in the first and second version of the "algorithm *a priori*".

In this case F_{Hill}^{Lam} has to be minimised with respect to three variables: the orthotropy orientation $\overline{\Omega}_1$ and the polar moduli $\overline{\Lambda}_{0L}$ and $\overline{\Lambda}_1$. The analytical solution of this problem will be realised within two consecutive phases: firstly the minimisation with respect to the orientation $\overline{\Omega}_1$ of the orthotropy axis and then, the minimisation with respect to the polar moduli $\overline{\Lambda}_{0L}$ and $\overline{\Lambda}_1$.

We can evaluate the optimal orientation $\overline{\Omega}_1^{opt}$ by the same procedure already used in Sec. 5.2 where the problem of minimising the failure index of a simple ply has been solved varying only the orthotropy orientation Ω_1. Thus, we present directly the results in Fig. 7.6 where

$$\begin{aligned} \mu &= \mathrm{dir}\left(\min\left\{|\varepsilon_I|,\,|\varepsilon_{II}|\right\}\right) \ , \\ \xi &= \frac{1}{2}\arccos\left(-\frac{\overline{\Lambda}_1 t}{\overline{\Lambda}_{0L} r}\right) \ . \end{aligned} \tag{7.39}$$

Fig. 7.6 shows that the orthotropy shape parameter $\overline{L}$ of the plate plays a decisive role in the evaluation of the optimal orthotropy orientation. We have, thus, two type of solutions concerning the optimal orthotropy orientation:

- a solution that does not include the term ξ, that we will call solution non-ξ;
- a solution including the term ξ, that we will call solution ξ.

If we put the expression of $\overline{\Omega}_1^{opt}$ in eq. (7.38), depending on the type of solution (non-ξ or ξ), $F_{Hill}^{Lam}(\overline{\Omega}_1^{opt})$ can assume two different expressions. Therefore, in the second minimisation phase, we have to minimise two different functions with respect to $\overline{\Lambda}_{0L}$ and $\overline{\Lambda}_1$:

$$\text{solution non-}\xi: \quad F_{Hill}^{Lam}(\overline{\Lambda}_{0L},\overline{\Lambda}_1,\overline{\Omega}_1^{opt}) = 4r^2\Gamma_0 + 8t^2\Gamma_1 + 4\overline{\Lambda}_{0L}r^2 - 16|t|r\overline{\Lambda}_1; \tag{7.40}$$

$$\text{solution } \xi: \quad F_{Hill}^{Lam}(\overline{\Lambda}_{0L}, \overline{\Lambda}_1, \overline{\Omega}_1^{opt}) = 4r^2\Gamma_0 + 8t^2\Gamma_1 - 4\overline{\Lambda}_0 r^2 - 8t^2\frac{\overline{\Lambda}_1^2}{\overline{\Lambda}_0} \ . \tag{7.41}$$

The optimal value of F_{Hill}^{Lam} obtained minimising eq. (7.40) will be, then, compared with that obtained minimising eq. (7.41). The solution that give the minimum value of F_{Hill}^{Lam} (and the corresponding values of the design variables $\overline{\Omega}_1$, $\overline{\Lambda}_{0L}$ and $\overline{\Lambda}_1$) will be the global optimal solution of problem (7.37).

In order to find an analytical solution, we can proceed by following the same logical steps described in Sec. 7.4.1.1. For the sake of brevity, the solutions of this case are directly summarised in Tab. 7.3, while the extended proof of solutions is reported in Appendix A.2. Also in this case, the solutions are numbered in order to have a map of "solution type" concerning the local minimisation of F_{Hill}^{Lam} in the section of numerical examples (Sec. 7.6). The first row of Tab. 7.3 gives the optimal value of $\overline{\Omega}_1$, while the rows below report the optimal values of the polar moduli $\overline{\Lambda}_{0L}$ and $\overline{\Lambda}_1$ depending on the value of L of the basic ply and, furthermore, on the strain field through the quantity $|t|/r$ with respect to ratio Λ_0/Λ_1 between the polar moduli of the basic ply.

In particular, the first row of Tab. 7.3 shows that the optimal orthotropy orientation to maximise the strength is always $\overline{\Omega}_1^{opt} = \text{dir}\left(\min\left\{|\varepsilon_I|, |\varepsilon_{II}|\right\}\right)$, eq. (7.39), for every value of L and $|t|/r$; so, the global minimum of F_{Hill}^{Lam} is always obtained from the problem of solution non-ξ, eq. (7.40).

This result leads to an important consequence: we know from Tab. 6.1 that the optimal orthotropy orientation that maximises the stiffness (for a given stress field) is always aligned with the directions of principal stresses, on the other hand, Tab. 7.3 shows that the optimal orthotropy orientation to maximise the strength (for a given strain field) is always aligned with the direction of the principal strains. Therefore, if in an anisotropic structure the stress and strain fields are such that the principal stresses and strains are aligned, the optimal orthotropy orientation maximising the strength will be aligned with that maximising the stiffness. Therefore, if the optimal solution carried out by the described algorithms, Secs. 7.2 and 7.3, leads to such a condition, we will have obtained a global optimal solution in terms of both the stiffness and the strength.

7.4.2 Numerical solution for minimum complementary energy with a fixed orthotropy orientation

The numerical approach described below is used in the first and second version of the algorithm *a priori* to solve the local minimisation phases of the local complementary energy, Sec. 7.3. The optimisation problem can be formalised as:

$$\min_{\left\{\overline{R}_{0K}, \overline{R}_1\right\}} W_c\left(\overline{R}_{0K}, \overline{R}_1\right) \tag{7.42}$$

with the constraints:

$$\begin{aligned} & 2\left(\frac{\overline{R}_1}{R_1}\right)^2 - 1 \leq \frac{\overline{R}_{0K}}{(-1)^K R_0}, \\ & |\overline{R}_{0K}| \leq R_0, \\ & \overline{R}_1 \geq 0; \end{aligned} \tag{7.43}$$

$\overline{\Omega}_1^{opt} = \mathrm{dir}\left(\min\left\{\lvert\varepsilon_I\rvert, \lvert\varepsilon_{II}\rvert\right\}\right) \forall$ **L, t, r**		
$\overline{\Lambda}_{0L}^{opt}$	$\overline{\Lambda}_1^{opt}$	$F_{Hill}^{Lam(opt)}$
L = 0, 1; r = 0, ∀t; Solution Type = 0		
any	*any*	$8t^2\Gamma_1$
L = 0		
$\frac{\lvert\mathbf{t}\rvert}{\mathbf{r}} \leq \frac{\Lambda_0}{\Lambda_1}$, **Solution Type = 11**		
$\left(\frac{2t^2\Lambda_1^2}{r^2\Lambda_0^2} - 1\right)\Lambda_0$	$\frac{\lvert t\rvert\Lambda_1^2}{r\Lambda_0}$	$4r^2\Gamma_0 + 8t^2\Gamma_1 - 4r^2\Lambda_0 - 8t^2\frac{\Lambda_1^2}{\Lambda_0}$
$\frac{\lvert\mathbf{t}\rvert}{\mathbf{r}} \geq \frac{\Lambda_0}{\Lambda_1}$, **Solution Type = 12**		
Λ_0	Λ_1	$4r^2\Gamma_0 + 8t^2\Gamma_1 + 4\Lambda_0 r^2 - 16\lvert t\rvert r\Lambda_1$
t = 0, Solution Type = 13		
$-\Lambda_0$	0	$4r^2\Gamma_0 - 4\Lambda_0 r^2$
L = 1		
t ≠ 0, Solution Type = 14		
$-\Lambda_0$	Λ_1	$4r^2\Gamma_0 + 8t^2\Gamma_1 - 4\Lambda_0 r^2 - 16\lvert t\rvert r\Lambda_1$
t = 0, Solution Type = 15		
$-\Lambda_0$	$[0, \Lambda_1]$	$4r^2\Gamma_0 - 4\Lambda_0 r^2$

Table 7.3: Global solution of the local minimisation of F_{Hill}^{Lam} including $\overline{\Omega}_1$ as optimisation parameter.

where:

$$W_c = \frac{1}{\Delta}\Big[2(T_0T_1 - \overline{R}_1^2)R^2 + (T_0^2 - \overline{R}_{0K}^2)T^2 + 2(\overline{R}_1^2 - T_1\overline{R}_{0K})R^2\cos 4(\overline{\Phi}_1 - \Phi) + -4\overline{R}_1(T_0 - (-1)^{\overline{K}}\overline{R}_{0K})TR\cos 2(\overline{\Phi}_1 - \Phi)\Big], \tag{7.44}$$

with:

$$\Delta = 4T_1(T_0^2 - \overline{R}_{0K}^2) - 8\overline{R}_1^2(T_0 - \overline{R}_{0K}); \tag{7.45}$$

and

$$\overline{\Phi}_1 = \begin{cases} \overline{\Omega}_1^{opt} & \text{or} \\ \overline{\Omega}_1^{opt} + \pi/2\ . \end{cases} \tag{7.46}$$

T, R and Φ are the polar parameters of $\mathbf{N}$. $\overline{\Omega}_1^{opt}$ is determined through the local minimisation of F_{Hill}^{Lam}. Thus, unlike the analytical solution of $(\overline{\Phi}_1 - \Phi)$ to problem (6.3) depicted in Tab. 6.1, in this case we know only the numerical value of such a angular difference, hence, we don't have an analytical expression of $(\overline{\Phi}_1 - \Phi)$ to put into eq. (7.44) in order to simplify the problem (7.42) like in [34].

The derivatives with respect to $\overline{R}_{0K}$ and $\overline{R}_1$ are rational functions of second order polynomials in terms of $\overline{R}_{0K}$ and $\overline{R}_1$. We can consider two separated cases: the first

one, where the principal stress and strains orientations are coincident, $\Phi = \phi$. In this circumstance, the analytical solution is the same presented in Tab. 6.1. In the second case the two orientations Φ and ϕ are different. In this circumstance, for what said above, the minimum of the local complementary energy is searched using a fixed point algorithm which consists in consecutive and alternated minimisations of the objective function with respect to the two design variables, in this case $\overline{R}_{0K}$ and $\overline{R}_1$. The procedure can be described as follows:

- the numerical iterations start by fixing an initial value of one of the two optimisation variables, for example we fix $\overline{R}_{0K} = \overline{R}^0_{0K}$ that belongs to the admissible domain described by the constraints (7.43);
- the simplified optimisation problem

$$\min_{\overline{R}_1} W_c \left(\overline{R}^0_{0K}, \overline{R}_1 \right) \ , \tag{7.47}$$

  is solved analytically and we find the value $\overline{R}_1 = \overline{R}^0_1$ that corresponds to the minimum of the objective function and that satisfies the geometric bounds;
- the optimisation problem

$$\min_{\overline{R}_{0K}} W_c \left(\overline{R}_{0K}, \overline{R}^0_1 \right) \ , \tag{7.48}$$

  is solved analytically and we find $\overline{R}_{0K} = \overline{R}^1_{0K}$ that minimises the objective function and satisfies the geometric bounds. Then, the last two step are iterated until convergence to a minimum.

Multiples starting points are considered in order to avoid a local minimum and converge to a global minimum. We found, numerically, that the local minimum obtained is the same using any starting point; hence, the convexity of the objective function is observed but not proved.

7.5 Summary of the computational procedure

We presented three different algorithms, the algorithm *a posteriori* to solve the optimisation problem (6.48) and two versions of the algorithm *a priori* to solve the optimisation problem (6.49).

The computational procedure of the structural optimisation step can be divided into three main phases as shown in Fig. 7.7. The entire computational procedure is programmed in the MATLAB environment except for the FE analyses that are conducted using the ANSYS software. The exchange of data between the MATLAB code and the FE code is obtained through writing and/or reading of text files containing the informations to be exchanged. The FE analysis is launched using a "dos" command line written in the MATLAB code.

Concerning the FE model, it is created using quadratic ANSYS SHELL281 elements based on the Kirchoff kinematic model with 8 nodes and 3 degrees of freedom per node. For this element the membrane option is activated, in this way there is no bending stiffness or rotational degrees of freedom, so, the elastic uncoupling is ensured. The mesh refinement, i.e. the dimension of the FEs, is chosen after preliminary mesh sensitivity analyses on the convergence of the maximum displacement for a given loading condition.

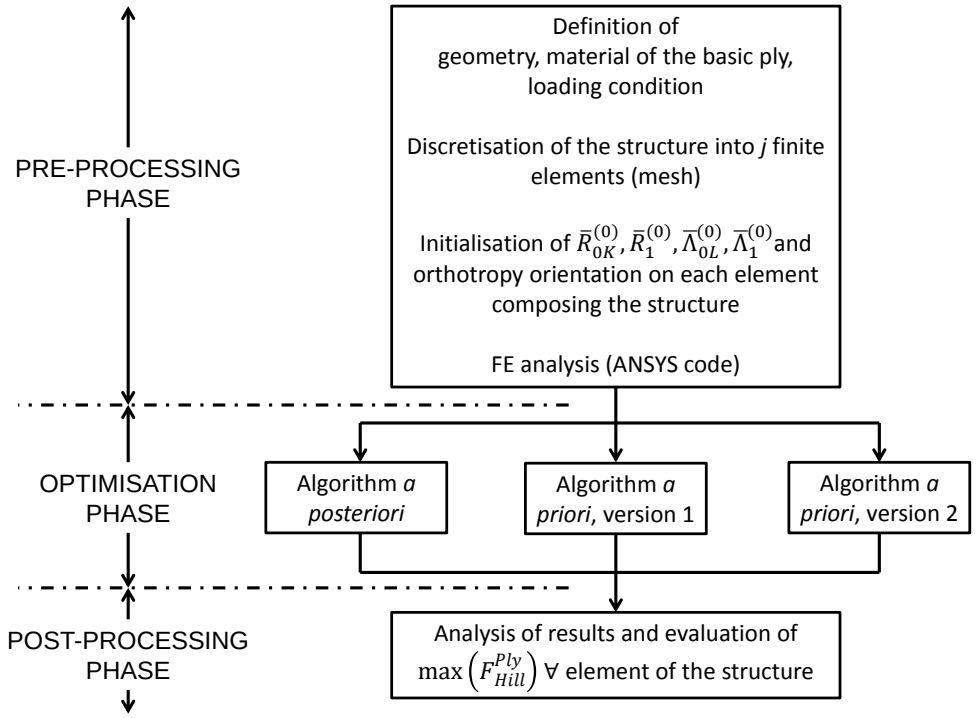

Figure 7.7: Main phases of the computational procedure.

7.5.1 Pre-processing phase

In the *pre-processing phase* we firstly define the geometry and loading conditions of the structure to be optimised. As we consider only the extension behaviour of the structure, we will consider only in-plane loading conditions. The point-wise optimisation of the properties of the structure, is realised discretising the structure into j finite elements. In this way the stiffness and strength properties of the structure are defined specifying the polar parameters of $\mathbf{A}^*$ and $\mathbf{G}^{A*}$, respectively, for every element of the structure. In particular, we define an initial stiffness distribution that is uniform over the plate in order to correspond to a classical laminated structure having a relevant value of the complementary energy W_c. Concerning the strength modules, we have chosen a starting value of the strength polar moduli equal to that of the basic ply $\overline{\Lambda}_{0L} = \Lambda_0$ and $\overline{\Lambda}_1 = \Lambda_1$. The pre-processing phase is terminated with a FE analysis that defines the starting stress and strain fields.

7.5.2 Optimisation phase

In the *optimisation phase* the user can chose the algorithm to be used to determine the optimal values of the design variables.

Let us start considering the algorithm *a posteriori*. A more precise flow-chart diagram of the optimisation phases is presented in Fig. 7.8. The internal actions field $\mathbf{N}^{(n)}$ at the iteration n is the input for the local minimisation of W_c^l, performed on every element of the structure, at the iteration $n+1$. Thanks to the analytical solution of Tab. 6.1 the new optimal stiffness distribution obtained by the MATLAB code is given, through a text file, to ANSYS in order to perform a new FE analysis. At the end of the FE analysis, ANSYS writes a text file giving the values, for every element, of the internal actions and strains

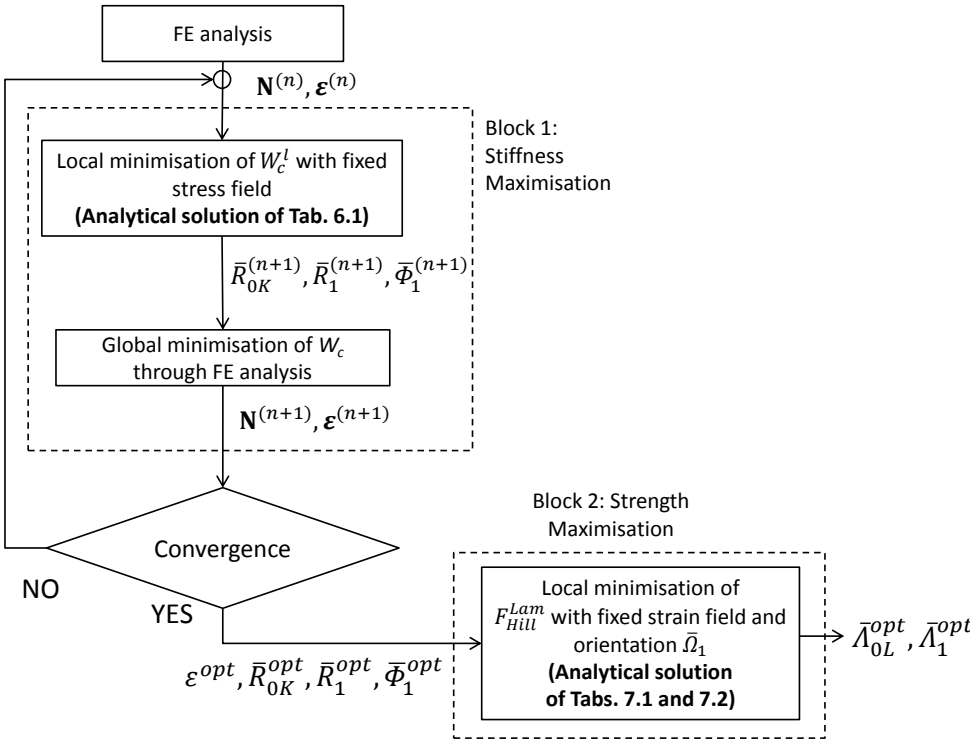

Figure 7.8: Detailed description of the algorithm *a posteriori*.

at the iteration $n+1$, that become the inputs for the new iteration. The convergence is achieved when a stop criterion is satisfied:

$$\frac{|W_c^{(n)} - W_c^{(n+1)}|}{W_c^{(n)}} < 0.001 \ , \tag{7.49}$$

such a condition has to be satisfied at least six consecutive times. Once the convergence is achieved, the optimal strain field is used as input to the local minimisation of F_{Hill}^{Lam} on every element. Thanks to the analytical solutions of Tabs. 7.1 and 7.2 the optimal strength distribution is obtained and the optimisation phase is terminated.

On the other hand, if we want to use the first version of the algorithm *a priori*, a detailed flow-chart diagram of the optimisation phases is presented in Fig. 7.9. The strain field $\boldsymbol{\varepsilon}^{(n)}$ at the iteration n is the input for the local minimisation of F_{Hill}^{Lam}, performed on every element of the structure, at the iteration $n+1$. Thanks to the analytical solution of Tab. 7.3 the new optimal strength distribution is obtained. Then, the internal actions field $\mathbf{N}^{(n)}$ at the iteration n and the orthotropy orientation $\overline{\Omega}_1$ at the iteration $n+1$ are used as input for the local minimisation of W_c^l, at the iteration $n+1$. Thanks to the numerical solution described in Sec. 7.4.2, the new optimal stiffness distribution is obtained and used by ANSYS in order to perform a new FE analysis. Then, the internal actions and strains at the iteration $n+1$ become the inputs for the next iteration. The iterations prosecute in this way until convergence. In Sec. 7.3 we have discussed the lack of the mathematical proof for the convergence of the first version of the algorithm *a priori*. From a numerical point of view we have observed that the amplitude of the oscillations linked to the variation of both laminate failure index F_{Hill}^{Lam} and complementary energy W_c reduces along the iterations. However, the relative variation of both these quantities (W_c and F_{Hill}^{Lam}) does not fall below $\sim 0.5\%$.

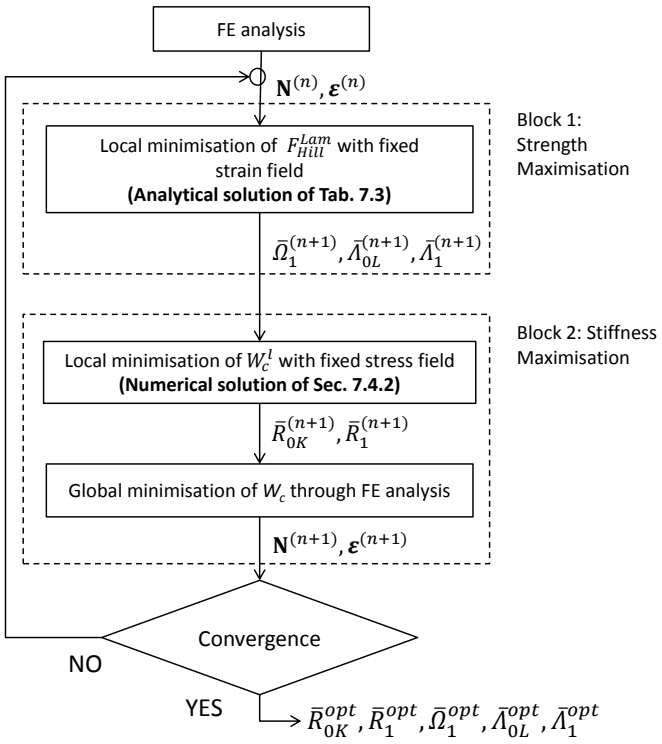

Figure 7.9: Detailed description of the first version of the algorithm *a priori*.

Finally, we can chose as optimisation algorithm, the second version of the algorithm *a priori*. A detailed flow-chart diagram of the computational phases is presented in Fig. 7.10. The strain $\boldsymbol{\varepsilon}^{(n)}$ field at the iteration n is the input for the local minimisation of F_{Hill}^{Lam}, performed on every element of the structure, at the iteration $n+1$:

$$\min_{\overline{\Omega}_1, \overline{\Lambda}_{0L}, \overline{\Lambda}_1} F_{Hill}^{Lam}(\overline{\Omega}_1, \overline{\Lambda}_{0L}, \overline{\Lambda}_1) \tag{7.50}$$

with no restrictions on the solution space of $\overline{\Omega}_1$. Thanks to the analytical solution of Tab. 7.3 the new optimal strength distribution is obtained. Then, the internal actions field $\mathbf{N}^{(n)}$ at the iteration n and the orthotropy orientation $\overline{\Omega}_1^{(n+1)}$ are used as input for the local minimisation of W_c^l, at the iteration $n+1$. Thanks to the numerical solution described in Sec. 7.4.2 we have the new optimal stiffness distribution. Until this point this algorithm is identical to the first version of the algorithm *a priori*.

In order to solve the constrained local minimisation problem of the F_{Hill}^{Lam} defined in Sec. 7.3.2, from a computational point of view, we have inserted a "check phase" on the reduction of W_c^l:

- if $W_c^{l(n+1)} \leq W_c^{l(n)}$ after the local minimisation, the MATLAB code gives the new values of the stiffness parameters to ANSYS;
- if $W_c^{l(n+1)} > W_c^{l(n)}$ after the local minimisation, the problem

$$\min_{\overline{R}_{0K}, \overline{R}_1} W_c(\overline{\Omega}_1, \overline{R}_{0K}, \overline{R}_1) \tag{7.51}$$

is solved, for every given value of $\overline{\Omega}_1 \in [-\pi/2, \pi/2]$ discretised with a step of $1°$. Thanks to the numerical solution described in Sec. 7.4.2 we have 181 values of

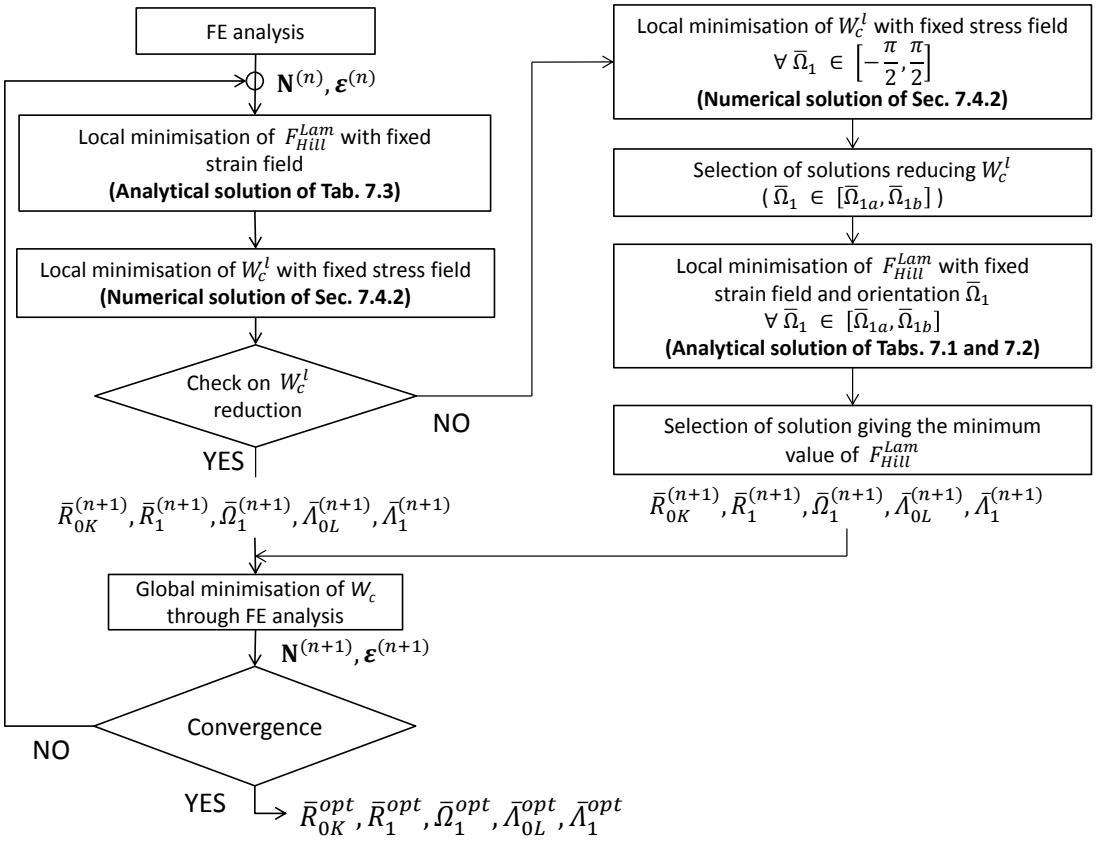

Figure 7.10: Detailed description of the second version of the algorithm *a priori*.

$W_c^{l(n+1)}$ along with their optimal stiffness parameters. A selection operator, now, chooses all $W_c^{l(n+1)} \leq W_c^{l(n)}$; after the selection phase, we have the range

$$\overline{\Omega}_1 \in [\overline{\Omega}_{1_a}, \overline{\Omega}_{1_b}] \ , \tag{7.52}$$

corresponding to the selected values of $W_c^{l(n+1)}$. At this point the local minimisation of F_{Hill}^{Lam}

$$\min_{\overline{\Lambda}_{0L}, \overline{\Lambda}_1} \ F_{Hill}^{Lam}(\overline{\Omega}_1, \overline{\Lambda}_{0L}, \overline{\Lambda}_1) \ , \tag{7.53}$$

is performed for every given value of $\overline{\Omega}_1 \in [\overline{\Omega}_{1_a}, \overline{\Omega}_{1_b}]$. Thanks to the analytical solutions of Tabs. 7.1 and 7.2 we obtain a set of values of $F_{Hill}^{Lam(n+1)}$ along with their optimal strength parameters. The optimal solution, for the finite element under consideration, will be the one giving the minimum value of F_{Hill}^{Lam} in the set of values determined for each $\overline{\Omega}_1 \in [\overline{\Omega}_{1_a}, \overline{\Omega}_{1_b}]$. Such a solution give us the stiffness and strength parameters, along with the orthotropy orientation, at the iteration $n+1$.

Once the procedure has been performed for all elements composing the structure, the MATLAB code gives to ANSYS the new stiffness distribution in order to perform a new FE analysis to determine the internal actions and strains fields at the iteration $n+1$, that become the inputs for the new iteration. The iterations prosecute in this way until convergence. The stop criterion to achieve the optimal condition is the same adopted for the algorithm *a posteriori*.

In order to better understand the second part of this algorithm, in Fig. 7.11 we show an example of the variation of minima of W_c^l and F_{Hill}^{Lam}, at the iteration $(n+1)$ for a fixed stress and strain state, varying only the orthotropy orientation. The red line corresponds to the value of the $W_c^{l(n)}$ at the previous iteration and represents the constraint on the admissible values of $W_c^{l(n+1)}$ and, so, on $\overline{\Omega}_1$. In particular we calculate, for each value of $\overline{\Omega}_1 \in [-\pi/2, \pi/2]$ the solution of the minimisation problem (7.51), for a given $\mathbf{N}^{(n)}$ field to obtain the curve of minima of $W_c^{l(n+1)}$.

Now, the two dashed vertical lines defines the range of values $\overline{\Omega}_1 \in \left[\overline{\Omega}_{1_a}, \overline{\Omega}_{1_b}\right]$ whose corresponding minimum values of $W_c^{l(n+1)}$ are such that $W_c^{l(n+1)} \leq W_c^{l(n)}$, i.e. satisfy the constraint on the reduction of W_c^l. Then, for each value of $\overline{\Omega}_1 \in \left[\overline{\Omega}_{1_a}, \overline{\Omega}_{1_b}\right]$ we solve the minimisation problem (7.53) for a given $\boldsymbol{\varepsilon}^{(n)}$ field to obtain the curve of minima of F_{Hill}^{Lam}. Thus, in this range of $\overline{\Omega}_1$ we look for the optimal value of orientation $\overline{\Omega}_1^{(n+1)}$ that, among all of the minima of F_{Hill}^{Lam} calculated for $\overline{\Omega}_1 \in \left[\overline{\Omega}_{1_a}, \overline{\Omega}_{1_b}\right]$ gives the lowest value of F_{Hill}^{Lam}. Such a value is placed on the black vertical line that just defines the optimal orthotropy orientation $\overline{\Omega}_1^{(n+1)}$. The values $\overline{R}_{0K}, \overline{R}_1$ and $\overline{\Lambda}_{0L}, \overline{\Lambda}_1$ corresponding to this point solution will be the optimal values of the iteration $(n+1)$ and will be stored by the algorithm in order to pass to the global optimisation phase.

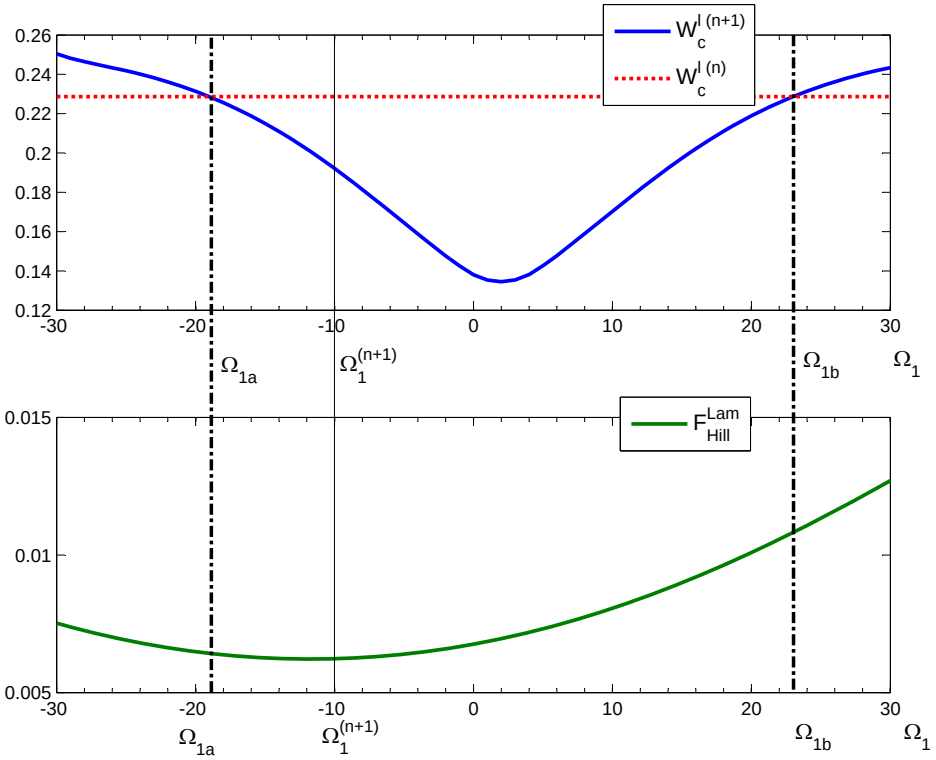

Figure 7.11: Curves of the minima of W_c^l and F_{Hill}^{Lam} corresponding to given values of the orthotropy orientation $\overline{\Omega}_1$.

7.5.3 Post-processing phase

At the end of the optimisation phase we have a homogenised structure whose optimal stiffness and strength distributions are known. Therefore, we can perform a final FE

analysis in order to determine the stress and strain states corresponding to the optimal condition.

We have still discussed in Sec. 6.4.1.2 about the Kirkhoff's kinematic model consequence, for an uncoupled plate subjected to a pure membrane loading, that the strain field of the whole laminate is identical to that of each constitutive layer. After the optimisation phase, we have a homogenised plate whose strain state (t, r, ϕ) is known, thus, we know also the strain state of each constitutive layer. Moreover, the polar parameters $(\Gamma_0, \Gamma_1, L, \Lambda_0, \Lambda_1)$ of the basic ply are given, so, we can evaluate the $\max(F_{Hill}^{Ply})$ for each element of the structure:

$$\max(F_{Hill}^{Ply}) = 4r^2\Gamma_0 + 8t^2\Gamma_1 + 4(-1)^L\Lambda_0 r^2\cos 4\left(\Omega_1 - \phi\right) + 16tr\Lambda_1\cos 2\left(\Omega_1 - \phi\right) \ , \qquad (7.54)$$

with Ω_1 set equal to the solution of Fig. 6.1 maximising the F_{Hill}^{Ply}. Then, such a value of $\max(F_{Hill}^{Ply})$ will be taken into account during the second step of the strategy in order to check the first-ply-failure and to define the admissible range of solutions of ply orientations to determine the stacking sequence of the laminate, see Chapter 8.

7.6 Numerical examples

In this Section, we present three numerical examples with different laminated plates that will be designed and optimised using the proposed optimisation algorithms of Secs. 7.2 and 7.3. The three plates are uncoupled and orthotropic and subject to pure membrane loading conditions. The mechanical properties and the numerical values of the polar parameters of the basic ply, for both stiffness and strength properties, are reported in Tab. 7.4. Concerning the strength properties, as we use the Tsai-Hill failure index we assume an identical strength behaviour in tension and compression, except for Sec. 7.6.3.3 where we take into account a different value of strength properties in tension and compression. The total thickness of the plates is fixed to $h = 3.75$ mm, that corresponds to a laminated plate composed by 30 identical plies of thickness $h_k = 0.125$ mm.

Mechanical properties			
Stiffness		Strength	
E_1 [MPa]	181000	X [MPa]	1500
E_2 [MPa]	10300	Y [MPa]	40
G_{12}^S [MPa]	7170	S [MPa]	68
ν_{12} [MPa]	0.28		
Polar parameters			
Parameters of $\mathbf{Q}$		Parameters of $\mathbf{G}$	
T_0 [MPa]	26880	Γ_0	11746
T_1 [MPa]	24744	Γ_1	15461
R_0 [MPa]	19710	Λ_0	628
R_1 [MPa]	21433	Λ_1	5898
K	0	L	0

Table 7.4: Mechanical properties and polar parameters of the basic ply, Carbon-Epoxy T300-5208.

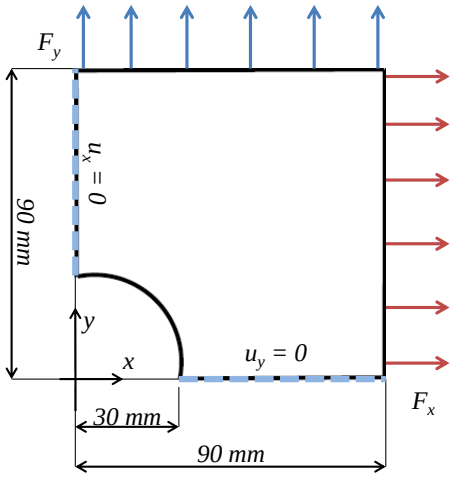

Figure 7.12: Geometry and boundary conditions, square plate.

		Alg. *posteriori*	Alg. *priori* v1	Alg. *priori* v2
	Starting condition	Optimal cond., (% reduction)	Optimal cond., (% reduction)	Optimal cond., (% reduction)
W_c [N mm]	10232.928	6921.054, (32.4)	7691.895, (24.8)	6931.053, (32.2)
Max F_{Hill}^{Lam}	8.358	0.476, (94.3)	0.447, (94.6)	0.449, (94.6)
Max F_{Hill}^{Ply}	-	0.476	1.43	0.459
Max displacement [mm]	0.317	0.138, (56.5)	0.155, (51.1)	0.139, (56.1)

Table 7.5: Main results, square plate.

7.6.1 First example: a holed square plate

We consider a square plate with a centered hole, subject to biaxial in-plane loading conditions. The geometry and the loading conditions of the plate are shown in Fig. 7.12. We consider only a quarter of the plate for symmetry reasons. The loading values are $F_x = 500$ N/mm and $F_y = 250$ N/mm.

The total number of elements n_{elem} is fixed to 1800: 60 partitions around the hole per 30 partitions along the side placed along the x axis. The starting values of the stiffness polar parameters are those of a cross-ply laminate oriented along x and y axis: $\overline{R}_0^{(0)} = R_0$ and $\overline{R}_1^{(0)} = 0$ over the whole plate.

In Tab. 7.5 we show the main results of the structural optimisation given by the three algorithms and their comparison with the starting condition. We present the values, at the starting and optimal conditions, of: the complementary energy, the maximum laminate and ply failure indexes and the maximum displacement. For all these quantities, a sensible reduction is obtained.

The lowest value of W_c is achieved with the algorithm *a posteriori*, that, according to the theory, favours the minimisation of the complementary energy. The optimal value of W_c when using the two algorithms *a priori* is still significantly reduced with respect to the starting condition, but it is greater than the optimal value obtained using the algorithm

a posteriori. On the other hand, both the versions of the algorithm *a priori* show lower values of $\max(F_{Hill}^{Lam})$, with a greater reduction with respect to that obtained with the algorithm *a posteriori*. This result can be explained by the mechanical nature of these algorithms *a priori*: the optimisation process favours the minimisation of F_{Hill}^{Lam}. However, the second version of the algorithm *a priori* has a mathematical convergence proof that finds confirmation in this numerical example, see Figs. 7.13 and 7.14, and gives a better solution than that obtained using the first version of the algorithm, see Figs. 7.15 and 7.16.

The comparison between the distribution, over the plate, of the local complementary energy W_c at the starting and the optimal conditions, using the three algorithms, is presented in Figs. 7.17. The red zone (maximal values of W_c) near the hole at the starting condition, see Fig. 7.17(a), completely disappears at the optimal conditions, see Fig. 7.17(b,c,d), and the blue zone (minimal values of W_c) is extremely extended. The lowest values of the local complementary energy are registered using the algorithm *a posteriori*, however, the second version of the algorithm *a priori* gives a very similar distribution of W_c, as shown in Figs. 7.17(b) and (d).

The comparison between the distribution of F_{Hill}^{Lam}, at the starting and at the optimal conditions for the three algorithms, is depicted in Figs. 7.18. Failure occurs when $F_{Hill}^{Lam} \geq 1$ and in Fig. 7.18(a) such a limit condition is verified in the plate regions coloured in red. Such a critical condition occurs in a large region of the plate at the initial condition, while it completely disappears for the optimal solution, Figs. 7.18(b,c,d), being the failure index of the laminate less or equal to about 0.5. The best distribution of F_{Hill}^{Lam}, over the plate, is achieved using the algorithm *a priori* version 1. However, this algorithm gives a $\max(F_{Hill}^{Ply})$ for the worst ply composing the laminate, see Sec. 6.4.1.2, greater than 1 (Tab. 7.5). Thus, the best compromise between the optimal distribution of F_{Hill}^{Lam} and that of the $\max(F_{Hill}^{Ply})$ is given by the optimal results of the algorithm *a priori* version 2, see Tab. 7.5.

Concerning the results of this first example we can say that we found:

- an optimal configuration, in terms of stiffness, having good strength properties using the algorithm *a posteriori*;
- an optimal configuration, in terms of strength, having good stiffness properties using the algorithms *a priori*;

In the following, concerning all the numerical test cases, we will discuss only the results obtained using the algorithm *a posteriori* and the algorithm *a priori* version 2, being this last more robust and effective than version 1. We pass now to assess in detail, the results obtained with the *a posteriori* and *a priori* version 2 algorithms.

7.6.1.1 Structural optimisation using the algorithm with *a posteriori* local maximisation of strength

The reduction of the complementary energy W_c along the iterations is shown in Fig. 7.19. In particular the most important reduction is obtained at the first iteration, we pass from 10232 N mm to 6977 N mm. This sensible reduction is due to the local minimisation of W_c: we have a starting condition that correspond to a cross-ply laminate with a constant value of orthotropy orientation and polar moduli of stiffness over all the plate. With the first iteration, after the local minimisation of W_c, we have still obtained a *variable stiffness plate* and the adaptation of the stiffness field to the stress field of each element of the

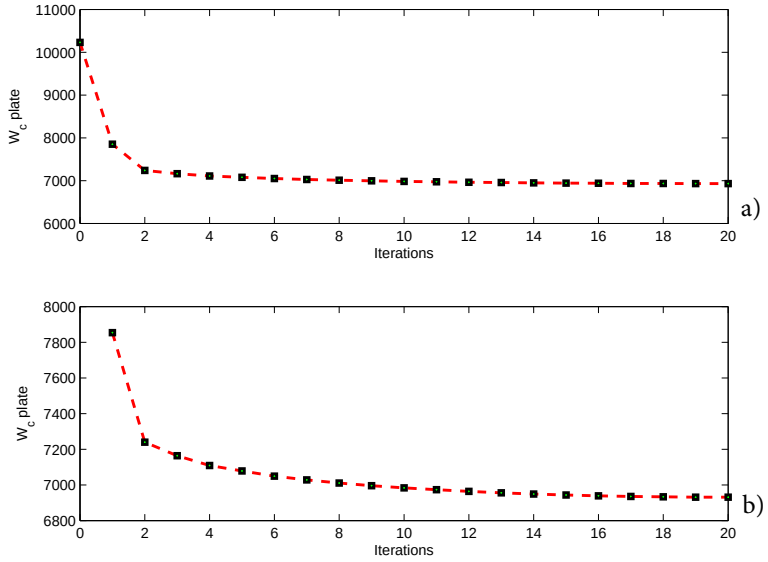

Figure 7.13: Complementary energy of the plate along the iterations (a) and its zoomed version (b), algorithm *a priori* version 2, square plate.

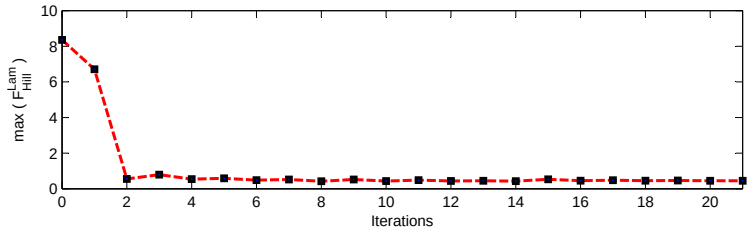

Figure 7.14: Maximum failure index of the plate along the iterations, algorithm *a priori* version 2, square plate.

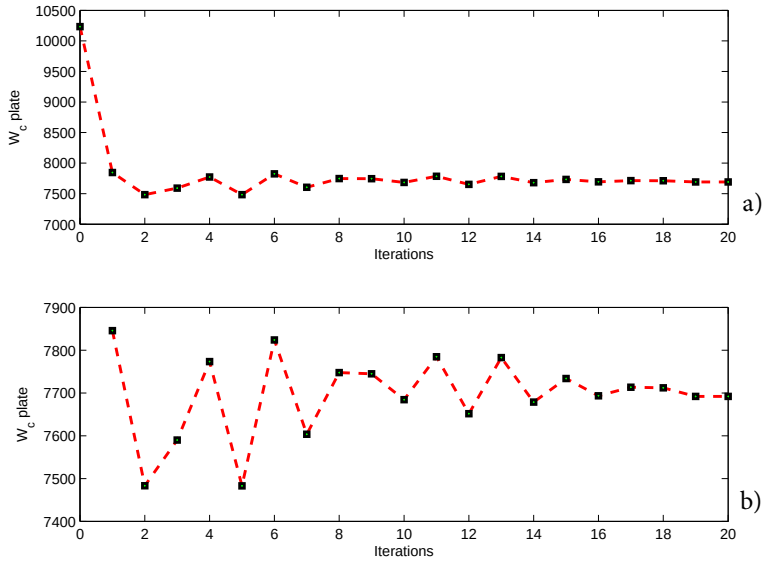

Figure 7.15: Complementary energy of the plate along the iterations (a) and its zoomed version (b), algorithm *a priori* version 1, square plate.

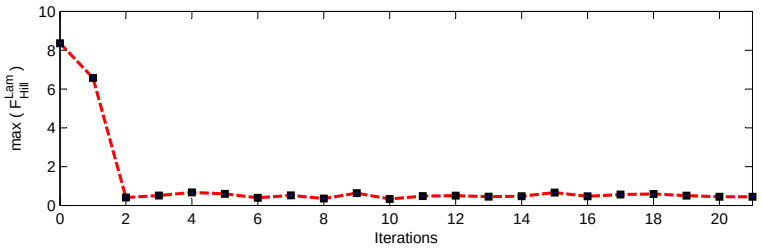

Figure 7.16: Maximum failure index of the plate along the iterations, algorithm *a priori* version 1, square plate.

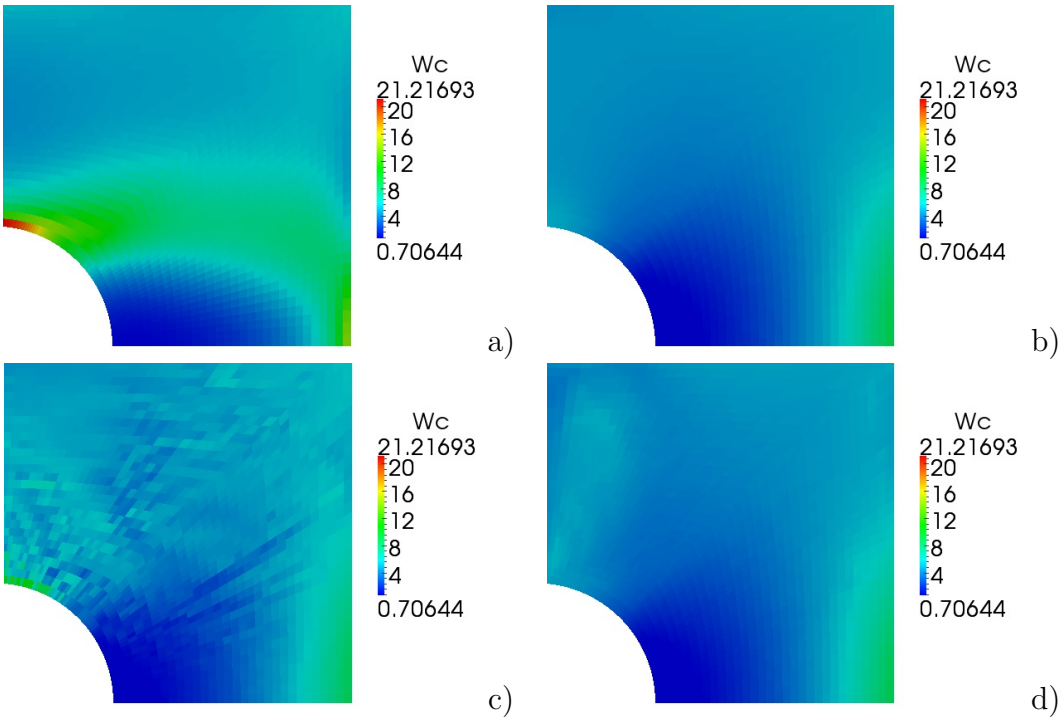

Figure 7.17: Complementary energy distribution for the starting (a) and optimal configuration using algorithm *a posteriori* (b), algorithm *a priori* vers. 1 (c) and algorithm *a priori* vers. 2 (d), square plate.

structure leads to a sensible increment of the local, and then global, stiffness of the plate. Such a result proves the interesting performances that a variable stiffness plate can have with respect to standard solutions. As proved by the theory, see Sec. 6.3.1, W_c reduces at each iteration, see Fig. 7.19(b) that shows a zoom of the first one.

The solution type of the local minimisation of W_c^l, see Tab. 6.1, is shown in Fig. 7.20(a). Almost the total surface of the plate is characterised by the solution type 1 while around the hole we have a thin area characterised by the solution type 2. We have already discussed about the peculiarity of the solution type 1 of the local minimisation of W_c^l in Sec. 6.3.1: such a stiffness distribution generates a pure spherical strain field (the deviatoric component of $\boldsymbol{\varepsilon}$ is null, $r = 0$), see Fig. 7.20(b). From Tab. 6.1 we can see that the solution type 1 gives a set of optimal values of $\overline{R}_{0K}$ and in Fig. 7.21(a) we have chosen $\overline{R}_{0K}^{opt} = R_0$ in the area characterised by the solution type 1. The distribution of $\overline{R}_1^{opt}$ is shown in Fig. 7.21(b).

In Figs. 7.22 we compare the distribution of F_{Hill}^{Lam} and $\max(F_{Hill}^{Ply})$ at the optimal

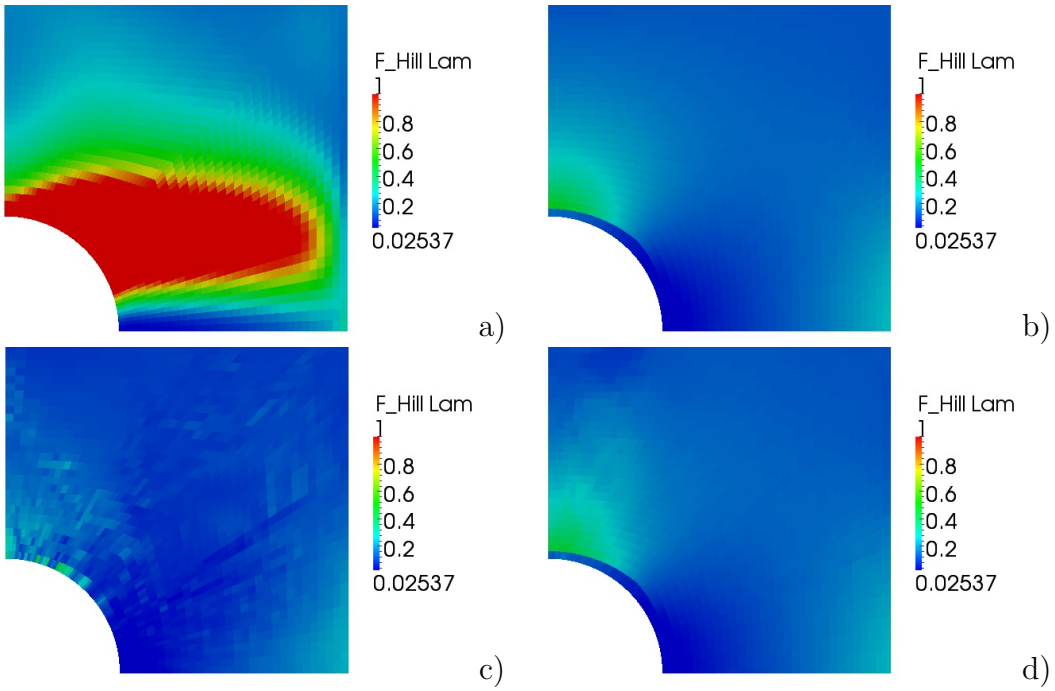

Figure 7.18: F_{Hill}^{Lam} distribution for the starting (a) and optimal configuration using algorithm *a posteriori* (b), algorithm *a priori* vers. 1 (c) and algorithm *a priori* vers. 2 (d), square plate.

condition. The maximum value of F_{Hill}^{Lam} occurs in the area characterised by $r = 0$. Also the highest value of $\max(F_{Hill}^{Ply})$, see Sec. 6.4.1, occurs at the same point, Fig. 7.22(b). A quick glance at eq. (6.18) is sufficient to assert that when $r = 0$ the contribution of Ω_1 vanishes, and we get:

$$F_{Hill}^{Lam} = F_{Hill}^{Ply} = 8t^2\Gamma_1 \ , \tag{7.55}$$

that explains the same values of $\max(F_{Hill}^{Lam})$ and $\max(F_{Hill}^{Ply})$ in Tab.7.5.

The solution type of the local minimisation of F_{Hill}^{Lam}, Tab. 7.1, is depicted in Fig. 7.23(b). The main part of the plate surface is characterised by the solution type 0 that corresponds to a pure spherical strain field ($r = 0$): thus $\overline{\Lambda}_{0L}^{opt}$ and $\overline{\Lambda}_1^{opt}$ can get any admissible value within the admissible design domain. Around the hole, the solution type is equal to 4 and 3, corresponding to a fixed optimal value of the strength moduli, see Tab. 7.1. Concerning the area characterised by the solution type 0 we have chosen $\overline{\Lambda}_{0L}^{opt} = \Lambda_0$ and $\overline{\Lambda}_1^{opt} = \Lambda_1$, see Figs. 7.24. Finally, the optimal orthotropy orientation $\overline{\Phi}_1^{opt}$ is reported in Fig. 7.23(a).

7.6.1.2 Structural optimisation using the algorithm with *a priori* maximisation of strength: version 2

In this algorithm the local minimisation of W_c^l is calculated through the numerical approach described in Sec. 7.4.2 for which we do not have an analytical solution. The distributions of $\overline{R}_{0K}^{opt}$ and of $\overline{R}_1^{opt}$ are reported in Figs. 7.25. Differently from the solution given by the algorithm *a posteriori*, in this case $\overline{R}_{0K}^{opt}$ does not belong to a set of solutions and varies over the plate surface.

The values of F_{Hill}^{Lam} and those of $\max(F_{Hill}^{Ply})$, at the optimal condition, are compared in Figs. 7.26. The maximum value of F_{Hill}^{Lam} occurs over a region near the hole, while the maximum value of F_{Hill}^{Ply} of the generic ply composing the laminate occurs on a very limited area around the hole and it is greater than $\max(F_{Hill}^{Lam})$ but still lower than 1, see

Fig. 7.26(b). This is due to the fact that in this case $r \neq 0$ and the orientation Ω_1 such that F_{Hill}^{Ply} is maximised leads to $\max(F_{Hill}^{Ply}) > \max(F_{Hill}^{Lam})$, see Sec. 6.4.1.

The solution type of the local minimisation of F_{Hill}^{Lam} is reported in Fig. 7.27(b). The plate surface is characterised by the solution types 3 and 4 of Tab. 7.1. The solution type 3 corresponds to $\overline{\Lambda}_{0L}^{opt} = \Lambda_0$ and $\overline{\Lambda}_1^{opt} = \Lambda_1$ and the solution type 4 gives also $\overline{\Lambda}_{0L}^{opt} = \Lambda_0$ and $\overline{\Lambda}_1^{opt} = \Lambda_1$ because $\dfrac{|t|}{r} > \dfrac{\Lambda_0 \cos 4\left(\overline{\Omega}_1 - \phi\right)}{\Lambda_1 |\cos 2\left(\overline{\Omega}_1 - \phi\right)|}$. Therefore, the optimal values of both the strength polar moduli over the whole plate surface correspond to the respective strength polar moduli of the basic ply. The optimal orthotropy orientation $\overline{\Omega}_1^{opt}$ is illustrated in Fig. 7.27(a). Except for small areas, wherein $\overline{\Omega}_1^{opt}$ is aligned with $\overline{\Phi}_1^{opt}$ given by the solution of the algorithm *a posteriori*, the distribution of $\overline{\Omega}_1^{opt}$ given by the algorithm *a priori* version 2, is different from the optimal orthotropy orientation given by the algorithm *a posteriori*. This is due to the different optimal stiffness distribution obtained with the two algorithms, that leads to a different state of stress and strain. In fact, the optimal solution given by the algorithm *a posteriori* generates a spherical strain field ($r = 0$), while the stiffness distribution obtained with the algorithm *a priori* version 2 generates a strain field with $r \neq 0$.

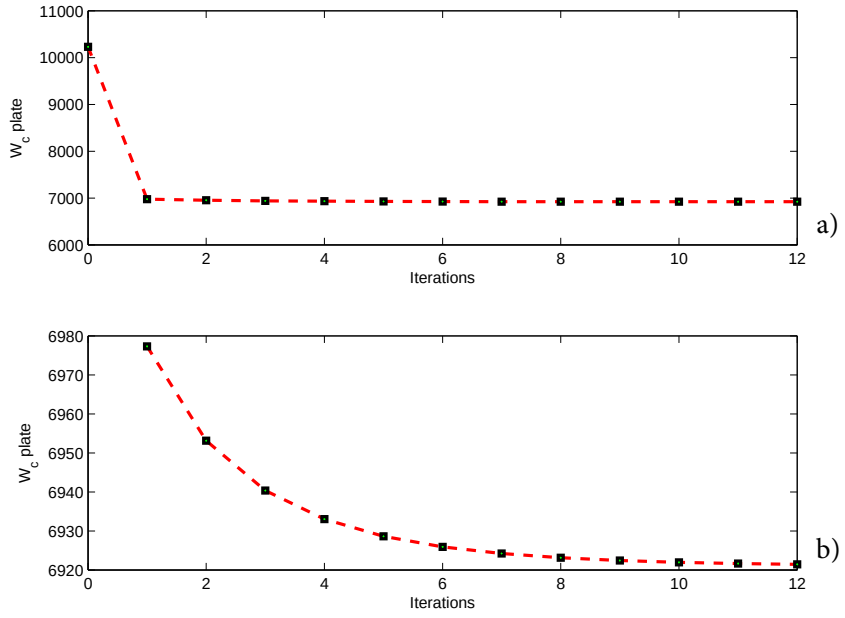

Figure 7.19: Complementary energy of the plate along the iterations (a) and its zoomed version (b), algorithm *a posteriori*, square plate.

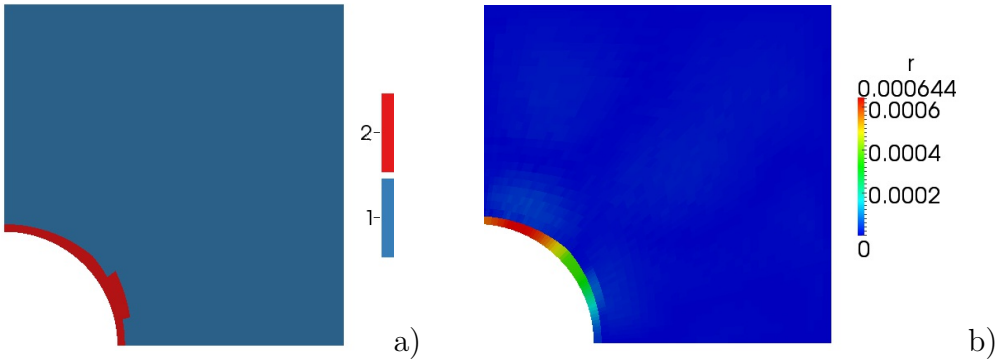

Figure 7.20: Solution type of local minimisation of W_c (a) and deviatoric strain component r (b) for the optimal configuration, algorithm *a posteriori*, square plate.

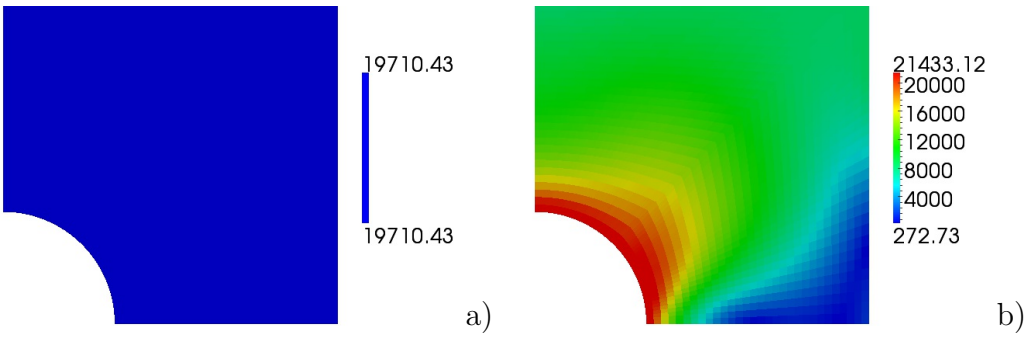

Figure 7.21: $\overline{R}_{0K}$ (a) and $\overline{R}_1$ (b) for the optimal configuration, algorithm *a posteriori*, square plate.

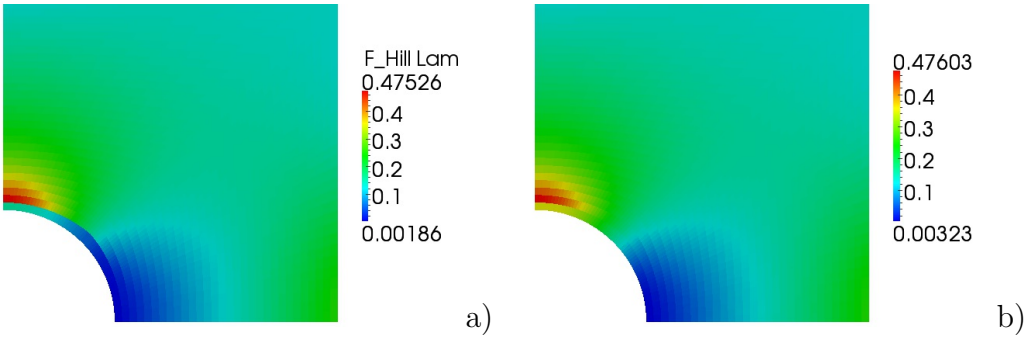

Figure 7.22: F_{Hill}^{Lam} distribution (a) and $\max(F_{Hill}^{Ply})$ of the generic ply (b) for the optimal configuration, algorithm *a posteriori*, square plate.

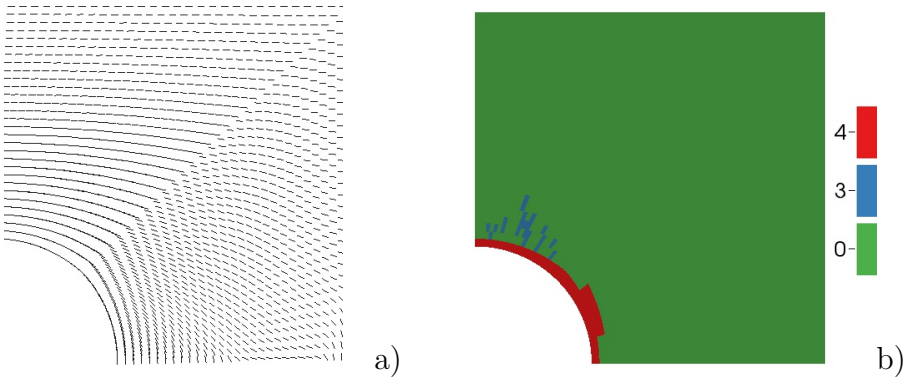

Figure 7.23: Optimal orthotropy orientation $\overline{\Phi}_1^{opt}$ (a) and solution type of local minimisation of F_{Hill}^{Lam} (b), algorithm *a posteriori*, square plate.

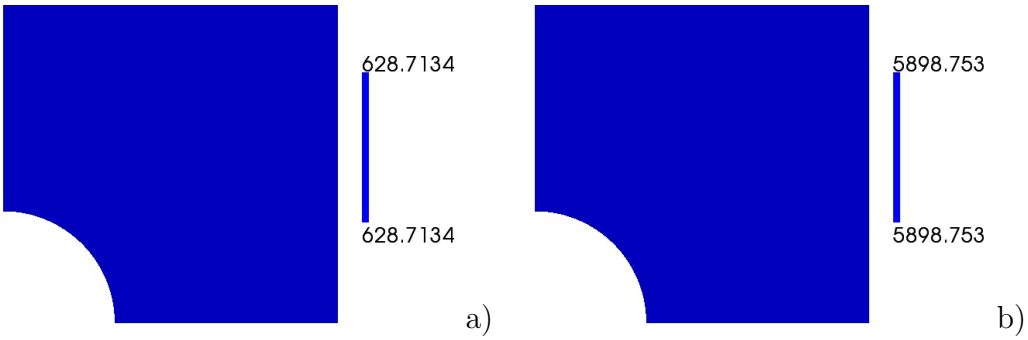

Figure 7.24: $\overline{\Lambda}_{0L}$ (a) and $\overline{\Lambda}_1$ (b) for the optimal configuration, algorithm *a posteriori*, square plate.

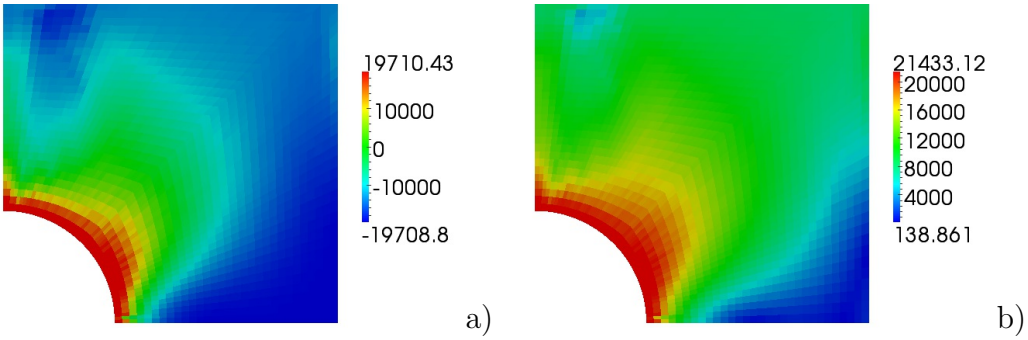

Figure 7.25: $\overline{R}_{0K}$ (a) and $\overline{R}_1$ (b) for the optimal configuration, algorithm *a priori* version 2, square plate.

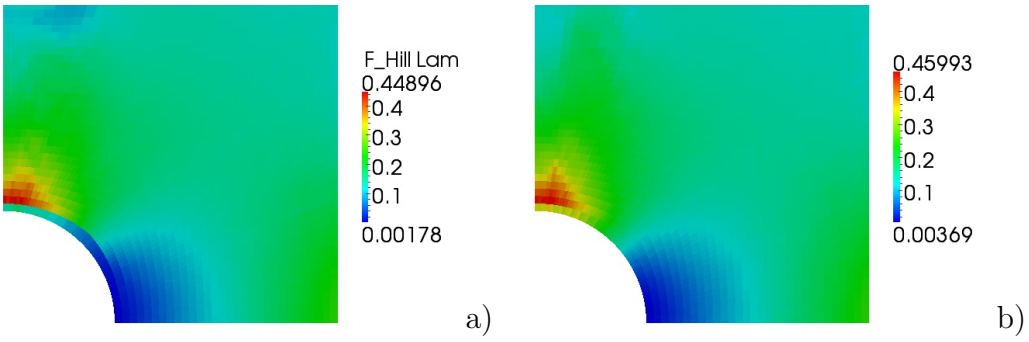

Figure 7.26: F_{Hill}^{Lam} distribution (a) and $\max(F_{Hill}^{Ply})$ of the generic ply (b) for the optimal configuration, algorithm *a priori* version 2, square plate.

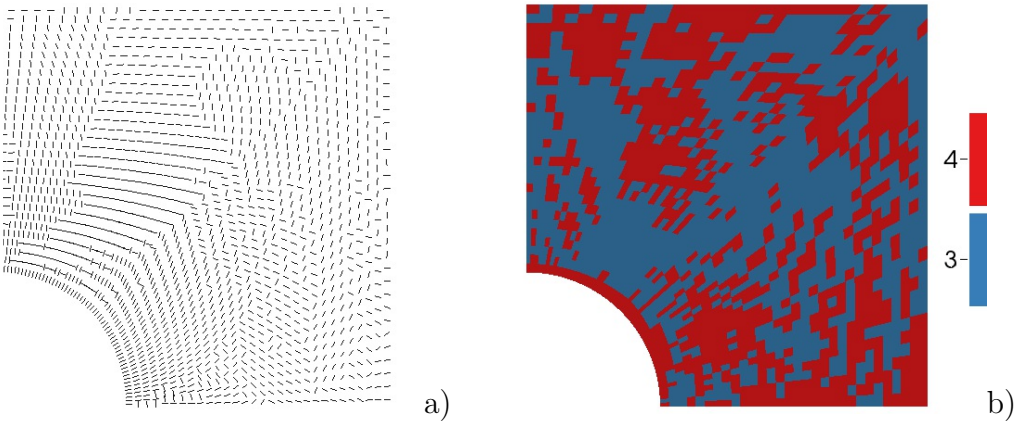

Figure 7.27: Optimal orthotropy orientation $\overline{\Omega}_1^{opt}$ (a) and solution type of local minimisation of F_{Hill}^{Lam} (b), algorithm *a priori* version 2, square plate.

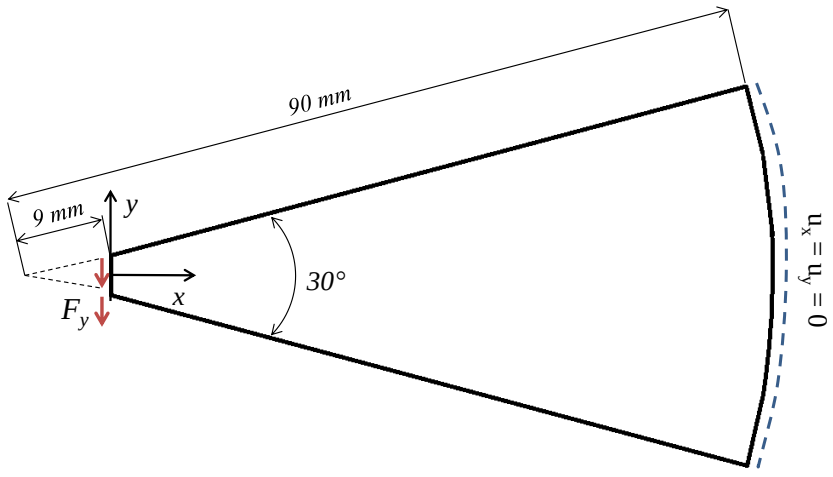

Figure 7.28: Geometry and boundary conditions, circular sector.

7.6.2 Second example: a circular sector

We consider a circular sector, subject to in-plane shear loading conditions. The geometry of the plate and the boundary conditions are shown in Fig. 7.28. The loading value is $F_y = 150$ N/mm. The total number of elements n_{elem} has been fixed to 1274 (14 circumferential partitions per 91 radial partitions). The starting values of the stiffness polar parameters correspond to a unidirectional lamina oriented along the x axis having the properties of the basic ply: $\overline{R}_0^{(0)} = R_0$, $\overline{R}_1^{(0)} = R_1$ and $\overline{\Phi}_1^{(0)} = 0$ everywhere in the plate. In order to avoid a singular point for stresses and strains, we have truncated the tip of the sector, see Fig. 7.28, and the load F_y is uniformly distributed on the vertical side of the wedge.

In Tab. 7.6 we show the main results of the structural optimisation step. For all the quantities, a sensible reduction is observed. Also in this case, the smallest value of W_c is achieved when using the algorithm *a posteriori*. The optimal value of W_c using the algorithm *a priori* version 2 is still significantly reduced with respect to the starting condition and gives the same percentage of reduction obtained using the algorithm *a posteriori*. On the other hand, the algorithm *a priori* version 2 presents the lowest value of $\max(F_{Hill}^{Lam})$, though its reduction with respect to the algorithm *a posteriori* is only about 0.1%.

The comparison between the distribution, over the plate, of the local complementary energy W_c at the starting and optimal configurations, using the two algorithms, is shown in Figs. 7.29. The red zone indicating the maximal values of W_c at the starting condition, Fig. 7.29(a), completely disappears at the optimal configurations, Fig. 7.29(b,c). Moreover, the optimal distribution of W_c given by the two algorithms is almost the same.

The comparison between the distribution of the F_{Hill}^{Lam} at the beginning and the end of iterations is illustrated in Figs. 7.30. The extended red area, indicating that $F_{Hill}^{Lam} \geq 1$, at the beginning, Fig. 7.30(a), completely disappears at the end, Figs. 7.30(b,c), and becomes a blue area corresponding to $F_{Hill}^{Lam} \leq 0.2$. The greatest values of F_{Hill}^{Lam} corresponding to $F_{Hill}^{Lam} \sim 0.5$ are confined in a very localised area corresponding to the loading application region, Figs. 7.30(b) and (c). The lowest distribution of the F_{Hill}^{Lam} is achieved using the algorithm *a priori* version 2. Also the maximum value of F_{Hill}^{Ply}, when using this algorithm, is lower than that obtained using the algorithm *a posteriori*.

We observe, again, that the algorithm *a priori* version 2 gives a smaller failure index at the price of a bigger complementary energy than those obtained with the algorithm *a posteriori*.

Let us now consider in detail the results concerning the two optimisation procedures used for this example.

7.6.2.1 Structural optimisation using the algorithm with *a posteriori* local maximisation of strength

The reduction of the complementary energy W_c along the iterations is shown in Fig. 7.31. The most important reduction is obtained at the first iteration, we pass from 1690 N mm to 755 N mm. W_c reduces at each iteration, see Fig. 7.31(b), up to the convergence. The solution type of the local minimisation of W_c is shown in Fig. 7.32(a). Almost the total surface of the plate is characterised by the solution type 2 corresponding to the unidirectional lamina (see Tab. 6.1), while around the geometrical symmetry axis we have a thin area characterised by the solution type 3. The optimal distribution of $\overline{R}_{0K}$ and $\overline{R}_1$ is given in Figs. 7.33.

		Alg. *posteriori*	Alg. *priori* v2
	Starting condition	Optimal cond., (% reduction)	Optimal cond., (% reduction)
W_c [N mm]	1690.356	749.473, (55.6)	750.072, (55.6)
Max F_{Hill}^{Lam}	15.392	0.530, (96.5)	0.515, (96.6)
Max F_{Hill}^{Ply}	-	0.591	0.570
Max displacement [mm]	0.715	0.318, (55.5)	0.319, (55.4)

Table 7.6: Main results, circular sector.

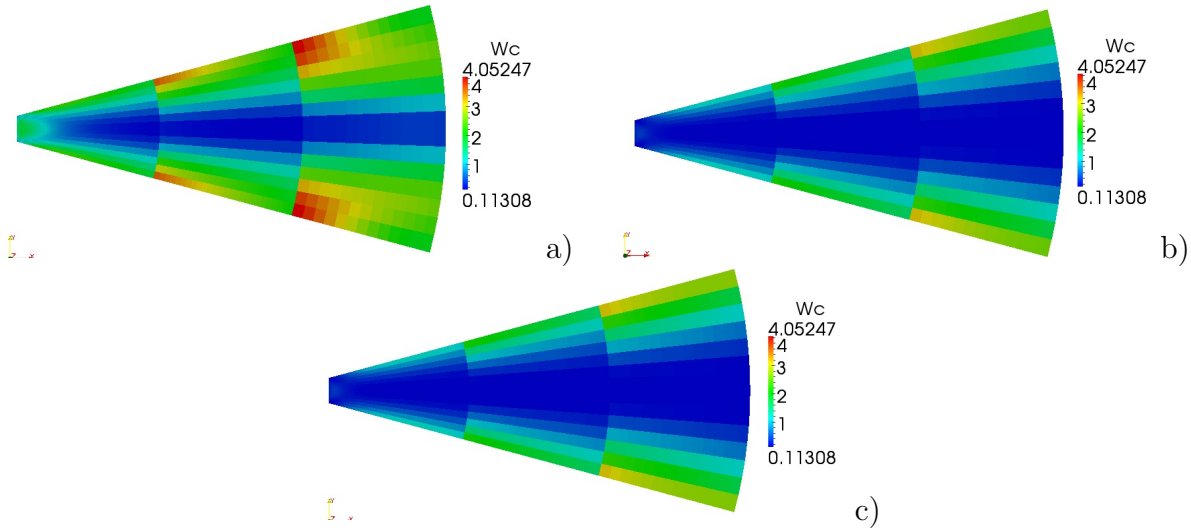

Figure 7.29: Complementary energy distribution for the starting (a) and optimal configuration using algorithm *a posteriori* (b) and algorithm *a priori* vers. 2 (c), circular sector.

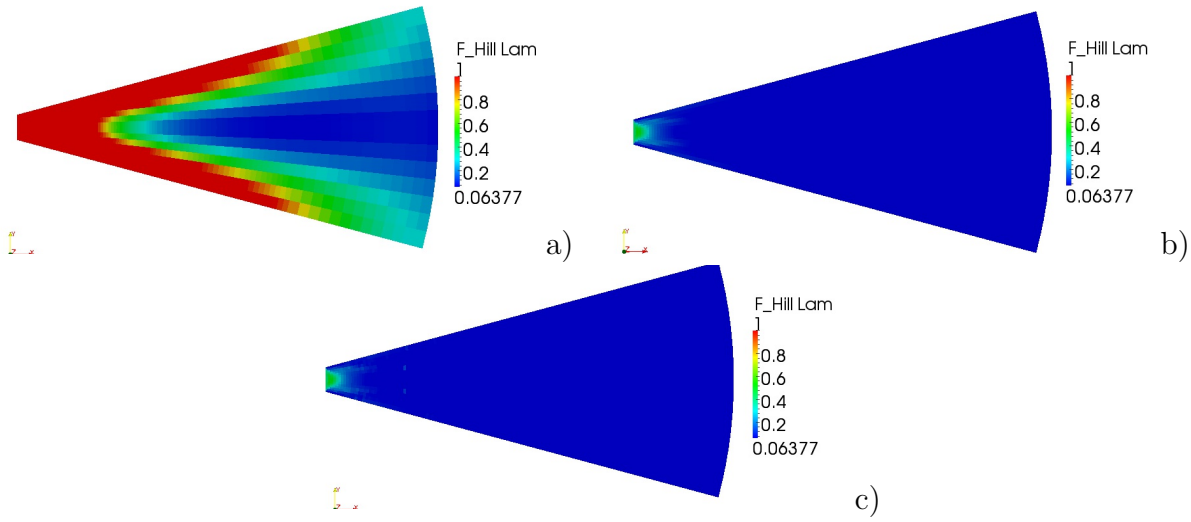

Figure 7.30: F_{Hill}^{Lam} distribution for the starting (a) and optimal configuration using algorithm *a posteriori* (b) and algorithm *a priori* vers. 2 (c), circular sector.

F_{Hill}^{Lam} and $\max(F_{Hill}^{Ply})$ are compared, at the optimal configuration, in Figs. 7.34. The maximum value of F_{Hill}^{Lam} occurs over the region where the load is applied. Also the $\max(F_{Hill}^{Ply})$ occurs in the same region, Fig. 7.34(b), and is greater than F_{Hill}^{Lam} because $r \neq 0$ in this case. The solution type of the local minimisation of F_{Hill}^{Lam} is illustrated in Fig. 7.32(b). The largest part of the plate surface is characterised by the solution type 4, that depends upon the ratio $\dfrac{|t|}{r}$ between the spherical and deviatoric component of strains. Along the geometric symmetry axis, the solution type is equal to 1 and corresponds to a fixed value of the strength moduli, see Tab. 7.1. The optimal distributions of $\overline{\Lambda}_{0L}$ and $\overline{\Lambda}_1$ are given in Figs. 7.35. Finally, the optimal orthotropy orientation $\overline{\Phi}_1^{opt}$ is depicted in Fig. 7.36. The distribution of $\overline{\Phi}_1^{opt}$ is symmetric with respect to the geometric symmetry axis, i.e. the x axis, and, with the exception of the area characterised by the solution type 3 (of the local minimisation of W_c^l), $\overline{\Phi}_1^{opt}$ is oriented along the radial direction. This solution is very similar to the analytical solution founded by Royer [63] and Pedersen [53] for the optimal fiber layout of a composite anisotropic wedge. In particular the area characterised by the solution type 3 for the local minimisation of W_c^l the optimal orientation $\overline{\Phi}_1^{opt}$ is identical to that found in [63]. While in the area characterised by the solution type 2, $\overline{\Phi}_1^{opt}$ is oriented along the radial direction, hence, the stress field is purely radial like the Michell's classical solution [68].

7.6.2.2 Structural optimisation using the algorithm with *a priori* maximisation of strength: version 2

We observe the numerical monotonic convergence for the complementary energy W_c, Fig. 7.37, and the oscillating convergence for the laminate failure index F_{Hill}^{Lam}, Fig. 7.38. The considerations made beforehand concerning the example of Sec. 7.6.1.2 can be repeated verbatim also in this case. The distributions of $\overline{R}_{0K}^{opt}$ and of $\overline{R}_1^{opt}$ are reported in Figs. 7.39. $\overline{R}_{0K}^{opt}$ is almost always equal to R_0. Also $\overline{R}_1^{opt} = R_1$ on the largest part of the surface, except for the thin area along the geometric symmetry axis.

The distribution of F_{Hill}^{Lam} and that of $\max(F_{Hill}^{Ply})$ are compared, at the optimal configuration, in Figs. 7.40. We can note that the maximum value of F_{Hill}^{Lam} and of $\max(F_{Hill}^{Ply})$ occurs near the loading application region. The solution type of the local minimisation of F_{Hill}^{Lam} is shown in Fig. 7.41. Almost the entire plate surface is characterised by the solution type 4 of Tab. 7.1, corresponding to $\overline{\Lambda}_{0L}^{opt} = \Lambda_0$ and $\overline{\Lambda}_1^{opt} = \Lambda_1$ because $\dfrac{|t|}{r} > \dfrac{\Lambda_0 \cos 4\left(\overline{\Omega}_1 - \phi\right)}{\Lambda_1 |\cos 2\left(\overline{\Omega}_1 - \phi\right)|}$. On the rest of the plate surface, $\overline{\Lambda}_{0L}^{opt}$ and $\overline{\Lambda}_1^{opt}$ vary, Figs. 7.42. The optimal orthotropy orientation $\overline{\Omega}_1^{opt}$ is illustrated in Fig. 7.43. On the greatest part of the surface, except for a localised region near the loading application region, $\overline{\Omega}_1^{opt}$ is oriented along the circumferential direction. If we compare such an optimal orientation with the distribution of $\overline{\Phi}_1^{opt}$ obtained with the algorithm *a posteriori*, Fig. 7.36, it is aligned or turned of $\pi/2$. Moreover, the optimal solution given by the algorithms *a posteriori* and *a priori* version 2 generate the same particular condition of coaxial stress and strain field (see for instance Figs. 7.44 concerning the principal stress and strain orientations for the optimal configuration obtained using the algorithm *a priori* version 2); so, the optimal orientation that maximises stiffness is the same that maximises strength, as already discussed in Sec. 7.4.1.2.

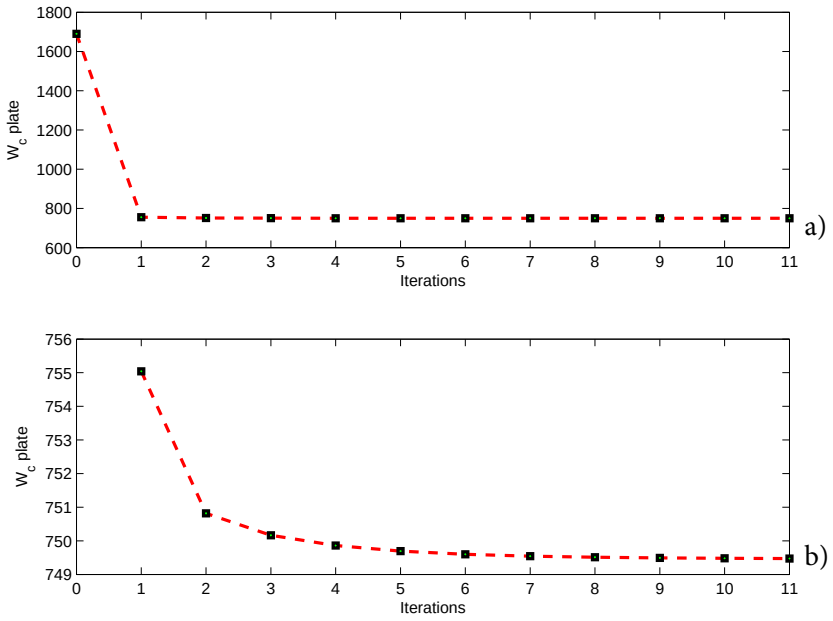

Figure 7.31: Complementary energy of the plate along the iterations (a) and its zoomed version (b), algorithm *a posteriori*, circular sector.

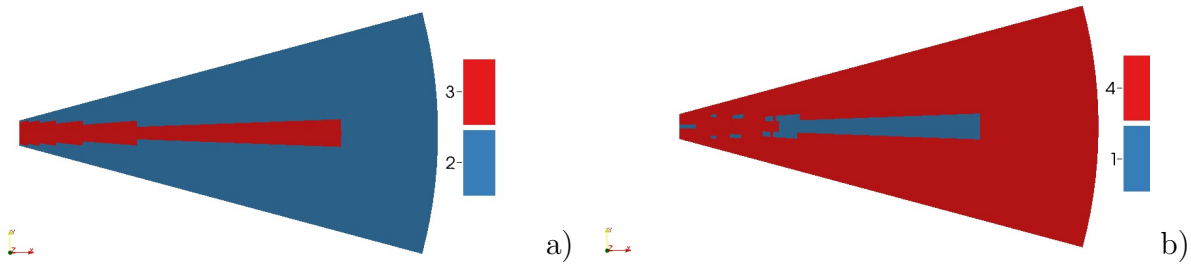

Figure 7.32: Solution type of local minimisation of W_c (a) and solution type of local minimisation of F_{Hill}^{Lam} (b) at optimal configuration, algorithm *a posteriori*, circular sector.

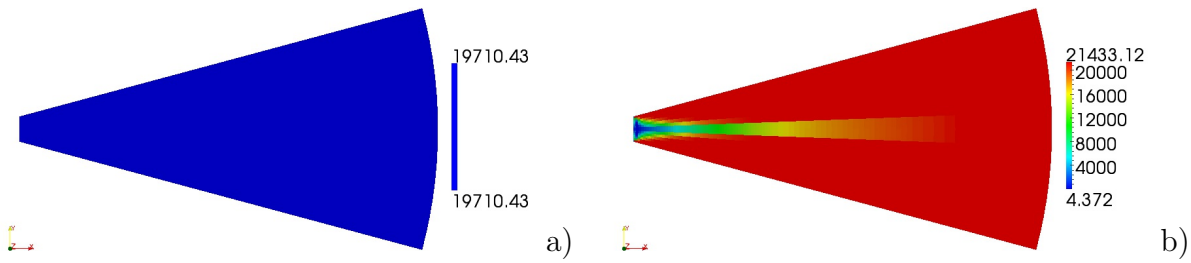

Figure 7.33: $\overline{R}_{0K}$ (a) and $\overline{R}_1$ (b) for the optimal configuration, algorithm *a posteriori*, circular sector.

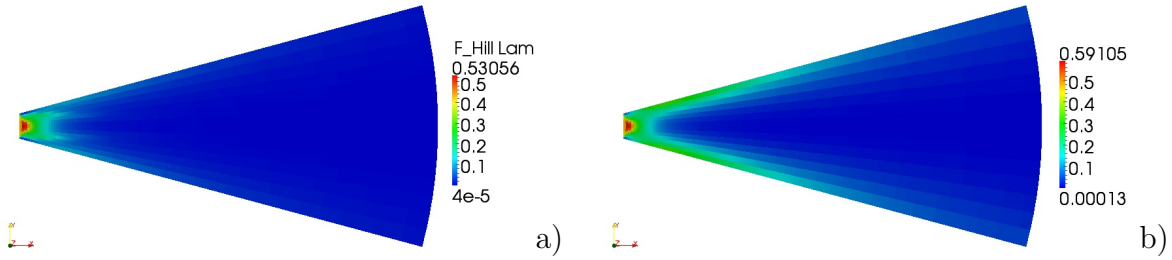

Figure 7.34: F_{Hill}^{Lam} distribution (a) and $\max(F_{Hill}^{Ply})$ of the generic ply (b) for the optimal configuration, algorithm *a posteriori*, circular sector.

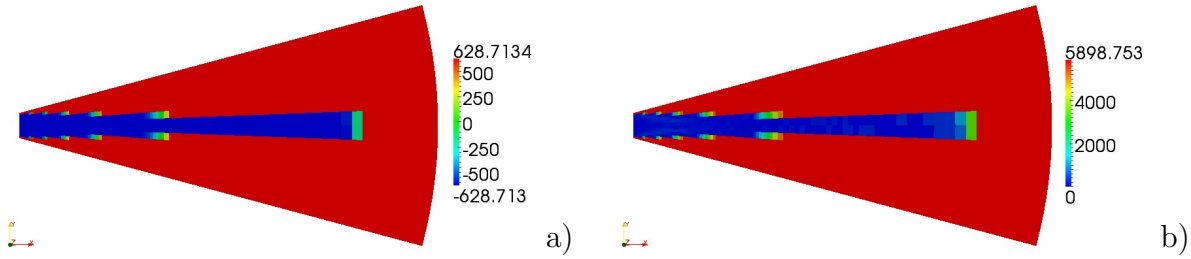

Figure 7.35: $\overline{\Lambda}_{0L}$ (a) and $\overline{\Lambda}_1$ (b) for the optimal configuration, algorithm *a posteriori*, circular sector.

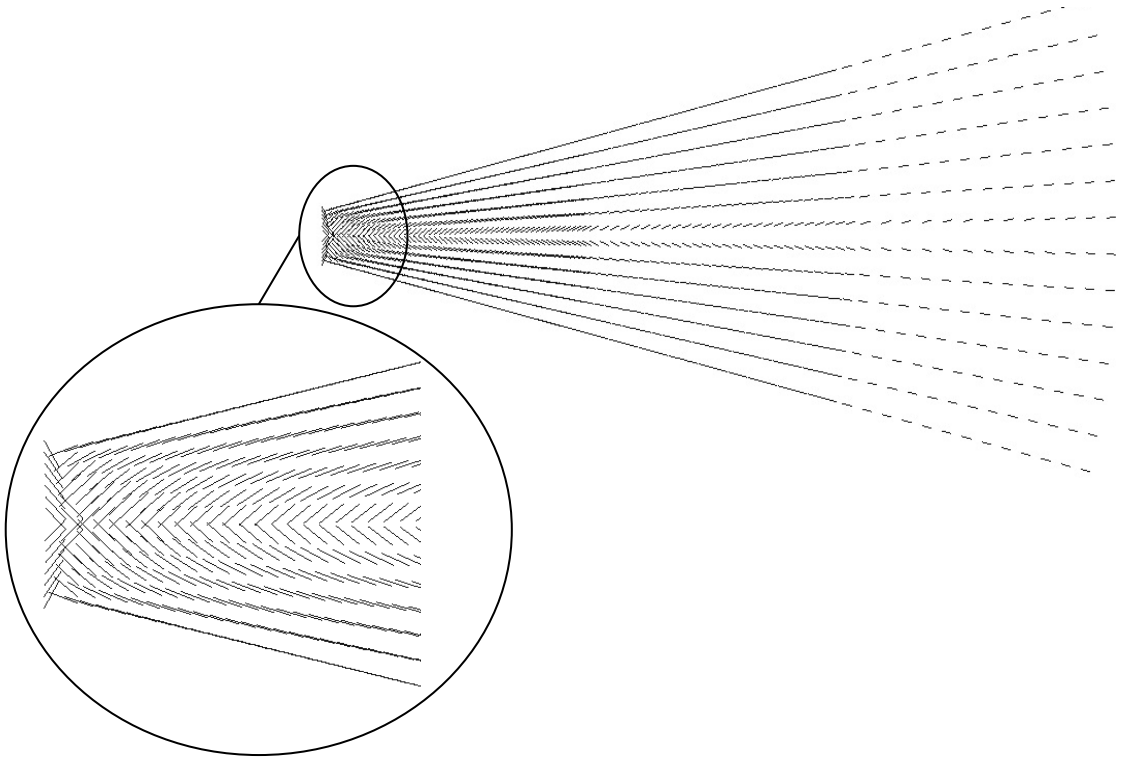

Figure 7.36: Optimal orthotropy orientation $\overline{\Phi}_1^{opt}$, algorithm *a posteriori*, circular sector.

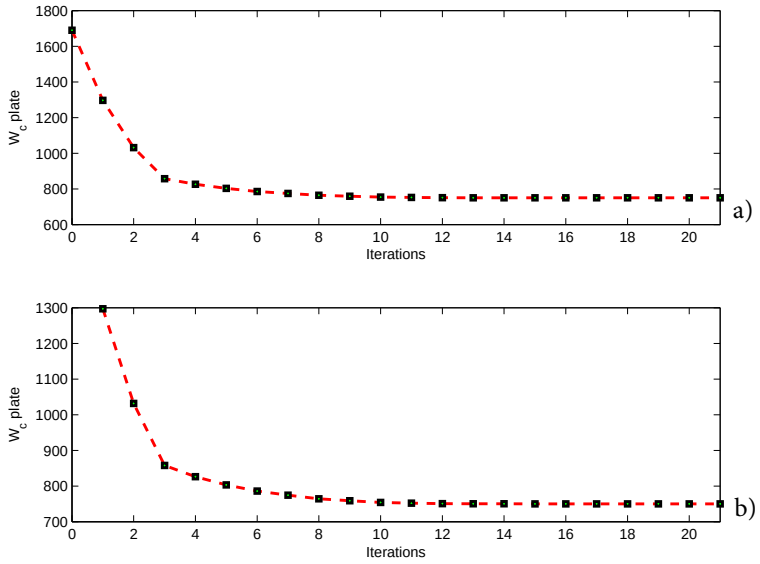

Figure 7.37: Complementary energy of the plate along the iterations (a) and its zoomed version (b), algorithm *a priori* version 2, circular sector.

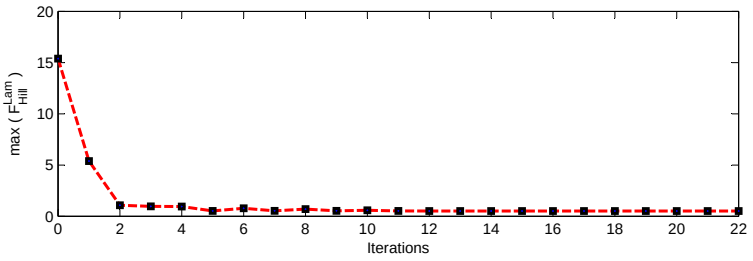

Figure 7.38: Maximum failure index of the plate along the iterations, algorithm *a priori* version 2.

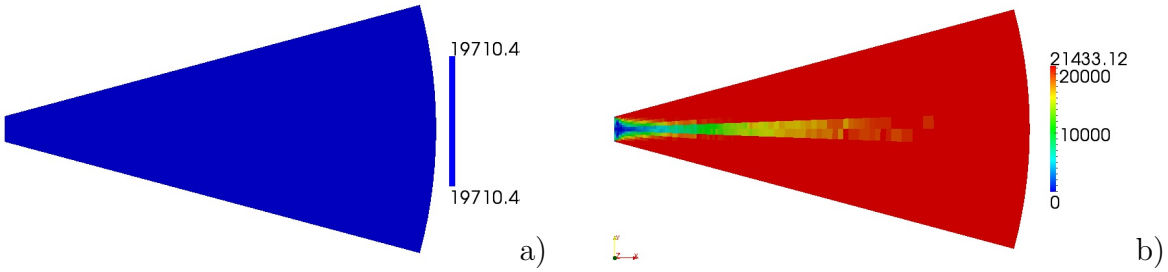

Figure 7.39: $\overline{R}_{0K}$ (a) and $\overline{R}_1$ (b) for the optimal configuration, algorithm *a priori* version 2, circular sector.

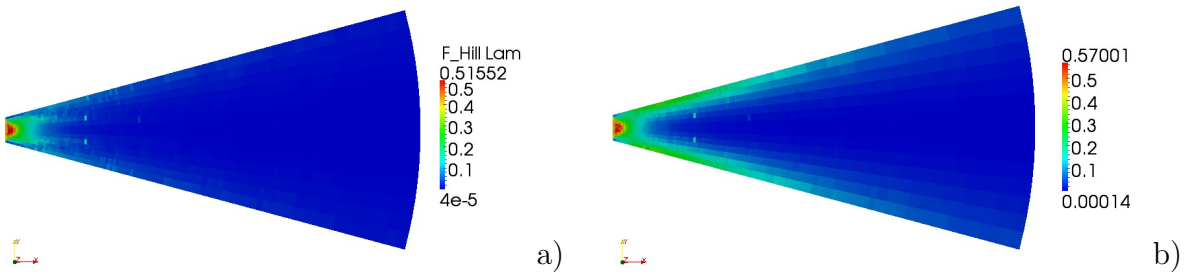

Figure 7.40: F_{Hill}^{Lam} distribution (a) and max(F_{Hill}^{Ply}) of the generic ply (b) for the optimal configuration, algorithm *a priori* version 2, circular sector.

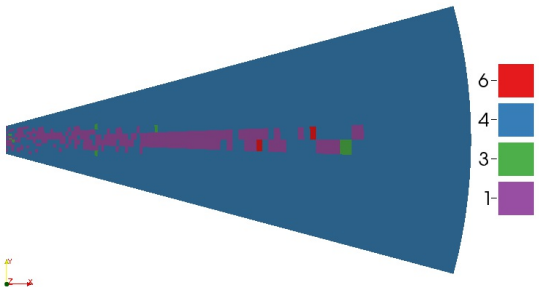

Figure 7.41: Solution type of local minimisation of F_{Hill}^{Lam}, algorithm *a priori* version 2, circular sector.

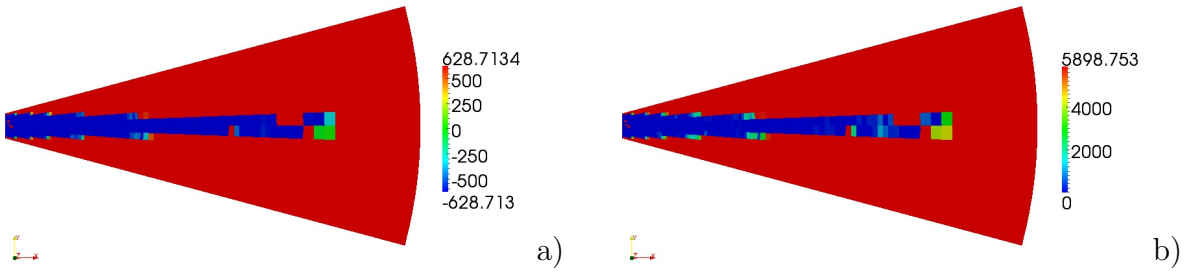

Figure 7.42: $\overline{\Lambda}_{0L}$ (a) and $\overline{\Lambda}_1$ (b) at optimal condition, algorithm *a priori* version 2, circular sector.

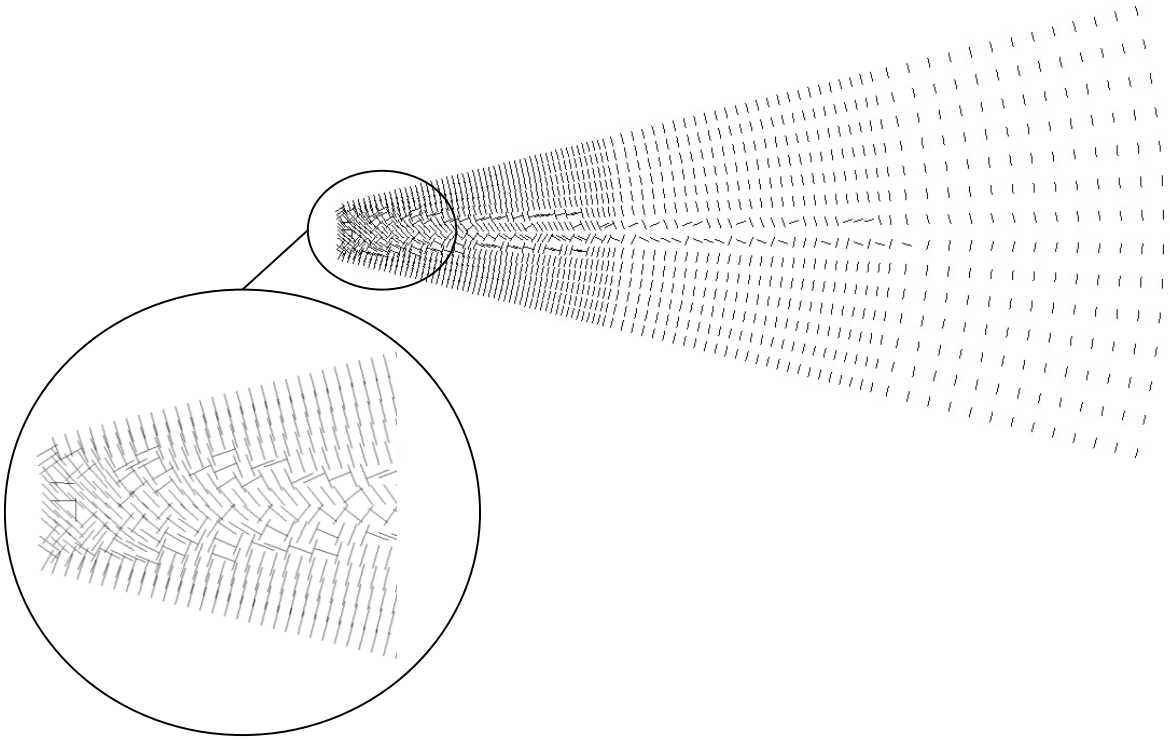

Figure 7.43: Optimal orthotropy orientation $\overline{\Omega}_1^{opt}$, algorithm *a priori* version 2, circular sector.

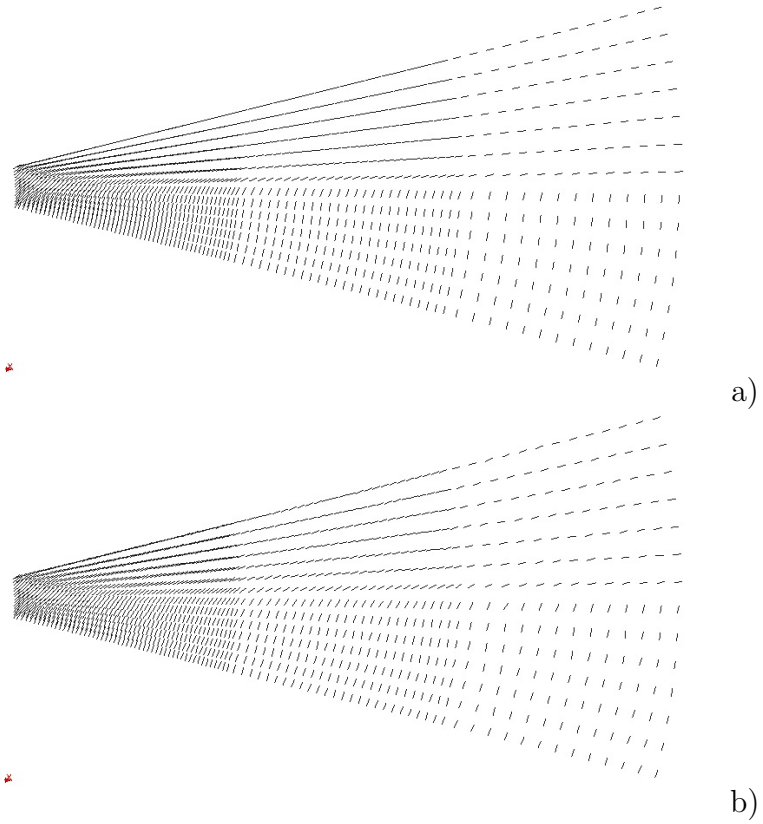

Figure 7.44: Direction of principal stress (a) and strain (b) components for the optimal configuration, algorithm *a priori* version 2, circular sector.

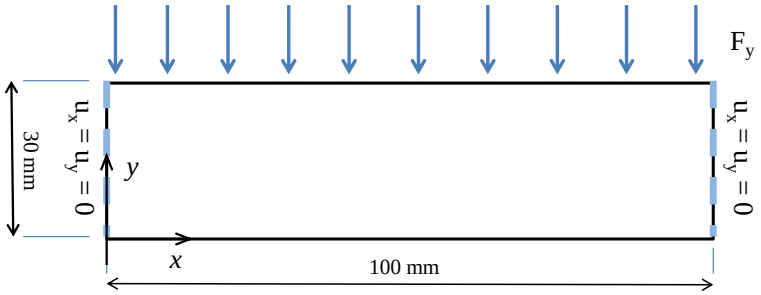

Figure 7.45: Geometry and boundary conditions, rectangular plate.

7.6.3 Third example: a rectangular plate

We consider now a rectangular plate whose geometry and boundary conditions are shown in Fig. 7.45. The loading value is $F_y = 200$ N/mm. The total number of elements n_{elem} is fixed to 1400 (70 partitions along the long side per 20 partitions along the short side). The starting values of the stiffness polar parameters are those of an equilibrated cross-ply laminate oriented at $\pm 45°$ with respect to the x axis: $\overline{R}_0^{(0)} = R_0$ and $\overline{R}_1^{(0)} = 0$ for the entire plate.

In Tab. 7.7 we show the main results of the structural optimisation step. Like the results of the first example, the reduction of W_c and of the maximum displacement given by the algorithm *a posteriori* is greater than that given by the algorithm *a priori* version 2. On the contrary, the reduction of F_{Hill}^{Lam} given by the algorithm *a priori* version 2 is greater of 0.2% than that obtained using the algorithm *a posteriori*.

The comparison between the distribution, over the plate, of the local W_c and F_{Hill}^{Lam} for the starting and final configurations are shown in Figs. 7.46 and Figs. 7.47, respectively.

		Alg. *posteriori*	Alg. *priori* v2
	Starting condition	Optimal cond., (% reduction)	Optimal cond., (% reduction)
W_c [N mm]	3064.960	1185.922, (61.3)	1191.130, (61.1)
Max F_{Hill}^{Lam}	6.427	0.325, (94.9)	0.317, (95.1)
Max F_{Hill}^{Ply}	-	0.520	0.528
Max displacement [mm]	0.275	0.096, (65.1)	0.097, (64.7)

Table 7.7: Main results, rectangular plate.

7.6.3.1 Structural optimisation using the algorithm with *a posteriori* local maximisation of strength

The reduction of the complementary energy W_c along the iterations is reported in Fig. 7.48. The solution type of the local minimisation of W_c is shown in Fig. 7.49(a). All of the three solution types are present. Thus, in Fig. 7.50(a) we have chosen $\overline{R}_{0K}^{opt} = R_0$ in the corresponding area with solution type 1. The distribution of $\overline{R}_1^{opt}$, Fig. 7.50(b), depends upon

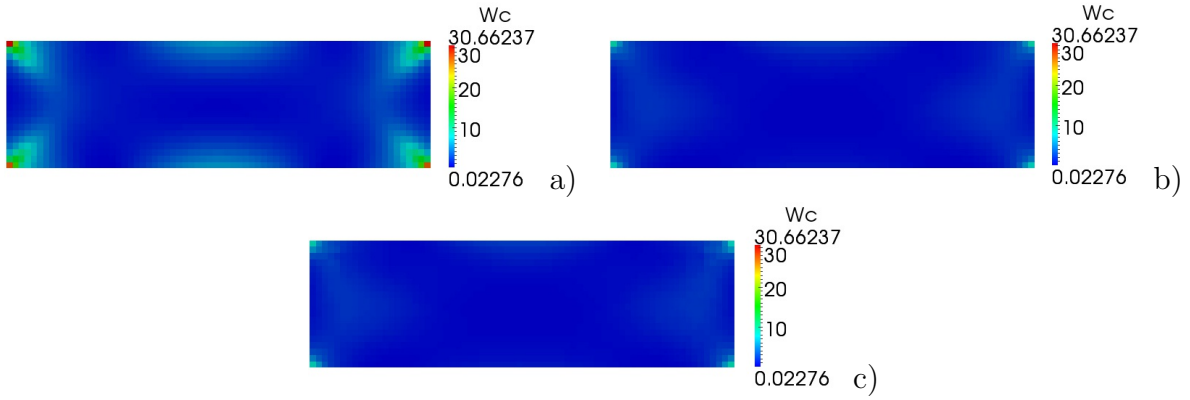

Figure 7.46: Complementary energy distribution for the starting (a) and optimal configuration using algorithm *a posteriori* (b) and algorithm *a priori* vers. 2 (c), rectangular plate.

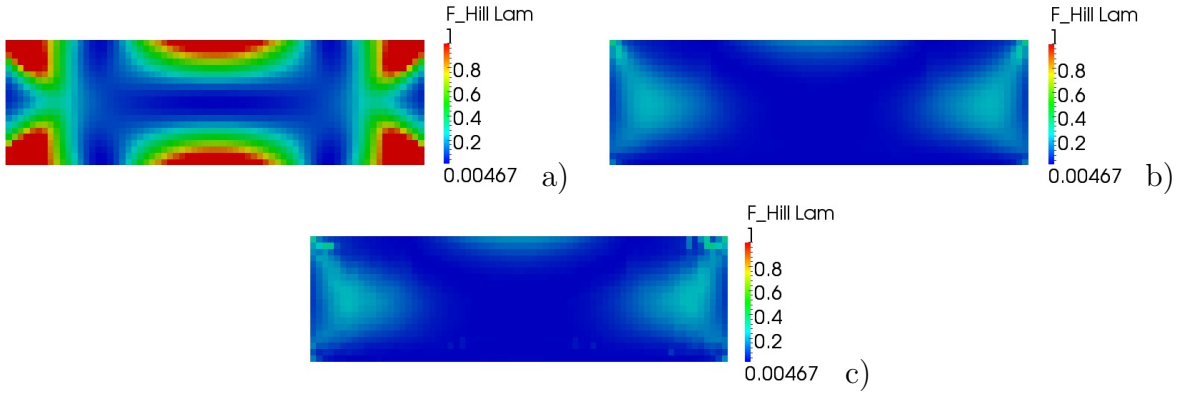

Figure 7.47: F_{Hill}^{Lam} distribution for the starting (a) and optimal configuration using algorithm *a posteriori* (b) and algorithm *a priori* vers. 2 (c), rectangular plate.

the ratio $R/|T|$ between the deviatoric and the spherical components of internal forces, in the areas with solution type 1 and 3, while is $\overline{R}_1^{opt} = R_1$ in the area characterised by the solution type 2, see Tab. 6.1.

The values of F_{Hill}^{Lam} and $\max(F_{Hill}^{Ply})$ are compared in Figs. 7.51. The maximum value of F_{Hill}^{Lam} and F_{Hill}^{Ply} occurs at the top corners.
The solution type of the local minimisation of F_{Hill}^{Lam} is reported in Fig. 7.49(b). Almost all the plate surface is characterised by the solution type 4 that depends upon the ratio $\dfrac{|t|}{r}$. The area characterised by the solution type 0 corresponds to the area characterised by the solution type 1 of the local minimisation of W_c^l, where $r = 0$. The optimal distribution of $\overline{\Lambda}_{0L}^{opt}$ and $\overline{\Lambda}_1^{opt}$ is shown in Figs. 7.52 (a) and (b), respectively. Finally, the optimal orthotropy orientation $\overline{\Phi}_1^{opt}$ is reported in Fig. 7.53. It is almost always oriented at $\pm\pi/4$ that corresponds to the starting distribution of orthotropy orientation. This explain the good values of W_c^l over the plate also at the starting condition. On the contrary, the values of F_{Hill}^{Lam} at the starting condition are greater than those obtained at the optimal condition. So the important result, in this case, concerns the significant reduction of the F_{Hill}^{Lam} over the whole plate surface.

7.6.3.2 Structural optimisation using the algorithm with *a priori* maximisation of strength: version 2

Fig. 7.54 shows the numerical convergence of the complementary energy W_c along the iterations. The variation of the laminate failure index F_{Hill}^{Lam}, Fig. 7.55, oscillates until the 14^{th} iteration. The convergence of the algorithm is achieved in 16 iterations.

The distribution of $\overline{R}_{0K}^{opt}$ and of $\overline{R}_1^{opt}$, given by the numerical solution of the algorithm of alternated directions is shown in Figs. 7.56. The optimal distribution of $\overline{R}_1$ is similar to that obtained using the algorithm *a posteriori*, see Figs. 7.50(b).

The values of F_{Hill}^{Lam} and those of $\max(F_{Hill}^{Ply})$ are compared, for the optimal configuration, in Figs. 7.57 (a) and (b), respectively. The maximum value of F_{Hill}^{Lam} and F_{Hill}^{Ply} occurs in the same area, like also to the solution given by the algorithm *a posteriori*, Figs. 7.51.

The solution type of the local minimisation of F_{Hill}^{Lam} is reported in Fig. 7.58. Also in this case, almost all of the plate surface is characterised by the solution type 4 of Tab. 7.1. The distribution of $\overline{\Lambda}_{0L}^{opt}$ and of $\overline{\Lambda}_1^{opt}$, Figs. 7.59 (a) and (b) respectively, is very similar to that obtained using the algorithm *a posteriori*, Figs. 7.52.

The optimal orthotropy orientation $\overline{\Omega}_1^{opt}$ is illustrated in Fig. 7.60 and is almost always aligned with $\overline{\Phi}_1^{opt}$ given by the algorithm *a posteriori*, Fig. 7.53. Moreover, the direction of the principal stress and strain components, for the optimal configuration obtained using this algorithm *a priori* version 2, are almost the same, see Figs. 7.61. As a consequence of these two aspects and recalling what discussed at the end of Sec. 7.4.1.2, we can assert that, except for some very localised areas, the optimal orthotropy orientation that maximises stiffness is the same that maximises strength and this optimal condition is achieved by both the algorithms. Thus, like the results of the previous example of the circular sector, the solution given by both the algorithms can be considered as a global optimal solution maximising simultaneously stiffness and strength, without one property clearly prevailing on the other one.

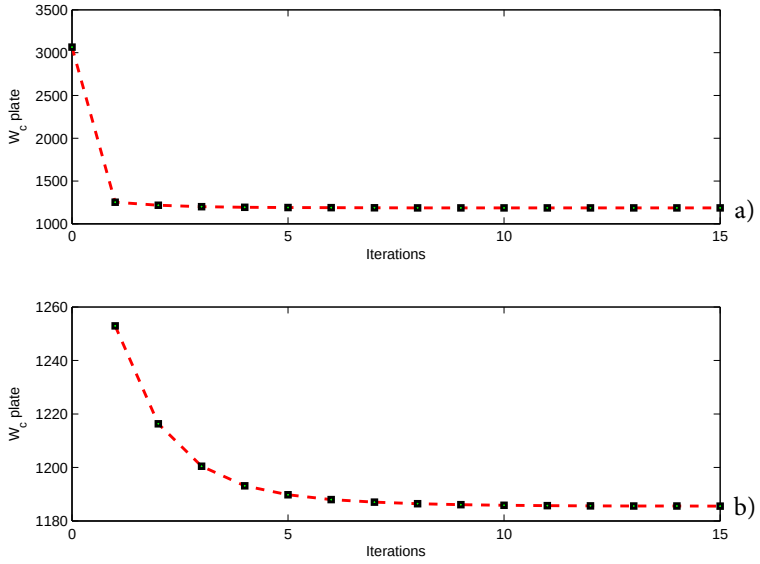

Figure 7.48: Complementary energy of the plate along the iterations (a) and its zoomed version (b), algorithm *a posteriori*, rectangular plate.

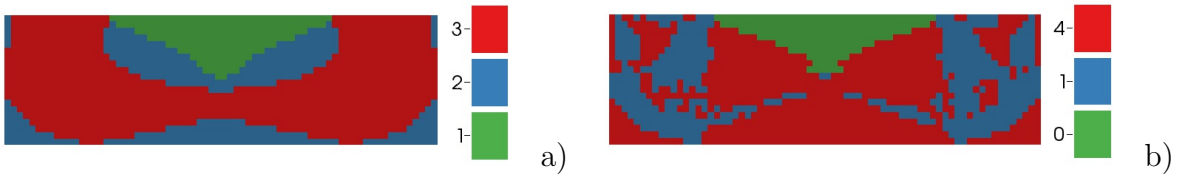

Figure 7.49: Solution type of local minimisation of W_c (a) and solution type of local minimisation of F_{Hill}^{Lam} (b) for the optimal configuration, algorithm *a posteriori*, rectangular plate.

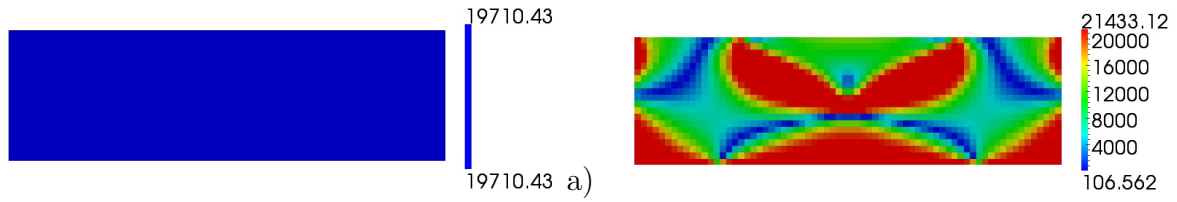

Figure 7.50: $\overline{R}_{0K}$ (a) and $\overline{R}_1$ (b) for the optimal configuration, algorithm *a posteriori*, rectangular plate.

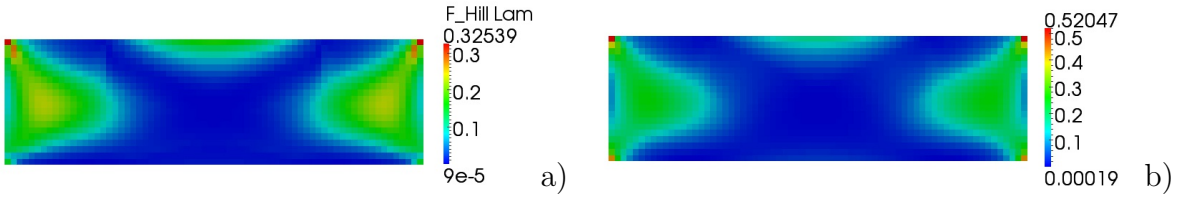

Figure 7.51: F_{Hill}^{Lam} distribution (a) and $\max(F_{Hill}^{Ply})$ of the generic ply (b) for the optimal configuration, algorithm *a posteriori*, rectangular plate.

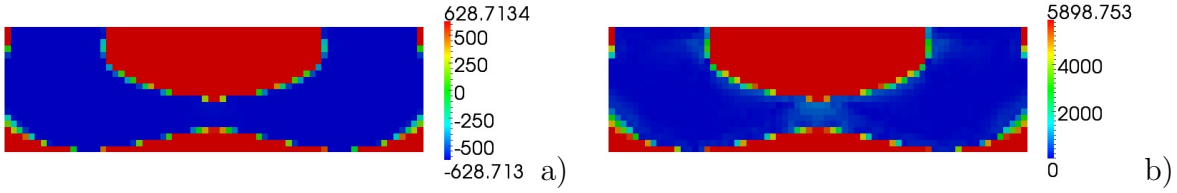

Figure 7.52: $\overline{\Lambda}_{0L}$ (a) and $\overline{\Lambda}_1$ (b) for the optimal configuration, algorithm *a posteriori*, rectangular plate.

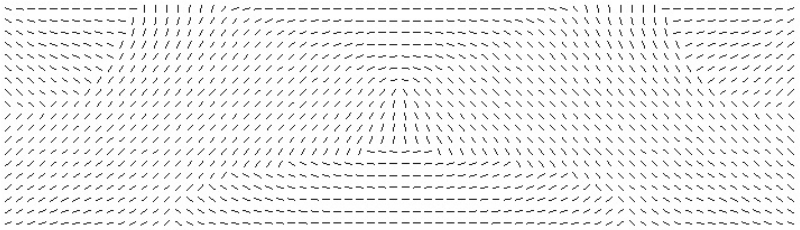

Figure 7.53: Optimal orthotropy orientation $\overline{\Phi}_1^{opt}$, algorithm *a posteriori*, rectangular plate.

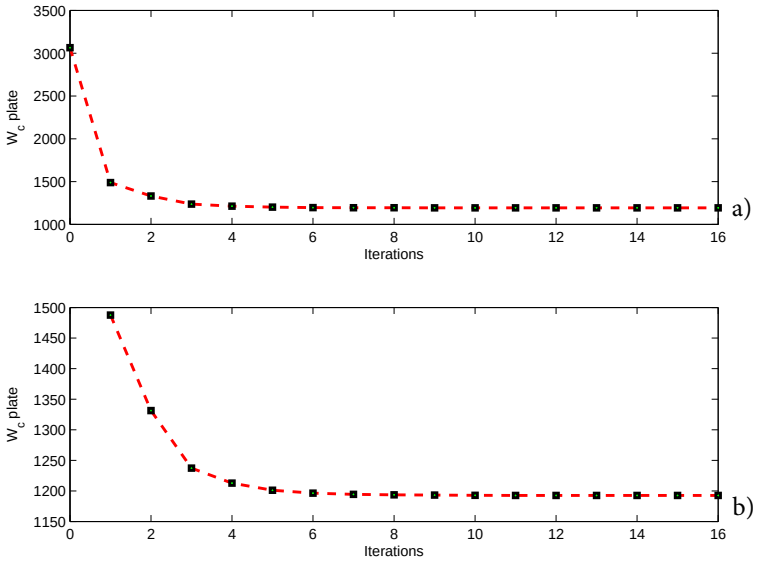

Figure 7.54: Complementary energy of the plate along the iterations (a) and its zoomed version (b), algorithm *a priori* version 2, rectangular plate.

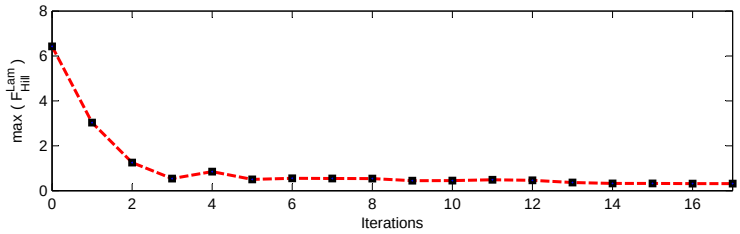

Figure 7.55: Maximum failure index of the plate along the iterations, algorithm *a priori* version 2, rectangular plate.

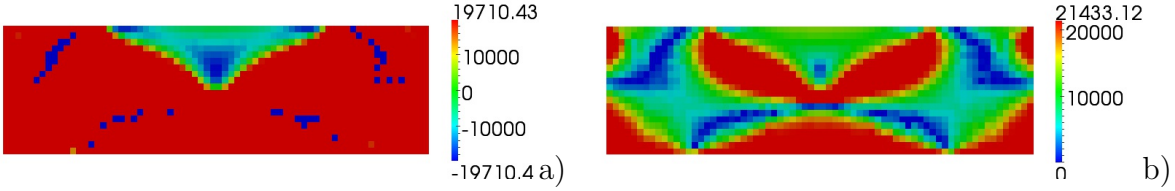

Figure 7.56: $\overline{R}_{0K}$ (a) and $\overline{R}_1$ (b) for the optimal configuration, algorithm *a priori* version 2, rectangular plate.

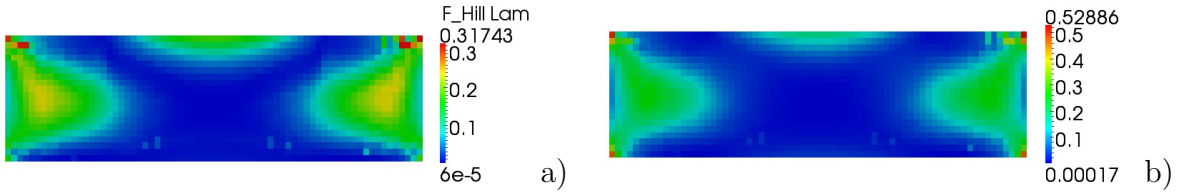

Figure 7.57: F_{Hill}^{Lam} distribution (a) and $\max(F_{Hill}^{Ply})$ of the generic ply (b) for the optimal configuration, algorithm *a priori* version 2, rectangular plate.

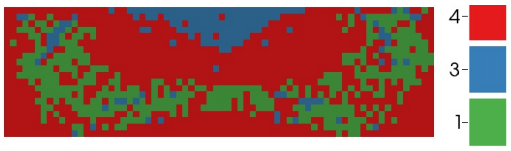

Figure 7.58: Solution type of local minimisation of F_{Hill}^{Lam}, algorithm *a priori* version 2, rectangular plate.

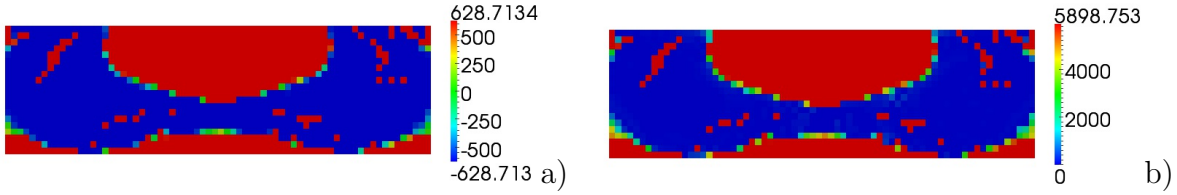

Figure 7.59: $\overline{\Lambda}_{0L}$ (a) and $\overline{\Lambda}_1$ (b) for the optimal configuration, algorithm *a priori* version 2, rectangular plate.

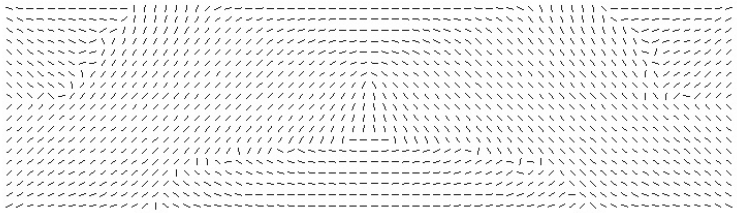

Figure 7.60: Optimal orthotropy orientation $\overline{\Omega}_1^{opt}$, algorithm *a priori* version 2, rectangular plate.

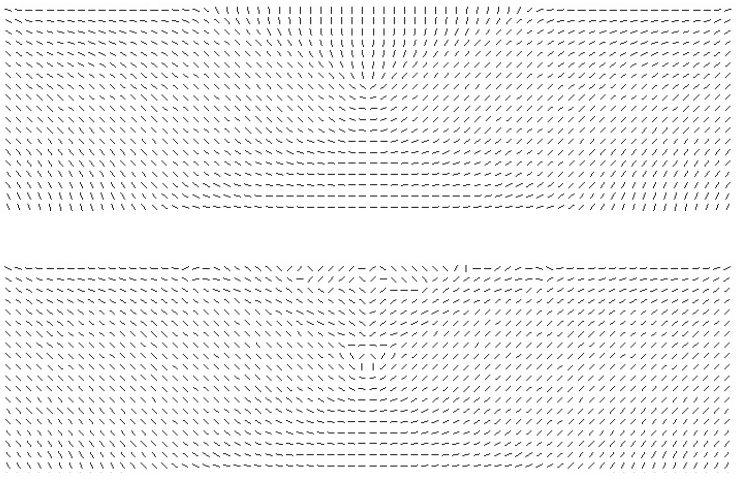

a)

b)

Figure 7.61: Direction of principal stress (a) and strain (b) components for the optimal configuration, algorithm *a priori* version 2, rectangular plate.

7.6.3.3 Structural optimisation taking into account for different strength in tension and compression: algorithm *a priori* version 2

In this section we want to perform an analysis closer to reality. Such an example is very similar to that of the Sec. 7.6.3.2, but, this time we take into account the difference of strength in tension and compression.

In Tab. 7.8 we show the strength properties of the material. The stiffness properties are still those of Tab. 7.4. In particular, as we use the Tsai-Hill criterion, we have four different combinations of strength properties. More precisely, the two different values of normal strength properties in tension and compression are used in relation with the sign of internal actions components N_{xx} and N_{yy}. Such an approach gives four different sets of invariants, one for the tension, one for the compression case, and the two others being a mix of tension and compression cases.

In terms of algorithm programming, we have simply inserted a check on the sign of the internal actions components N_{xx} and N_{yy} in order to select the corresponding values of the strength polar parameters of Tab. 7.8. In Tab. 7.9 we show the main results of the structural optimisation step. For all of the considered quantities, a sensible reduction is obtained. However, the difference of strength in tension and compression has influenced the results; in fact we have an optimal value of the W_c a bit higher with respect to the previous case, where we have considered equal strength properties in tension and compression, and a maximum F_{Hill}^{Lam} a bit lower, see Tab. 7.7.

The trend of the numerical convergence of the complementary energy W_c and of the laminate failure index F_{Hill}^{Lam} along the iterations is very similar to that of the previous case and, so, is not reported here for the sake of brevity.

In Figs. 7.62 the components N_{xx} and N_{yy} of the internal actions field are shown to better understand the results presented below. In particular Figs. 7.62 shows that all the combinations of signs of N_{xx} and N_{yy} are present and, thus, the different combinations of strength properties of Tab. 7.8 have to be considered.

Let us now compare these results and those obtained in Sec. 7.6.3.2 in order to show how the different strength behaviour in tension and compression can influence the results.

Strength properties, [MPa]							
$X = X_t$	1500	$X = X_c$	900	$X = X_t$	1500	$X = X_c$	900
$Y = Y_t$	40	$Y = Y_c$	246	$Y = Y_c$	246	$Y = Y_t$	40
S	68	S	68	S	68	S	68
Polar parameters of **G**							
Γ_0	11746	Γ_0	10819	Γ_0	7525	Γ_0	15040
Γ_1	15461	Γ_1	5250	Γ_1	2122	Γ_1	18589
Λ_0	628	Λ_0	299	Λ_0	3592	Λ_0	3922
Λ_1	5898	Λ_1	4819	Λ_1	1604	Λ_1	2683
L	0	L	1	L	1	L	0

Table 7.8: Strength properties and polar parameters of the basic ply.

		Alg. *priori* v2
	Starting condition	Optimal cond., (% reduction)
W_c [N mm]	3064.960	1225.063, (60.0)
Max F_{Hill}^{Lam}	4.288	0.287, (93.3)
Max F_{Hill}^{Ply}	-	0.520
Max displacement [mm]	0.275	0.1, (63.6)

Table 7.9: Main results, rectangular plate: different tension/compression strength.

The distribution of $\overline{R}_{0K}^{opt}$ and of $\overline{R}_1^{opt}$, given by the numerical solution of the algorithm of alternated directions is shown in Figs. 7.63. Both optimal distributions of $\overline{R}_{0K}$ and of $\overline{R}_1$ are similar to that of Figs. 7.56, hence, the different strength behaviour in tension and compression has not influenced sensibly the optimal stiffness distribution.

The values of F_{Hill}^{Lam} and those of $\max(F_{Hill}^{Ply})$ are compared, for the optimal configuration, in Figs. 7.64 (a) and (b), respectively. The maximum value of F_{Hill}^{Lam} occurs in different localised regions, while the highest value of $\max(F_{Hill}^{Ply})$ occurs only in the same localised region observed also in the previous results, Fig. 7.57(b), at the top corners of the plate. Of course, the values of F_{Hill}^{Lam} and $\max(F_{Hill}^{Ply})$ for the optimal configuration are different to those presented in Figs. 7.57.

The solution type of the local minimisation of F_{Hill}^{Lam} is reported in Fig. 7.65. A great part of the plate surface is characterised by the solution type 9 of Tab. 7.2 corresponding to a solution for $L = 1$ of the basic ply. The distribution of $\overline{\Lambda}_{0L}^{opt}$ and of $\overline{\Lambda}_1^{opt}$, Figs. 7.66 (a) and (b) respectively, is completely different to that of Figs. 7.59 as Λ_0 and Λ_1 can assume four different values due to the four different combinations of strength properties, see Tab. 7.8.

The optimal orthotropy orientation $\overline{\Omega}_1^{opt}$ is illustrated in Fig. 7.67 and, also in this case, the solution is different from that given by the previous case, Fig. 7.60.

To conclude we can assert that the different strength behaviour in tension and compression has a bit influenced the results of the structural optimisation in terms of stiffness

and, on the contrary, has sensibly influenced the results in terms of strength. In any case, the optimal stiffness and strength distribution lead to an important reduction of both the complementary energy and the laminate failure index with respect to the starting condition.

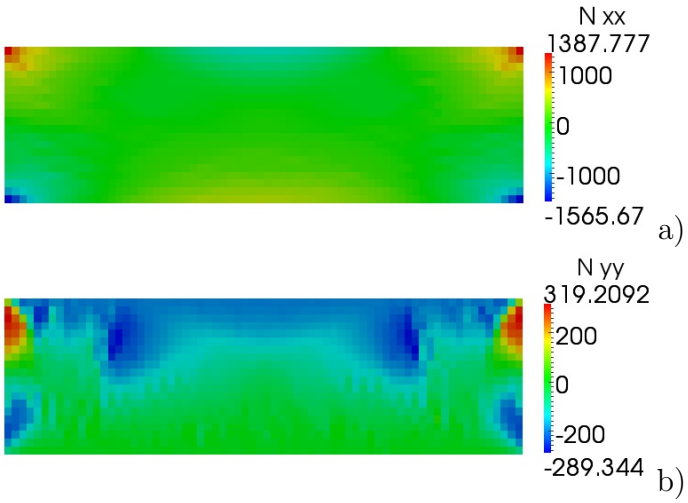

Figure 7.62: Internal actions field components N_{xx} (a) and N_{yy} (b) for the optimal configuration, algorithm *a priori* version 2, rectangular plate: different tension/compression strength.

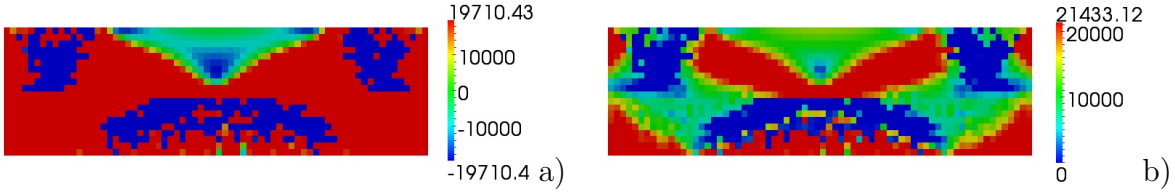

Figure 7.63: $\overline{R}_{0K}$ (a) and $\overline{R}_1$ (b) for the optimal configuration, algorithm *a priori* version 2, rectangular plate: different tension/compression strength.

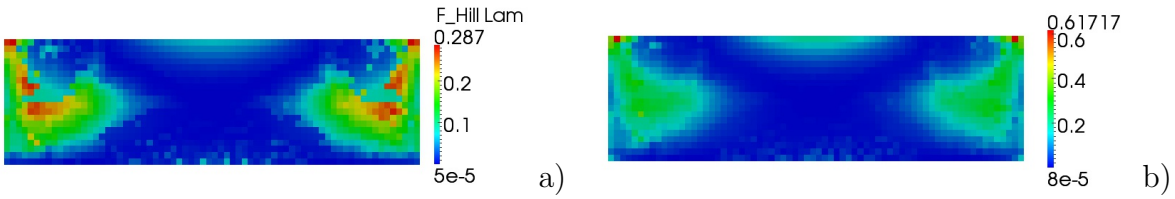

Figure 7.64: F_{Hill}^{Lam} distribution (a) and $\max(F_{Hill}^{Ply})$ of the generic ply (b) for the optimal configuration, algorithm *a priori* version 2, rectangular plate: different tension/compression strength.

Figure 7.65: Solution type of local minimisation of F_{Hill}^{Lam}, algorithm *a priori* version 2, rectangular plate: different tension/compression strength.

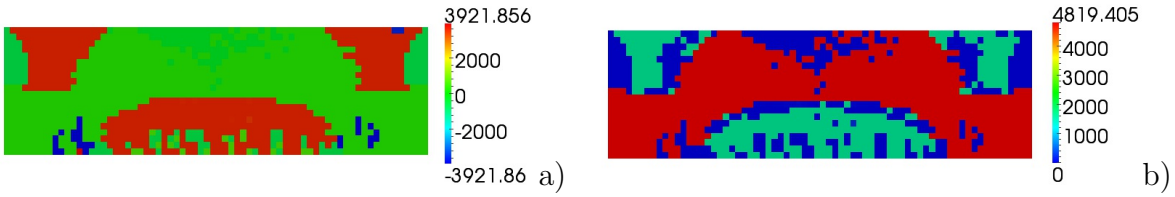

Figure 7.66: $\overline{\Lambda}_{0L}$ (a) and $\overline{\Lambda}_1$ (b) for the optimal configuration, algorithm *a priori* version 2, rectangular plate: different tension/compression strength.

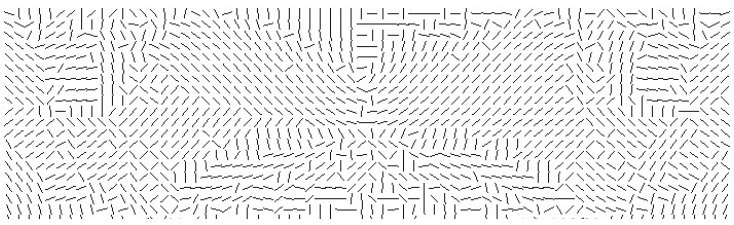

Figure 7.67: Optimal orthotropy orientation $\overline{\Omega}_1^{opt}$, algorithm *a priori* version 2, rectangular plate: different tension/compression strength.

7.7 Concluding remarks

In this Chapter we presented three different algorithms used to solve the first step of the hierarchical strategy proposed in Chapter 6. As already said, the goal of this first step of the hierarchical strategy consists in determining the optimal distribution of material parameters, represented by the polar parameters, of a structure with a given geometry and boundary conditions.

The first proposed algorithm is a simple modification of the optimisation algorithm introduced by Allaire and Kohn [2]. Particularly, we have added a further phase to the original version of the algorithm in which we introduce the strength optimisation phase. We considered the stiffness functional, i.e. the complementary energy, as the main objective to be minimised in terms of all the stiffness material parameters. On the contrary, the strength functional, i.e. the laminate failure index, is considered as the secondary objective to be minimised and the strength orthotropy orientation is taken equal to the optimal orthotropy orientation of stiffness.

The second algorithm can be considered, in some sense, as the "converse" version of the previous one. The failure index is minimised in terms of all the strength polar parameters while the complementary energy is minimised only in terms of the stiffness polar moduli, being the stiffness orthotropy orientation equal to the optimal orthotropy orientation of strength. Moreover, we proposed a modified version of this algorithm in order to match the mathematical convergence proof and this last version demonstrates to be more effective and robust than the previous one.

A point of originality of these new algorithms resides in the fact that we considered *two functional* to be minimised: one describing the stiffness of the structure (the complementary energy) and the other one describing the strength (the homogenised failure criterion). *The complementary energy and the laminate failure index have been taken into account to develop two algorithms able to deal with the optimisation problem of maximising simultaneously the strength and the stiffness of a structure and to have a control on which property should be privileged.* The decision of using two functional instead of only one, as in [30] and [38] wherein stiffness and strength fields are included in an unique function, is taken for having the control on which of the two mechanical property must be the leading one. Indeed, the use of an unique objective function implies that, before obtaining and evaluating an optimal solution, we are not able to know *a priori* which quantity, between stiffness and strength, will have better qualities at the end of the optimisation process.

After developing the two algorithms, we deal with the problem of finding *an analytical solution to the minimisation of the strength functional, with respect to the material parameters, for linear elastic plane structures composed of orthotropic materials*, see Sec. 7.4.1. Concerning the analytical solution, an important result has been obtained: *when the directions of the principal stress and strain components are the same, the solution given by both algorithms represents a real global optimum for both stiffness and strength properties.*

Finally, we performed some numerical tests in order to prove the effectiveness and the robustness of the proposed algorithms and to evaluate the computational costs of this first step of the hierarchical strategy. Although we used a laminate level failure criterion based on the same assumptions of the Tsai-Hill criterion, we have shown in Sec. 7.6.3.3 a numerical example, using the modified version of the algorithm *a priori*, wherein we take into account the different strength behaviour in tension and compression. All the results show a considerable incrementation in terms of stiffness and strength and also in terms of computational costs. Concerning the reduction of both functional, we achieve an

average of 50 % of reduction of the global complementary energy and an average of 70 % of the laminate failure index. Regarding the computational costs, thanks to the adoption of the hierarchical strategy, we are able to solve the structural optimisation within about 5 minutes, using the algorithm *a posteriori*, 15 minutes using the first version of the algorithm *a priori* and 40 minutes using the second version of the algorithm *a priori* on an Intel® *i*5 Dual Core 2.5GHz processor. In all the cases, in less than one hour, we are able to determine the optimal anisotropy distribution of a plate similar to those considered in the numerical examples.

A last remark concerns the results of the second and third test cases: the optimal solution achieved by the two algorithms, *a posteriori* and *a priori* second version, corresponds to the particular case of coaxiality between the stress and strain fields, hence, in terms of both stiffness and strength properties we obtain a global optimal solution.

8

Second step: optimal lay-up including strength

8.1 Introduction

In this Chapter we are concerned with the second step of the hierarchical strategy: the lay-up design. As still explained in Chapter 6, the lay-up design in the framework of the hierarchical strategy corresponds to determine a laminate stacking sequence satisfying the optimal distribution of material parameters issued from the first step of the strategy.

We already talked about the non-bijectivity and non-convexity of this design problem that is due to the relations that link the design variables, the plies orientations, to the material parameters, see Sec. 6.3.2. In order to ensure the existence of at least one stacking sequence satisfying such optimal distribution of material parameters we have imposed some constraints, i.e. the geometric constraints, on the admissible values of the material parameters during the resolution of the structural optimisation step.

In Sec. 6.4.3 we have already introduced the problem of the lay-up design linked to the solutions of the structural optimisation found in Chapter 7. The fundamental difference between problems (6.10) and (6.50) resides in the addition, in the last one, of some material parameters: the polar invariants that describe strength. In the next Sections we will face the problem (6.50) through a numerical method in order to find, at least, one stacking sequence meeting the optimal requirements of both stiffness and strength.

8.2 The lay-up design respecting the optimal solution of the first step

The optimal material parameters of the structure issued from the structural optimisation step vary point-wise: the homogenised structure issued from the the first step of the hierarchical strategy is a *variable stiffness and strength structure*. Therefore, problem (6.50):

$$\text{find, for a given set } \left\{\overline{K}^{opt}, \overline{R}_0^{opt}, \overline{R}_1^{opt}, \overline{L}^{opt}, \overline{\Lambda}_0^{opt}, \overline{\Lambda}_1^{opt}\right\}$$
$$\text{a vector of plies orientations } (\delta_1, \delta_2, ..., \delta_n) \text{ such that :}$$

$$\begin{cases} \overline{R}_0 = \overline{R}_0^{opt} \ , \\ \overline{R}_1 = \overline{R}_1^{opt} \ , \\ \overline{\Lambda}_0 = \overline{\Lambda}_0^{opt} \ , \\ \overline{\Lambda}_1 = \overline{\Lambda}_1^{opt} \ , \\ \overline{\Phi}_0 - \overline{\Phi}_1 = \overline{K}^{opt}\pi/4 \ , \\ \overline{\Omega}_0 - \overline{\Omega}_1 = \overline{L}^{opt}\pi/4 \ , \\ \overline{\Phi}_1 - \overline{\Omega}_1 = 0; \pi/2 \ , \\ \overline{\Phi}_1 = \overline{\Phi}_1^{opt} \ , \\ \mathbf{B} = 0 \ , \end{cases} \tag{8.1}$$

needs to be solved at any point of the structure. In the discretised FE approach introduced in the previous Chapter, Sec. 7.5, this means that the above problem must be written and solved for every element of the discretised model of the structure.

8.2.1 Mathematical statement of the problem

The optimisation parameters of (8.1) are the ply orientations δ_k. In the framework of this thesis, we decided to formulate this problem through the minimisation of an unconstrained objective function introduced by Vannucci in [78]. We recall its general expression, already given in eq. (6.11):

$$\min_{\delta_k} I(f_i(\delta_k)) = \sum_j f_j^2(\delta_k) \text{ with } \ k = 1, 2, .., n \ , \tag{8.2}$$

where the sub-objectives $f_j^2(\delta_k)$ are quadratic functions, each one representing a requirement to be satisfied. In our case we have:

$$\begin{gathered} f_1(\delta_k) = \left(\frac{|\overline{\Phi}_0(\delta_k) - \overline{\Phi}_1(\delta_k)|}{\pi/4} - \overline{K}^{opt} \right), \quad f_2(\delta_k) = \left(\frac{|\overline{\Omega}_0(\delta_k) - \overline{\Omega}_1(\delta_k)|}{\pi/4} - \overline{L}^{opt} \right), \\ f_3(\delta_k) = \left(\frac{\overline{\Omega}_1(\delta_k) - \overline{\Phi}_1(\delta_k)}{\pi/4} \right), \quad f_4(\delta_k) = \left(\frac{\overline{R}_0(\delta_k) - \overline{R}_0^{opt}}{R_0} \right), \quad f_5(\delta_k) = \left(\frac{\overline{R}_1(\delta_k) - \overline{R}_1^{opt}}{R_1} \right), \\ f_6(\delta_k) = \left(\frac{\overline{\Lambda}_0(\delta_k) - \overline{\Lambda}_0^{opt}}{\Lambda_0} \right), \quad f_7(\delta_k) = \left(\frac{\overline{\Lambda}_1(\delta_k) - \overline{\Lambda}_1^{opt}}{\Lambda_1} \right), \\ f_8(\delta_k) = \left(\frac{||\mathbf{B}(\delta_k)||}{||\mathbf{Q}||} \right) \ , \quad f_9(\delta_k) = \left(\frac{\overline{\Phi}_1(\delta_k) - \overline{\Phi}_1^{opt}}{\pi/4} \right), \end{gathered} \tag{8.3}$$

Hence, the problem (8.1) can be formulated as the search for an absolute minimum of the global objective function (8.2), composed by 9 positive semi-definite sub-objectives functions (8.3), each one satisfying one of the imposed requirements. In addition, the function $I(f_i(\delta_k))$ has a great advantage: being composed by the sum of semi-definite positive functions, its minimum is known *a priori*, it is zero. This aspect can help us in the identification of an absolute minimum.

8.2.2 Check on the first ply failure

Concerning the check on the first-ply-failure, the evaluation of $\max(\eta) = \max(F_{Hill}^{Ply})/F_{Hill}^{Lam}$ discussed in Sec. 6.4.1 and in the post-processing phase of Sec. 7.5, will be now, very helpful. After the structural optimisation step we have $F_{Hill}^{Lam} < 1$ everywhere, but the calculation of $\max(\eta)$ can lead to three different situations:

1. $\max(\eta) < 1 \Longrightarrow \max(F_{Hill}^{Ply}) < F_{Hill}^{Lam}$, therefore, we will have no limits to impose on the plies orientations when searching the stacking sequence;

2. $\max(\eta) = 1 \Longrightarrow$ at most $\max(F_{Hill}^{Ply}) = F_{Hill}^{Lam}$ and being $F_{Hill}^{Lam} < 1$ we can still consider all the possible plies orientations to determine the stacking sequence;

3. $\max(\eta) > 1 \Longrightarrow$ there are some orientations $(\Omega_1)_k$ such that $F_{Hill}^{Ply} > F_{Hill}^{Lam}$. In this case, we can evaluate the range of values of $(\Omega_1)_k$ such that $F_{Hill}^{Ply} > F_{Hill}^{Lam}$. We can have two different situations:

   - $F_{Hill}^{Ply}[(\Omega_1)_k] < 1 \Rightarrow$ even if the failure index of the ply is greater than that of the laminate, the first-ply-failure will not happen. We can define such a situation a "partially unsafe condition". In this case we can decide to include or not the values $(\Omega_1)_k$ among the admissible orientations. The range of values of Ω_1 such that $F_{Hill}^{Ply} > F_{Hill}^{Lam}$ can be calculated as follows:

$$\eta = \frac{4r^2\Gamma_0 + 8t^2\Gamma_1 + 4(-1)^L\Lambda_0 r^2\cos 4\left(\Omega_1 - \phi\right) + 16tr\Lambda_1\cos 2\left(\Omega_1 - \phi\right)}{F_{Hill}^{Lam}} \geq 1, \tag{8.4}$$

with

$$\cos 4\left(\Omega_1 - \phi\right) = 2\cos^2 2\left(\Omega_1 - \phi\right) - 1 \ , \tag{8.5}$$

so,

$$\begin{aligned} 8(-1)^L\Lambda_0 r^2\cos^2 2\left(\Omega_1 - \phi\right) + 16tr\Lambda_1\cos 2\left(\Omega_1 - \phi\right) + \\ +4r^2\Gamma_0 + 8t^2\Gamma_1 - 4(-1)^L\Lambda_0 r^2 - F_{Hill}^{Lam} \quad \geq 0, \end{aligned} \tag{8.6}$$

Eq. (8.6) represents a classical second degree inequality in terms of $\cos 2\left(\Omega_1 - \phi\right)$. If we set the constant term:

$$4r^2\Gamma_0 + 8t^2\Gamma_1 - 4(-1)^L\Lambda_0 r^2 - F_{Hill}^{Lam} = 8c \ , \tag{8.7}$$

and

$$\cos 2\left(\Omega_1 - \phi\right) = u \ , \tag{8.8}$$

eq. (8.6) becomes:

$$(-1)^L\Lambda_0 r^2 u^2 + 2tr\Lambda_1 u + c \geq 0 \ . \tag{8.9}$$

The solution of such an inequality will give us all values of Ω_1 that have to be removed from the solution space of problem (8.1).
The solution of (8.9) depends upon the sign of its discriminant

$$\Delta = t^2r^2\Lambda_1^2 - (-1)^L\Lambda_0 r^2 c \ , \tag{8.10}$$

and upon the shape of orthotropy described by the parameter L.

Let us start with the case $\Delta < 0$. This is a trivial case where for $L = 0$ eq. (8.9) is always verified; thus, problem (8.1) has no feasible solutions in terms of first ply failure. Whereas for $L = 1$ the situation is completely inverted: eq. (8.9) is never verified and the solution space of problem (8.1) can include all values of Ω_1.

Also the case $\Delta = 0$ is trivial. The root of the second order equation associated to the inequality (8.9) is:

$$u_1 = -(-1)^L \frac{t\Lambda_1}{\Lambda_0 r} \ . \tag{8.11}$$

that represents the limit condition for which $\eta = 1$. For $L = 0$ eq. (8.9) is always satisfied; thus, problem (8.1) has no feasible solutions in terms of first ply failure. Whereas, for $L = 1$ eq. (8.9) is satisfied by only one condition $u = u_1$; hence, the solution space of problem (8.1) can include all values of Ω_1.

Finally, let us consider the case $\Delta > 0$. The roots of the second order equation associated to the inequality (8.9) are:

$$\begin{aligned} u_1 &= -(-1)^L \frac{t}{r}\frac{\Lambda_1}{\Lambda_0} - \sqrt{\left(\frac{t}{r}\frac{\Lambda_1}{\Lambda_0}\right)^2 - \frac{(-1)^L c}{\Lambda_0 r^2}} \ , \\ u_2 &= -(-1)^L \frac{t}{r}\frac{\Lambda_1}{\Lambda_0} + \sqrt{\left(\frac{t}{r}\frac{\Lambda_1}{\Lambda_0}\right)^2 - \frac{(-1)^L c}{\Lambda_0 r^2}} \ , \end{aligned} \tag{8.12}$$

The range of solution varies with the value of L. In particular we have two sub-cases:

(a) $L = 0$, the solution is

$$u \le u_1 \text{ and } u \ge u_2 \ , \tag{8.13}$$

with $u_1 < u_2$. We have to consider also some particular cases:
1. $|u_1| \le 1$ and $|u_2| \le 1$, the solution is:

$$-1 \le u \le u_1 \text{ and } u_2 \le u \le 1 \ . \tag{8.14}$$

2. $|u_1| \ge 1$ and $|u_2| \le 1$, the solution is:

$$u_2 \le u \le 1 \ . \tag{8.15}$$

3. $|u_1| \le 1$ and $|u_2| \ge 1$, the solution is:

$$-1 \le u \le u_1 \ . \tag{8.16}$$

4. $u_1 \le -1$ and $u_2 \le -1$, the solution is:

$$-1 \le u \le 1 \ . \tag{8.17}$$

5. $u_1 \ge 1$ and $u_2 \ge 1$, the solution is:

$$-1 \le u \le 1 \ . \tag{8.18}$$

6. $u_1 \le -1$ and $u_2 \ge 1$, the solution does not exist.

(b) $L = 1$, the solution is

$$u_1 \le u \le u_2 \ , \tag{8.19}$$

with $u_1 < u_2$. Also here we have to consider some particular cases:
1. $|u_1| \le 1$ and $|u_2| \le 1$, the solution is:

$$u_1 \le u \le u_2 \ . \tag{8.20}$$

2. $|u_1| \geq 1$ and $|u_2| \leq 1$, the solution is:

$$-1 \leq u \leq u_2 \ . \tag{8.21}$$

3. $|u_1| \leq 1$ and $|u_2| \geq 1$, the solution is:

$$u_1 \leq u \leq 1 \ . \tag{8.22}$$

4. $u_1 \leq -1$ and $u_2 \leq -1$, the solution does not exist.

5. $u_1 \geq 1$ and $u_2 \geq 1$, the solution does not exist.

6. $u_1 \leq -1$ and $u_2 \geq 1$, the solution is:

$$-1 \leq u \leq 1 \ . \tag{8.23}$$

We remark that the value of the roots depend upon the ratios $\frac{t}{r}$ and $\frac{\Lambda_1}{\Lambda_0}$, i.e. upon the strain state and the anisotropy moduli. The sign of the roots depends only upon the sign of the spherical component of strains t. Moreover, also concerning this problem, we show that the shape of orthotropy, i.e. the value of L, can change completely the results.

All of these solutions give the range of the orthotropy orientations Ω_1 of the ply such that the failure index of the ply F_{Hill}^{Ply} is greater than the failure index of the laminate;

- $F_{Hill}^{Ply}[(\Omega_1)_k] \geq 1$: the firs-ply-failure happens; this situation represents an unsafe condition, we must exclude all the orientations $(\Omega_1)_k$ such that $F_{Hill}^{Ply} \geq 1$ among the admissible orientations when searching the stacking sequence. In this case, such values of $(\Omega_1)_k$ are still the solutions of the inequality (8.9) calculated beforehand, but now it is $c = 4r^2\Gamma_0 + 8t^2\Gamma_1 - 4(-1)^L\Lambda_0 r^2 - 1$.

Finally, we can assert that we are able to compare F_{Hill}^{Lam} and the maximum value of F_{Hill}^{Ply}, in order to check the first-ply-failure of plies and to determine the admissible range of orientations to exclude the failure of any ply. This last result will be used in the definition of the orientations search domain to determine the optimal stacking sequence.

A last remark: if we had expressed F_{Hill}^{Lam} and F_{Hill}^{Ply} in terms of stresses, such a comparison should not be possible. In fact, the variation of the stresses through the thickness of the laminate is not continuous, also in the case of pure membrane loading. In addition, the variation of stresses through the thickness depends upon the plies orientation, that are known only at the end of the lay-up design.

8.3 Resolution: using the genetic algorithm BIANCA

Eq. (8.2) represents a classical unconstrained minimum problem with 9 partial objective functions. Nevertheless, in the domain of ply orientations, eqs. (1.62) and (1.64), $I(f_i(\delta_k))$ is a highly non-convex function; hence, for the search of a solution, the use of a performing numerical strategy is of the greatest importance.

At this point we are faced to the following decision: which numerical strategy can be more advantageous when dealing with the unconstrained minimisation of a non-convex function?

As well known, the universal best optimisation algorithm does not exist: the choice of the best suited numerical strategy for the resolution of an optimum problem depends upon the problem itself. In the field of laminates lay-up design, methods inspired by heuristics have imposed, in this last decades, an almost complete supremacy. This is mainly due to their insensitivity to non-convexity and to the possibility of easy handling discrete design variables. So, we decided to use such a kind of strategy too; namely, thanks to the previous works on the matter [45–47], we decided to solve the second step problem using the Genetic Algorithm (GA) BIANCA (BIological ANalysis of Composite Assemblages), originally developed by Vincenti et al. [87] since 2002.

GAs present an approach to the search of minima of a function completely different from that of classical numerical methods like gradient-based algorithms, that need the evaluation of gradients and whose strategy depends upon the chosen starting point and, as a consequence, can fail reaching convergence to an absolute minimum when dealing with non-convex problems. Fundamentally, GAs replies, numerically, the Darwinian natural selection and the transmission of the genetic characters: they do not work on a single point, but on a set of possible solutions, called a population of individuals. The best individuals of a population are then selected in order to create a new generation of the offspring, see [18, 29]. The main advantages in using GAs are:

1. GAs work on a population of points, not on a single point, distributed over the whole design space. This fact improves the chance to reach an absolute minimum, though this cannot be mathematically ensured;

2. GAs are *zero-order* methods: they only require the evaluation of the objective function without other additional informations; namely, the knowledge of the derivatives of the objective is not needed, so, discrete variables can be easily handled.

The main components of a standard GA are:

- generation operator: it creates, usually by a random low, a starting population of N_{ind} individuals. Each individual represents a potential solution to the problem, it can be a scalar, a vector, and so on;

- evaluation operator: it evaluates the adaptation of each individual through an adaptation function, the *fitness*, that measures the quality of the individual as a solution of the problem;

- selection operator: using the value of the fitness function of each individual, it selects, by a given rule, N_{ind} individuals having a good fitness function; hence, the best individuals have a greater probability to be chosen for the following phase of reproduction;

- reproduction operator: it generates the new population starting from the set of parents chosen through the selection operator. The most common reproduction operators are the *cross-over* and *mutation* operators. The first one couples, randomly, two among the N_{ind} selected individuals, so creating the parent couples that will be crossed in order to generate the new couples of offspring. The second one, the mutation operator, acts in a random way, with a certain probability, mutating the genes of the new individuals and increasing, in this way, the biodiversity among the individuals of the population.

After the reproduction operator the new generation undergoes the selection operator and the iterative process restarts and prosecute until convergence. The convergence is achieved when a certain criterion is satisfied. Generally, the stop criterion corresponds to fixing the number of generations.

The main features of the GA BIANCA are described in [44, 87]. It has the classical operators of a standard GA along with new features concerning mainly the algebraic structure of the information and an Automatic Dynamic Penalisation (ADP) method for handling constraints of both the equality and inequality type, [44].

The generic individual of the GA BIANCA represents a solution, hence, in the framework of the present thesis it represents a stacking sequence of one finite element of the structure. Each individual, in a GA, is composed by a certain number of chromosomes. In this case, the genotype of the generic individual has n chromosomes representing, each one, one of the n plies composing the laminate. The chromosomes, in turn, are constituted by a certain number of genes, each one representing one optimisation variable of the k^{th} chromosome. In this case, each chromosome is characterised by only one gene representing the unique design variable: the ply orientation δ_k. If the ply thickness was also included among the optimisation variables, the number of genes would be increased to 2 and so on for taking into account other variables.

It is not the subject of this thesis to discuss about the characteristics of GAs; the reader is addressed to the scientific literature on this matter for a better description and discussion on the matter. Nevertheless, we want to remark again that these algorithms have proven to be very robust for handling problems of the type considered herein. Also, the experience previously made in the use of the GA BIANCA, on problems even more complicated than (8.2), has always been very satisfactory. So, this choice is really well motivated by the experience.

8.4 A numerical example

The problem of finding the stacking sequence of the generic element of the laminate has been solved using the GA BIANCA. On the other hand, thanks to the interface with external codes programmed in [44], the procedure has been automated interfacing the GA BIANCA with the MATLAB code. In particular the rule of the MATLAB code is to select automatically one element of the structure, pass to BIANCA the informations necessary to determine the stacking sequence, then get, from the code BIANCA, the resulting lay-up and finally store the informations. This procedure is automated in order to execute the procedure sequentially for all the elements of the structure.

We have chosen, as a demonstration of the effectiveness of the approach, to consider only the first example, the holed plate of Sec. 7.6.1, and in particular the anisotropy field obtained by the *a posteriori* optimisation algorithm, Sec. 7.2.

Concerning the settings of BIANCA to solve the second step problem we have imposed for all the elements:

- the ply orientations δ_k belong to $[-90°, 90°]$ with a discrete interval of $1°$. We can consider all the possible orientations because the $\max(F_{Hill}^{Lam})$ and the $\max(F_{Hill}^{Ply})$ of the generic ply are less than 1, see Tab. 7.5;

- the population size has been set to $\mathrm{N}_{ind} = 500$ and the maximum number of generations to $\mathrm{N}_{gen} = 500$;

- the crossover and mutation probability are $p_{cross} = 0.85$ and $p_{mut} = 1/N_{ind}$, respectively;
- selection is performed by the roulette-wheel strategy and the elitism operator is active.

Tabs. 8.1 and 8.2 show two examples of stacking sequences found using the GA BIANCA. We show the value of the partial objectives and the value of the global objective function $I(f_i(\delta_k))$. We remind that exact solutions correspond to the zeroes of the partial objective functions. In Tab. 8.1 we have considered an element of the plate characterised by fixed optimisation values of $\overline{R}_1$, $\overline{\Lambda}_{0L}$ and $\overline{\Lambda}_1$ and a free optimisation value of $\overline{R}_{0K}$. Such solution corresponds to the solution type 1 of the local minimisation of W_c, see Tab. 6.1. Therefore, we don't have imposed a given value of $\overline{R}_{0K}$ and the number of partial objective functions of eq. (8.3) pass from 9 to 8.

The example of Tab. 8.2 corresponds to an element of the plate presenting a fixed optimal value for each optimisation parameter, hence, in this case we have 9 partial objectives. In both these examples, the resulting laminate is uncoupled (the value of the corresponding partial function varies from 0.37×10^{-6} to 0.41×10^{-3}) and orthotropic (the value of the corresponding partial function is always about 10^{-7}). Similar considerations can be done for the other elements composing the plate structure, whose results are not shown here for the sake of brevity.

In Figs. 8.1 we show the optimal orientation of the first four plies composing the plate. The plate is composed by 30 plies (each elementary ply having a thickness of 0.125 mm). In Fig. 8.2 we map the value of the total objective function $I(f_i(\delta_k))$ for each element.

Thanks to the GA BIANCA, we determined the lay-up of every element composing the plate and being the plate composed by 1800 elements, we determined for 1800 different combinations of polar parameters, a lay-up satisfying all the different requirements in eq. (8.2).

	Given values	Partial obj. funct.
Uncoupling	$\mathbf{B} = 0$	$0.37E-06$
$\overline{R}_0$ [MPa]	any	-
$\overline{R}_1$ [MPa]	19909.481	$0.51E-02$
$\overline{\Lambda}_0$	628.713	$0.33E-03$
$\overline{\Lambda}_1$	2291.85	$0.21E-04$
$\overline{\Phi}_0 - \overline{\Phi}_1$	0	$0.12E-06$
$\overline{\Omega}_0 - \overline{\Omega}_1$	$\pi/2$	$0.12E-06$
$\overline{\Phi}_1 - \overline{\Omega}_1$	$\pi/2$	$0.12E-06$
Total obj. funct. $f(\delta_k) = 5 \times 10^{-3}$		
Sequence	2/1/4/-3/-3/2/0/-1/1/2/0/1/1/1/-2/ -10/-2/-2/-2/-2/0/0/4/4/3/3/0/-1/0/-2	

Table 8.1: Stacking sequence design, first example.

	Given values	Partial obj. funct.
Uncoupling	$\mathbf{B} = 0$	$0.41E-03$
$\overline{R}_0$ [MPa]	19710.431	$0.67E-04$
$\overline{R}_1$ [MPa]	8746.335	$0.34E-03$
$\overline{\Lambda}_0$	628.713	$0.11E-02$
$\overline{\Lambda}_1$	1998.75	$0.65E-04$
$\overline{\Phi}_0 - \overline{\Phi}_1$	0	$0.15E-06$
$\overline{\Omega}_0 - \overline{\Omega}_1$	$\pi/2$	$0.15E-06$
$\overline{\Phi}_1 - \overline{\Omega}_1$	$\pi/2$	$0.15E-06$
Total obj. funct. $f(\delta_k) = 2 \times 10^{-3}$		
Sequence	5/-90/5/3/-10/-6/89/5/3/-10/90/0/ -1/2/-90/1/-7/1/-90/89/2/89/-3/2/90/-90/1/2/-3/1	

Table 8.2: Stacking sequence design, second example.

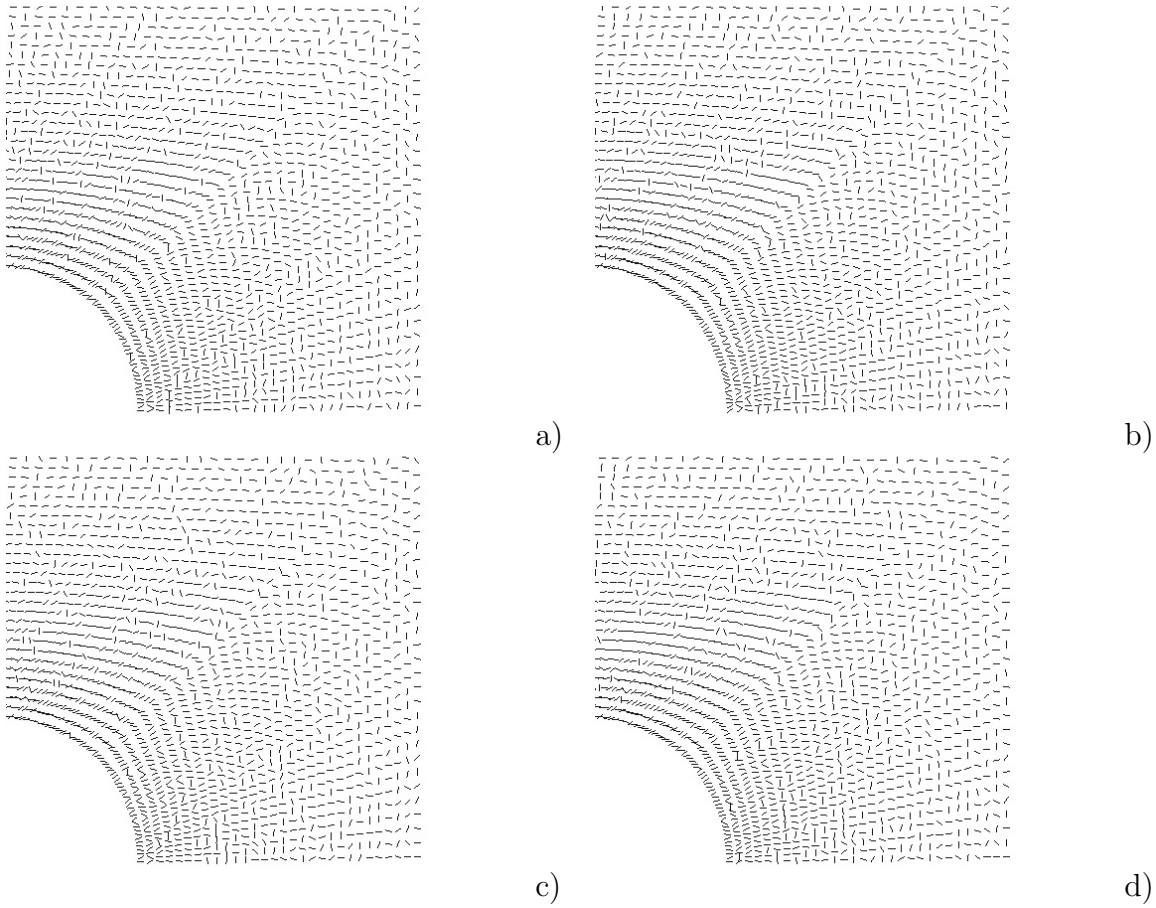

Figure 8.1: Optimal stacking sequence.

8.5 Concluding remarks

In this Chapter we dealt with the problem of determining the laminate stacking sequence satisfying the optimal distribution of material parameters issued from the first step of the hierarchical strategy. We formulated this problem as an optimisation problem of minimum

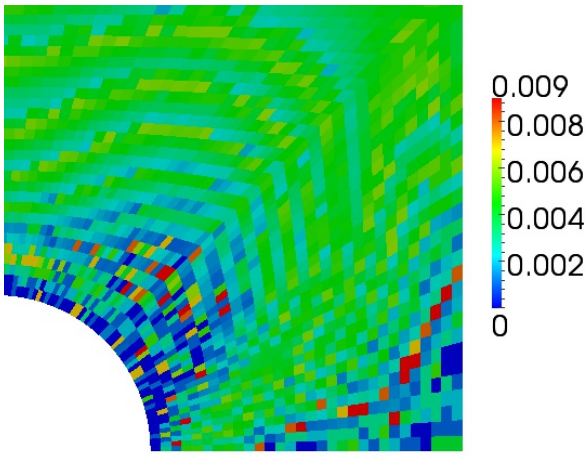

Figure 8.2: Distribution of the total objective function.

distance between the material parameters of the laminate solution and those issued from the structural optimisation step. In particular, this objective function is composed by nine positive semi-definite sub-objectives, each one linked to one material parameter of the homogenised structure, whose optimum value is calculated during the first step, Chapter 7. Due to the non-convexity of the objective function, we solved this optimisation problem by the genetic code BIANCA developed by Montemurro, Vincenti and Vannucci in [44] and used here in an automated procedure for the sequential solution of the lay-up problem for each one of the finite elements discretising the structure. We demonstrated, by a numerical example, the existence of stacking sequences satisfying a given local optimal distribution of anisotropy. In fact, being the optimal homogenised structure a variable stiffness and strength structure, we defined an optimal stacking sequence for every element belonging to the laminate. This was not evident in our procedure, and the fact that it is possible to find a lay-up corresponding to the set of optimal design variables, for each finite element in the discretised structural model is essentially due to three facts:

- the assumption of independent stiffness and strength parameters for the final laminated structure;
- the correct definition of the so called geometrical bounds on the polar parameters, for both stiffness and strength:
- the redundancy of the lay-up solutions, due to the non bijectivity between the mechanical behaviour of a laminate and the stacking sequences.

Concerning this last aspect, the redundancy, as already explained in Chapter 6, greatly increases with the number of plies. Just for giving an idea about that, when passing from 20 to 30 layers, the number of exact quasi-homogeneous solutions passes from 40 to 6146; the increase is not monotonic and the 29-ply case is rather spectacular: 45441 solutions, all of them unsymmetric, [82]. Nevertheless, though it is not possible to ensure *a priori* the existence of a solution to the lay-up problem, the probability of finding at least one solution to a give problem tends very quickly to 1 increasing the number of plies n. What can be said, however, is that, as we design a laminate for matching 8 independent invariants ($\overline{R}_0$, $\overline{R}_1$, $\overline{\Lambda}_0$, $\overline{\Lambda}_1$, $\overline{K}$, $\overline{L}$, $\widehat{R}_0$, $\widehat{R}_1$) at least 8 layers are necessary to find a solution.

In practical structural applications, with standard pre-pregs layers, the number of layers is generally greater than 8, say about 20 or much more. So, though it is not possible to prove the existence of a solution to the lay-up problem of the type considered in this thesis, the probability of finding at least one solution is very close to 1.

General conclusions and future perspectives

In this thesis we deal with the problem of determining the best distribution of the anisotropy for a laminated structure that has to be simultaneously the stiffest and the strongest one. The work has been divided into three main parts: in the first part we presented all the concepts and tools that we have used to develop the research, the second part is devoted to the analysis of strength and its maximisation for orthotropic sheets and, finally, in the third part we face the problem of designing a laminated structure to be optimal for both stiffness and strength.

Particularly, in the second part we have proposed a tensor invariant formulation, through the polar method, of four different polynomial failure criteria for orthotropic sheets. We have given also a mechanical interpretation of the polar parameters with respect to the strength properties and material symmetries of the sheet. Then, we considered the problem of determining the optimal material orientation to maximise strength by the minimisation of the failure index. Thanks to the polar formalism, we presented a general analytical solution whose formulation is valid for different criteria that can be expressed, indifferently, in terms of stresses or strains. With this study we have shown that the type of orthotropy, characterised by the polar parameter L, plays a decisive role in the optimisation of strength and that, depending on the values of the stresses or strains and of the polar parameters of the failure criteria, the optimal orientation of the material that maximises strength can be equal to different from that maximising stiffness. This means that it is possible to obtain, in some cases, an orthotropic plate that is simultaneously optimised with respect to two important engineering requirements, stiffness and strength.

The last part of the thesis is dedicated to the development of a new strategy to solve a non conventional problem: the simultaneous optimisation of stiffness and strength for a laminated structure. Our aim concerned the optimisation of the anisotropy distribution of a variable stiffness laminated structure whose geometry and boundary conditions are given. In this part of the thesis we proved that we are able to state and to solve such a problem. Our approach is inspired from an already existing *hierarchical strategy* for the only stiffness maximisation.

First of all we defined *a new laminate level failure criterion* valid for an equivalent homogenised plate. Then, conscious of having two functional, the complementary energy and the laminate failure index, to be minimised at the same time, we have proved that the first step of the hierarchical strategy, where the laminate is modelled as an equivalent homogenised single-layer, can be alternatively stated as two problems taking into account for both stiffness and strength maximisation. These problems are characterised by *two functional* that are sequentially minimised, preserving only the orthotropy direction. Each problem has a different leading objective: stiffness or strength.

In order to face the first step of the strategy we developed three different algorithms to determine the optimal distribution of material parameters for a given structure. In the first algorithm, called *a posteriori*, the stiffness is the leading objective and in the other two, called *a priori*, the strength is the leading objective. We also found an analytical solution to the problem of minimising the strength functional with respect to the material parameters and an important result has been obtained: *when the tensors of stress and strain are coaxial, the optimal solution given by the algorithms represents a real global optimum for both stiffness and strength properties.* For instance, in the presented test cases the optimal solutions achieved by the two algorithms, *a posteriori* and second version of the algorithm *a priori*, correspond to the particular case of coaxiality between the stress and strain fields, hence, in terms of both stiffness and strength properties we obtain a global optimal solution. Moreover the test cases showed that we can achieve an average reduction of about 50 % for the global complementary energy and an average reduction of about 70 % for the local laminate failure index with respect to the starting configuration. The structural optimisation procedure here proposed, is not time consuming: the longest computational time for the most difficult case takes about 40 minutes on an Intel® *i*5 Dual Core 2.5GHz processor.

Finally, using the genetic code BIANCA, we dealt with the problem of determining the laminate stacking sequence satisfying the optimal distribution of material parameters issued from the first step of the hierarchical strategy. In particular, the solution space of ply orientations can vary in order to exclude the first-ply-failure. We demonstrated, by a numerical example, the existence of stacking sequences satisfying a given local optimal distribution of anisotropic stiffness and strength fields.

The true objective of this thesis was, we have seen, to propose a new approach to the design of laminated structures having a variable anisotropy. So, we have chosen to concentrate our efforts on giving an as much as possible mathematically rigorous procedure, not based upon simplifying but polluting assumptions and in showing that such a procedure, conciliating stiffness and strength as design objectives, is truly possible.

Nevertheless, we are perfectly conscious that in doing this, we have left apart some points that should be developed in future works for, on one side, to fill the gap towards practical applications and, on the other side, to improve the scientific quality of the results found herein.

Some points should be, to our opinion, investigated in the next future, let us briefly list them:

- the only failure criterion used in this thesis for developing the optimisation strategy of the laminates has been the Tsai-Hill one but other criteria, namely those presented in Chapters 4 and 5, should also be considered; the global procedure is not affected by a change of the criterion, nevertheless this needs a particular attention in the theoretical developments given in Chapter 6, because the presence, in criteria like those of Hoffmann or Tsai-Wu, of a linear term besides the quadratic one gives supplementary terms in the expression of the failure index for both the ply and the laminate;

- all the developments have been done for the only case of simple in-plane actions; the case of a pure bending state should also be considered, and this should not imply substantial modifications to the procedure; more complicate, is the case of contemporary in-plane and bending actions, because in such a case it is not possible to define analytically the bounds on the polar components for the laminate; actually,

this is still an open problem in laminates design, also when the description of the behaviour is not done by the polar formalism;

- all the numerical tests done with the first version of the algorithm *a priori* have clearly shown, without exception, that such a procedure gives an alternate convergence, for both the complementary energy and the failure index, towards a minimum; nevertheless, a convergence proof for this algorithm is still lacking and it should be studied in the future;

- considering the numerical results, we can formulate a conjecture, that should be proved: the structural optimisation with the *a posteriori* algorithm leads to the same overall optimal values of the complementary energy and of the highest failure index than those obtained with the *a priori* algorithm, version 2, see Tabs. 7.5, 7.6 and 7.7; nevertheless, the solution, i.e. the optimal distribution of the anisotropy, is not necessarily the same for the two cases; in other words, the optimal solution is not unique and probably, as it often happens with anisotropic problems, there are infinitely many solutions, continuously varying;

- this coincidence of results for the two algorithms disappears when the difference of strength in tension and compression is taken into account, Tab. 7.7 and 7.8; seemingly, this is due to the same structure of the Tsai-Hill failure index functional, quite similar to that of the complementary energy; this is a key point to prove, probably, the above conjecture, and at the same time the fact that when difference of strength in tension and compression is introduced in the calculations, the coincidence of the optimal final values for the *a posteriori* and *a priori*, version 2, algorithms, do not coincide any more; all these facts should, of course, be mathematically proved;

- the results of the optimisation procedure give n fields of orientations for the laminate, a field for each one of the n layers; nevertheless, we have not considered in this study an important point, necessary to ensure the results, found with the optimisation procedure, to be actually interesting from a practical point of view; namely, the orientation of the fibers cannot vary, locally, more than some giving technological limits; such a constraint should be taken into account, for obtaining a really manufacturable laminate; no general solutions exist in the literature to our knowledge, and actually this problem is particularly hard to be solved; in practice, it should be seen, to our opinion, as another optimum problem, where the distances between n fields of orientations, taking into account for technological constraints on their variation, and n fields of target, optimal orientations, are to be minimised; in addition, some constraints are to be satisfied for the whole laminate, namely on bending-extension uncoupling, orthotropy and so on; this problem is rather complicate but more important, and this point confers to it a strange mathematical character, the *n target fields are not fixed*; in fact, what is to be ensured are the fields of stiffness and strength properties, while, as already said, their is not a unique set of n orientation fields realising the optimal laminate; so, the n target fields can vary and this renders the problem of finding n technologically interesting orientation fields rather complicate, though not impossible; to our opinion, this is another genuine optimisation problem, that should be considered apart, why not in another thesis;

- as already said, we have wanted to deal with the optimum problem in the most

general way, without making use of some practical rules often used by laminates designers; some of these rules are imposed in aircraft structural design, and they can be very easily inserted in the procedure; actually, they concern only the second step of the design procedure, the lay-up design, and the code BIANCA accepts all the types of constraints on the staking sequence design (symmetric and/or balanced stacks, quasi-isotropic sequences and so on), what has been already done in previous works, for instance in the thesis of M. Montemurro.

The points listed above could, hopefully, improve the results found in this thesis; we hope only that the way we have traced in this work can constitute, in the future, a valuable tool for the optimal design of advanced laminated structures.

Appendix A

Analytical solution for minimum laminate failure index

A.1 First problem: fixed orthotropy orientation

The optimisation problem can be formalised as:

$$\min_{\left\{\overline{\Lambda}_{0L},\overline{\Lambda}_1\right\}} F_{Hill}^{Lam}\left(\overline{\Lambda}_{0L},\overline{\Lambda}_1,\overline{\Phi}_1^{opt}\right) \ , \tag{A.1}$$

with:

$$\begin{cases} 2\left(\dfrac{\overline{\Lambda}_1}{\Lambda_1}\right)^2 - 1 \leq \dfrac{\overline{\Lambda}_{0L}}{(-1)^L\Lambda_0} \ , \\ |\overline{\Lambda}_{0L}| \leq \Lambda_0 \ , \\ \overline{\Lambda}_1 \geq 0 \ . \end{cases} \tag{A.2}$$

and

$$\overline{\Omega}_1 = \begin{cases} \overline{\Phi}_1^{opt} & \text{or} \\ \overline{\Phi}_1^{opt} + \pi/2 \ . \end{cases} \tag{A.3}$$

The extended expression of the objective function is

$$F_{Hill}^{Lam} = 4r^2\Gamma_0 + 8t^2\Gamma_1 + 4\overline{\Lambda}_{0L}r^2\cos 4\left(\overline{\Omega}_1 - \phi\right) + 16tr\overline{\Lambda}_1\cos 2\left(\overline{\Omega}_1 - \phi\right) \ , \tag{A.4}$$

First of all, we have to consider an important case: the spherical strain field, characterised by $r = 0$. If we impose $r = 0$ in eq. (A.4), the two optimisation parameters are no longer present in the equation of F_{Hill}^{Lam}. This means that, for a spherical strain field, any value of $\overline{\Lambda}_{0L}$ and $\overline{\Lambda}_1$ within the admissible design region can be optimal for the failure index functional. From a mechanical point of view this means that when the strain field is purely spherical, we can place the fibres, of the corresponding laminate, in any direction and we will have still an optimal solution in terms of strength. Hence, now we consider $r \neq 0$. The two partial derivatives of F_{Hill}^{Lam} with respect to $\overline{\Lambda}_{0L}$ and $\overline{\Lambda}_1$ are:

$$\begin{aligned} \frac{\partial F_{Hill}^{Lam}}{\partial\overline{\Lambda}_{0L}} &= 4r^2\cos 4(\overline{\Omega}_1 - \phi) \ , \\ \frac{\partial F_{Hill}^{Lam}}{\partial\overline{\Lambda}_1} &= 16tr\cos 2(\overline{\Omega}_1 - \phi) \ . \end{aligned} \tag{A.5}$$

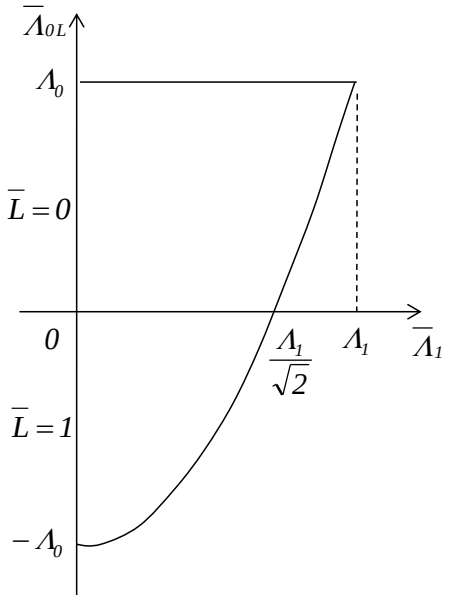

Figure A.1: Admissible domain of $\overline{\Lambda}_{0L}$ and $\overline{\Lambda}_1$ for $L = 0$.

Both derivatives are constants for a fixed strain field. F_{Hill}^{Lam} is a linear function of $\overline{\Lambda}_{0L}$ and $\overline{\Lambda}_1$. Therefore, the minimum value of F_{Hill}^{Lam} necessarily lies on the boundary of the domain defined in the plane $(\overline{\Lambda}_{0L}, \overline{\Lambda}_1)$ by eqs. (A.2), see Figs. A.1 and A.2. In addition, the area of admissible values of $\overline{\Lambda}_{0L}$ and $\overline{\Lambda}_1$ changes together with the value of the orthotropy shape parameter L of the basic ply, see eq. (A.2). Moreover, the sign of the partial derivatives (A.5) depends upon the signs of $\cos 4\left(\overline{\Omega}_1 - \phi\right)$ and $\cos 2\left(\overline{\Omega}_1 - \phi\right)$, Fig. 7.4, and upon the sign of t, the spherical part of strains.

Solution for a basic ply with $L = 0$

As the solution depends upon the sign of t, $\cos 4\left(\overline{\Omega}_1 - \phi\right)$ and $\cos 2\left(\overline{\Omega}_1 - \phi\right)$, we start our analysis by considering the case

1. Solution with $t > 0$;

   - $\left(\overline{\Omega}_1 - \phi\right) \in \left]-\frac{\pi}{8}, \frac{\pi}{8}\right[$

     In this case we have:

     $$\begin{cases} \cos 4\left(\overline{\Omega}_1 - \phi\right) > 0 , \\ \cos 2\left(\overline{\Omega}_1 - \phi\right) > 0 ; \end{cases} \tag{A.6}$$

     so,

     $$\frac{\partial F_{Hill}^{Lam}}{\partial \overline{\Lambda}_{0L}} > 0, \ \frac{\partial F_{Hill}^{Lam}}{\partial \overline{\Lambda}_1} > 0 \ . \tag{A.7}$$

     The two design variables $\overline{\Lambda}_{0L}$ and $\overline{\Lambda}_1$ being independent, the point corresponding to the minimum of F_{Hill}^{Lam} is placed where $\overline{\Lambda}_{0L}$ and $\overline{\Lambda}_1$ get their lowest admissible value:

     $$\begin{aligned} \overline{\Lambda}_{0L}^{opt} &= -\Lambda_0, \\ \overline{\Lambda}_1^{opt} &= 0 \ . \end{aligned} \tag{A.8}$$

     The objective function takes, thus, the following value:

     $$F_{Hill}^{Lam} = 4r^2\Gamma_0 + 8t^2\Gamma_1 - 4\Lambda_0 r^2 \cos 4\left(\overline{\Omega}_1 - \phi\right) \ . \tag{A.9}$$

- $\left(\overline{\Omega}_1 - \phi\right) \in \left]-\frac{\pi}{4}, -\frac{\pi}{8}\right[\cup \left]\frac{\pi}{8}, \frac{\pi}{4}\right[$

  The procedure to calculate the optimal values of the optimisation variables is identical to that of the previous case.

$$\left\{ \begin{array}{ll} \cos 4\left(\overline{\Omega}_1 - \phi\right) & < 0 \ , \\ \cos 2\left(\overline{\Omega}_1 - \phi\right) & > 0 \ ; \end{array} \right. \Rightarrow \left\{ \begin{array}{l} \overline{\Lambda}_{0L}^{opt} = \Lambda_0 \ , \\ \overline{\Lambda}_1^{opt} = 0 \ . \end{array} \right. \tag{A.10}$$

  The objective function assumes the following shape:

$$F_{Hill}^{Lam} = 4r^2\Gamma_0 + 8t^2\Gamma_1 + 4\Lambda_0 r^2 \cos 4\left(\overline{\Omega}_1 - \phi\right) \ . \tag{A.11}$$

- $\left(\overline{\Omega}_1 - \phi\right) \in \left]-\frac{3\pi}{8}, -\frac{\pi}{4}\right[\cup \left]\frac{\pi}{4}, \frac{3\pi}{8}\right[$

$$\left\{ \begin{array}{ll} \cos 4\left(\overline{\Omega}_1 - \phi\right) & < 0 \ , \\ \cos 2\left(\overline{\Omega}_1 - \phi\right) & < 0 \ ; \end{array} \right. \Rightarrow \left\{ \begin{array}{l} \overline{\Lambda}_{0L}^{opt} = \Lambda_0 \ , \\ \overline{\Lambda}_1^{opt} = \Lambda_1 \ ; \end{array} \right. \tag{A.12}$$

  and

$$F_{Hill}^{Lam} = 4r^2\Gamma_0 + 8t^2\Gamma_1 + 4\Lambda_0 r^2 \cos 4\left(\overline{\Omega}_1 - \phi\right) + 16tr\Lambda_1 \cos 2\left(\overline{\Omega}_1 - \phi\right) \ . \tag{A.13}$$

- $\left(\overline{\Omega}_1 - \phi\right) \in \left]-\frac{\pi}{2}, -\frac{3\pi}{8}\right[\cup \left]\frac{3\pi}{8}, \frac{\pi}{2}\right[$

$$\left\{ \begin{array}{ll} \cos 4\left(\overline{\Omega}_1 - \phi\right) & > 0 \ , \\ \cos 2\left(\overline{\Omega}_1 - \phi\right) & < 0 \ . \end{array} \right. \tag{A.14}$$

  and we have

$$\frac{\partial F_{Hill}^{Lam}}{\partial \overline{\Lambda}_{0L}} > 0 \ . \tag{A.15}$$

  For a fixed $\overline{\Lambda}_1$ the optimum value of $\overline{\Lambda}_{0L}$ is placed where it gets its lowest admissible value, hence, on the parabola, see Fig. A.1. We can explicitly write $\overline{\Lambda}_{0L}$ in the equation of the parabola

$$\overline{\Lambda}_{0L} = \Lambda_0 \left(2\frac{\overline{\Lambda}_1^2}{\Lambda_1^2} - 1 \right) \ , \tag{A.16}$$

  and replace it in eq. (A.4) of the objective function,

$$\begin{aligned} F_{Hill}^{Lam} = \ & 4r^2\Gamma_0 + 8t^2\Gamma_1 + 4r^2 \cos 4\left(\overline{\Omega}_1 - \phi\right) \Lambda_0 \left(2\frac{\overline{\Lambda}_1^2}{\Lambda_1^2} - 1 \right) + \\ & + 16tr\overline{\Lambda}_1 \cos 2\left(\overline{\Omega}_1 - \phi\right) \ . \end{aligned} \tag{A.17}$$

  We can derive F_{Hill}^{Lam} with respect to $\overline{\Lambda}_1$:

$$\frac{\partial F_{Hill}^{Lam}}{\partial \overline{\Lambda}_1} = 16r^2 \frac{\overline{\Lambda}_1}{\Lambda_1^2} \Lambda_0 \cos 4\left(\overline{\Omega}_1 - \phi\right) + 16tr \cos 2\left(\overline{\Omega}_1 - \phi\right) \ . \tag{A.18}$$

  The stationary value of $\overline{\Lambda}_1$ can be calculated imposing

$$\frac{\partial F_{Hill}^{Lam}}{\partial \overline{\Lambda}_1} = 0 \text{ for } \overline{\Lambda}_1^{stat} = \frac{t|\cos 2\left(\overline{\Omega}_1 - \phi\right)|\Lambda_1^2}{r\Lambda_0 \cos 4\left(\overline{\Omega}_1 - \phi\right)} \ . \tag{A.19}$$

In addition

$$\frac{\partial^2 F_{Hill}^{Lam}}{\partial \overline{\Lambda}_1^2} = \frac{16r^2}{\Lambda_1^2}\Lambda_0 \cos 4\left(\overline{\Omega}_1 - \phi\right) \geq 0, \ \forall\ \overline{\Lambda}_1; \tag{A.20}$$

so,

$$\overline{\Lambda}_1^{stat} = \overline{\Lambda}_1^{opt}\ . \tag{A.21}$$

This value of $\overline{\Lambda}_1$ corresponds, on the parabola, to

$$\overline{\Lambda}_{0L}^{opt} = \left(\frac{2t^2 \cos^2 2\left(\overline{\Omega}_1 - \phi\right)\Lambda_1^2}{r^2 \cos^2 4\left(\overline{\Omega}_1 - \phi\right)\Lambda_0^2} - 1\right)\Lambda_0. \tag{A.22}$$

In order to respect the bounds on $\overline{\Lambda}_1$, eq. (A.2), this solution is valid for

$$\frac{t}{r} \leq \frac{\Lambda_0 \cos 4\left(\overline{\Omega}_1 - \phi\right)}{\Lambda_1 |\cos 2\left(\overline{\Omega}_1 - \phi\right)|}, \tag{A.23}$$

and the objective function assumes the following shape:

$$F_{Hill}^{Lam} = \ 4r^2\Gamma_0 + 8t^2\Gamma_1 + 24\frac{t^2 \cos^2 2\left(\overline{\Omega}_1 - \phi\right)\Lambda_1^2}{\Lambda_0 \cos 4\left(\overline{\Omega}_1 - \phi\right)} - 4r^2\Lambda_0 \cos 4\left(\overline{\Omega}_1 - \phi\right)\ . \tag{A.24}$$

Otherwise, for $\dfrac{t}{r} \geq \dfrac{\Lambda_0 \cos 4\left(\overline{\Omega}_1 - \phi\right)}{\Lambda_1 |\cos 2\left(\overline{\Omega}_1 - \phi\right)|}$, we have

$$\begin{array}{l} \overline{\Lambda}_{0L}^{opt} = \Lambda_0, \\ \overline{\Lambda}_1^{opt} = \Lambda_1\ . \end{array} \tag{A.25}$$

In this case, the objective function is:

$$F_{Hill}^{Lam} = 4r^2\Gamma_0 + 8t^2\Gamma_1 + 4\Lambda_0 r^2 \cos 4\left(\overline{\Omega}_1 - \phi\right) + 16tr\Lambda_1 cos2\left(\overline{\Omega}_1 - \phi\right)\ . \tag{A.26}$$

- $\left(\overline{\Omega}_1 - \phi\right) = \pm\dfrac{\pi}{8}$

$$\left\{ \begin{array}{rcl} \cos 4\left(\overline{\Omega}_1 - \phi\right) & = & 0\ , \\ \cos 2\left(\overline{\Omega}_1 - \phi\right) & > & 0\ ; \end{array} \right. \Rightarrow \left\{ \begin{array}{l} \overline{\Lambda}_{0L}^{opt} \in [-\Lambda_0, \Lambda_0]\,, \\ \overline{\Lambda}_1^{opt} = 0\ ; \end{array} \right. \tag{A.27}$$

$$F_{Hill}^{Lam} = 4r^2\Gamma_0 + 8t^2\Gamma_1\ . \tag{A.28}$$

- $\left(\overline{\Omega}_1 - \phi\right) = \dfrac{3\pi}{8}$

$$\left\{ \begin{array}{rcl} \cos 4\left(\overline{\Omega}_1 - \phi\right) & = & 0\ , \\ \cos 2\left(\overline{\Omega}_1 - \phi\right) & < & 0\ ; \end{array} \right. \Rightarrow \left\{ \begin{array}{l} \overline{\Lambda}_{0L}^{opt} = \Lambda_0\ , \\ \overline{\Lambda}_1^{opt} = \Lambda_1\ ; \end{array} \right. \tag{A.29}$$

$$F_{Hill}^{Lam} = 4r^2\Gamma_0 + 8t^2\Gamma_1 + 16tr\Lambda_1 \cos 2\left(\overline{\Omega}_1 - \phi\right)\ . \tag{A.30}$$

- $\left(\overline{\Omega}_1 - \phi\right) = \pm\dfrac{\pi}{4}$

$$\left\{ \begin{array}{rcl} \cos 4\left(\overline{\Omega}_1 - \phi\right) & < & 0\ , \\ \cos 2\left(\overline{\Omega}_1 - \phi\right) & = & 0\ . \end{array} \right. \Rightarrow \left\{ \begin{array}{l} \overline{\Lambda}_{0L}^{opt} = \Lambda_0\ , \\ \overline{\Lambda}_1^{opt} \in [0, \Lambda_1]\ ; \end{array} \right. \tag{A.31}$$

$$F_{Hill}^{Lam} = 4r^2\Gamma_0 + 8t^2\Gamma_1 + 4\Lambda_0 r^2 \cos 4\left(\overline{\Omega}_1 - \phi\right)\ . \tag{A.32}$$

2. Solution with $t = 0$.
In this case $\overline{\Lambda}_1$ vanishes from the equation of the objective function, hence, we have only to find the optimum value of $\overline{\Lambda}_{0L}$.

- $\left(\overline{\Omega}_1 - \phi\right) \in \left]-\frac{\pi}{2}, -\frac{3\pi}{8}\right[\cup \left]-\frac{\pi}{8}, \frac{\pi}{8}\right[\cup \left]\frac{3\pi}{8}, \frac{\pi}{2}\right[$

$$\cos 4\left(\overline{\Omega}_1 - \phi\right) > 0 \Rightarrow \begin{cases} \overline{\Lambda}_{0L}^{opt} = -\Lambda_0 \ , \\ \overline{\Lambda}_1^{opt} = 0 \ ; \end{cases} \tag{A.33}$$

and

$$F_{Hill}^{Lam} = 4r^2\Gamma_0 + 8t^2\Gamma_1 - 4\Lambda_0 r^2 \cos 4\left(\overline{\Omega}_1 - \phi\right) \ . \tag{A.34}$$

- $\left(\overline{\Omega}_1 - \phi\right) \in \left]-\frac{3\pi}{8}, -\frac{\pi}{8}\right[\cup \left]\frac{\pi}{8}, \frac{3\pi}{8}\right[$

$$\cos 4\left(\overline{\Omega}_1 - \phi\right) < 0 \Rightarrow \begin{cases} \overline{\Lambda}_{0L}^{opt} = \Lambda_0 \ , \\ \overline{\Lambda}_1^{opt} \in [0, \Lambda_1] \, ; \end{cases} \tag{A.35}$$

and

$$F_{Hill}^{Lam} = 4r^2\Gamma_0 + 8t^2\Gamma_1 + 4\Lambda_0 r^2 \cos 4\left(\overline{\Omega}_1 - \phi\right) \ . \tag{A.36}$$

- $\left(\overline{\Omega}_1 - \phi\right) = \pm\frac{3\pi}{8}, \pm\frac{\pi}{8},$

$$\cos 4\left(\overline{\Omega}_1 - \phi\right) = 0 \Rightarrow \begin{cases} \overline{\Lambda}_{0L}^{opt} \text{ any} \ , \\ \overline{\Lambda}_1^{opt} \text{ any} \ ; \end{cases} \tag{A.37}$$

belonging to the admissible domain of Fig. A.1.

$$F_{Hill}^{Lam} = 4r^2\Gamma_0 + 8t^2\Gamma_1 \ , \tag{A.38}$$

so, the anisotropic distribution of strength does not take part to the optimal distribution of strength.

3. Solution with $t < 0$.

- $\left(\overline{\Omega}_1 - \phi\right) \in \left]-\frac{\pi}{8}, \frac{\pi}{8}\right[$

$$\begin{cases} \cos 4\left(\overline{\Omega}_1 - \phi\right) > 0 \ , \\ \cos 2\left(\overline{\Omega}_1 - \phi\right) > 0 \ . \end{cases} \Rightarrow \tag{A.39}$$

$$\begin{cases} \overline{\Lambda}_{0L}^{opt} = \left(\dfrac{2t^2 \cos^2 2\left(\overline{\Omega}_1 - \phi\right)\Lambda_1^2}{r^2 \cos^2 4\left(\overline{\Omega}_1 - \phi\right)\Lambda_0^2} - 1\right)\Lambda_0 \ , \\ \overline{\Lambda}_1^{opt} = \dfrac{|t| \cos 2\left(\overline{\Omega}_1 - \phi\right)\Lambda_1^2}{r\Lambda_0 \cos 4\left(\overline{\Omega}_1 - \phi\right)} \ . \end{cases} \quad \text{for } \frac{|t|}{r} < \frac{\Lambda_0 \cos 4\left(\overline{\Omega}_1 - \phi\right)}{\Lambda_1 \cos 2\left(\overline{\Omega}_1 - \phi\right)} \tag{A.40}$$

and

$$F_{Hill}^{Lam} = 4r^2\Gamma_0 + 8t^2\Gamma_1 + 24\frac{t^2 \cos^2 2\left(\overline{\Omega}_1 - \phi\right)\Lambda_1^2}{\Lambda_0 \cos 4\left(\overline{\Omega}_1 - \phi\right)} - 4r^2\Lambda_0 \cos 4\left(\overline{\Omega}_1 - \phi\right) \ . \tag{A.41}$$

Otherwise

$$\left\{ \begin{array}{l} \overline{\Lambda}_{0L}^{opt} = \Lambda_0 \ , \\ \overline{\Lambda}_1^{opt} = \Lambda_1 \ . \end{array} \right. \text{ for } \frac{|t|}{r} \geq \frac{\Lambda_0 \cos 4\left(\overline{\Omega}_1 - \phi\right)}{\Lambda_1 \cos 2\left(\overline{\Omega}_1 - \phi\right)} \tag{A.42}$$

and

$$F_{Hill}^{Lam} = 4r^2\Gamma_0 + 8t^2\Gamma_1 + 4\Lambda_0 r^2 \cos 4\left(\overline{\Omega}_1 - \phi\right) + 16tr\Lambda_1 \cos 2\left(\overline{\Omega}_1 - \phi\right) \ . \tag{A.43}$$

- $\left(\overline{\Omega}_1 - \phi\right) \in \ \left]-\frac{\pi}{4}, -\frac{\pi}{8}\right[\ \cup \ \left]\frac{\pi}{8}, \frac{\pi}{4}\right[$

$$\left\{ \begin{array}{l} \cos 4\left(\overline{\Omega}_1 - \phi\right) \ < \ 0 \ , \\ \cos 2\left(\overline{\Omega}_1 - \phi\right) \ > \ 0 \ ; \end{array} \right. \Rightarrow \left\{ \begin{array}{l} \overline{\Lambda}_{0L}^{opt} = \Lambda_0 \ , \\ \overline{\Lambda}_1^{opt} = \Lambda_1 \ ; \end{array} \right. \tag{A.44}$$

and

$$F_{Hill}^{Lam} = 4r^2\Gamma_0 + 8t^2\Gamma_1 + 4\Lambda_0 r^2 \cos 4\left(\overline{\Omega}_1 - \phi\right) + 16tr\Lambda_1 \cos 2\left(\overline{\Omega}_1 - \phi\right) \ . \tag{A.45}$$

- $\left(\overline{\Omega}_1 - \phi\right) \in \ \left]-\frac{3\pi}{8}, -\frac{\pi}{4}\right[\ \cup \ \left]\frac{\pi}{4}, \frac{3\pi}{8}\right[$

$$\left\{ \begin{array}{l} \cos 4\left(\overline{\Omega}_1 - \phi\right) \ < \ 0 \ , \\ \cos 2\left(\overline{\Omega}_1 - \phi\right) \ < \ 0 \ ; \end{array} \right. \Rightarrow \left\{ \begin{array}{l} \overline{\Lambda}_{0L}^{opt} = \Lambda_0 \ , \\ \overline{\Lambda}_1^{opt} = 0 \ ; \end{array} \right. \tag{A.46}$$

and

$$F_{Hill}^{Lam} = 4r^2\Gamma_0 + 8t^2\Gamma_1 + 4\Lambda_0 r^2 \cos 4\left(\overline{\Omega}_1 - \phi\right) \ . \tag{A.47}$$

- $\left(\overline{\Omega}_1 - \phi\right) \in \left]-\frac{\pi}{2}, -\frac{3\pi}{8}\right[\ \cup \ \left]\frac{3\pi}{8}, \frac{\pi}{2}\right[,$

$$\left\{ \begin{array}{l} \cos 4\left(\overline{\Omega}_1 - \phi\right) \ > \ 0 \ , \\ \cos 2\left(\overline{\Omega}_1 - \phi\right) \ < \ 0 \ ; \end{array} \right. \Rightarrow \left\{ \begin{array}{l} \overline{\Lambda}_{0L}^{opt} = -\Lambda_0 \ , \\ \overline{\Lambda}_1^{opt} = 0 \ ; \end{array} \right. \tag{A.48}$$

and

$$F_{Hill}^{Lam} = 4r^2\Gamma_0 + 8t^2\Gamma_1 - 4\Lambda_0 r^2 \cos 4\left(\overline{\Omega}_1 - \phi\right) \ . \tag{A.49}$$

- $\left(\overline{\Omega}_1 - \phi\right) = \pm\frac{\pi}{8}$

$$\left\{ \begin{array}{l} \cos 4\left(\overline{\Omega}_1 - \phi\right) \ = \ 0 \ , \\ \cos 2\left(\overline{\Omega}_1 - \phi\right) \ > \ 0 \ ; \end{array} \right. \Rightarrow \left\{ \begin{array}{l} \overline{\Lambda}_{0L}^{opt} = \Lambda_0 \ , \\ \overline{\Lambda}_1^{opt} = \Lambda_1 \ ; \end{array} \right. \tag{A.50}$$

and

$$F_{Hill}^{Lam} = 4r^2\Gamma_0 + 8t^2\Gamma_1 + 16tr\Lambda_1 \cos 2\left(\overline{\Omega}_1 - \phi\right) \ . \tag{A.51}$$

- $\left(\overline{\Omega}_1 - \phi\right) = \pm\frac{3\pi}{8}$

$$\left\{ \begin{array}{l} \cos 4\left(\overline{\Omega}_1 - \phi\right) \ = \ 0 \ , \\ \cos 2\left(\overline{\Omega}_1 - \phi\right) \ < \ 0 \ ; \end{array} \right. \Rightarrow \left\{ \begin{array}{l} \overline{\Lambda}_{0L}^{opt} \in [-\Lambda_0, \Lambda_0] \ , \\ \overline{\Lambda}_1^{opt} = 0 \ ; \end{array} \right. \tag{A.52}$$

and

$$F_{Hill}^{Lam} = 4r^2\Gamma_0 + 8t^2\Gamma_1 \ . \tag{A.53}$$

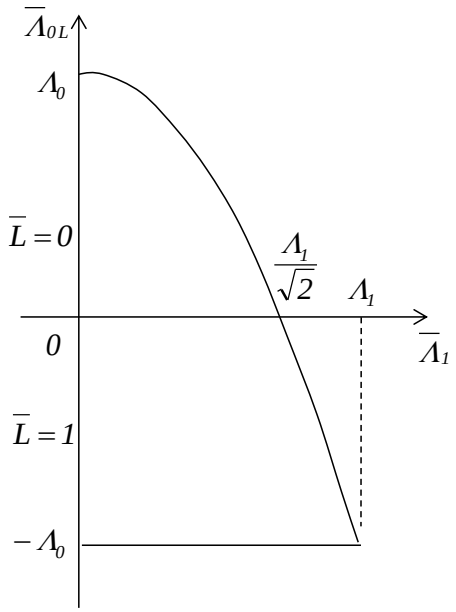

Figure A.2: Admissible domain of $\overline{\Lambda}_{0L}$ and $\overline{\Lambda}_1$ for $L = 1$.

- $\left(\overline{\Omega}_1 - \phi\right) = \pm\dfrac{\pi}{4}$

$$\left\{ \begin{array}{lcl} \cos 4\left(\overline{\Omega}_1 - \phi\right) & < & 0\ , \\ \cos 2\left(\overline{\Omega}_1 - \phi\right) & = & 0\ . \end{array} \right. \Rightarrow \left\{ \begin{array}{l} \overline{\Lambda}_{0L}^{opt} = \Lambda_0\ , \\ \overline{\Lambda}_1^{opt} \in [0, \Lambda_1]\ ; \end{array} \right. \tag{A.54}$$

and

$$F_{Hill}^{Lam} = 4r^2\Gamma_0 + 8t^2\Gamma_1 + 4\Lambda_0 r^2 \cos 4\left(\overline{\Omega}_1 - \phi\right)\ . \tag{A.55}$$

Solution for a basic ply with $L = 1$
Also here we consider different cases that depend upon the sign of t, $\cos 4\left(\overline{\Omega}_1 - \phi\right)$ and $\cos 2\left(\overline{\Omega}_1 - \phi\right)$, see Fig. 7.4. The way to get the optimal values of the optimisation parameters is identical to the previous case characterised by $L = 0$.

1. Solution with $t > 0$.

- $\left(\overline{\Omega}_1 - \phi\right) \in \left]-\dfrac{\pi}{8}, \dfrac{\pi}{8}\right[$

$$\left\{ \begin{array}{lcl} \cos 4\left(\overline{\Omega}_1 - \phi\right) & > & 0\ , \\ \cos 2\left(\overline{\Omega}_1 - \phi\right) & > & 0\ ; \end{array} \right. \Rightarrow \left\{ \begin{array}{l} \overline{\Lambda}_{0L}^{opt} = -\Lambda_0\ , \\ \overline{\Lambda}_1^{opt} = 0\ ; \end{array} \right. \tag{A.56}$$

and

$$F_{Hill}^{Lam} = 4r^2\Gamma_0 + 8t^2\Gamma_1 - 4\Lambda_0 r^2 \cos 4\left(\overline{\Omega}_1 - \phi\right)\ . \tag{A.57}$$

- $\left(\overline{\Omega}_1 - \phi\right) \in \left]-\dfrac{\pi}{4}, -\dfrac{\pi}{8}\right[\cup \left]\dfrac{\pi}{8}, \dfrac{\pi}{4}\right[$

$$\left\{ \begin{array}{lcl} \cos 4\left(\overline{\Omega}_1 - \phi\right) & < & 0\ , \\ \cos 2\left(\overline{\Omega}_1 - \phi\right) & > & 0\ ; \end{array} \right. \Rightarrow \left\{ \begin{array}{l} \overline{\Lambda}_{0L}^{opt} = \Lambda_0\ , \\ \overline{\Lambda}_1^{opt} = 0\ ; \end{array} \right. \tag{A.58}$$

and

$$F_{Hill}^{Lam} = 4r^2\Gamma_0 + 8t^2\Gamma_1 + 4\Lambda_0 r^2 \cos 4\left(\overline{\Omega}_1 - \phi\right) \ . \tag{A.59}$$

$\circ$ $\left(\overline{\Omega}_1 - \phi\right) \in \left]-\frac{3\pi}{8}, -\frac{\pi}{4}\right[\cup \left]\frac{\pi}{4}, \frac{3\pi}{8}\right[$

$$\left\{ \begin{array}{rcl} \cos 4\left(\overline{\Omega}_1 - \phi\right) & < & 0 \ , \\ \cos 2\left(\overline{\Omega}_1 - \phi\right) & < & 0 \ . \end{array} \right. \Rightarrow \tag{A.60}$$

$$\left\{ \begin{array}{l} \overline{\Lambda}_{0L}^{opt} = \left(1 - \dfrac{2t^2 \cos^2 2\left(\overline{\Omega}_1 - \phi\right) \Lambda_1^2}{r^2 \cos^2 4\left(\overline{\Omega}_1 - \phi\right) \Lambda_0^2}\right) \Lambda_0 \ , \\ \overline{\Lambda}_1^{opt} = \dfrac{t \cos 2\left(\overline{\Omega}_1 - \phi\right) \Lambda_1^2}{r\Lambda_0 \cos 4\left(\overline{\Omega}_1 - \phi\right)} \ ; \end{array} \right. \quad \text{for } \frac{t}{r} < \frac{\Lambda_0 \cos 4\left(\overline{\Omega}_1 - \phi\right)}{\Lambda_1 \cos 2\left(\overline{\Omega}_1 - \phi\right)} \ , \tag{A.61}$$

and

$$F_{Hill}^{Lam} = \ 4r^2\Gamma_0 + 8t^2\Gamma_1 + 8\frac{t^2 \cos^2 2\left(\overline{\Omega}_1 - \phi\right) \Lambda_1^2}{\Lambda_0 \cos 4\left(\overline{\Omega}_1 - \phi\right)} + 4r^2\Lambda_0 \cos 4\left(\overline{\Omega}_1 - \phi\right) \ . \tag{A.62}$$

Otherwise

$$\left\{ \begin{array}{l} \overline{\Lambda}_{0L}^{opt} = -\Lambda_0 \ , \\ \overline{\Lambda}_1^{opt} = \Lambda_1 \ ; \end{array} \right. \quad \text{for } \frac{t}{r} \geq \frac{\Lambda_0 \cos 4\left(\overline{\Omega}_1 - \phi\right)}{\Lambda_1 \cos 2\left(\overline{\Omega}_1 - \phi\right)} \ , \tag{A.63}$$

and

$$F_{Hill}^{Lam} = 4r^2\Gamma_0 + 8t^2\Gamma_1 - 4\Lambda_0 r^2 \cos 4\left(\overline{\Omega}_1 - \phi\right) + 16tr\Lambda_1 \cos 2\left(\overline{\Omega}_1 - \phi\right) \ . \tag{A.64}$$

$\circ$ $\left(\overline{\Omega}_1 - \phi\right) \in \left]-\frac{\pi}{2}, -\frac{3\pi}{8}\right[\cup \left]\frac{3\pi}{8}, \frac{\pi}{2}\right[$,

$$\left\{ \begin{array}{rcl} \cos 4\left(\overline{\Omega}_1 - \phi\right) & > & 0 \ , \\ \cos 2\left(\overline{\Omega}_1 - \phi\right) & < & 0 \ ; \end{array} \right. \Rightarrow \left\{ \begin{array}{l} \overline{\Lambda}_{0L}^{opt} = -\Lambda_0 \ , \\ \overline{\Lambda}_1^{opt} = \Lambda_1 \ ; \end{array} \right. \tag{A.65}$$

and

$$F_{Hill}^{Lam} = 4r^2\Gamma_0 + 8t^2\Gamma_1 - 4\Lambda_0 r^2 \cos 4\left(\overline{\Omega}_1 - \phi\right) + 16tr\Lambda_1 \cos 2\left(\overline{\Omega}_1 - \phi\right) \ . \tag{A.66}$$

$\circ$ $\left(\overline{\Omega}_1 - \phi\right) = \pm\frac{\pi}{8}$

$$\left\{ \begin{array}{rcl} \cos 4\left(\overline{\Omega}_1 - \phi\right) & = & 0 \ , \\ \cos 2\left(\overline{\Omega}_1 - \phi\right) & > & 0 \ ; \end{array} \right. \Rightarrow \left\{ \begin{array}{l} \overline{\Lambda}_{0L}^{opt} \in [-\Lambda_0, \Lambda_0] \, , \\ \overline{\Lambda}_1^{opt} = 0 \ ; \end{array} \right. \tag{A.67}$$

and

$$F_{Hill}^{Lam} = 4r^2\Gamma_0 + 8t^2\Gamma_1 \ . \tag{A.68}$$

$\circ$ $\left(\overline{\Omega}_1 - \phi\right) = \pm\frac{3\pi}{8}$

$$\left\{ \begin{array}{rcl} \cos 4\left(\overline{\Omega}_1 - \phi\right) & = & 0 \ , \\ \cos 2\left(\overline{\Omega}_1 - \phi\right) & < & 0 \ ; \end{array} \right. \Rightarrow \left\{ \begin{array}{l} \overline{\Lambda}_{0L}^{opt} = -\Lambda_0 \ , \\ \overline{\Lambda}_1^{opt} = \Lambda_1 \ ; \end{array} \right. \tag{A.69}$$

and

$$F_{Hill}^{Lam} = 4r^2\Gamma_0 + 8t^2\Gamma_1 + 16tr\Lambda_1 \cos 2\left(\overline{\Omega}_1 - \phi\right) \ . \tag{A.70}$$

- $\left(\overline{\Omega}_1 - \phi\right) = \pm\dfrac{\pi}{4}$

$$\left\{ \begin{array}{l} \cos 4\left(\overline{\Omega}_1 - \phi\right) \ < \ 0 \ , \\ \cos 2\left(\overline{\Omega}_1 - \phi\right) \ = \ 0 \ . \end{array} \right. \Rightarrow \left\{ \begin{array}{l} \overline{\Lambda}_{0L}^{opt} = \Lambda_0 \ , \\ \overline{\Lambda}_1^{opt} = 0 \ ; \end{array} \right. \tag{A.71}$$

and

$$F_{Hill}^{Lam} = 4r^2\Gamma_0 + 8t^2\Gamma_1 + 4\Lambda_0 r^2 \cos 4\left(\overline{\Omega}_1 - \phi\right) \ . \tag{A.72}$$

2. Solution with $t = 0$.

- $\left(\overline{\Omega}_1 - \phi\right) \in \ \left]-\dfrac{\pi}{2}, -\dfrac{3\pi}{8}\right[\ \cup \ \left]-\dfrac{\pi}{8}, \dfrac{\pi}{8}\right[\ \cup \ \left]\dfrac{3\pi}{8}, \dfrac{\pi}{2}\right[$

$$\cos 4\left(\overline{\Omega}_1 - \phi\right) \ > \ 0 \ \Rightarrow \left\{ \begin{array}{l} \overline{\Lambda}_{0L}^{opt} = -\Lambda_0 \ , \\ \overline{\Lambda}_1^{opt} \in [0, \Lambda_1] \ ; \end{array} \right. \tag{A.73}$$

and

$$F_{Hill}^{Lam} = 4r^2\Gamma_0 + 8t^2\Gamma_1 - 4\Lambda_0 r^2 \cos 4\left(\overline{\Omega}_1 - \phi\right) \ . \tag{A.74}$$

- $\left(\overline{\Omega}_1 - \phi\right) \in \ \left]-\dfrac{3\pi}{8}, -\dfrac{\pi}{8}\right[\ \cup \ \left]\dfrac{\pi}{8}, \dfrac{3\pi}{8}\right[$

$$\cos 4\left(\overline{\Omega}_1 - \phi\right) \ < \ 0 \ \Rightarrow \left\{ \begin{array}{l} \overline{\Lambda}_{0L}^{opt} = \Lambda_0 \ , \\ \overline{\Lambda}_1^{opt} = 0 \ ; \end{array} \right. \tag{A.75}$$

and

$$F_{Hill}^{Lam} = 4r^2\Gamma_0 + 8t^2\Gamma_1 + 4\Lambda_0 r^2 \cos 4\left(\overline{\Omega}_1 - \phi\right) \ . \tag{A.76}$$

- $\left(\overline{\Omega}_1 - \phi\right) = \pm\dfrac{3\pi}{8}, \pm\dfrac{\pi}{8}$

$$\cos 4\left(\overline{\Omega}_1 - \phi\right) \ = \ 0 \ \Rightarrow \left\{ \begin{array}{l} \overline{\Lambda}_{0L}^{opt} \text{ any}, \\ \overline{\Lambda}_1^{opt} \text{ any}; \end{array} \right. \tag{A.77}$$

that belong to the admissible region of Fig. A.2.

$$F_{Hill}^{Lam} = 4r^2\Gamma_0 + 8t^2\Gamma_1 \ . \tag{A.78}$$

Also in this case the anisotropic distribution of strength does not take part to the optimal solution.

3. Solution with $t < 0$.

- $\left(\overline{\Omega}_1 - \phi\right) \in \ \left]-\dfrac{\pi}{8}, \dfrac{\pi}{8}\right[$

$$\left\{ \begin{array}{l} \cos 4\left(\overline{\Omega}_1 - \phi\right) \ > \ 0 \ , \\ \cos 2\left(\overline{\Omega}_1 - \phi\right) \ > \ 0 \ ; \end{array} \right. \Rightarrow \left\{ \begin{array}{l} \overline{\Lambda}_{0L}^{opt} = -\Lambda_0 \ , \\ \overline{\Lambda}_1^{opt} = \Lambda_1 \ ; \end{array} \right. \tag{A.79}$$

and

$$F_{Hill}^{Lam} = 4r^2\Gamma_0 + 8t^2\Gamma_1 - 4\Lambda_0 r^2 \cos 4\left(\overline{\Omega}_1 - \phi\right) + 16tr\Lambda_1 \cos 2\left(\overline{\Omega}_1 - \phi\right) \ . \tag{A.80}$$

$\circ$ $\left(\overline{\Omega}_1 - \phi\right) \in \left]-\frac{\pi}{4}, \frac{\pi}{8}\right[\cup \left]\frac{\pi}{8}, \frac{\pi}{4}\right[$

$$\left\{ \begin{array}{l} \cos 4\left(\overline{\Omega}_1 - \phi\right) < 0 \ , \\ \cos 2\left(\overline{\Omega}_1 - \phi\right) > 0 \ . \end{array} \right. \Rightarrow \tag{A.81}$$

$$\left\{ \begin{array}{l} \overline{\Lambda}_{0L}^{opt} = \left(\dfrac{2t^2 \cos^2 2\left(\overline{\Omega}_1 - \phi\right) \Lambda_1^2}{r^2 \Lambda_0^2 \cos^2 4\left(\overline{\Omega}_1 - \phi\right)} - 1 \right) \Lambda_0 \ , \\ \overline{\Lambda}_1^{opt} = \dfrac{t \cos 2\left(\overline{\Omega}_1 - \phi\right) \Lambda_1^2}{r \Lambda_0 \cos 4\left(\overline{\Omega}_1 - \phi\right)} \ ; \end{array} \right. \quad \text{for } \frac{t}{r} < \frac{\Lambda_0 \cos 4\left(\overline{\Omega}_1 - \phi\right)}{\Lambda_1 \cos 2\left(\overline{\Omega}_1 - \phi\right)} \ ; \tag{A.82}$$

and

$$F_{Hill}^{Lam} = \ 4r^2 \Gamma_0 + 8t^2 \Gamma_1 + 8 \frac{t^2 \cos^2 2\left(\overline{\Omega}_1 - \phi\right) \Lambda_1^2}{\Lambda_0 \cos 4\left(\overline{\Omega}_1 - \phi\right)} + 4r^2 \Lambda_0 \cos 4\left(\overline{\Omega}_1 - \phi\right) \ . \tag{A.83}$$

$$\left\{ \begin{array}{l} \overline{\Lambda}_{0L}^{opt} = \Lambda_0 \ , \\ \overline{\Lambda}_1^{opt} = \Lambda_1 \ ; \end{array} \right. \text{for } \frac{t}{r} \geq \frac{\Lambda_0 \cos 4\left(\overline{\Omega}_1 - \phi\right)}{\Lambda_1 \cos 2\left(\overline{\Omega}_1 - \phi\right)} \ ; \tag{A.84}$$

and

$$F_{Hill}^{Lam} = 4r^2 \Gamma_0 + 8t^2 \Gamma_1 + 4\Lambda_0 r^2 \cos 4\left(\overline{\Omega}_1 - \phi\right) + 16tr\Lambda_1 \cos 2\left(\overline{\Omega}_1 - \phi\right) \ . \tag{A.85}$$

$\circ$ $\left(\overline{\Omega}_1 - \phi\right) \in \left]-\frac{3\pi}{8}, -\frac{\pi}{4}\right[\cup \left]\frac{\pi}{4}, \frac{3\pi}{8}\right[$

$$\left\{ \begin{array}{l} \cos 4\left(\overline{\Omega}_1 - \phi\right) < 0 \ , \\ \cos 2\left(\overline{\Omega}_1 - \phi\right) < 0 \ ; \end{array} \right. \Rightarrow \left\{ \begin{array}{l} \overline{\Lambda}_{0L}^{opt} = \Lambda_0 \ , \\ \overline{\Lambda}_1^{opt} = 0 \ ; \end{array} \right. \tag{A.86}$$

and

$$F_{Hill}^{Lam} = 4r^2 \Gamma_0 + 8t^2 \Gamma_1 + 4\Lambda_0 r^2 \cos 4\left(\overline{\Omega}_1 - \phi\right) \ . \tag{A.87}$$

$\circ$ $\left(\overline{\Omega}_1 - \phi\right) \in \left]-\frac{\pi}{2}, -\frac{3\pi}{8}\right[\cup \left]\frac{3\pi}{8}, \frac{\pi}{2}\right[$,

$$\left\{ \begin{array}{l} \cos 4\left(\overline{\Omega}_1 - \phi\right) > 0 \ , \\ \cos 2\left(\overline{\Omega}_1 - \phi\right) < 0 \ ; \end{array} \right. \Rightarrow \left\{ \begin{array}{l} \overline{\Lambda}_{0L}^{opt} = -\Lambda_0 \ , \\ \overline{\Lambda}_1^{opt} = 0 \ ; \end{array} \right. \tag{A.88}$$

and

$$F_{Hill}^{Lam} = 4r^2 \Gamma_0 + 8t^2 \Gamma_1 - 4\Lambda_0 r^2 \cos 4\left(\overline{\Omega}_1 - \phi\right) \ . \tag{A.89}$$

$\circ$ $\left(\overline{\Omega}_1 - \phi\right) = \pm\frac{\pi}{8}$,

$$\left\{ \begin{array}{l} \cos 4\left(\overline{\Omega}_1 - \phi\right) = 0 \ , \\ \cos 2\left(\overline{\Omega}_1 - \phi\right) > 0 \ ; \end{array} \right. \Rightarrow \left\{ \begin{array}{l} \overline{\Lambda}_{0L}^{opt} = -\Lambda_0 \ , \\ \overline{\Lambda}_1^{opt} = \Lambda_1 \ ; \end{array} \right. \tag{A.90}$$

and

$$F_{Hill}^{Lam} = 4r^2 \Gamma_0 + 8t^2 \Gamma_1 + 16tr\Lambda_1 \cos 2\left(\overline{\Omega}_1 - \phi\right) \ . \tag{A.91}$$

$\circ$ $\left(\overline{\Omega}_1 - \phi\right) = \pm\frac{3\pi}{8}$

$$\left\{ \begin{array}{l} \cos 4\left(\overline{\Omega}_1 - \phi\right) = 0 \ , \\ \cos 2\left(\overline{\Omega}_1 - \phi\right) < 0 \ ; \end{array} \right. \Rightarrow \left\{ \begin{array}{l} \overline{\Lambda}_{0L}^{opt} \in [-\Lambda_0, \Lambda_0] \, , \\ \overline{\Lambda}_1^{opt} = 0 \ ; \end{array} \right. \tag{A.92}$$

and

$$F_{Hill}^{Lam} = 4r^2\Gamma_0 + 8t^2\Gamma_1 \ . \tag{A.93}$$

- $\left(\overline{\Omega}_1 - \phi\right) = \pm\dfrac{\pi}{4}$

$$\left\{ \begin{array}{l} \cos 4\left(\overline{\Omega}_1 - \phi\right) \ < \ 0 \ , \\ \cos 2\left(\overline{\Omega}_1 - \phi\right) \ = \ 0 \ . \end{array} \right. \Rightarrow \left\{ \begin{array}{l} \overline{\Lambda}_{0L}^{opt} = \Lambda_0 \ , \\ \overline{\Lambda}_1^{opt} = 0 \ ; \end{array} \right. \tag{A.94}$$

and

$$F_{Hill}^{Lam} = 4r^2\Gamma_0 + 8t^2\Gamma_1 + 4\Lambda_0 r^2 \cos 4\left(\overline{\Omega}_1 - \phi\right) \ . \tag{A.95}$$

A.2 Second problem: including the orthotropy orientation as an optimisation variable

The optimisation problem can be formalised as:

$$\underset{\left\{\overline{\Lambda}_{0L}, \overline{\Lambda}_1, \overline{\Omega}_1\right\}}{min} F_{Hill}^{Lam}\left(\overline{\Lambda}_{0L}, \overline{\Lambda}_1, \overline{\Omega}_1\right) \ , \tag{A.96}$$

along with the constraints (A.2). The objective function is:

$$F_{Hill}^{Lam} = 4r^2\Gamma_0 + 8t^2\Gamma_1 + 4\overline{\Lambda}_{0L} r^2 \cos 4\left(\overline{\Omega}_1 - \phi\right) + 16tr\overline{\Lambda}_1 \cos 2\left(\overline{\Omega}_1 - \phi\right) \ . \tag{A.97}$$

Also in this case firstly we have to consider the important case of spherical strain field, characterised by $r = 0$. If we impose $r = 0$ in eq. (A.97), the two optimisation parameters are not longer present in the expression of F_{Hill}^{Lam}, so, the optimal value of $\overline{\Lambda}_{0L}$ and $\overline{\Lambda}_1$ is any value belonging to the admissible design region of the plane ($\overline{\Lambda}_{0L}$, $\overline{\Lambda}_1$). Hence, now we consider $r \neq 0$.

In this case F_{Hill}^{Lam} has to be minimised with respect to three variables: the orthotropy orientation $\overline{\Omega}_1$ and the polar moduli $\overline{\Lambda}_{0L}$ and $\overline{\Lambda}_1$. The analytical solution of this problem will be realised within two successive phases: firstly the minimisation with respect to the orientation $\overline{\Omega}_1$ of the orthotropy axis and then, the minimisation with respect to the polar moduli $\overline{\Lambda}_{0L}$ and $\overline{\Lambda}_1$.

The optimal orientation $\overline{\Omega}_1^{opt}$ can be determined in analogue way as done in Sec. 5.2. Thus, we show directly the results in Fig. A.3 where

$$\begin{aligned} \mu &= \mathrm{dir}\left(\min\left\{|\varepsilon_I|, \ |\varepsilon_{II}|\right\}\right) \ , \\ \xi &= \frac{1}{2}\arccos\left(-\frac{\overline{\Lambda}_1 t}{\overline{\Lambda}_{0L} r}\right) \ . \end{aligned} \tag{A.98}$$

Fig. A.3 shows that the shape of orthotropy of the plate ($\overline{L}$) plays a decisive role in the evaluation of the optimal orthotropy orientation. We have, thus, two type of solutions concerning the optimal orthotropy orientation:

- a solution that does not include the term ξ, that we will call solution non-ξ;
- a solution including the term ξ, that we will call solution ξ.

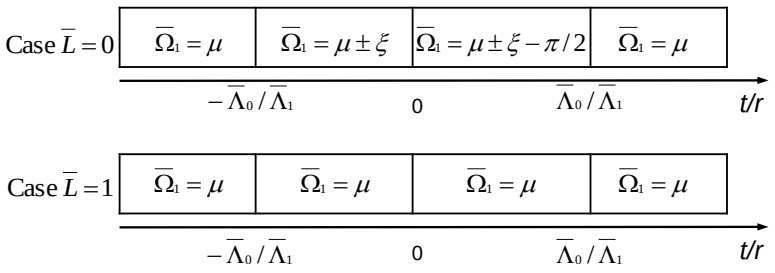

Figure A.3: Optimal material orientation to minimise F_{Hill}^{Lam}.

If we put the expression of $\overline{\Omega}_1^{opt}$ in eq. (A.97), depending on the type of solution of $\overline{\Omega}_1^{opt}$, $F_{Hill}^{Lam}(\overline{\Omega}_1^{opt})$ that will be used in the second minimisation phase concerning the evaluation of $\overline{\Lambda}_{0L}^{opt}$ and $\overline{\Lambda}_1^{opt}$ can assume two different shapes. Therefore, in the second minimisation phase, we have to minimise two different functions with respect to $\overline{\Lambda}_{0L}$ and $\overline{\Lambda}_1$:

$$\text{solution non-}\xi: \quad F_{Hill}^{Lam}(\overline{\Lambda}_{0L},\overline{\Lambda}_1,\overline{\Omega}_1^{opt}) = 4r^2\Gamma_0 + 8t^2\Gamma_1 + 4\overline{\Lambda}_{0L}r^2 - 16|t|r\overline{\Lambda}_1; \tag{A.99}$$

$$\text{solution } \xi: \quad F_{Hill}^{Lam}(\overline{\Lambda}_{0L},\overline{\Lambda}_1,\overline{\Omega}_1^{opt}) = 4r^2\Gamma_0 + 8t^2\Gamma_1 - 4\overline{\Lambda}_0r^2 - 8t^2\frac{\overline{\Lambda}_1^2}{\overline{\Lambda}_0}\ . \tag{A.100}$$

The optimal value of F_{Hill}^{Lam} obtained minimising eq. (A.99) will be, then, compared with that obtained minimising eq. (A.100). The solution that give the minimum value of F_{Hill}^{Lam} (and the corresponding values of the design variables $\overline{\Omega}_1$, $\overline{\Lambda}_{0L}$ and $\overline{\Lambda}_1$) will be the global optimal solution of problem (A.96).

Moreover, the range of the solutions non-ξ is characterised by the following strain field:

$$\begin{cases} \dfrac{t}{r} \le -\dfrac{\overline{\Lambda}_0}{\overline{\Lambda}_1}\ , \\ \dfrac{t}{r} \ge \dfrac{\overline{\Lambda}_0}{\overline{\Lambda}_1}\ , \end{cases} \Rightarrow \frac{|t|}{r} \ge \frac{\overline{\Lambda}_0}{\overline{\Lambda}_1}\ ; \tag{A.101}$$

while, the solutions ξ is characterised by the following strain field:

$$\begin{cases} \dfrac{t}{r} \ge -\dfrac{\overline{\Lambda}_0}{\overline{\Lambda}_1}\ , \\ \dfrac{t}{r} \le \dfrac{\overline{\Lambda}_0}{\overline{\Lambda}_1}\ , \end{cases} \Rightarrow \frac{|t|}{r} \le \frac{\overline{\Lambda}_0}{\overline{\Lambda}_1}\ ; \tag{A.102}$$

The separation between these two types of solutions (non-ξ and ξ) is represented by the equality

$$\overline{\Lambda}_{0L} = \frac{|t|}{r}\overline{\Lambda}_1 \tag{A.103}$$

that is a straight-line in the space $(\overline{\Lambda}_{0L},\overline{\Lambda}_1)$. The ratio $|t|/r$ between the spherical and deviatoric components of the strain tensor represents the angular coefficient of the straight-line and is a positive quantity.

In order to find an analytical solution, we can proceed by following the same logical steps as already done in Sec. A.1.

Solution for a basic ply with $L = 0$

- Solution non-ξ.
  We have:
$$F_{Hill}^{Lam} = 4r^2\Gamma_0 + 8t^2\Gamma_1 + 4\overline{\Lambda}_{0L}r^2 - 16|t|r\overline{\Lambda}_1 \ . \tag{A.104}$$
  The two partial derivatives of F_{Hill}^{Lam} with respect to $\overline{\Lambda}_{0L}$ and $\overline{\Lambda}_1$ are:
$$\begin{aligned} \frac{\partial F_{Hill}^{Lam}}{\partial \overline{\Lambda}_{0L}} &= 4r^2 \ , \\ \frac{\partial F_{Hill}^{Lam}}{\partial \overline{\Lambda}_1} &= -16|t|r \ . \end{aligned} \tag{A.105}$$
  Both the derivatives are constant for a fixed strain field. In particular, the derivative with respect to $\overline{\Lambda}_{0L}$ is always positive, while the first derivative with respect to $\overline{\Lambda}_1$ is always negative or equal to zero if $t = 0$.

  A particular case is represented by the pure deviatoric strain field characterised by $t = 0$; the angular coefficient $|t|/r$ becomes null and the separation between the two solutions (non-ξ and ξ) is aligned with the axis $\overline{\Lambda}_1$ of Fig. A.4. In addition, $\overline{\Lambda}_1$ is not longer present in the equation of F_{Hill}^{Lam} and being $\dfrac{\partial F_{Hill}^{Lam}}{\partial \overline{\Lambda}_{0L}} > 0$, the optimal value of $\overline{\Lambda}_{0L}$ is:
$$\overline{\Lambda}_{0L}^{opt} = -\Lambda_0 \ , \tag{A.106}$$
  so,
$$\overline{\Lambda}_1^{opt} = 0 \ , \tag{A.107}$$
  see Fig. A.4.

  For $t \neq 0$
$$\frac{\partial F_{Hill}^{Lam}}{\partial \overline{\Lambda}_{0L}} = 4r^2 \ . \tag{A.108}$$
  For a fixed value of $\overline{\Lambda}_1$ the optimum value of $\overline{\Lambda}_{0L}$ is placed on the parabola. The expression of the parabola, explicitly writing $\overline{\Lambda}_{0L}$, is:
$$\overline{\Lambda}_{0L} = \Lambda_0 \left(2\frac{\overline{\Lambda}_1^2}{\Lambda_1^2} - 1 \right) \ . \tag{A.109}$$
  Putting eq. (A.109) in eq. (A.104), we have
$$F_{Hill}^{Lam} = 4r^2\Gamma_0 + 8t^2\Gamma_1 + 4r^2\Lambda_0 \left(2\frac{\overline{\Lambda}_1^2}{\Lambda_1^2} - 1 \right) - 16|t|r\overline{\Lambda}_1 \ , \tag{A.110}$$
  and deriving with respect to $\overline{\Lambda}_1$, we have:
$$\frac{\partial F_{Hill}^{Lam}}{\partial \overline{\Lambda}_1} = 16r^2\frac{\overline{\Lambda}_1}{\Lambda_1^2}\Lambda_0 - 16|t|r = 0 \ , \tag{A.111}$$
  then, the stationary value of $\overline{\Lambda}_1$ is:
$$\overline{\Lambda}_1^{stat} = \frac{|t|\Lambda_1^2}{r\Lambda_0}. \tag{A.112}$$

The second derivative of F_{Hill}^{Lam} with respect to $\overline{\Lambda}_1$ is always positive:

$$\frac{\partial^2 F_{Hill}^{Lam}}{\partial \overline{\Lambda}_1^2} = \frac{16 r^2 \Lambda_0}{\Lambda_1^2} > 0 \ , \tag{A.113}$$

so,

$$\overline{\Lambda}_1^{stat} = \overline{\Lambda}_1^{opt} \ . \tag{A.114}$$

The corresponding value of $\overline{\Lambda}_{0L}$ on the parabola is

$$\overline{\Lambda}_{0L}^{opt} = \left(\frac{2t^2 \Lambda_1^2}{r^2 \Lambda_0^2} - 1 \right) \Lambda_0 \ . \tag{A.115}$$

In order to respect the bounds on $\overline{\Lambda}_1$, eq. (A.2), this solution is valid for

$$\frac{|t|}{r} \leq \frac{\Lambda_0}{\Lambda_1} \ , \tag{A.116}$$

that correspond also to the graphical condition of Fig. A.4(c).
The associated value of the objective function is

$$F_{Hill}^{Lam} = 4r^2 \Gamma_0 + 8t^2 \Gamma_1 - 4r^2 \Lambda_0 - 8t^2 \frac{\Lambda_1^2}{\Lambda_0} \tag{A.117}$$

For $|t|/r \geq \Lambda_0/\Lambda_1$, eq. (A.112) gives a value of $\overline{\Lambda}_1^{opt}$ greater than Λ_1 violating the bounds of eq. (A.2). In this case we have to impose:

$$\overline{\Lambda}_1^{opt} = \Lambda_1 \ , \tag{A.118}$$

and the unique corresponding admissible value of $\overline{\Lambda}_{0L}$ is

$$\overline{\Lambda}_{0L}^{opt} = \Lambda_0 \ , \tag{A.119}$$

see Fig. A.4(a). The objective function becomes

$$F_{Hill}^{Lam} = 4r^2 \Gamma_0 + 8t^2 \Gamma_1 + 4r^2 \Lambda_0 - 16|t| r \Lambda_1 \ . \tag{A.120}$$

- Solution ξ.
  This optimal solution of $\overline{\Omega}_1$ leads to the following form of the objective function:

$$F_{Hill}^{Lam} = 4r^2 \Gamma_0 + 8t^2 \Gamma_1 - 4\overline{\Lambda}_0 r^2 - 8t^2 \frac{\overline{\Lambda}_1^2}{\overline{\Lambda}_0} \ . \tag{A.121}$$

The first derivatives with respect to $\overline{\Lambda}_0$ and $\overline{\Lambda}_1$ are:

$$\begin{aligned} \frac{\partial F_{Hill}^{Lam}}{\partial \overline{\Lambda}_0} &= -4r^2 + 8t^2 \frac{\overline{\Lambda}_1^2}{\overline{\Lambda}_0^2} \ , \\ \frac{\partial F_{Hill}^{Lam}}{\partial \overline{\Lambda}_1} &= -16t^2 \frac{\overline{\Lambda}_1}{\overline{\Lambda}_0} \leq 0 \ . \end{aligned} \tag{A.122}$$

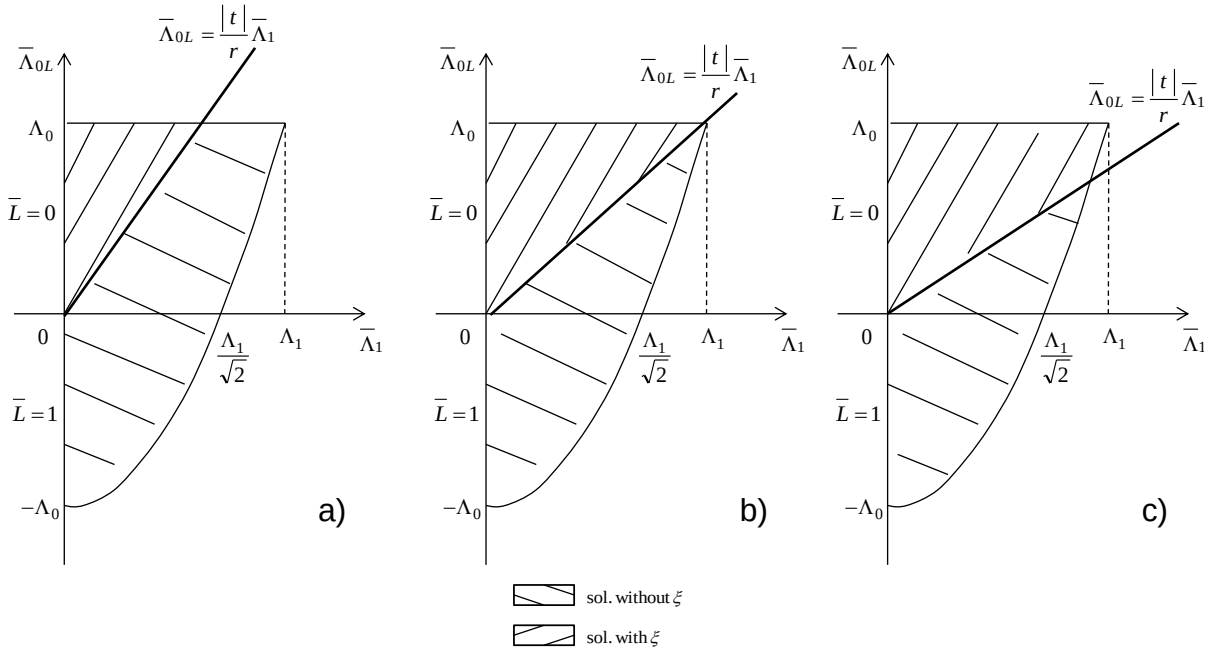

Figure A.4: Admissible domain of $\overline{\Lambda}_0$ and $\overline{\Lambda}_1$ for $L = 0$ and for $|t|/r > \Lambda_0/\Lambda_1$ (a), $|t|/r = \Lambda_0/\Lambda_1$ (b), $|t|/r < \Lambda_0/\Lambda_1$ (c).

A particular case is represented by the pure deviatoric strain field ($t = 0$): the straight-line separating the two solutions, non-ξ and ξ, is aligned with the axis of $\overline{\Lambda}_1$, Fig. A.4, and the variable $\overline{\Lambda}_1$ is not more present in the equation of F^{Lam}_{Hill}. Being the derivative with respect to $\overline{\Lambda}_{0L}$ constant and negative, the optimal solution is:

$$\overline{\Lambda}^{opt}_{0L} = \Lambda_0 \ , \overline{\Lambda}^{opt}_1 \in [0, \Lambda_1] \ . \tag{A.123}$$

For $t \neq 0$, the first derivative with respect to $\overline{\Lambda}_1$ is always negative, so, for a fixed value of $\overline{\Lambda}_0$ the optimum value of $\overline{\Lambda}_1$ corresponds to its maximum value belonging to the admissible region.

To this purpose we have to separate three different cases, see Fig. A.4:

1. $|t|/r \geq \Lambda_0/\Lambda_1$.
   $\overline{\Lambda}^{opt}_1$ is placed on the straight-line, hence, we can explicitly write $\overline{\Lambda}_1$ in the straight-line equation
   $$\overline{\Lambda}_1 = \overline{\Lambda}_0 \frac{r}{|t|} \ , \tag{A.124}$$
   and replace it in the eq. (A.121)
   $$F^{Lam}_{Hill} = 4r^2\Gamma_0 + 8t^2\Gamma_1 - 12r^2\overline{\Lambda}_0 \ . \tag{A.125}$$
   Deriving F^{Lam}_{Hill} with respect to $\overline{\Lambda}_0$ we have
   $$\frac{\partial F^{Lam}_{Hill}}{\partial \overline{\Lambda}_0} = -12r^2 \leq 0 \ . \tag{A.126}$$

The optimum value of $\overline{\Lambda}_0$ is:

$$\overline{\Lambda}_0^{opt} = \Lambda_0 \ , \tag{A.127}$$

and

$$\overline{\Lambda}_1^{opt} = \Lambda_0 \frac{r}{|t|} \ . \tag{A.128}$$

2. $|t|/r < \Lambda_0/\Lambda_1$ and $\frac{|t|\Lambda_1}{4r^2\Lambda_0}\left[|t|\Lambda_1 + \sqrt{t^2\Lambda_1^2 + 8r^2\Lambda_0^2}\right] \leq \overline{\Lambda}_0 \leq \Lambda_0$ (intersection between the parabola and the straight-line).
$\overline{\Lambda}_1^{opt}$ is placed on the parabola. We can explicitly write $\overline{\Lambda}_1$ in the parabola equation

$$\overline{\Lambda}_1^2 = \frac{\Lambda_1^2}{2}\left(\frac{\overline{\Lambda}_0}{\Lambda_0} + 1\right) \ , \tag{A.129}$$

replace it in the eq. (A.121) of the objective function

$$F_{Hill}^{Lam} = 4r^2\Gamma_0 + 8t^2\Gamma_1 - 4r^2\overline{\Lambda}_0 - \frac{4t^2\Lambda_1^2}{\Lambda_0} - \frac{4t^2\Lambda_1^2}{\overline{\Lambda}_0} \ , \tag{A.130}$$

and derive F_{Hill}^{Lam} with respect to $\overline{\Lambda}_0$

$$\frac{\partial F_{Hill}^{Lam}}{\partial \overline{\Lambda}_0} = -4r^2 + \frac{4t^2\Lambda_1^2}{\overline{\Lambda}_0^2} \ . \tag{A.131}$$

The first derivative gives us a stationary value for $\overline{\Lambda}_0$

$$\frac{\partial F_{Hill}^{Lam}}{\partial \overline{\Lambda}_0} = 0 \text{ for } \overline{\Lambda}_0^{stat} = \frac{|t|}{r}\Lambda_1 \ , \tag{A.132}$$

and for $\overline{\Lambda}_0 = \overline{\Lambda}_0^{stat}$ the second derivative of F_{Hill}^{Lam} is

$$\left.\frac{\partial^2 F_{Hill}^{Lam}}{\partial \overline{\Lambda}_0^2}\right|_{\overline{\Lambda}_0^{stat}} = -\frac{8r^3}{|t|\Lambda_1} < 0 \ . \tag{A.133}$$

$\overline{\Lambda}_0^{stat}$ does not correspond to a minimum for F_{Hill}^{Lam}, so, we need to compare the value of the objective function on the two extremes of the portion of the parabola:

$$\begin{aligned} a &= (\overline{\Lambda}_1 = \Lambda_1, \overline{\Lambda}_0 = \Lambda_0) \ ; \\ b &= (\overline{\Lambda}_1 = \frac{\Lambda_1}{4r\Lambda_0}\left[|t|\Lambda_1 + \sqrt{t^2\Lambda_1^2 + 8r^2\Lambda_0^2}\right], \cdots \\ &\cdots \overline{\Lambda}_0 = \frac{|t|\Lambda_1}{4r^2\Lambda_0}\left[|t|\Lambda_1 + \sqrt{t^2\Lambda_1^2 + 8r^2\Lambda_0^2}\right]) \ ; \end{aligned} \tag{A.134}$$

then, we have to compare

$$\begin{aligned} F_{Hill}^{Lam}|_a &= 4r^2\Gamma_0 + 8t^2\Gamma_1 - 4r^2\Lambda_0 - 8t^2\frac{\Lambda_1^2}{\Lambda_0^2} \ ; \\ F_{Hill}^{Lam}|_b &= 4r^2\Gamma_0 + 8t^2\Gamma_1 - \frac{3|t|\Lambda_1}{\Lambda_0}\left[t\Lambda_1 + \sqrt{t^2\Lambda_1^2 + 8r^2\Lambda_0^2}\right] \ . \end{aligned} \tag{A.135}$$

3. $|t|/r < \Lambda_0/\Lambda_1$ and $0 \leq \overline{\Lambda_0} \leq \dfrac{|t|\Lambda_1}{4r^2\Lambda_0}\left[|t|\Lambda_1 + \sqrt{t^2\Lambda_1^2 + 8r^2\Lambda_0^2}\right]$.

$\overline{\Lambda}_1^{opt}$ is placed on the straight-line. Thus, the optimum value of $\overline{\Lambda}_0$ is placed at the intersection with the parabola:

$$\begin{cases} \overline{\Lambda}_0^{opt} = \dfrac{|t|\Lambda_1}{4r^2\Lambda_0}\left[|t|\Lambda_1 + \sqrt{t^2\Lambda_1^2 + 8r^2\Lambda_0^2}\right] \ , \\ \overline{\Lambda}_1^{opt} = \dfrac{\Lambda_1}{4r\Lambda_0}\left[|t|\Lambda_1 + \sqrt{t^2\Lambda_1^2 + 8r^2\Lambda_0^2}\right] \ ; \end{cases} \tag{A.136}$$

and

$$F_{Hill}^{Lam} = 4r^2\Gamma_0 + 8t^2\Gamma_1 - \frac{3|t|\Lambda_1}{\Lambda_0}\left[t\Lambda_1 + \sqrt{t^2\Lambda_1^2 + 8r^2\Lambda_0^2}\right] \ . \tag{A.137}$$

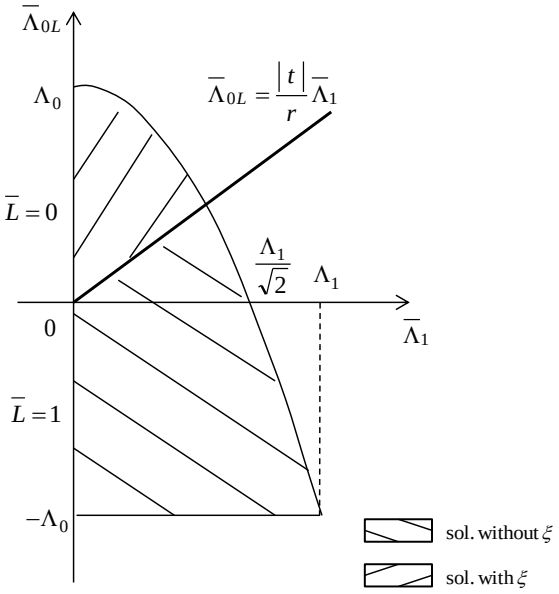

Figure A.5: Admissible domain of $\overline{\Lambda}_{0L}$ and $\overline{\Lambda}_1$ for $L = 1$.

Solution for a basic ply with $L = 1$
The region of admissible values of $\overline{\Lambda}_{0L}$ and $\overline{\Lambda}_1$ for $L = 1$ is showed in Fig. A.5.

- Solution non-ξ.
  The associated value of the objective function is

$$F_{Hill}^{Lam} = 4r^2\Gamma_0 + 8t^2\Gamma_1 + 4\overline{\Lambda}_{0L}r^2 - 16|t|r\overline{\Lambda}_1 \ . \tag{A.138}$$

  The way to find the optimal solution is analogue to that discussed beforehand. In the case of pure deviatoric strain field, $t = 0$, the variable $\overline{\Lambda}_1$ is not present in the equation of the objective function F_{Hill}^{Lam}, so, we have:

$$\overline{\Lambda}_0^{opt} = -\Lambda_0 \ , \overline{\Lambda}_1^{opt} \in [0, \Lambda_1] \ . \tag{A.139}$$

  For $t \neq 0$, we have

$$\forall \ \overline{\Lambda}_1 \ : \ \overline{\Lambda}_{0L}^{opt} = -\Lambda_0 \ . \tag{A.140}$$

If we fix $\overline{\Lambda}_{0L} = -\Lambda_0$ in the equation of the objective function F_{Hill}^{Lam} and we calculate the first derivative, we have

$$\frac{\partial F_{Hill}^{Lam}}{\partial \overline{\Lambda}_1} = -16|t|r < 0 \ , \tag{A.141}$$

hence,

$$\overline{\Lambda}_1^{opt} = \Lambda_1 \ , \tag{A.142}$$

see Fig. A.5.

- Solution ξ.
  The objective function is

$$F_{Hill}^{Lam} = 4r^2\Gamma_0 + 8t^2\Gamma_1 - 4\overline{\Lambda}_0 r^2 - 8t^2\frac{\overline{\Lambda}_1^2}{\overline{\Lambda}_0} \ . \tag{A.143}$$

In the case of pure deviatoric strain field ($t = 0$) the variable $\overline{\Lambda}_1$ is not present in the equation of F_{Hill}^{Lam}. The first derivative of F_{Hill}^{Lam} with respect to $\overline{\Lambda}_0$ is

$$\frac{\partial F_{Hill}^{Lam}}{\partial \overline{\Lambda}_{0L}} = -4r^2 < 0 \ , \tag{A.144}$$

so, we have:

$$\overline{\Lambda}_0^{opt} = \Lambda_0 \ , \overline{\Lambda}_1^{opt} = 0 \ . \tag{A.145}$$

For $t \neq 0$ it is

$$\begin{aligned} \frac{\partial F_{Hill}^{Lam}}{\partial \overline{\Lambda}_0} &= -4r^2 + 8t^2\frac{\overline{\Lambda}_1^2}{\overline{\Lambda}_0^2} \ , \\ \frac{\partial F_{Hill}^{Lam}}{\partial \overline{\Lambda}_1} &= -16t^2\frac{\overline{\Lambda}_1}{\overline{\Lambda}_0} \leq 0 \ . \end{aligned} \tag{A.146}$$

For a fixed value of $\overline{\Lambda}_0$, the optimum value of $\overline{\Lambda}_1$ is its minimum value belonging to the admissible region. Hence, $\overline{\Lambda}_1^{opt}$ is placed on the straight-line up to a certain value of $\overline{\Lambda}_0$ and then on the parabola.

The analysis of the first and second derivatives of (A.143) lead us to two solutions, placed at the two extremes of the portion of the parabola, that has to be compared:

$$\begin{aligned} F_{Hill}^{Lam}|_a &= 4r^2\Gamma_0 + 8t^2\Gamma_1 - 4r^2\Lambda_0 \ ; \\ F_{Hill}^{Lam}|_b &= 4r^2\Gamma_0 + 8t^2\Gamma_1 + \frac{3|t|\Lambda_1}{\Lambda_0}\left[t\Lambda_1 + \sqrt{t^2\Lambda_1^2 + 8r^2\Lambda_0^2}\right] \ . \end{aligned} \tag{A.147}$$

with

$$\begin{aligned} a = \ & (\overline{\Lambda}_1 = 0, \overline{\Lambda}_0 = \Lambda_0) \ ; \\ b = \ & (\overline{\Lambda}_1 = \frac{\Lambda_1}{4r\Lambda_0}\left[-|t|\Lambda_1 + \sqrt{t^2\Lambda_1^2 + 8r^2\Lambda_0^2}\right], \cdots \\ & \cdots \overline{\Lambda}_0 = \frac{|t|\Lambda_1}{4r^2\Lambda_0}\left[-|t|\Lambda_1 + \sqrt{t^2\Lambda_1^2 + 8r^2\Lambda_0^2}\right]) \ ; \end{aligned} \tag{A.148}$$

We have:

$$F_{Hill}^{Lam}|_a \leq F_{Hill}^{Lam}|_b \ . \tag{A.149}$$

so

$$\begin{aligned} \overline{\Lambda}_1^{opt} &= 0 \ , \\ \overline{\Lambda}_0^{opt} &= \Lambda_0 \ ; \end{aligned} \tag{A.150}$$

and

$$F_{Hill}^{Lam} = 4r^2\Gamma_0 + 8t^2\Gamma_1 - 4r^2\Lambda_0 \ . \tag{A.151}$$

****

The global minimum of (A.97) can be determined comparing the solutions of the two studied cases: solution non-ξ and solution ξ. In particular:

- for $L = 0$ and $|t|/r \leq \Lambda_0/\Lambda_1$ the solution is always placed on the parabola for both solutions non-ξ and ξ. Moreover, the solution ξ is placed at the intersection between the parabola and the straight-line so it belongs to both regions of solution ξ and non-ξ, see Fig. A.4. The others two solutions, non-ξ and ξ, lead to the same value of the objective function. Thus, *the global minimum is given by the solution non-ξ*;

- for $L = 0$ and $|t|/r \geq \Lambda_0/\Lambda_1$ the comparison between the two solutions can be done analytically.
  For $\dfrac{|t|}{r} = \dfrac{\Lambda_0}{\Lambda_1}$ we have:

$$F_{Hill}^{Opt}(sol.\ non-\xi) = 4r^2\Gamma_0 + 8t^2\Gamma_1 - 12r^2\Lambda_0 = F_{Hill}^{Opt}(sol.\xi) \ . \tag{A.152}$$

  Whereas, for $\dfrac{|t|}{r} > \dfrac{\Lambda_0}{\Lambda_1}$ we have:

$$F_{Hill}^{Opt}(sol.\ non-\xi) < F_{Hill}^{Opt}(sol.\xi) \ ; \tag{A.153}$$

- for $L = 0$ and $t = 0$ the two solutions are coincident;

- for $L = 1$ and $t \neq 0$ we have:

$$F_{Hill}^{Opt}(sol.\ non-\xi) - F_{Hill}^{Opt}(sol.\xi) = -16|t|r\Lambda_1 \ , \tag{A.154}$$

  so,

$$F_{Hill}^{Opt}(sol.\ non-\xi) < F_{Hill}^{Opt}(sol.\xi) \ ; \tag{A.155}$$

- for $L = 1$ and $t = 0$ the two solutions are coincident.

As a conclusion, it is proved that the global minimum, in both cases for $L = 0$ and $L = 1$ is given by the solution non-xi. The results are summarised in Tab. A.1.

	$\overline{\Lambda}_{0L}^{opt}$	$\overline{\Lambda}_1^{opt}$	$F_{Hill}^{Lam(opt)}$
	$\mathbf{L=0,1;\ r=0,\forall t}$		
	any	*any*	$8t^2\Gamma_1$
$\mathbf{L=0}$			
	$\frac{\lvert\mathbf{t}\rvert}{\mathbf{r}} \leq \frac{\Lambda_0}{\Lambda_1}$		
sol. non-ξ	$\left(\frac{2t^2\Lambda_1^2}{r^2\Lambda_0^2}-1\right)\Lambda_0$	$\frac{\lvert t\rvert\Lambda_1^2}{r\Lambda_0}$	$(*)4r^2\Gamma_0+8t^2\Gamma_1-4r^2\Lambda_0-8t^2\frac{\Lambda_1^2}{\Lambda_0}$
sol. ξ	$\overline{\Lambda}_0^{int}$	$\overline{\Lambda}_1^{int}$	$4r^2\Gamma_0+8t^2\Gamma_1-4r^2\overline{\Lambda}_0^{int}-8t^2\frac{\overline{\Lambda}_1^{int\ 2}}{\Lambda_0}$
	Λ_0	Λ_1	$4r^2\Gamma_0+8t^2\Gamma_1-4r^2\Lambda_0-8t^2\frac{\Lambda_1^2}{\Lambda_0}$
	$\frac{\lvert\mathbf{t}\rvert}{\mathbf{r}} \geq \frac{\Lambda_0}{\Lambda_1}$		
sol. non-ξ	Λ_0	Λ_1	$(*)\ 4r^2\Gamma_0+8t^2\Gamma_1+4\Lambda_0r^2-16\lvert t\rvert r\Lambda_1$
sol. ξ	Λ_0	$\Lambda_0\frac{r}{\lvert t\rvert}$	$4r^2\Gamma_0+8t^2\Gamma_1-12\Lambda_0r^2$
	$\mathbf{t=0}$		
sol. non-ξ	$-\Lambda_0$	0	$(*)\ 4r^2\Gamma_0-4\Lambda_0r^2$
sol. ξ	Λ_0	$[0,\Lambda_1]$	$(*)\ 4r^2\Gamma_0-4\Lambda_0r^2$
$\mathbf{L=1}$			
	$\mathbf{t\neq 0}$		
sol. non-ξ	$-\Lambda_0$	Λ_1	$(*)\ 4r^2\Gamma_0+8t^2\Gamma_1-4\Lambda_0r^2-16\lvert t\rvert r\Lambda_1$
sol. ξ	Λ_0	0	$4r^2\Gamma_0+8t^2\Gamma_1-4\Lambda_0r^2$
	$\mathbf{t=0}$		
sol. non-ξ	$-\Lambda_0$	$[0,\Lambda_1]$	$(*)\ 4r^2\Gamma_0-4\Lambda_0r^2$
sol. ξ	Λ_0	0	$(*)\ 4r^2\Gamma_0-4\Lambda_0r^2$

(*) global minimum.
$\overline{\Lambda}_0^{int}$ and $\overline{\Lambda}_1^{int}$ correspond to the intersection point between the straight-line and the parabola.

Table A.1: Solutions of the local minimisation of F_{Hill}^{Lam} including $\overline{\Omega}_1$ as optimisation parameter.

Bibliography

[1] S. Abrate. Optimal design of laminates plates and shells. *Composite Structures*, 29:269–286, 1994.

[2] G. Allaire and R. Khon. Optimal design for minimum weight and compliance in plane stress using extremal micro structures. *European Journal of Mechanics, A/Solids*, 12(6):839–878, 1993.

[3] J.S. Arora. *Optimization of structural and mechanical systems*. World Scientific, 2007.

[4] M. Autio. Determining the real lay-up of a laminate corresponding to optimal lamination parameters by genetic search. *Structural and Multidisciplinary Optimisation*, 20:301–310, 2000.

[5] N.V. Banichuk. *Problems and methods of optimal structural design*. Plenum Press, 1983.

[6] H.E. Brandmaier. Optimum filament orientation criteria. *Journal of Composite Materials*, 4:422–425, 1970.

[7] C. Caprino and I. Crivelli-Visconti. A note on specially orthotropic laminates. *Journal of Composite Materials*, 16(5):395399, 1982.

[8] A. Catapano, B. Desmorat, and P. Vannucci. Invariant formulation of phenomenological failure criteria for orthotropic sheets and optimisation of their strength. *Mathematical Methods in Applied Sciences*, 35(15):1842–1858, 2012.

[9] G. Cheng, N. Kikuchi, and Z.D. Ma. An improved approach for determining the optimal orientation of orthotropic materials. *Structural Optimization*, 8:101–112, 1994.

[10] G. Cheng and P. Pedersen. On sufficiency conditions for optimal design based on extremum principles of mechanics. *Journal on Mechanical Physics and Solids*, 45:135–150, 1997.

[11] R.M. Christensen. Yield functions/failure criteria for isotropic materials. *Proceedings of the Royal Society of London*, 453:1473–1491, 1997.

[12] R.M. Christensen. A comprehensive theory of yielding and failure for isotropic materials. *Journal of Engineering Material and Technology*, 129:173–181, 2007.

[13] P. De Buhan. Homogenisation and yield design theory: the case of the multi-layered composite material. *C. R. Acad. Sc. Paris, II*, 296:933–936, 1983.

[14] P. De Buhan and A. Taliercio. A homogenisation approach to the yield strength of composite materials. *European Journal of Mechanics, A/Solids*, 10(2):129–154, 1991.

[15] J.F. Ferrero, J.J. Barrau, J.M. Segura, M. Sudre, and B. Castanie. Analytical theory for an approach calculation of non-balanced composite box beams. *Thin-Walled Structures*, 39(8):709–729, 2001.

[16] H. Fukunaga and G.N. Vanderplaats. Stiffness optimization of orthotropic laminated composites usign lamination parameters. *AIAA Journal*, 29:641–646, 1991.

[17] H. Fukunaga and G.N. Vanderplaats. Optimum design of composite structures for shape, layer angle and layer thickness distributions. *Journal of Composite Materials*, 27:1479–1492, 1993.

[18] D.E. Goldberg. *Genetic algorithms*. Addison-Wesley Publishing Co., Massachussets, USA, 1991.

[19] J.H. Gosse and S. Christensen. Strain invariant failure criteria for polymers in composite materials. *AIAA Journal*, page 1184, 2001.

[20] A.A. Groenwold and R.T. Haftka. Optimisation with non-homogeneous failure criteria like tsai-wu for composite laminates. *Structural Multidisciplinary Optimisation*, 32:183–190, 2006.

[21] Z. Gürdal, R.T. Haftka, and P. Hajela. *Design and optimization of laminated composite materials*. Wiley-Interscience, 1999.

[22] V.B. Hammer, M.P. Bendsoe, R. Lipton, and P. Pedersen. Parametrization in laminate design for optimal compliance. *International Journal of Solids and Structures*, 34(4):415–434, 1997.

[23] R. Hill. A theory of the yielding and plastic flow of anisotropic metals. *Proceedings of the Royal Society of London. Series A, Mathematical and Physical Sciences*, 193(1033):281–297, 1948.

[24] H.H. Hilton and Ariaratnam S.T. Invariant anisotropic large deformation deterministic and stochastic combined load failure criteria. *International Journal of Solids ans Structures*, 31(23):3285–3293, 1994.

[25] M.J. Hinton, A.S. Kaddour, and P.D. Soden. *Failure criteria in fibre reinforced polymer composites: the World Wide Failure Exercise, part A*, volume 58. Composites Science and Technology, Elsevier Science Ltd, 1998.

[26] M.J. Hinton, A.S. Kaddour, and P.D. Soden. *Failure criteria in fibre reinforced polymer composites: the World Wide Failure Exercise, part B*, volume 62. Composites Science and Technology, Elsevier Science Ltd, 2002.

[27] M.J. Hinton, A.S. Kaddour, and P.D. Soden. *Failure criteria in fibre reinforced polymer composites: the World Wide Failure Exercise, part C*, volume 64. Composites Science and Technology, Elsevier Science Ltd, 2004.

[28] O. Hoffman. The brittle strength of orthotropic materials. *Journal of Composite Materials*, 1(2):200–206, 1967.

[29] J.H. Holland. *Adaptation of natural and artidicial systems*. University of Michigan Press, Ann Arbor, MI, USA, 1975.

[30] S.T. IJsselmuiden, M.M. Abdalla, and Z. Gürdal. Implementation of strength-based failure criteria in the lamination parameter design space. *AIAA Journal*, 46(7):1826–1834, 2008.

[31] A. Jibawy, C. Julien, B. Desmorat, A. Vincenti, and F. Léné. Hierarchical structural optimization of laminated plates using polar representation. *International Journal of Solids and Structures*, 48:25762584, 2011.

[32] Ali Jibawy. *Optimisation structurale de coques minces composites stratifiées*. PhD thesis, UPMC, Paris 6, Paris (France), 2010.

[33] R.M. Jones. *Mechanics of composite materials*. Taylor & Francis, 1999.

[34] C. Julien. *Conception Optimale de l'Anisotropie dans les Structures Stratifiees à Rigiditè Variable par la Méthode Polaire-Génétique*. PhD thesis, UPMC, Paris 6, Paris (France), 2010.

[35] R. Kathiravan and R. Ganguli. Strength design of composite beam using gradient and particle swarm optimization. *Composite Structures*, (81):471–479, 2007.

[36] P. Kere and J. Koski. Multicriterion optimization of composite laminates for maximum failure margin with an interactive descent algorithm. *Structural and Multidisciplinary Optimization*, (23):436–447, 2002.

[37] P. Kere, M. Lyly, and J. Koski. Using multicriterion optimization for strength design of composite laminates. *Composite Structures*, (62):329–333, 2003.

[38] A. Khani, S.T. IJsselmuiden, M.M. Abdalla, and Z. Gürdal. Design of variable stiffness panels for maximum strength using lamination parameter. *Composites: Part B*, 42:546–552, 2011.

[39] K.S. Liu and S.W. Tsai. A progressive quadratic failure criterion for a laminate. *Composites Science and Technology*, (58):1023–1032, 1998.

[40] J. Majak and S. Hannus. Orientational design of anisotropic materials using the hill and tsai-wu strength criteria. *Mechanics of Composite Materials*, 39(6), 2003.

[41] J. Majak and M. Pohlak. Optimal material orientation of linear and non-linear elastic 3d anisotropic materials. *Meccanica*, 45:671–680, 2010.

[42] M. Miki. Material design of composite laminates with required in-plane elastic properties. In T. Hayashi, K. Kawata, and S. Umekawa, editors, *Progress in Science and Engineering of Composites*, pages 1725–1731, Tokyo, 1982. ICCM-IV.

[43] M. Miki. Design of laminated fibrous composite plates with required flexural stiffness. *ASTM STP*, 864:387–400, 1985.

[44] M. Montemurro. *Optimal Design of Advanced Engineering Modular Systems through a New Genetic Approach*. PhD thesis, Université U.P.M.C. Paris VI, 2012.

[45] M. Montemurro, A. Vincenti, and P. Vannucci. Design of elastic properties of laminates with minimum number of plies. *Mechanics of Composite Materials*, 48:369–390, 2012.

[46] M. Montemurro, A. Vincenti, and P. Vannucci. A two-level procedure for the global optimum design of composite modular structures - application to the design of an aircraft wing. part 1: theoretical formulation. *Journal of Optimization Theory and Applications*, 155(1):1–23, 2012.

[47] M. Montemurro, A. Vincenti, and P. Vannucci. A two-level procedure for the global optimum design of composite modular structures - application to the design of an aircraft wing. part 2: numerical aspects and examples. *Journal of Optimization Theory and Applications*, 155(1):24–53, 2012.

[48] M. Montemurro, A. Vincenti, and P. Vannucci. The authomatic dynamic penalisation method (ADP) for handling constraints with genetic algorithms. *Computer Methods in Applied Mechanics and Engineering*, 256:70–87, 2013.

[49] D. Orvosh and L. Davis. Shall we repair? genetic algorithms, combinatorial optimization, and feasibility constraints. volume 650, pages 17–21. Proceedings of the fifth International Conference on Genetic Algorithms, 1993.

[50] Y. Özgür. Penalty function methods for constrained optimization with genetic algorithms. *Mathematical and Computational Applications*, 10(1):45–56, 2005.

[51] M. Palantera, J.P. Karjalainen, and O. Saarela. Laminate level failure criteria based on FPF analyses. volume SP-428. Proceeding European Conference on Spacecraft Structures, Materials and Mechanical Testing, 1998.

[52] J.H. Park, J.H. Hwang, C.S. Lee, and W. Hwang. Stacking sequence design of composite laminates for maximum strength using genetic algorithms. *Composite Structures*, (52):217–231, 2001.

[53] G. Pedersen. A note on design of fiber-nets for maximum stiffness. *Journal of Elasticity*, 73:127145, 2003.

[54] P. Pedersen. On optimal orientation of orthotropic materials. *Structural Optimization*, 1:101–106, 1989.

[55] P. Pedersen. Bounds on elastic energy in solids of orthotropic materials. *Structural Optimization*, 2:55–63, 1990.

[56] P. Pedersen. On thickness and orientational design with orthotropic materials. *Structural Optimization*, 3:69–78, 1991.

[57] P. Pedersen and J.E. Taylor. *Optimal design based on power law nonlinear elasticity. In: Optimal design with advances materials.* Elsevier, 1993.

[58] J.H. Puck and H. Schürmann. Failure analysis of FRP laminates by means of physically based phenomenological failure criteria. *Composites Science and Technology*, (58):1045–1067, 1998.

[59] J.N. Reddy. *Theory and analysis of elastic plates and shells*. 2nd ed., Boca Raton, CRC Press, 2007.

[60] M. Rovati and A. Taliercio. Optimal orientation of the symmetry axes of orthotropic 3-D materials. *Engineering Optimization in Design Processes*, 63:127–134, 1991.

[61] M. Rovati and A. Taliercio. Stationarity of the strain energy density for some classes of anisotropic solids. *International Journal of Solids and Structures*, 40(22):6043–6075, 2003.

[62] R.E. Rowlands. *Strength (failure) theories and their experimental correlation*, volume III. Handbook of Composite Materials, Elsevier Scientific, Oxford, 1984.

[63] G. Royer-Carfagni. Optimal fiber-mesh layout for a composite anisotropic elastic wedge. *Journal of Elasticity*, 60:103–117, 2000.

[64] G. Sacchi Landriani and M. Rovati. Optimal design of two-dimensional structures made of composite materials. *Journal of Mechanical Design*, 113(1):88–92, 1991.

[65] R. S. Sandhu. Parametric study of tsai's strength criteria for filamentary composites. *Air Force Flight Dynamic Laboratory, AFF-TR-68-168*, 1969.

[66] F. R. Shanley and E. I. Ryder. Stress ratios : the answer to the combined loading problem. *Aviation*, 36, 1937.

[67] T. M. Thauchert and S. Adibatla. Design of laminated plates for maximum stiffness. *Journal of Composite Materials*, 18:58–69, 1984.

[68] S.P. Timoshenko and J.N. Goodier. *Theory of Elasticity.* McGraw-Hill, Singapore, 1970.

[69] A. Todoroki and M. Sekishiro. Stacking sequence optimization to maximize the buckling load of blade-stiffened panels with strength constraints using the iterative fractal branch and bound method. *Composites : Part B*, 39:842850, 2008.

[70] U. Topal and Ü. Uzman. Strength optimization of laminated composite plates. *Journal of Composite Materials*, 42(17):1731–1746, 2008.

[71] S.W. Tsai and H.T. Hahn. *Introduction to composite materials.* Technomic Press, New York, 1980.

[72] S.W. Tsai and N. Pagano. Invariant properties of composite materials. In Halpin Tsai and Pagano, editors, *Composite Material Workshop*, pages 233–253. Technomic Publishing Co., 1968.

[73] S.W. Tsai and E.M. Wu. A general theory of strength for anisotropic materials. *Journal of Composite Materials*, 5:58–80, 1971.

[74] J. Van Campen, C. Kassapoglou, and Z. Gürdal. Generating realistic laminate fiber angle distributions for optimal variable stiffness laminates. *Composites: part B*, 43(2):354–360, 2011.

[75] P. Vannucci. A special planar orthotropic material. *Journal of Elasticity*, 67:81–96, 2002.

[76] P. Vannucci. Un parcours de recherche multidisciplinaire en mécanique. Université de Bourgogne, Thèse de HDR, 2002. http://tel.archives-ouvertes.fr/docs/00/62/59/58/PDF/HDR.pdf.

[77] P. Vannucci. Plane anisotropy by the polar method. *Meccanica*, 40:437–454, 2005.

[78] P. Vannucci. Designing the elastic properties of laminates as an optimisation problem: a unified approach based on polar tensor invariants. *Structural and Multidisciplinary Optimisation*, 31(5):378387, 2006.

[79] P. Vannucci. The polar analysis of a third order piezoelecticity-like plane tensor. *International Journal of Solids and Structures*, 44:7803–7815, 2007.

[80] P. Vannucci. Influence of invariant material parameters on the flexural optimal design of thin anisotropic laminates. *International Journal of Mechanical Sciences*, 51:192–203, 2009.

[81] P. Vannucci. A note on the elastic and geometric bounds for composite laminates. *Journal of Elasticity*, 2013 (in press.).

[82] P. Vannucci and G. Verchery. A special class of uncoupled and quasi-homogeneous laminates. *Composite Science and Technology*, 61(10):14651473, 2001.

[83] P. Vannucci and G. Verchery. Stiffness design of laminates using the polar method. *International Journal of Solids and Structures*, 38(50):92819294, 2001.

[84] P. Vannucci and G. Verchery. Anisotropy of plane complex elastic body. *International Journal of Solids and Structures*, 47:1154–1166, 2010.

[85] P. Vannucci and A. Vincenti. The design of laminates with given thermal/hygral expansion coefficients: a general approach based upon the polar-genetic method. *Composite Structures*, 79:454466, 2007.

[86] G. Verchery. Les invariants des tenseurs d'ordre 4 du type de l'élasticité. In *Proceeding of the Euromech Colloquium 115*, volume 115, pages 93–104, Villard-de-Lans, France, 1979.

[87] A. Vincenti. *Conception et optimisation de composites par m'ethode polaire et algorithmes génétiques*. PhD thesis, Universite de Bourgogne, France, 2002.

[88] A. Vincenti and B. Desmorat. Optimal orthotropy for minimum elastic energy by the polar method. *Journal of Elasticity*, 102(1):55–78, 2010.

[89] A. Vincenti, P. Vannucci, and M.R. Ahmadian. Optimization of laminated composites by using genetic algorithm and the polar description of plane anisotropy. *Mechanics of Advanced Materials and Structures*, 20:242–255, 2013.

[90] W. Voigt. *Lehrbuch der Kristallphysik : mit Ausschlu d. Kristalloptik*. Teubner, Leipzig, 1910.

[91] M. Yong, B.G. Falzon, and L. Iannucci. On the application of genetic algorithms for optimising composites against impact loading. *International Journal of Impact Engineering*, 35:12931302, 2008.

[92] W. Zhang and K.E. Evans. A strain-based tensor polynomial failure criterion for anisotropic materials. *Journal of Strain Analysis for Engineering Design*, 23:179–186, 1988.

[93] W. Zhang and K.E. Evans. Correlation between stress and strain based polynomial failure criteria. *Composite Structures*, 13:115–121, 1989.

List of publications

1. A. Catapano, B. Desmorat and P. Vannucci, Invariant formulation of phenomenological failure criteria for orthotropic sheets and optimisation of their strength, *Mathematical Methods in the Applied Sciences*, 35(15): pp. 1842-1858, 2012.
   http://onlinelibrary.wiley.com/doi/10.1002/mma.2530

2. A. Catapano, G. Giunta, S. Belouettar and E. Carrera, Static analysis of laminated beams via a unified formulation, *Composite Structures*, 94(1): pp. 75-83, 2011.
   http://dx.doi.org/10.1016/j.compstruct.2011.07.015

3. G. Giunta, A. Catapano, S. Belouettar, P. Vannucci and E. Carrera, Failure Analysis of Composite Plates Subjected to Localized Loadings via a Unified Formulation, *Journal of Engineering Mechanics*, 138(5): pp. 458-467, 2012.
   http://dx.doi.org/10.1061/(ASCE)EM.1943-7889.0000358

4. G. Giunta, A. Catapano and S. Belouettar, Failure indentation analysis of composite sandwich plates via hierarchical models, *Journal of Sandwich Structures and Materials*, 15(1): pp. 45-70, 2013.
   doi:10.1177/1099636212460539

5. A. Catapano, B. Desmorat and P. Vannucci, Stiffness and strength optimisation of the anisotropy distribution for laminated structures, *Journal of Optimization Theory and Applications*, submitted.